



UNIVERSITY OF <sup>TM</sup>  
**KWAZULU-NATAL**  

---

**INYUVESI**  
**YAKWAZULU-NATALI**

**Fusaric Acid-Induced Epigenetic Modifications  
*in vitro* and *in vivo*: Alternative Mechanisms of  
Hepatotoxicity**

By

**TERISHA GHAZI**

*BSc. (Biomedical Science), B. Med. Sc. (Hons) (Medical Biochemistry), M. Med. Sc.  
(Medical Biochemistry)*

**Submitted in fulfilment for the degree of Doctor of Philosophy (Medical  
Biochemistry), School of Laboratory Medicine and Medical Science, College of  
Health Sciences, University of KwaZulu-Natal**

**Supervisor**

**Professor Anil A. Chuturgoon**

**2019**

## DECLARATION

I, **Terisha Ghazi**, declare that:

- i. The research reported in this thesis, except where otherwise indicated, is my original work.
- ii. This thesis has not been submitted for any degree or examination at another university.
- iii. This thesis does not contain other persons' data, pictures, graphs, or other information, unless specifically acknowledged as being sourced from other persons.
- iv. This thesis does not contain other person's writing, unless specifically acknowledged as being sourced from other researchers. Where other written sources have been quoted, then:
  - a. their words have been re-written but the general information sourced has been referenced to the authors;
  - b. where their exact words have been used, their writing has been placed within quotation marks, and referenced.
- v. Where I have reproduced a publication of which I am an author, co-author, or editor, I have indicated in detail which part of the publication was written by myself alone and have fully referenced such publications.
- vi. This thesis does not contain text, graphics, or tables copied and pasted from the internet, unless specifically acknowledged, and the source being detailed in the thesis and reference section.

Signed: 

**Miss Terisha Ghazi**

Date: 8 November 2019

## DEDICATION

To my parents, **Prasanth** and **Nireka Ghazi**, for always believing in me and encouraging me to strive for excellence.

## ACKNOWLEDGMENTS

### **My Family**

Thank you for all your love, support and encouragement. Thank you for always believing in me and providing me with the opportunity to pursue my dreams. Without you my success would not be possible.

### **Professor Anil A. Chuturgoon**

I am truly grateful for all the support, guidance and motivation that you have given me throughout the years. Thank you for believing in me and my ideas and allowing me the freedom to express myself. Your passion for science and innovation has been an inspiration and I am truly fortunate to have you as my supervisor.

### **Dr Savania Nagiah**

Thank you for your dedication towards this study. Your patience, assistance and constructive criticism have made this journey a pleasant experience.

### **Friends and Colleagues of Medical Biochemistry**

Thank you for your friendship and help throughout the years. A special thanks to **Dr Pragalathan Naidoo** and **Miss Thilona Arumugam** for always being someone I could count on. Your enthusiasm, curiosity, and willingness to assist in the laboratory have always been greatly appreciated.

### **Funding Sources**

I would like to thank the National Research Foundation (Grant no.: SFH160703175722) and the University of KwaZulu-Natal College of Health Sciences (Grant no.: 570869) for financially supporting this study.

## PUBLICATIONS

1. Ghazi, T., Nagiah, S., Tiloke, C., Abdul, N.S., and Chuturgoon, A.A. (2017). Fusaric acid induces DNA damage and post-translational modifications of p53 in human hepatocellular carcinoma (HepG2) cells. **Journal of Cellular Biochemistry** 118 (11), 3866-3874. DOI: [10.1002/jcb.26037](https://doi.org/10.1002/jcb.26037).
2. Ghazi, T., Nagiah, S., Naidoo, P., and Chuturgoon, A.A. (2019). Fusaric acid-induced promoter methylation of DNA methyltransferases triggers DNA hypomethylation in human hepatocellular carcinoma (HepG2) cells. **Epigenetics** 14 (8), 804-817. DOI: [10.1080/15592294.2019.1615358](https://doi.org/10.1080/15592294.2019.1615358).
3. Ghazi, T., Nagiah, S., Dhani, S., and Chuturgoon, A.A. (2019). Fusaric acid-induced epigenetic modulation of hepatic H3K9me3 triggers apoptosis *in vitro* and *in vivo*. **Future Medicine: Epigenomics** (*In Review*). Manuscript ID: EPI-2019-0284.
4. Ghazi, T., Nagiah, S., and Chuturgoon, A.A. (2019). Fusaric acid regulates p53 expression via promoter methylation and m6A RNA methylation *in vitro* and *in vivo*. **Scientific Reports** (*In Review*). Manuscript ID: SREP-19-40805

## PRESENTATIONS

### International

1. Ghazi, T., Nagiah, S., Tiloke, C., Abdul, N.S., and Chuturgoon, A.A. (2018). Fusaric acid induces DNA damage and post-translational modifications of p53 in human hepatocellular carcinoma (HepG2) cells. National Conference on “Integrative Medicine: Emerging Scientific Knowledge and New Therapies”, Mysore, Karnataka, India, Oral presentation.
2. Ghazi, T., Nagiah, S., Pillay, Y., and Chuturgoon, A.A. (2018). Fusaric acid upregulates miR-200a and attenuates H3K9me3 in HepG2 cells. Cold Spring Harbor Meeting: Regulatory and non-coding RNAs, New York, USA, Poster presentation.
3. Ghazi, T., Nagiah, S., Naidoo, P., and Chuturgoon, A.A. (2019). Fusaric acid-induced promoter methylation of DNA methyltransferases triggers DNA hypomethylation in HepG2 cells. IUTOX 15<sup>th</sup> International Congress of Toxicology (co-hosted by Society of Toxicology), Honolulu, Hawaii, USA, Poster presentation.

### National

4. Ghazi, T., Nagiah, S., Tiloke, C., Abdul, N.S., and Chuturgoon, A.A. (2017). Fusaric acid induces DNA damage and post-translational modifications of p53 in human hepatocellular carcinoma (HepG2) cells. Cape Town 8<sup>th</sup> International Conference on “Medical, Medicine and Health Sciences” (MMHS-2017), Cape Town, South Africa, Oral presentation.
5. Ghazi, T., Nagiah, S., and Chuturgoon, A.A. (2018). Fusaric acid causes DNA hypomethylation by upregulating miR-29b and methyl-CpG binding domain protein 2 in human liver (HepG2) cells. School of Laboratory Medicine and Medical Science Research Day 2018, University of KwaZulu-Natal, Durban, South Africa, Oral presentation (3<sup>rd</sup> Prize).

6. Ghazi, T., Nagiah, S., Pillay, Y., and Chuturgoon, A.A. (2018). Fusaric acid upregulates miR-200a and attenuates SUV39H1-mediated H3K9me3 in human hepatocellular carcinoma (HepG2) cells. College of Health Sciences Research Symposium 2018, University of KwaZulu-Natal, Durban, South Africa, Oral presentation.
7. Ghazi, T., Nagiah, S., Dhani, S., Baijnath, S., Singh, S.D., and Chuturgoon, A.A. (2019). Fusaric acid-induced epigenetic modulation of hepatic H3K9me3 triggers apoptosis *in vivo*: a pilot study. School of Laboratory Medicine and Medical Science Research Day 2019, University of KwaZulu-Natal, Durban, South Africa, Poster presentation (1<sup>st</sup> Prize).
8. Ghazi, T., Nagiah, S., Dhani, S., Baijnath, S., Singh, S.D., and Chuturgoon, A.A. (2019). Fusaric acid regulates p53 expression via promoter methylation and m6A RNA methylation *in vivo*: a pilot study. College of Health Sciences Research Symposium 2019, University of KwaZulu-Natal, Durban, South Africa, Oral presentation (2<sup>nd</sup> Prize).

## TABLE OF CONTENTS

Declaration .....	ii
Dedication .....	iii
Acknowledgments .....	iv
Publications .....	v
Presentations .....	vi
Table of Contents .....	viii
List of Figures .....	x
List of Tables.....	xii
Abbreviations .....	xiii
Abstract .....	xix
Chapter 1: Introduction .....	1
Chapter 2: Literature Review .....	6
2.1. Mycotoxins.....	6
2.2. Fusaric Acid .....	7
2.2.1. Structure of FA.....	8
2.2.2. Effects of FA.....	9
2.3. Epigenetics .....	11
2.4. Structure of Chromatin.....	12
2.5. DNA Methylation.....	13
2.5.1. Structure of DNMTs.....	15
2.5.2. Regulation of DNMTs.....	16
2.5.2.1.Regulation of DNMTs via Promoter Methylation .....	17
2.5.2.2.Regulation of DNMTs via Post-Translational Modifications: Acetylation and Ubiquitination .....	18
2.6. Methyl-CpG Binding Proteins .....	20
2.6.1. MBD2.....	21
2.6.2. Regulation of MBD2 via Promoter Methylation.....	21
2.7. Histone Modifications .....	22
2.7.1 H3K9me3 .....	22
2.7.2 Structure of SUV39H1 .....	23
2.7.3 Post-Translational Regulation of SUV39H1: Acetylation and Ubiquitination .....	24
2.7.4 The Relationship between DNA Methylation and H3K9me3.....	25
2.7.5 H2Ax .....	25
2.8. Apoptosis.....	26

2.8.1. Caspases .....	26
2.8.2. Pathways of Apoptosis .....	27
2.8.2.1.The Intrinsic Apoptotic Pathway.....	27
2.8.2.2.The Extrinsic Apoptotic Pathway .....	27
2.9. The p53 Tumour Suppressor Protein.....	28
2.9.1. Regulation of p53 .....	30
2.9.1.1.Promoter Methylation of p53 .....	30
2.9.1.2.M6A RNA Methylation .....	31
2.10. MicroRNAs .....	33
2.10.1. Biogenesis of MiRNAs .....	34
2.10.2. MiRNAs and DNA Methylation .....	35
2.10.3. MiRNAs and Histone Methylation .....	36
2.11. The Role of Epigenetics in Mycotoxicology.....	36
2.12. References .....	38
Chapter 3: Fusaric acid-induced promoter methylation of DNA methyltransferases triggers DNA hypomethylation in human hepatocellular carcinoma (HepG2) cells .....	58
Chapter 4: Fusaric acid-induced epigenetic modulation of hepatic H3K9me3 triggers apoptosis <i>in vitro</i> and <i>in vivo</i> .....	89
Chapter 5: Fusaric acid regulates p53 expression via promoter methylation and m6A RNA methylation <i>in vitro</i> and <i>in vivo</i> .....	126
Chapter 6: Conclusion.....	157
Addendum A .....	162
Addendum B: Ethical Approval Letter – <i>In Vitro</i> Study.....	172
Addendum C: Ethical Approval Letter – <i>In Vivo</i> Study .....	173
Addendum D: Quantification of DNA Methylation .....	174
Addendum E: Quantification of M6A RNA Methylation.....	175

## LIST OF FIGURES

<b>Figure 2.1</b> Chemical structure of nicotinic acid (A), picolinic acid (B), and Fusaric acid (C) (May et al., 2000) .....	9
<b>Figure 2.2</b> Structure of chromatin (Pieterman et al., 2014) .....	13
<b>Figure 2.3</b> Process of DNA methylation (Miranda-Gonçalves et al., 2018) .....	14
<b>Figure 2.4</b> Structure of DNMT proteins (Jeltsch and Jurkowska, 2016) .....	16
<b>Figure 2.5</b> Regulation of gene expression via promoter methylation (Dabrowski and Wojtas, 2019) .....	17
<b>Figure 2.6</b> Regulation of DNMT1 by acetylation and ubiquitination .....	19
<b>Figure 2.7</b> Structure of MBD1 to MBD6 (Du et al., 2015) .....	21
<b>Figure 2.8</b> Structure of SUV39H1 (Firestein et al., 2000) .....	24
<b>Figure 2.9</b> Intrinsic and extrinsic pathways of apoptosis (Favaloro et al., 2012) .....	28
<b>Figure 2.10</b> Activation and functions of p53 (Bieging et al., 2014) .....	30
<b>Figure 2.11</b> Regulation and function of m6A RNA methylation (Liao et al., 2018) .....	33
<b>Figure 2.12</b> The canonical pathway of microRNA biogenesis (Winter et al., 2009) .....	35
<b>Figure 3.1</b> Fusaric acid induced global DNA hypomethylation in HepG2 cells .....	63
<b>Figure 3.2</b> The effect of FA on DNA methyltransferases in HepG2 cells .....	64
<b>Figure 3.3</b> The effect of FA on the promoter methylation of <i>DNMT1</i> , <i>DNMT3A</i> , and <i>DNMT3B</i> in HepG2 cells .....	65
<b>Figure 3.4</b> The effect of FA on miR-29b and <i>Sp1</i> in HepG2 cells .....	66
<b>Figure 3.5</b> The effect of FA on the ubiquitination of DNMT1, DNMT3A, and DNMT3B in HepG2 cells .....	67
<b>Figure 3.6</b> The effect of FA on <i>MBD2</i> promoter methylation and MBD2 expression in HepG2 cells .....	68
<b>Figure 3.7</b> Proposed mechanism of FA-induced global DNA hypomethylation in HepG2 cells .....	72
<b>Supplementary Figure S3.1</b> CpG islands within the <i>DNMT1</i> , <i>DNMT3A</i> , <i>DNMT3B</i> , and <i>MBD2</i> promoter regions obtained using the MethPrimer software version 2.0. [65] .....	81
<b>Figure 4.1</b> FA upregulates miR-200a in HepG2 cells and mice livers .....	99
<b>Figure 4.2</b> FA decreases Sirt1 mRNA and protein expression in HepG2 cells and mice livers .....	101
<b>Figure 4.3</b> FA alters SUV39H1 ubiquitination and increases MDM2 expression in HepG2 cells .....	102
<b>Figure 4.4</b> FA alters expression levels of nuclear and cytoplasmic SUV39H1 in HepG2 cells .....	103

<b>Figure 4.5</b> FA alters SUV39H1 mRNA and protein expression in HepG2 cells and mice livers .....	104
<b>Figure 4.6</b> FA decreases H3K9me3 and increases H3K9me1 in HepG2 cells and mice livers .....	105
<b>Figure 4.7</b> FA induces genome instability and alters p-S139-H2Ax in HepG2 cells and mice livers.....	107
<b>Figure 4.8</b> FA decreases cell viability and increases caspase-3/7 activity in HepG2 cells and mice livers .....	108
<b>Supplementary Figure S4.1</b> FA alters miR-141 expression in HepG2 cells and mice livers. .	117
<b>Supplementary Figure S4.2</b> TargetScan analyses of miR-141 to the 3' UTR of <i>Sirt1</i> in humans and mice .....	117
<b>Supplementary Figure S4.3</b> FA decreased caspase -8 and -9 activities in HepG2 cells and mice livers.....	118
<b>Figure 5.1</b> FA alters p53 expression in HepG2 cells and mice livers .....	131
<b>Figure 5.2</b> FA alters <i>p53</i> promoter methylation in HepG2 cells and mice livers.....	132
<b>Figure 5.3</b> FA alters m6A- <i>p53</i> levels in HepG2 cells and mice livers.....	133
<b>Figure 5.4</b> FA alters the expression of m6A methyltransferases and demethylases in HepG2 cells and mice livers .....	134
<b>Figure 5.5</b> FA alters the expression of m6A readers in HepG2 cells and mice livers.....	136
<b>Supplementary Figure S5.1</b> Full size western blot images for Figure 5.1b.....	148
<b>Supplementary Figure S5.2</b> Full size western blot images for Figure 5.1d.....	148
<b>Figure A1</b> Standard curve used to determine 5-methylcytosine in DNA.....	174
<b>Figure A2</b> Standard curve used to determine m6A levels in total RNA .....	175
<b>Figure A3</b> The effect of FA on total m6A levels in HepG2 cells.....	176

## LIST OF TABLES

<b>Supplementary Table S3.1:</b> The effect of FA on the mRNA expression of <i>MBD1</i> , <i>MBD2</i> , <i>MBD3</i> , <i>MBD4</i> , <i>MBD5</i> , and <i>MBD6</i> in HepG2 cells.....	79
<b>Supplementary Table S3.2:</b> qPCR primer sequences and annealing temperatures .....	80
<b>Supplementary Table S4.1:</b> qPCR primer sequences and annealing temperatures .....	116
<b>Supplementary Table S5.1:</b> qPCR primer sequences and annealing temperatures .....	145

## ABBREVIATIONS

ADP	Adenosine di-phosphate
AFB <sub>1</sub>	Aflatoxin B <sub>1</sub>
Ago2	Argonaute 2
AIF	Apoptosis inducing factor
AKT	Protein kinase B
ALKBH5	ALK B homolog 5
AML	Acute myeloid leukemia
ANOVA	One-way analysis of variance
ANT	Adenine nucleotide translocator
Apaf1	Apoptotic protease activating factor 1
ATM	Ataxia telangiectasia mutated
ATP	Adenosine tri-phosphate
ATR	ATM and Rad3-related
BAH	Bromo-adjacent homology
BCA	Bicinchoninic acid
BSA	Bovine serum albumin
CBP	CREB-binding protein
CC	Coiled coil domain
CCM	Complete culture media
CDC42	Cell division cycle 42
cDNA	complementary DNA
CH <sub>3</sub>	Methyl group

CpG	Cytosine phosphate guanine
Ct	Comparative threshold cycle
CXXC	Cysteine-rich zinc binding domain
DAS	Diacetoxyscirpenol
DGCR8	DiGeorge syndrome critical region 8
DICER	Ribonuclease III enzyme
DISC	Death inducing signaling complex
DMAP1	DNMT-associated protein 1
DNA	Deoxyribonucleic acid
DNA-PK	DNA-dependent protein kinase
DNMT	DNA methyltransferase
DON	Deoxynivalenol
DR4/5	Death receptor 4/5
DROSHA	Ribonuclease III enzyme
EDTA	Ethylene diamine tetra-acetic acid
EGF	Epithelial growth factor
EHMT2/G9a	Euchromatic-histone lysine N-methyltransferase 2
EMEM	Eagles minimum essentials medium
FA	Fusaric acid
FADD	Fas-associated death domain
FAO	Food and Agriculture Organization
FasL	Fas ligand
FasR	Fas receptor

FB <sub>1</sub>	Fumonisin B <sub>1</sub>
FTO	Fat mass and obesity-associated protein
GAPDH	Glyceraldehyde-3-phosphate dehydrogenase
GR	Glycine-arginine-rich
H	Histone
H3K9Ac	Histone 3 lysine 9 acetylation
H3K9me3	Histone 3 lysine 9 trimethylation
H3K9me1	Histone 3 lysine 9 mono-methylation
H3K4me2	Histone 3 lysine 4 di-methylation
H4K20me3	Histone 4 lysine 20 trimethylation
HDAC	Histone deacetylase
HepG2	Human liver cell line
HNSCC	Head and neck squamous cell carcinoma
HP1	Heterochromatin protein 1
IL	Interleukin
K	Lysine
KDM4B	Lysine demethylase 4B
KG	Lysine-Glycine
M6A	N-6-methyladenosine
MAPK	Mitogen-activated protein kinase
MBD	Methyl-CpG binding domain
MDM2	Murine double minute 2
METTL3	Methyltransferase-like 3

METTL14	Methyltransferase-like 14
MiRNA/MiR	MicroRNA
MPTP	Mitochondrial permeability transition pore
mRNA	Messenger RNA
NAD <sup>+</sup>	Nicotinamide adenine dinucleotide
NFDM	Non-fat dry milk
NLS	Nuclear localization signal
OTA	Ochratoxin A
PARP1	Poly-ADP-ribose polymerase 1
PAT	Patulin
PBD	Proliferating cell nuclear antigen-binding domain
PBMCs	Peripheral blood mononuclear cells
PBR	Peripheral benzodiazepine receptor
PBS	Phosphate buffered saline
PCNA	Proliferating cell nuclear antigen
PI3K	Phospho-inositol-3 kinase
Pre-miRNA	Precursor microRNA
Pri-miRNA	Primary microRNA
p-S139-H2Ax	Histone H2Ax phosphorylated on serine residue 139
PTMs	Post-translational modifications
PWWP	Proline-tryptophan-tryptophan-proline
R	Arginine
RBD	Relative band density

RBM15	RNA binding motif 15
RFTD	Replication foci targeting domain
RISC	RNA-induced silencing complex
RLU	Relative light units
RNA	Ribonucleic acid
RT	Room temperature
SAM	S-adenosyl methionine
SD	Standard deviation
SDS	Sodium dodecyl sulphate
SEM	Standard error of the mean
Sir2	Silencing information regulator 2
Sirt	Sirtuin
SRA	SET and Ring-associated
SUV39H1	Suppressor of variegation 3-9 homolog 1
SUV39H2	Suppressor of variegation 3-9 homolog 2
TGF- $\beta$	Transforming growth factor beta
TNF- $\alpha$	Tumor necrosis factor alpha
TNFR1	Type 1 TNF receptor
TRADD	TNFR-associated death domain
TRAIL	TNF-related apoptosis inducing ligand
TRBP	Trans-activation response (TAR) RNA-binding protein
TRD	Transcriptional repression domain
TTBS	Tris buffered saline with Tween 20

UHRF1	Ubiquitin-like and ring finger domain 1
USP7	Ubiquitin specific peptidase 7
UTR	Untranslated region
VDAC	Voltage-dependent anion channel
VIRMA	Vir-like m6A methyltransferase-associated
WHO	World Health Organization
WTAP	Wilm's tumor 1-associated protein
YTHDC	YT521-B homology domain containing
YTHDF	YT521-B homology domain family
ZC3H13	Zinc finger CCH-type containing 13
ZEB	Zinc finger E-box binding protein

## ABSTRACT

The *Fusarium*-produced mycotoxin, Fusaric acid (FA), is a frequent contaminant of agricultural foods that exhibits toxicity in plants and animals with little information on its molecular and epigenetic mechanisms. Epigenetic modifications including DNA methylation, histone methylation, N-6-methyladenosine (m6A) RNA methylation, and microRNAs are central mediators of cellular function and may constitute novel mechanisms of FA toxicity. This study aimed to determine epigenetic mechanisms of FA-induced hepatotoxicity *in vitro* and *in vivo* by specifically investigating DNA methylation, histone 3 lysine (K) 9 trimethylation (H3K9me3), and m6A-mediated regulation of p53 expression in human liver (HepG2) cells and C57BL/6 mice livers.

FA induced global DNA hypomethylation in HepG2 cells; decreased the expression of DNA methyltransferases (*DNMT1*, *DNMT3A*, and *DNMT3B*) by inducing promoter hypermethylation and upregulated expression of miR-29b. Further, FA decreased the ubiquitination of DNMT1, DNMT3A, and DNMT3B by decreasing the expression of the ubiquitination regulators, *UHRF1* and *USP7*. FA induced promoter hypomethylation of the demethylase, *MBD2* and increased *MBD2* expression contributing to global DNA hypomethylation in HepG2 cells.

DNA methylation and H3K9me3 function in concert to regulate genome integrity and gene transcription. Sirtuin (Sirt) 1 is a histone deacetylase and direct target of miR-200a that regulates the repressive H3K9me3 mark by post-translationally modifying both H3K9Ac and the histone methyltransferase, SUV39H1. FA upregulated miR-200a and decreased Sirt1 expression in HepG2 cells and C57BL/6 mice livers. FA decreased the expression of SUV39H1 and histone demethylase, *KDM4B* which led to a decrease in H3K9me3 and an increase in H3K9me1. FA also decreased cell viability via apoptosis as evidenced by the significant increase in the activity of the executioner caspase-3/7.

The tumor suppressor protein, p53 regulates cell cycle arrest and apoptosis in response to cellular stress. The expression of p53 is regulated at the transcriptional and post-transcriptional level by promoter methylation and m6A RNA methylation. In HepG2 cells, FA induced *p53* promoter hypermethylation and decreased *p53* expression. FA also decreased m6A-*p53* levels by decreasing the expression of the methyltransferases, *METTL3* and *METTL14*, and the m6A readers, *YTHDF1*, *YTHDF3*, and *YTHDC2*, thereby, decreasing p53 translation. In C57BL/6 mice livers FA, however, induced *p53* promoter hypomethylation and increased *p53* expression. FA increased m6A-*p53* levels by increasing the expression of *METTL3* and *METTL14*; and increased expression of *YTHDF1*, *YTHDF3*, and *YTHDC2* increased p53 translation.

In conclusion, this study provides evidence for alternative mechanisms of FA-induced hepatotoxicity (*in vitro* and *in vivo*) by modulating DNA methylation, H3K9me3, m6A RNA methylation, and epigenetically regulating p53 expression ultimately leading to genome instability and apoptotic cell death. These results provide insight into a better understanding of FA induced hepatic toxicity at the epigenetic and cellular level and may assist in the development of preventative and therapeutic measures against FA toxicity. It also suggests that exposure to FA may lead to the onset of human diseases via epigenetic changes/modifications. This is particularly relevant in under privileged communities where the food supply and storage conditions are inadequate.

## CHAPTER 1

### INTRODUCTION

The contamination of foods and feeds with pathogenic fungi and mycotoxins is a global problem that threatens food security. Every year, approximately 25% of the global food and feed output is contaminated by mycotoxins (Smith et al., 2016); and the exposure to mycotoxin-contaminated commodities has been linked with adverse effects in humans and animals (Zain, 2011).

Fusaric acid (FA; 5-butyl picolinic acid) is a secondary metabolite and mycotoxin produced by several *Fusarium* species that parasitize agricultural foods consumed by humans and animals (Bacon et al., 1996). Previously, approximately 643µg/kg (Streit et al., 2013) and 18µg/kg (Chen et al., 2017b) FA were found to contaminate animal feeds and commercial foods, respectively. Many of these foods are a staple in human and animal diets and the regular consumption of FA-contaminated commodities may have serious health implications. Currently, a maximum dietary safety limit for FA has not been established; and humans and animals are continuously exposed to both low and extremely high concentrations of FA.

FA was initially patented for its use in treating drug addiction and alleviating the cravings for and withdrawal from narcotics and amphetamines in humans (Pozuelo, 1978). It was also patented for its antiviral and anti-proliferative effects and used in creams for the treatment of warts, psoriasis, and skin cancer (Fernandez-Pol, 1998). Later it was determined that FA was in fact toxic; however, the molecular mechanisms underlying its toxicity were unknown.

FA is a lipophilic toxin that traverses cellular membranes and affects multiple biochemical pathways exerting low to moderate toxicity in both plants (Singh et al., 2017, D'Alton and Etherton, 1984, Diniz and Oliveira, 2009, Pavlovkin et al., 2004) and animals (Diringer et al., 1982, Hidaka et al., 1969, Reddy et al., 1996, Yin et al., 2015). In plants, FA-induced phytotoxicity has been attributed to alterations in plant physiology and cellular function, ultimately leading to wilt disease symptoms and death of the plant (Singh et al., 2017, D'Alton and Etherton, 1984, Pavlovkin et al., 2004).

FA is a divalent metal chelator that has been implicated as a possible etiological agent in hypotension (Hidaka et al., 1969, Toshiharu et al., 1970, Terasawa and Kameyama, 1971), notochord malformation (Yin et al., 2015), and delayed growth in animals (Reddy et al., 1996). It also acts synergistically with other food-borne mycotoxins such as fumonisin B<sub>1</sub> (FB<sub>1</sub>) (Bacon

et al., 1995), deoxynivalenol (DON) (Smith et al., 1997) and 4,15-diacetoxyscirpenol (DAS) (Fairchild et al., 2005), thereby, mediating toxicity in various animal models.

Studies evaluating the toxicity of FA in humans are limited. Recently, *in vitro* studies on several human cell lines indicated that FA is toxic by inducing oxidative stress (Abdul et al., 2016, Devnarain et al., 2017, Dhani et al., 2017), mitochondrial dysfunction (Abdul et al., 2016), DNA damage (Ghazi et al., 2017, Mamur et al., 2018), and apoptosis (Abdul et al., 2016, Devnarain et al., 2017, Dhani et al., 2017, Ghazi et al., 2017, Ogata et al., 2001).

Despite studies evaluating the toxic effects of FA, there are currently no studies on the effects of FA-induced epigenetic changes both *in vitro* and *in vivo*. Our preliminary work on FA in human liver (HepG2) cells indicated that FA induced genotoxic effects (Addendum A) (Ghazi et al., 2017); and it was this study that prompted further investigation of FA-induced epigenetic changes in the liver. The elucidation of cellular epigenetic mechanisms can lead to a better understanding of FA toxicity as well as assist in the development of preventative and therapeutic measures against FA exposure and toxicity. This will be beneficial in underprivileged communities where the food supply and storage methods are inadequate.

Epigenetic mechanisms influence gene expression in response to environmental stimuli and are essential in regulating various cell signaling pathways. DNA methylation, promoter methylation, histone modifications, N<sup>6</sup>-methyladenosine (m<sup>6</sup>A) RNA methylation, and variations in microRNA (miRNA) expression are common epigenetic modifications that may provide alternative mechanisms of FA-induced toxicity (Handy et al., 2011, Moore et al., 2009, Moarii et al., 2015).

Promoter methylation, methylation of CpG islands within the promoter region of genes, regulates gene transcription by controlling the accessibility of transcription factors to the gene promoter region. Promoter hypermethylation masks gene promoter regions, prevents binding of transcription factors, and inhibits gene transcription whereas promoter hypomethylation activates gene transcription (Moarii et al., 2015).

DNA methylation occurs on the 5<sup>th</sup> position of cytosine in CpG islands and is regulated by DNA methyltransferases (DNMTs; DNMT1, DNMT3A, and DNMT3B) and demethylases (MBD2) (Lin and Wang, 2014). The expression of DNMTs and MBD2 is regulated at the transcriptional level by promoter methylation (Novakovic et al., 2010, Naghitorabi et al., 2013) and at the post-transcriptional level by miRNAs such as miR-29b (Garzon et al., 2009, Fabbri et al., 2007). MiR-29b negatively regulates DNA methylation by targeting *DNMT1*, *DNMT3A*, and *DNMT3B* (Garzon et al., 2009, Fabbri et al., 2007). The activity and stability of DNMTs are also regulated

by post-translational modifications. Post-translational modifications such as ubiquitination are mediated by the E3 ligase, ubiquitin-like and ring finger domain 1 (UHRF1) and the deubiquitylating enzyme, ubiquitin specific peptidase 7 (USP7), and mark DNMTs for proteasomal degradation (Lin and Wang, 2014, Scott et al., 2014, Denis et al., 2011).

A complex relationship exists between DNA methylation and histone modifications. DNA methylation is a pre-requisite for histone methylation and changes in global DNA methylation regulate histone modifications by recruiting histone modifying enzymes. Histone methylation can also control DNA methylation by recruiting DNMTs (Rose and Klose, 2014, Jin et al., 2011). The dynamic relationship between DNA methylation and histone methylation plays a crucial role in maintaining genome integrity, gene transcription, and cell death (Rose and Klose, 2014, Espada et al., 2004, Estève et al., 2006).

Histone 3 lysine (K) 9 trimethylation (H3K9me3) is mediated by the histone methyltransferase, suppressor of variegation 3-9 homolog 1 (SUV39H1) and is associated with a closed tightly compacted and repressed chromatin structure (Bosch-Presegué et al., 2011). SUV39H1-mediated H3K9me3 is crucial for regulating genome integrity (Peters et al., 2001), cell division (Melcher et al., 2000), cell viability (Reimann et al., 2010), and apoptosis (Watson et al., 2014).

Post-translational modifications such as acetylation and ubiquitination regulate SUV39H1 and H3K9me3 (Bosch-Presegué et al., 2011). The acetylation of SUV39H1 decreases SUV39H1 activity and mediates proteasomal degradation by promoting SUV39H1 polyubiquitination (Bosch-Presegué et al., 2011). The histone deacetylase, Sirtuin (Sirt) 1 is a direct target of miR-200a that maintains H3K9me3 by deacetylating SUV39H1 thus increasing its catalytic activity and preventing its proteasomal degradation (Eades et al., 2011, Bosch-Presegué et al., 2011, Vaquero et al., 2007).

Histone methylation can regulate m6A RNA methylation by recruiting m6A methyltransferases; and a decrease in H3K9me3 was associated with a decrease in m6A levels (Wang et al., 2018). Additionally, m6A RNA methylation can influence histone methylation by destabilizing transcripts that encode histone modifying enzymes (Wang et al., 2018, Li et al., 2018, Chen et al., 2019, Lai et al., 2018).

M6A RNA methylation is an epi-transcriptomic mark and one of the most prevalent post-transcriptional modifications of messenger RNA (mRNA) (Fu et al., 2014, Geula et al., 2015). M6A methylation is regulated by the methyltransferases, METTL3, METTL14, and WTAP, and the demethylases, FTO and ALKBH5; and recruits the m6A-dependent readers, YTHDF1, YTHDF2, YTHDF3, YTHDC1, and YTHDC2 to regulate RNA transcripts, splicing, and

protein translation (Geula et al., 2015, Fu et al., 2014, Jia et al., 2011, Xiao et al., 2016). To date, several RNA transcripts have been found to be regulated by m6A methylation (Li et al., 2019, Li et al., 2017a). Additionally, m6A patterns were shown to be dysregulated during cellular stress (Engel et al., 2018), and may play a crucial role in regulating the expression of the tumor suppressor and stress response protein, p53. Studies on m6A and p53 indicate that m6A located within the coding region of p53 leads to the translation of mutant p53 that alters the p53 signaling pathway and contributes to tumor formation and progression (Uddin et al., 2019, Kwok et al., 2017).

The role of epigenetics in mycotoxicology is limited. The liver, due to its detoxification and metabolizing functions as well as its close relationship with the gastrointestinal tract, is highly susceptible to damage by chemical substances and mycotoxins. The HepG2 cell line is a common *in vitro* liver model for evaluating drug/mycotoxin metabolism and hepatotoxicity as it displays similar physiological functions to primary human hepatocytes (Ruoß et al., 2019). It is enriched with cytochrome P450 enzymes that enable toxins to undergo first pass metabolism and are thus susceptible to damage. In addition to its increased metabolic capacity, the HepG2 cell line displays an epigenetic profile that is similar to primary human hepatocytes; and the regulation of epigenetic enzymes such as SUV39H1 in HepG2 cells is most comparable to the expression in primary human hepatocytes (Ruoß et al., 2019). This indicates that HepG2 cells may also be used as a reliable model for determining mycotoxin-induced epigenetic changes. *In vivo* animal models, due to its functional organ systems and absence of diseases, are analogous to humans and are also able to provide a reliable link between epigenetic changes and cellular outcomes (Rosenfeld, 2010). In particular, the inbred C57BL/6 mice model lacks genetic variation and, in response to dietary factors, is capable of exhibiting changes in DNA and histone methylation patterns that can be linked with developmental and cellular abnormalities in the various organs (Rosenfeld, 2010). Previous studies have highlighted key roles for epigenetic mechanisms in mycotoxin-induced adverse health effects in the liver; FB<sub>1</sub> was shown to have carcinogenic potential by altering global DNA methylation (Chaturgoon et al., 2014a), promoter methylation (Demirel et al., 2015), histone methylation (Chaturgoon et al., 2014a, Sancak and Ozden, 2015), and miRNA expression (Chaturgoon et al., 2014b). Similarly, other *Fusarium* mycotoxins such as zearalenone, DON, and T2-toxin were shown to exert its toxic effects by altering DNA methylation (So et al., 2014, Han et al., 2016) and histone methylation (Han et al., 2016, Zhu et al., 2016, Zhu et al., 2014). This suggests a possible role for epigenetics in FA-mediated hepatotoxicity.

In this study, we hypothesized that FA induced genotoxic and cytotoxic effects *in vitro* and *in vivo* via alterations in epigenetic mechanisms. This hypothesis was tested by measuring changes in global DNA methylation, promoter DNA methylation, H3K9me3, miRNAs (miR-29b and miR-200a), and m6A-mediated regulation of p53 expression; and relating these changes in epigenetic modifications with the genotoxic and cytotoxic effects of FA.

The aim of this study was to determine epigenetic changes of FA-induced hepatotoxicity *in vitro* (HepG2 cells) and *in vivo* (C57BL/6 mice). The specific objectives of the study were to determine the effect of FA on:

1. Global DNA methylation as well as FA-induced changes in DNA methylation by transcriptional (promoter methylation), post-transcriptional (miR-29), and post-translational (ubiquitination) regulation of DNMTs and MBD2 in HepG2 cells.
2. miR-200a, SUV39H1-mediated H3K9me3, genome integrity, and apoptosis in HepG2 cells and C57BL/6 mice livers.
3. p53 expression and its epigenetic regulation at the transcriptional and post-transcriptional level by promoter methylation and m6A RNA methylation in HepG2 cells and C57BL/6 mice livers.

Ethical approval for this study was obtained from the University of Kwazulu-Natal Biomedical Research Ethics Committee (Ethical approval number: BE316/19; Addendum B) for procedures involving the HepG2 cells and from the University of KwaZulu-Natal Animal Research Ethics Committee (Ethical approval number: AREC/079/016; Addendum C) for all procedures involving mice.

## CHAPTER 2

### LITERATURE REVIEW

#### 2.1. Mycotoxins

Mycotoxins are low molecular weight natural compounds produced as secondary metabolites of fungi and toxigenic molds (Bennett and Klich, 2003, Zain, 2011). These toxins are produced in cereal grains and animal feeds before, during, and after harvests, in various environmental conditions (Yiannikouris and Jouany, 2002); and are capable of exerting harmful effects in humans and animals.

There are currently over 300 compounds that have been identified as mycotoxins since 1960 following the outbreak of Turkey X Disease in which 100,000 turkey poultts died as a result of consuming aflatoxin B<sub>1</sub> (AFB<sub>1</sub>; a mycotoxin produced by *Aspergillus flavus*) contaminated peanut meal (Bennett and Klich, 2003, Zain, 2011); the most common mycotoxins of human and agro-economic importance include AFB<sub>1</sub>, FB<sub>1</sub>, ochratoxin A (OTA), DON, T2-toxin, patulin (PAT), and zearalenone (Zain, 2011). These mycotoxins frequently contaminate a wide variety of food sources and have been classified by the Food and Agriculture Organization (FAO) and World Health Organization (WHO) as potent neurotoxins, nephrotoxins, hepatotoxins, immuno-toxins, and carcinogens (Bennett and Klich, 2003, Yiannikouris and Jouany, 2002, Zain, 2011, Omotayo et al., 2019).

The worldwide contamination of foods and feeds with mycotoxins is a significant problem (Zain, 2011). The global prevalence of mycotoxins in foods and feeds has dramatically increased over the past five years due to global warming, pest infestation, and poor harvest and storage practices (Meyer et al., 2019, Omotayo et al., 2019); and each year, an estimated 25% of the world's agricultural food and feed output is contaminated by mycotoxins (Omotayo et al., 2019). This threatens food security and puts humans at a high risk of exposure to mycotoxin-contaminated commodities. Human exposure to mycotoxins can occur via the consumption of contaminated plant-derived foods, from the carry-over of mycotoxins and toxic metabolites in animal products such as milk, meat and eggs, skin-contact with mold-infested substrates, and inhalation of spore-borne toxins (Bennett and Klich, 2003, Yiannikouris and Jouany, 2002, Zain, 2011, Omotayo et al., 2019).

Exposure to mycotoxins can lead to several, often unrecognized, diseases known as mycotoxicoses (Bennett and Klich, 2003). Mycotoxicoses are common in developing countries

and poverty stricken areas where malnutrition is a major concern and where contaminated maize and cereal grains form a staple diet for many people (Omotayo et al., 2019). It also commonly occurs in areas where there are poor methods of food handling and improper storage of foods (Bennett and Klich, 2003, Yiannikouris and Jouany, 2002, Zain, 2011, Omotayo et al., 2019). The severity of mycotoxicoses varies among individuals and is dependent on the type of mycotoxin, dose and length of exposure, routes of exposure as well as the health and sex of the affected individual (Bennett and Klich, 2003, Zain, 2011). Synergistic interactions between the mycotoxin and other mycotoxins or chemicals to which the individual may have been exposed is also a major determinant of toxicity (Yiannikouris and Jouany, 2002). While it often occurs that mycotoxicoses can be treated, chronic toxicity can have irreversible and life-changing effects (Zain, 2011).

Fungi are natural contaminants of food and therefore, the presence of mycotoxins is often unavoidable. Several efforts to minimize mycotoxin contamination and exposure include the application of modern agricultural practices to prevent fungal growth and mycotoxin production, establishing maximum food safety limits for mycotoxins, and removing unsafe contaminated commodities from the food supply by regular government screening (Bennett and Klich, 2003, Yiannikouris and Jouany, 2002, Zain, 2011). Despite this, extensive mycotoxin contamination still continues to occur in foods and feeds around the world.

## **2.2. Fusaric Acid**

Fusaric acid (FA) is a mycotoxin produced by fungi of the genus *Fusarium* that contaminates agricultural foods and feeds (Bacon et al., 1996). These foods are an integral part of the human and animal diet and regular consumption of FA-contaminated commodities may have adverse effects on human and animal health.

To date, only a few studies have measured FA concentration in foods and feeds, although its presence has been detected in various corn and wheat-based foods and feeds worldwide (Placinta et al., 1999). A study conducted on mycotoxins in corn and wheat silages reported that FA had the highest prevalence and concentration (765µg/kg FA) compared to 22 other common mycotoxins (Shimshoni et al., 2013); feed samples were reported to contain an average of 643µg/kg FA (Streit et al., 2013) and approximately 2.5-18µg/kg FA were reported to contaminate commercial foods and feeds (Chen et al., 2017b). It was also found that corn and swine feeds were contaminated with up to 36µg/kg FA (Smith and Sousadias, 1993) and approximately 12.4µg/kg FA was found in livestock and poultry feeds (Voss et al., 1999).

FA is a neglected mycotoxin that is usually not monitored and to date a maximum dietary safety limit has not been determined, this puts humans and animals at a high risk of exposure to FA at both low and extremely high concentrations.

### **2.2.1. Structure of FA**

FA is an aromatic carboxylic acid and picolinic acid derivative that consists of the chemical formula,  $C_{10}H_{13}NO_2$  (ŠroBároVá et al., 2009). The structure of FA is based on the structure of picolinic acid (2-pyridine carboxylic acid) which is an isomer of nicotinic acid that consists of a six membered pyridine ring structure (Figure 2.1A and B) (Grant et al., 2009). The structure of FA resembles picolinic acid in that it contains the pyridine ring structure of picolinic acid as well as an additional fused aromatic ring or 5-butyl side chain (Figure 2.1C). The butyl side chain is responsible for increasing the lipophilicity of FA and enables it to penetrate cell membranes that are mostly composed of lipids (Bochner et al., 1980). The structure of FA also consists of a hydroxyl ( $OH^-$ ) group that acts as a proton donor and is responsible for the acidic properties of FA.

FA is a chelator of divalent cations, and similar to picolinic acid which is a bidentate metal chelating agent (Grant et al., 2009); it is capable of forming conjugates with essential ions such as zinc, iron, copper, and manganese (Li et al., 2013). Mechanistically, this occurs via the N-atom of the pyridine ring of FA which binds with the carboxyl group of the metal to form chelates that prevent these ions from functioning in biological processes (Li et al., 2013).

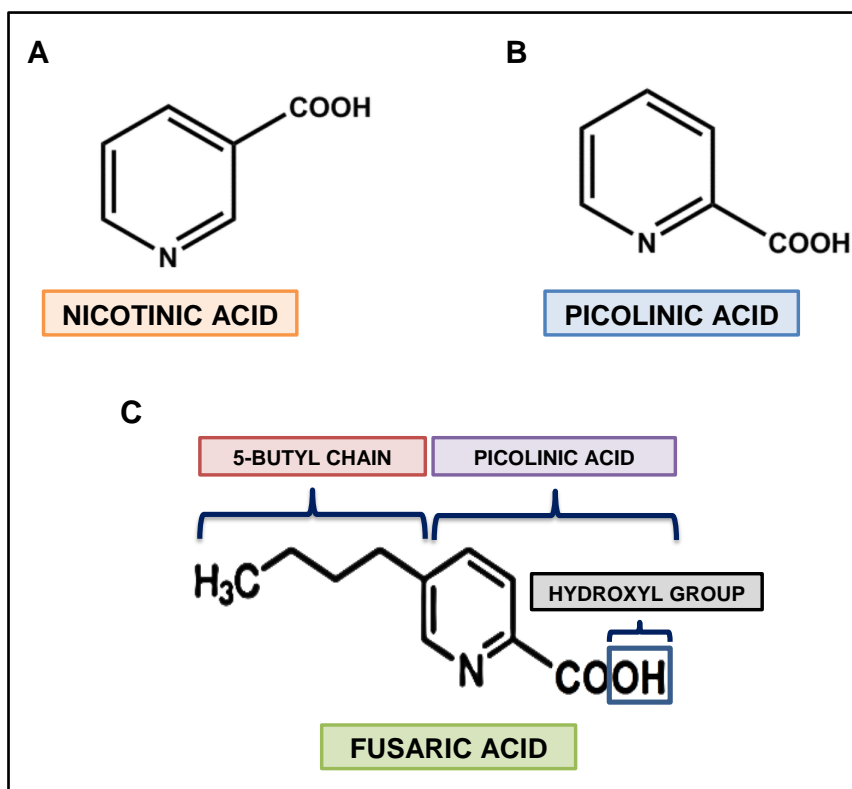


**Figure 2.1** Chemical structure of nicotinic acid (A), picolinic acid (B), and Fusaric acid (C) (May et al., 2000)

### 2.2.2. *Effects of FA*

FA is a non-specific mycotoxin known to have diverse toxicological effects in plants and animals (Singh et al., 2017, D'Alton and Etherton, 1984, Diniz and Oliveira, 2009, Pavlovkin et al., 2004, Diringer et al., 1982, Hidaka et al., 1969, Reddy et al., 1996, Yin et al., 2015); however, studies evaluating the effects of FA on humans and its mechanisms of toxicity are limited. In plants, FA is phytotoxic and has been implicated in the pathogenesis of wilt diseases (Singh et al., 2017, Diniz and Oliveira, 2009, D'Alton and Etherton, 1984, Pavlovkin et al., 2004). Other effects of FA on plants include alterations in membrane permeability (D'Alton and Etherton, 1984, Pavlovkin et al., 2004), increased electrolyte leakage (Pavlovkin et al., 2004, D'Alton and Etherton, 1984, Singh et al., 2017), damage to plant photosynthetic machinery (Singh et al., 2017), and inhibition of respiration (Singh et al., 2017, D'Alton and Etherton, 1984). It also reduces leaf protein content by increasing the activity of proteolytic enzymes and inhibits root and leaf cell function leading to necrotic cell death (Singh et al., 2017).

FA is a cell membrane permeating weak acid ( $pK_a = 5.04$ ) and is therefore, potentially toxic as a proton conductor (Bochner et al., 1980). It alters the mitochondrial membrane potential of

cells and decreases ATP production by inhibiting cytochrome c oxidase and the ATPase/ATP synthase pump (Köhler and Bentrup, 1983, D'Alton and Etherton, 1984, Telles-Pupulin et al., 1996). FA impairs mitochondrial function and biogenesis in HepG2 liver cells; and induces apoptosis by increasing the activity of caspases -8, -9, and -3/7 (Abdul et al., 2016, Devnarain et al., 2017, Ogata et al., 2001, Ghazi et al., 2017). FA also elevates oxidative stress, induces lipid peroxidation, and increases the activity of anti-oxidant enzymes: superoxide dismutase (SOD), catalase (CAT), and ascorbate peroxidase (Abdul et al., 2016, Devnarain et al., 2017, Sapko et al., 2011, Kuźniak, 2001).

FA is immuno-toxic to peripheral blood mononuclear cells (PBMCs) and human monocytic (THP-1) cells by altering the MAPK signaling pathway (Dhani et al., 2017); it increases cytokine production in human cervical carcinoma (Hep-2) cells and docetaxel-resistant Hep-2 cells (Ye et al., 2013). FA also has immuno-suppressive activity in HepG2 cells by inhibiting the activation of the NRLP3 inflammasome, and disrupting the synthesis and maturation of interleukin-1-beta (IL-1 $\beta$ ) (Abdul et al., 2019); however, no effect was observed between FA and the production of interleukin-2 (IL-2) and interleukin-5 (IL-5) in murine thymoma (EL-4) cells (Marin et al., 1996).

FA is a potent chelator of divalent cations and the removal of essential metal ions may serve as a mechanism by which this mycotoxin exerts its effects. FA has anti-proliferative and anti-tumor effects in several human cancer cell lines (Fernandez-Pol et al., 1993); it has anti-tumor activity against head and neck squamous cell carcinoma (HNSCC) by chelating divalent cations from catalytic DNA-associated metalloproteins, thereby, increasing DNA damage and preventing its synthesis and repair (Stack Jr et al., 2004). FA has anti-proliferative effects in WI-38 fibroblasts, and is a potent inhibitor of DNA synthesis in breast cancer (MDA-MB-468) cells and WI-38 fibroblasts (Fernandez-Pol et al., 1993). Additionally, FA was shown to induce DNA damage and decrease HepG2 cell viability by post-translationally modifying the tumor suppressor protein, p53 (Mamur et al., 2018, Ghazi et al., 2017).

FA is toxic to mice (intra-peritoneal LD<sub>50</sub> = 80mg/kg and intravenous LD<sub>50</sub> = 100mg/kg) and death caused by the lethal dose has been attributed to its hypotensive effect (Hidaka et al., 1969, Toshiharu et al., 1970, Terasawa and Kameyama, 1971). FA has hypotensive activity in cats, dogs, rabbits, and rats by inhibiting the copper-dependent enzyme, dopamine-beta-hydroxylase, a key enzyme in the synthesis of the neurotransmitter noradrenaline (Hidaka et al., 1969, Terasawa and Kameyama, 1971, Toshiharu et al., 1970). The FA-induced decrease in noradrenaline was also shown to prevent the formation of gastric ulcers in rats (Osumi et al., 1973).

FA has neurochemical effects in mice (Diringer et al., 1982), rats (Porter et al., 1995), and pigs (Smith and MacDonald, 1991), and reduced aggressive behavior and motor activity (Diringer et al., 1982). FA attenuates isoproterenol-induced heart failure in mice by inactivating the PI3K/AKT and TGF-beta/SMAD signaling pathways, thereby, preventing the development of cardiac hypertrophy and fibrosis (Li et al., 2017b).

FA is toxic to zebrafish by chelating copper and inhibiting the enzyme lysyl oxidase resulting in notochord malformation (Yin et al., 2015) whereas calcium chelation was shown to cause toxicity in mice by affecting blood coagulation (Devaraja et al., 2013), delaying the bone ossification process, and affecting the growth of fetuses (Reddy et al., 1996).

Synergistic interactions between FA and other co-produced *Fusarium* mycotoxins have also been demonstrated. Studies conducted in pigs indicate that FA enhances the toxicity of DON by decreasing feed intake and reducing body weight (Smith et al., 1997); it increases tryptophan uptake and serotonin synthesis by competing with tryptophan for binding to blood albumin and increases the concentration of free tryptophan in the blood (Smith et al., 1997). Exposure to FA also increases vomiting, feed refusal, and brain metabolism in pigs given trichothecenes (Smith and MacDonald, 1991); although no toxic synergistic effects were observed in broiler chicks and young turkey poults fed a combination of FA and T2-toxin (Ogunbo et al., 2007). Synergism between FA and DAS has been demonstrated in insects; FA enhances the toxicity of DAS in insects by increasing mortality from 5% with DAS alone to over 20% with DAS and FA combined (Dowd, 1988). Contrastingly, a recovery in body weight and body weight gains were observed in turkey poults fed a combination of FA and DAS as opposed to a diet with FA and DAS alone (Fairchild et al., 2005). FA also has a toxic synergistic interaction with FB<sub>1</sub> in chicken embryos (Bacon et al., 1995); although no synergistic toxic effects were observed between FA and FB<sub>1</sub> in rats (Voss et al., 1999).

### **2.3. Epigenetics**

The term “epigenetics” was coined in 1942 by Conrad H. Waddington to describe the relationship between genes and the cellular phenotype. Epigenetics refers to inherited modifications that influence gene expression by regulating the structure and function of the genome (Handy et al., 2011). These modifications occur independently of the DNA sequence and play a crucial role in regulating cell signaling pathways that are essential for the normal growth and development of higher organisms (Handy et al., 2011, Moore et al., 2013).

Epigenetic phenomena are mediated by a variety of molecular mechanisms including DNA methylation, promoter DNA methylation, histone modifications, RNA methylation, and microRNAs (miRNAs). Among those, DNA methylation, promoter methylation, and histone modifications are the most studied epigenetic mediators that regulate gene transcription by altering chromatin structure and DNA accessibility (Handy et al., 2011, Moore et al., 2013) whereas RNA methylation and miRNAs function post transcription and directly target RNA transcripts to regulate protein expression (Shi et al., 2019, Winter et al., 2009).

Epigenetic mechanisms can be modified by exogenous influences and as a result can contribute to or be a consequence of environmental alterations of the cells phenotype or patho-phenotype (Handy et al., 2011). The role of epigenetics in various human diseases such as cancer (Gopalakrishnan et al., 2008), cardiovascular disease (Handy et al., 2011), and neurodegenerative disorders (Iraola-Guzmán et al., 2011) are well established; however, studies concerning the association between epigenetics and mycotoxicology are still limited (see section 2.11: The Role of Epigenetics in Mycotoxicology; Page 36-37).

#### **2.4. Structure of Chromatin**

Chromatin is a complex of DNA and histone proteins that form the scaffold for the packaging of the entire genome. The nucleus, approximately 6µm in diameter, consists of nearly 2 meters of DNA packaged into chromatin (Handy et al., 2011, Moore et al., 2013). Nucleosomes are the basic functional units of chromatin and consist of approximately 147 base pairs of negatively charged DNA wrapped around an octamer of positively charged histone proteins, two copies each of H2A, H2B, H3, and H4 (Figure 2.2) (Handy et al., 2011, Moore et al., 2013). Linker histones such as H1 interact with linker DNA situated between nucleosomes and organize nucleosomes and intervening linker DNA into higher order chromatin structures (Handy et al., 2011, Moore et al., 2013).

The structure of chromatin is important in regulating gene expression and can be divided into either a closed tightly compacted and transcriptionally silent, heterochromatin or a relatively open loosely packed and transcriptionally active, euchromatin (Figure 2.2) (Handy et al., 2011, Moore et al., 2013, Pieterman et al., 2014). The structure of chromatin is regulated by post-translational modifications to both DNA and histone tails (Handy et al., 2011).

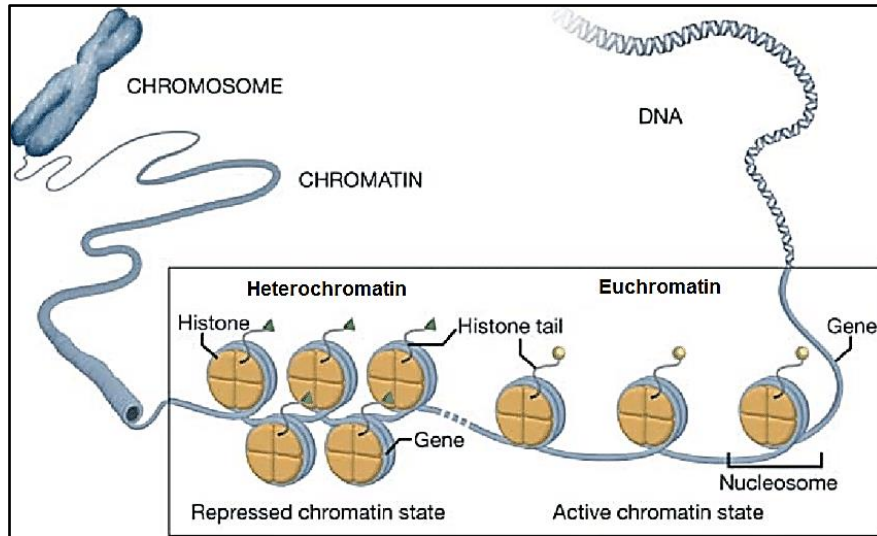


**Figure 2.2** Structure of chromatin (Pieterman et al., 2014)

## 2.5. DNA Methylation

DNA methylation is an important biochemical process that maintains genomic stability and is often associated with a repressed chromatin structure and gene silencing (Handy et al., 2011). DNA methylation plays a major role in the regulation of pluripotency genes, transposon silencing, genomic imprinting, and X-chromosome inactivation (Handy et al., 2011). It controls transcriptional gene silencing during development and differentiation and is involved in creating distinct cell lineages in adult organisms (Handy et al., 2011, Moore et al., 2013).

DNA methylation occurs almost exclusively at CpG dinucleotides where a cytosine nucleotide occurs next to a guanine nucleotide (Hervouet et al., 2018), and nearly 70-80% of CpG dinucleotides are methylated in mammalian DNA (Hervouet et al., 2018). DNA methylation is catalyzed by DNA methyltransferases (DNMTs) that transfer a methyl ( $\text{CH}_3$ ) group from the methyl donor, *s*-adenosyl methionine (SAM) to the fifth carbon of cytosine residues (Figure 2.3) (Moore et al., 2013, Thankam et al., 2019). This process yields 5-methylcytosine which can undergo spontaneous deamination to produce thymine.

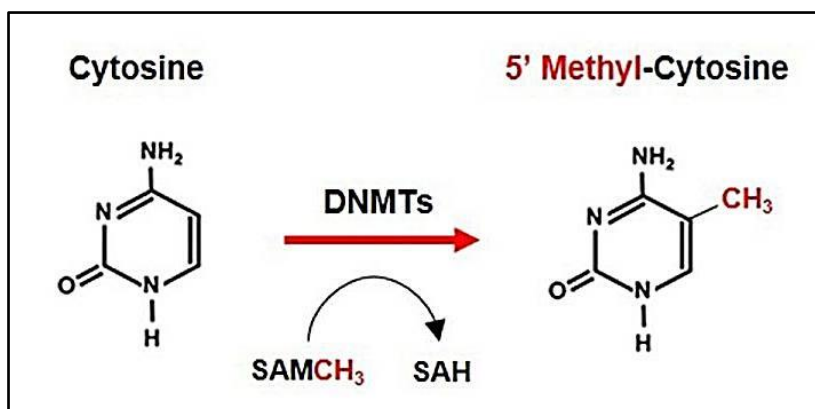


**Figure 2.3** Process of DNA methylation (Miranda-Gonçalves et al., 2018)

The most common DNMTs include DNMT1, DNMT3A, DNMT3B, and DNMT3L. DNMT1 is a maintenance DNMT that functions during DNA replication where it recognizes and binds specifically to hemi-methylated (CpG dinucleotides on only one of the two DNA strands are methylated) DNA and is responsible for conserving the methylation pattern from one generation to the next (Lin and Wang, 2014). Additionally, DNMT1 has the ability to repair DNA methylation patterns (Moore et al., 2013); and knockout of *DNMT1* in mice embryos exhibited a two-thirds loss of DNA methylation, increased apoptosis, and embryonic lethality (Moore et al., 2013).

DNMT3A and DNMT3B are *de novo* DNMTs that establish DNA methylation patterns by targeting unmethylated (CpG dinucleotides on both DNA strands are unmethylated) cytosine bases to initiate methylation (Lin and Wang, 2014). DNMT3A and DNMT3B are functionally active during embryogenesis; and knockout studies in mice indicate that *de novo* DNA methylation is essential for early development and differentiation since *DNMT3A-null* mice die shortly after birth and *DNMT3B-null* mice die *in utero* with multiple developmental defects (Okano et al., 1999). Additionally, *DNMT3A* and *DNMT3B* double knockout mice embryos arrest shortly after gastrulation (Okano et al., 1999), and mouse embryonic fibroblasts deleted of both *DNMT3A* and *DNMT3B* are susceptible to genomic instability and spontaneous immortalization (Dodge et al., 2005).

DNMT3L is a DNMT3-related protein homologous to DNMT3A and DNMT3B that lacks catalytic activity and functions to stimulate the methyltransferase activity of DNMT3A and DNMT3B by increasing their ability to bind to SAM (Moore et al., 2013). DNMT3L is expressed mainly during development and in germ cells where it is required for establishing maternal and paternal genomic imprinting, methylates retrotransposons, and compaction of the X-chromosome (Zamudio et al., 2011). Male *DNMT3L* knockout mice display defects in

spermatogenesis and are unable to produce mature sperm cells (Webster et al., 2005) whereas female *DNMT3L* knockout mice produce methylation-deficient oocytes that result in embryos that die during gestation (Kobayashi et al., 2012).

### 2.5.1. *Structure of DNMTs*

The *DNMT1* gene is located on human chromosome 19 (19p13.2) and encodes a 183 kDa protein upon translation. This protein comprises of 1616 amino acids and is made up of three main regions – an N-terminal regulatory region, a series of lysine-glycine (KG)-repeats, and a C-terminal catalytic region (Figure 2.4) (Hervouet et al., 2018). The N-terminal region includes a DNMT-associated protein 1 (DMAP1) interaction domain, a proliferating cell nuclear antigen (PCNA) binding domain (PBD), a nuclear localization signal (NLS), a replication foci targeting domain (RFTD), a cysteine-rich zinc (CXXC) binding domain, and two bromo-adjacent homology (BAH1 and BAH2) domains (Cheng and Blumenthal, 2008, Hervouet et al., 2018). The DMAP1 domain interacts with the transcriptional repressor, DMAP1 and targets it to replication foci where it maintains DNA methylation patterns during early development (Jeltsch and Jurkowska, 2016). The PBD domain contains the DNA-binding motif and is involved in recruiting DNMT1 to the replication fork during DNA replication (Jeltsch and Jurkowska, 2016). The NLS is responsible for importing DNMT1 into the nucleus (Hervouet et al., 2018), and the RFTD domain targets DNMT1 to replication foci and centromeric chromatin (Jeltsch and Jurkowska, 2016). The CXXC domain follows the RFTD domain and functions by binding to unmethylated CpG dinucleotides (Cheng and Blumenthal, 2008). The BAH1 and BAH2 domains are required for the folding of the DNMT1 protein (Jeltsch and Jurkowska, 2016). The N- and C-terminal regions are linked via a series of KG-repeats that can undergo post-translational modifications to regulate the stability and activity of the DNMT1 protein (Yarychkivska et al., 2018). The C-terminal region consists of the catalytic domain and is essential in mediating the interaction between SAM and DNMT1. It favours the binding of DNMT1 for hemi-methylated CpG dinucleotides and is responsible for the DNMT activity of DNMT1 (Hervouet et al., 2018, Jeltsch and Jurkowska, 2016). DNMT1 also contains an allosteric site that is independent of the catalytic domain and binds to 5-methylcytosine to increase the affinity of DNMT1 for both SAM and DNA (Hervouet et al., 2018).

The *DNMT3A* and *DNMT3B* gene, located on human chromosome 2 (2p23.3) and human chromosome 20 (20q11.2), encodes a 101 and 130 kDa protein upon translation. These proteins comprising of 912 and 853 amino acids for DNMT3A and DNMT3B, respectively, are structurally similar and vary only in the length of their variable regions (Cheng and Blumenthal,

2008). The structure of DNMT3A and DNMT3B is made up of two main regions – an N-terminal region and a C-terminal region (Figure 2.4) (Hervouet et al., 2018). The N-terminal region is further subdivided into a variable region, a proline-tryptophan-tryptophan-proline (PWWP) domain, and a DNMT3L-type zinc finger (ADD) domain (Hervouet et al., 2018, Cheng and Blumenthal, 2008). The PWWP domain non-specifically binds to DNA and is responsible for targeting DNMT3A and DNMT3B to pericentric heterochromatin (Cheng and Blumenthal, 2008). The ADD domain contains six CXXC motifs (Cheng and Blumenthal, 2008) and a DNMT3L-type zinc finger that binds to the regulatory DNMT3L and mediates protein-protein interactions (Hervouet et al., 2018). The C-terminal region contains the catalytic domain which is responsible for the DNMT activity of DNMT3A and DNMT3B (Hervouet et al., 2018).

The structure of DNMT3L (*DNMT3L* gene is located on human chromosome 21 (21q22.3) and encodes a 44 kDa protein) is similar to DNMT3A and DNMT3B; however, it lacks the PWWP domain and the C-terminal catalytic region found in both DNMT3A and DNMT3B (Figure 2.4) (Hervouet et al., 2018, Jeltsch and Jurkowska, 2016).

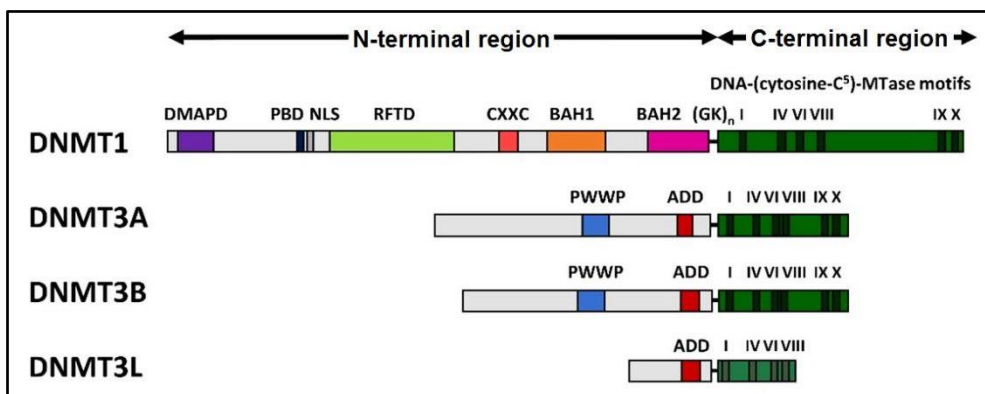


**Figure 2.4** Structure of DNMT proteins (Jeltsch and Jurkowska, 2016)

### 2.5.2. Regulation of DNMTs

DNMTs are the major regulators of DNA methylation and alterations in their expression and activity affects DNA methylation patterns and many cellular functions (Lin and Wang, 2014). Previously, aberrant DNA methylation patterns owing to dysregulated and dysfunctional DNMTs have been implicated in the pathogenesis of several human diseases especially, cancer (Gopalakrishnan et al., 2008). The expression of *DNMT1*, *DNMT3A*, and *DNMT3B* were reportedly elevated in various malignancies including hepatomas, prostate, colorectal, and breast tumors (Girault et al., 2003, Saito et al., 2003, Eads et al., 1999, Patra et al., 2002); and *DNMT1* and *DNMT3B* were elevated in lung cancer (Kim et al., 2006). These changes in *DNMT*

expression as well as the methylation pattern were correlated with a poor prognosis in the affected patients (Kim et al., 2006).

Numerous studies have aimed to elucidate the mechanisms of DNMT regulation *in vitro* and *in vivo*, and it was determined that the DNMTs are regulated at the transcriptional level by promoter methylation and at the protein level by post-translational modifications (Scott et al., 2014, Lin and Wang, 2014, Denis et al., 2011, Peng et al., 2011).

### 2.5.2.1. Regulation of DNMTs via Promoter Methylation

Promoter methylation refers to the methylation of CpG dinucleotides within the promoter region of target genes (Moore et al., 2013, Moarii et al., 2015). Promoter methylation plays a crucial role in regulating gene transcription by either promoting or preventing the binding of transcription factors to gene promoter regions (Moarii et al., 2015). Promoter hypermethylation prevents transcription factors from binding to gene promoters and as a result inhibits gene transcription (Moarii et al., 2015) whereas promoter hypomethylation enables transcription factors to bind to gene promoters and activate its transcription (Figure 2.5) (Moore et al., 2013).

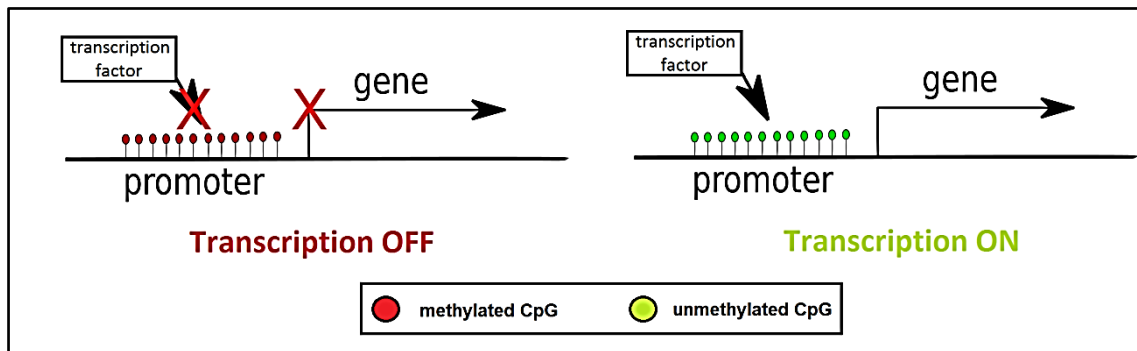


**Figure 2.5** Regulation of gene expression via promoter methylation (Dabrowski and Wojtas, 2019)

Studies conducted on the regulation of DNMTs at the transcriptional level indicate that promoter methylation plays an important role in controlling *DNMT* transcript levels (Naghitorabi et al., 2013, Novakovic et al., 2010). Promoter hypermethylation of *DNMT1* was associated with a decrease in *DNMT1* expression in both cancerous (Rajendran et al., 2011) and non-cancerous (Novakovic et al., 2010) cells. Similarly, promoter hypomethylation of *DNMT3A* and *DNMT3B* was accompanied with an increased expression of *DNMT3A* and *DNMT3B* in embryonic tissues (Novakovic et al., 2010), glioma tumors (Rajendran et al., 2011), and breast cancer cells (Naghitorabi et al., 2013). The silencing of genes by aberrant promoter methylation is a major initiating event in various human diseases, especially cancer where the silencing of

tumor suppressor genes by changes in promoter methylation is required for both the onset and progression of cancer (Gopalakrishnan et al., 2008, Naghitorabi et al., 2013, Rajendran et al., 2011).

#### *2.5.2.2. Regulation of DNMTs via Post-Translational Modifications: Acetylation and Ubiquitination*

DNMTs are synthesized in the cytoplasm and imported into the nucleus where they perform their enzymatic functions; thereafter, they are exported out of the nucleus to the cytoplasm where they are degraded by the proteasome (Scott et al., 2014). The DNMTs are subject to a variety of post-translational modifications that regulate its cellular localization, catalytic activity, stability, and protein-protein interactions (Lin and Wang, 2014). These modifications occur in the N- and C-terminal regions of the protein and include acetylation and ubiquitination, (Lin and Wang, 2014).

The acetylation-mediated ubiquitination of DNMTs plays a major role in inhibiting DNMT activity and stability as well as promoting its proteasomal degradation (Jeltsch and Jurkowska, 2016, Lin and Wang, 2014, Scott et al., 2014, Denis et al., 2011). The acetyltransferase, Tip60 promotes the acetylation of DNMTs which triggers ubiquitination by the E3 ligase, ubiquitin-like and ring finger domain 1 (UHRF1); thereby, targeting the DNMTs for proteasomal degradation (Jeltsch and Jurkowska, 2016, Lin and Wang, 2014, Scott et al., 2014, Denis et al., 2011). Conversely, the deacetylases, HDAC1 and HDAC2, and the deubiquitylating enzyme, ubiquitin specific peptidase 7 (USP7) protect the DNMTs from degradation via deacetylation and deubiquitination, respectively (Lin and Wang, 2014).

The role of acetylation and ubiquitination on the regulation of DNMT1 is well understood. Previously, the acetylation of DNMT1 on lysine (K) residues (K1111, K1113, K1115, and K1117) in the KG-repeat was shown to increase the transcriptional repressor activity of DNMT1 (Lin and Wang, 2014, Jeltsch and Jurkowska, 2016, Peng et al., 2011) and promote the ubiquitination and degradation of DNMT1 by increasing the DNMT1-UHRF1 interaction and impairing the DNMT1-USP7 interaction (Figure 2.6) (Cheng et al., 2015). Additionally, HDAC1-mediated deacetylation of DNMT1 in the KG-repeat restores the DNMT1-USP7 interaction and increases the stability of DNMT1 by preventing its ubiquitination and proteosomal degradation (Cheng et al., 2015, Jeltsch and Jurkowska, 2016). Deacetylation of DNMT1 at K1111, K1113, K1115, and K1117 in the KG-repeat also reduces its transcriptional repressor activity; however, no effect was observed on the methyltransferase activity of DNMT1 (Peng et al., 2011).

The acetylation of DNMT1 on K1349 and K1415 in the catalytic domain decreases DNMT1 activity and the deacetylase, Sirtuin (Sirt) 1 was shown to physically interact with DNMT1 both *in vitro* and *in vivo* (Peng et al., 2011). Deacetylation of DNMT1 at K1349 and K1415 by Sirt1 increases the methyltransferase activity of DNMT1 (Figure 2.6) (Peng et al., 2011).

DNMT1 is also acetylated in the N-terminal region containing the NLS and RFTD domain on K160, K188, K259, and K266 and in the BAH1 and BAH2 domains on K749, K861, K957, K961, and K975 affecting DNMT1 localization and protein-protein interactions (Peng et al., 2011).

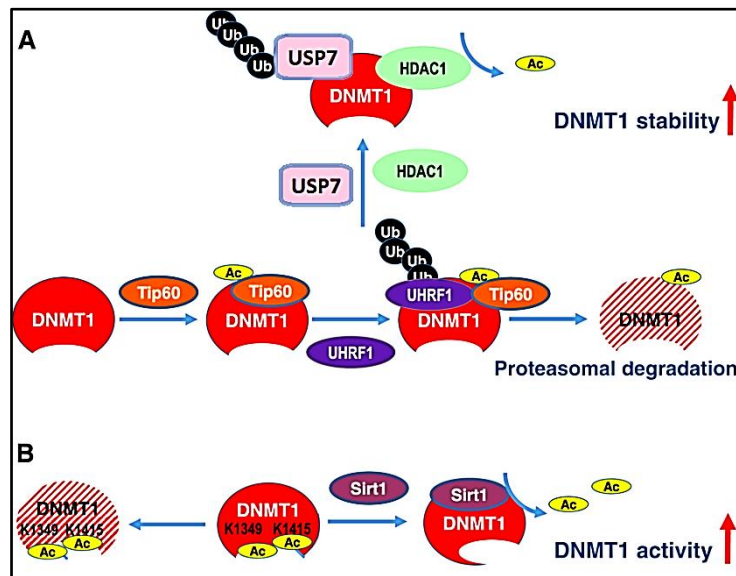


**Figure 2.6** Regulation of DNMT1 by acetylation and ubiquitination. (A) Tip60 acetylates DNMT1 promoting UHRF1-mediated ubiquitination and proteasomal degradation. (B) Sirt1 deacetylates DNMT1 preventing its proteasomal degradation and increasing its DNMT activity (Lin and Wang, 2014)

Studies determining the role of acetylation and ubiquitination on the regulation of DNMT3A and DNMT3B are limited. Previously, UHRF1 was shown to physically interact with both DNMT3A and DNMT3B leading to a reduction in its catalytic activity as well as its ubiquitination and proteasomal degradation (Jia et al., 2016). Additionally, UHRF2 was also shown to inhibit DNA methylation in a DNMT3A and/or DNMT3B-dependent manner by negatively regulating the protein expression of DNMT3A and DNMT3B (Jia et al., 2016). UHRF2 enhances the ubiquitination and proteasomal degradation of both DNMT3A and DNMT3B as determined via knockout studies in various cancer cell lines (Jia et al., 2016).

## 2.6. Methyl-CpG Binding Proteins

DNA methylation forms a platform for several methyl binding proteins (Du et al., 2015). Methyl-CpG binding domain (MBD) proteins are a family of nuclear proteins that have a high affinity for 5-methylcytosine and regulate DNA methylation and gene transcription by recruiting chromatin remodelling complexes to regions of methylated DNA (Du et al., 2015, Jeltsch and Jurkowska, 2016).

MBD proteins, comprising of MBD1 to MBD6, play a crucial role in mammalian development where they regulate cell proliferation, genome integrity, embryonic stem cell pluripotency, cell differentiation, and neurogenesis (Du et al., 2015, Detich et al., 2002, Liu et al., 2010). The structure of all MBD proteins consist of the highly conserved MBD that binds single symmetrically methylated CpG dinucleotides as well as additional domains such as the CXXC domain of MBD1 that enables MBD1 to maintain heterochromatin structure/transcriptional repression by binding to both methylated and unmethylated DNA (Figure 2.7) (Du et al., 2015). The transcriptional repression domain (TRD) found in MBD1 and MBD2 as well as the coiled coil (CC) domain found in MBD2 and MBD3 mediate protein-protein interactions and are responsible for recruiting chromatin repressor proteins (Figure 2.7) (Du et al., 2015). MBD2 also contains an N-terminal glycine-arginine (GR) rich domain that undergoes post-translational modifications (Figure 2.7); and although MBD2 shares the highest amino acid sequence similarity with MBD3, MBD3 lacks the GR-rich domain and is unable to bind to methylated DNA due to a tyrosine to phenylalanine substitution in the MBD domain (Figure 2.7) (Hendrich et al., 2001, Du et al., 2015). MBD4, due to the presence of a C-terminal glycosylase domain (Figure 2.7), plays an important role in repairing mismatched DNA (Hendrich et al., 1999). MBD5 and MBD6 consist of a proline-rich domain and PWWP domain that binds methylated histones and regulates heterochromatin (Figure 2.7) (Du et al., 2015).

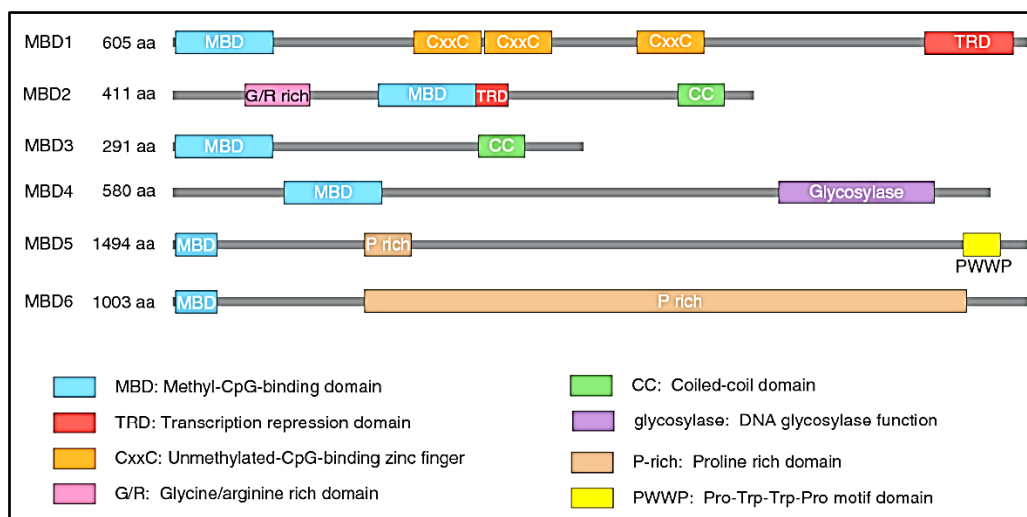


**Figure 2.7** Structure of MBD1 to MBD6 (Du et al., 2015)

### 2.6.1. *MBD2*

*MBD2* is the major MBD protein that binds to methylated DNA and functions as both a methylation-dependent transcriptional repressor and DNA demethylase (Detich et al., 2002). Studies conducted on *MBD2* knockout mice indicate that *MBD2* is dispensible for embryonic development but is required for maternal behaviour and neurogenesis (Hendrich et al., 2001). Deletion of *MBD2* inhibits cell proliferation *in vitro* (Cheng et al., 2018); however, overexpression of *MBD2* contributes to tumourigenesis by causing DNA hypomethylation and genome instability, and silencing methylated tumour suppressor genes such as *p16* and *p14* (Magdinier and Wolffe, 2001). *MBD2* is also involved in the activation of pro-metastatic genes (Cheishvili et al., 2014).

### 2.6.2. *Regulation of MBD2 via Promoter Methylation*

Similar to the DNMTs, *MBD2* is regulated at the transcriptional level by promoter methylation. Hypomethylation of the *MBD2* gene promoter activates *MBD2* transcription leading to increased *MBD2* expression and DNA hypomethylation (a hallmark of cancer) in cancerous liver tissue (Liu et al., 2016). Additionally, hypermethylation of the *MBD2* promoter was associated with an inhibition in *MBD2* expression (Cheishvili et al., 2014). Dysregulations in *MBD2* promoter methylation has been observed in neurological disorders (Liu et al., 2010), cancer (Liu et al., 2016), defective embryonic development and differentiation (Du et al., 2015, Detich et al., 2002).

## **2.7. Histone Modifications**

A loss in DNA methylation is associated with a loss in genome integrity which leads to irreparable DNA damage and mutations (Hervouet et al., 2018, Moore et al., 2013). In eukaryotes, DNA interacts with histone proteins that help package it into higher order chromatin structures and thus the orientation and structure of histone proteins and chromatin are important in regulating genome integrity. Post-translational modifications that occur on the N- and C-terminal histone tails alter chromatin structure and influence the orientation in which DNA is packaged as well as its transcriptional activity (Moore et al., 2013).

The most common post-translational modifications of histones include acetylation and methylation. Acetylation occurs on the K residues of histone tails and facilitates decondensation of chromatin by neutralizing the positive charge of histones and loosening the interaction between DNA and histone proteins (Moore et al., 2013, Thankam et al., 2019). This modification exposes genes making them accessible to transcription factors and enhances gene transcription (Moore et al., 2013, Thankam et al., 2019). Conversely, histone deacetylation reinforces the positive charge of histones and tightens the interaction between DNA and histone proteins producing a condensed chromatin structure that represses gene transcription (Moore et al., 2013, Thankam et al., 2019).

Histone methylation occurs on both arginine (R) and K residues and can have different effects on gene expression depending on the R or K residue being methylated as well as the degree of methylation (Moore et al., 2013, Thankam et al., 2019). The methylation of K residues are best characterized; K residues can be mono-, di-, or tri- methylated providing functional diversity to each site of methylation (Moore et al., 2013, Thankam et al., 2019). Several methylation sites have been identified for H3 (K4, K9, K27, K36, and K79) and H4 (K20). Methylation of H3K4, H3K36, and H3K79 is often associated with active genes whereas methylation of H3K9, H3K27, and H4K20 is associated with inactive genes (Morales et al., 2017).

In this study, the interest is focused on histone 3 lysine 9 trimethylation (H3K9me<sub>3</sub>) due to its distinct role in maintaining heterochromatin structure and genome stability as well as its possible susceptibility to alteration by genotoxic agents.

### **2.7.1 H3K9me<sub>3</sub>**

H3K9me<sub>3</sub> is regulated by the histone methyltransferase, suppressor of variegation 3-9 homolog 1 (SUV39H1) and the lysine demethylase 4B (KDM4B). KDM4B specifically demethylates H3K9me<sub>3</sub> by catalyzing the removal of H3K9 di- and tri- methyl marks and converts H3K9me<sub>3</sub>

to its mono-methylated state (H3K9me1), which then forms a substrate for trimethylation by SUV39H1 (Zheng et al., 2014). H3K9 is mono-methylated by the histone methyltransferase, G9a (also known as EHMT2, euchromatic histone-lysine N-methyltransferase 2).

H3K9me3 is a functionally important histone mark associated with transcriptional inactivation and gene silencing (Bosch-Presegué et al., 2011, Vaquero et al., 2007). Previously SUV39H1-mediated H3K9me3 was shown to play a crucial role in maintaining genome stability (Peters et al., 2001), heterochromatin organization (Vaquero et al., 2007), chromosome segregation (Park et al., 2011), and mitosis (Melcher et al., 2000). H3K9me3 is essential in determining cell fates during development and differentiation (Nicetto et al., 2019); and it is involved in telomere maintenance and aging (García-Cao et al., 2004).

The inactivation of SUV39H1 and H3K9me3 causes ectopic expression of cell-inappropriate genes leading to various human pathologies (Nicetto et al., 2019). Dysregulation of H3K9me3 has been associated with diseases marked by oxidative stress and inflammation (Chen et al., 2017a), and H3K9me3-mediated loss in heterochromatin and genome instability has been shown to be a hallmark in the onset of cancer (Dong et al., 2013).

Defects in heterochromatin are most evident in *SUV39H1* and *SUV39H2* double knockout mice which lose H3K9me3 and display a significant reduction in embryonic viability, small stature, chromosome instability, and increased susceptibility to tumors (Peters et al., 2001). Evidence from transgenic mice also reveals that a loss or overexpression of *SUV39H1* and *SUV39H2* is associated with severe defects in growth and development due to alterations in cell cycle (Chiba et al., 2015), and apoptosis (Watson et al., 2014).

### **2.7.2 Structure of *SUV39H1***

The *SUV39H1* gene is located on human chromosome X (Xp11.23) and encodes a 48 kDa protein that comprises of an N-terminal chromo-domain and a C-terminal SET domain (Figure 2.8) (Wang et al., 2012, Firestein et al., 2000). The chromo-domain consists of a highly conserved motif that functions to target SUV39H1 to chromosomal loci and is involved in DNA, RNA, and histone binding (Wang et al., 2012). The SET domain together with the adjacent cysteine-rich domain is responsible for the catalytic histone methyltransferase activity of SUV39H1 (Wang et al., 2012).

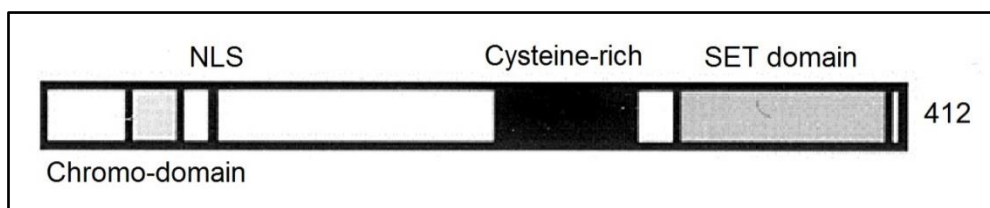


**Figure 2.8** Structure of SUV39H1 (Firestein et al., 2000)

### 2.7.3 *Post-Translational Regulation of SUV39H1: Acetylation and Ubiquitination*

The regulation of SUV39H1 expression and activity is critical for maintaining heterochromatin and genome stability (Bosch-Presegué et al., 2011). The acetylation-mediated ubiquitination of SUV39H1 controls the activity, stability, and cellular localization of SUV39H1 (Bosch-Presegué et al., 2011, Vaquero et al., 2007). The acetylation of SUV39H1 on K266 in the catalytic SET domain is mediated by the acetyltransferase, CREB-binding protein (CBP)/p300, and decreases SUV39H1 activity (Bosch-Presegué et al., 2011). The acetylation of SUV39H1 on K266 also enables the E3 ubiquitin ligase, murine double minute 2 (MDM2) to polyubiquitinate SUV39H1 on K87, thereby, targeting it for proteasomal degradation (Bosch-Presegué et al., 2011).

Sirt1 is a class III NAD<sup>+</sup>-dependent lysine deacetylase closely related to the yeast counterpart, *Sir2* (silencing information regulator 2). Sirt1 is one of four chromatin-associated sirtuins (Sirt1, Sirt2, Sirt3, and Sirt6) that is predominantly localized in the nucleus where it regulates chromatin structure by catalyzing the deacetylation of acetyl-lysine residues of histones (H3K9, H3K4, and H4K16) and non-histone proteins in a reaction that cleaves NAD<sup>+</sup> and generates O-acetyl ADP-ribose (Vaquero et al., 2007). RNA-mediated silencing of *Sirt1* expression in human liver cells led to hyper-acetylation of H3K9 and H4K16, and a reduction in H3K9me3 (Zhang et al., 2014).

Previously, co-immunoprecipitation studies have shown that Sirt1 interacts with SUV39H1 *in vitro* and this interaction between Sirt1 and SUV39H1 is essential in regulating SUV39H1 activity and expression as well as maintaining H3K9me3 (Vaquero et al., 2007, Bosch-Presegué et al., 2011). Sirt1 interacts with the chromo-domain of SUV39H1 and deacetylates SUV39H1 on K266, thereby, enhancing the catalytic activity of SUV39H1 and facilitating heterochromatin formation (Vaquero et al., 2007, Bosch-Presegué et al., 2011). Interestingly, other chromatin-associated Sirtuins such as Sirt2, Sirt3, and Sirt6 failed to co-localize with SUV39H1 and suggested that SUV39H1-mediated deacetylation is Sirt1-dependent (Bosch-Presegué et al.,

2011). No interaction was observed between Sirt1 and the H3K9 mono-methyltransferase, G9a *in vitro* and *in vivo* (Bosch-Presegué et al., 2011).

Sirt1 also regulates SUV39H1 protein expression by inhibiting polyubiquitination of K87 in the SUV39H1 chromo-domain, preventing its proteasomal degradation and increasing its half-life by nearly four times (Bosch-Presegué et al., 2011). This was also observed in cervical cancer (HELA) cells where an increase in Sirt1 expression was positively correlated with an increase in SUV39H1 protein levels (Bosch-Presegué et al., 2011). Sirt1 also deacetylates H3K9Ac and recruits SUV39H1 promoting H3K9me3 and heterochromatin formation (Bosch-Presegué et al., 2011).

#### **2.7.4 *The Relationship between DNA Methylation and H3K9me3***

A complex interplay exists between DNA methylation and H3K9me3 (Fuks et al., 2003). DNA methylation forms a scaffold for MBD proteins to recruit SUV39H1 and maintain H3K9me3 *in vivo* (Fuks et al., 2003). DNMTs directly interact with enzymes that regulate H3K9me3, and both DNMT1 and DNMT3A are known to bind to SUV39H1 and mediate H3K9me3 (Fuks et al., 2003). DNMT1 and DNMT3B can also bind to histone deacetylases that remove acetyl residues from H3K9Ac enabling SUV39H1 to mediate H3K9me3 (Fuks et al., 2003). Furthermore, H3K9me3 can recruit DNMT3A and DNMT3B to unmethylated CpG dinucleotides in order to initiate methylation (Cedar and Bergman, 2009). This occurs via DNMT3L which binds to H3K9me3 and recruits DNMT3A and DNMT3B to methylate DNA (Ooi et al., 2007). A loss in DNA methylation and H3K9me3 is associated with a loss in heterochromatin and genome stability (Rose and Klose, 2014, Espada et al., 2004, Estève et al., 2006).

#### **2.7.5 *H2Ax***

Histone modifications are also central regulators of the DNA damage response. The phosphorylation of histone H2Ax on serine 139 (p-S139-H2Ax) is an early response to DNA double-strand breaks that is essential in mediating cell cycle arrest and initiating DNA repair pathways (Podhorecka et al., 2010). During DNA damage several protein kinases such as ataxia telangiectasia mutated (ATM), DNA-dependent protein kinase (DNA-PK), and ATM and RAD3-related protein (ATR) are triggered (Podhorecka et al., 2010). These protein kinases rapidly phosphorylate H2Ax on serine 139 causing a conformational change in the DNA-H2Ax complex that enables DNA repair proteins such as poly (ADP-ribose) polymerase 1 (PARP1) to be recruited to sites of DNA double-strand breaks and initiate DNA repair (Podhorecka et al.,

2010). Previously, mouse embryonic stem cells deficient in *H2Ax* showed an increase in chromosomal aberrations and an inefficiency of DNA repair (Celeste et al., 2003, Bassing et al., 2002). It was also found that *H2Ax* knockout cells have impaired recruitment of DNA repair proteins that are consistent with genome instability (Bassing et al., 2002).

## **2.8. Apoptosis**

Irreparable DNA damage is a major initiating event of apoptosis. Apoptosis, also referred to as programmed cell death, is a physiological process that is responsible for the removal of cells in normal tissues as well as in some pathological states (Kerr et al., 1972). It is a sequential process involving cell shrinkage, chromatin condensation, DNA fragmentation, membrane blebbing, and the formation of apoptotic bodies (Hengartner, 2000, Kerr et al., 1994). The apoptotic bodies are phagocytosed and digested by nearby resident cells such as phagocytes and macrophages, preventing the spillage of intracellular contents and avoiding an inflammatory response (Kerr et al., 1994). Apoptotic bodies not subjected to phagocytosis are released into the adjacent lumen where they exhibit progressive dilation and degradation of cytoplasmic organelles in a process known as necrosis. Necrosis differs from apoptosis in which the cell swells and the plasma membrane ruptures releasing cytosolic contents into the extracellular space where they produce an inflammatory response (Kerr et al., 1994).

Apoptosis has an indispensable role in both physiological and pathological conditions and anomalies in the apoptotic pathway are associated with various pathological conditions such as developmental defects, autoimmune diseases, and cancer with some diseases pertaining to excessive apoptosis or its absence thereof (Kerr et al., 1994).

### **2.8.1. Caspases**

Caspases, also referred to as death proteases, are a family of cysteine aspartate proteases responsible for the initiation and execution of apoptosis (Hengartner, 2000). Caspases consist of an active site cysteine and are able to cleave proteins at aspartic acid residues (Hengartner, 2000). To control the apoptotic process, caspases are initially synthesized as inactive zymogens that consist of three domains, an N-terminal pro-domain, a p20 domain, and a p10 domain. Proteolytic cleavage of these zymogens between the pro-domain and p20 domain as well as between the p20 domain and p10 domain leads to the activation of caspases (Hengartner, 2000). Caspases act by activating or inactivating apoptotic regulatory proteins and are responsible for majority of the morphological changes observed during apoptosis (Hengartner, 2000).

Initiator caspases such as caspase -2, -8, and -9 are the apical caspases in apoptosis and their cleavage and activation is required for the cleavage and activation of the downstream executioner caspases -3, -6, and -7. The activation of the executioner caspases is usually irreversible and ensures that apoptosis occurs (Hengartner, 2000).

### **2.8.2. Pathways of Apoptosis**

Apoptosis is initiated by a variety of physiological death signals as well as pathological cellular insults (Hengartner, 2000). It is an energy-dependent process that occurs via several pathways of which the two main pathways involve caspase activation and are referred to as the intrinsic and extrinsic apoptotic pathways.

#### **2.8.2.1. The Intrinsic Apoptotic Pathway**

In the intrinsic apoptotic pathway, a death signal such as irreparable DNA damage or oxidative stress causes the pro-apoptotic molecule, BAX to translocate from the cytosol to the mitochondria where it undergoes a conformational change allowing it to act as an integral membrane protein (Elmore, 2007). BAX then interacts with members of the mitochondrial permeability transition pore (MPTP; adenine nucleotide translocator (ANT), voltage-dependent anion channel (VDAC), and peripheral benzodiazepine receptor (PBR)) resulting in the opening of the MPTP and release of cytochrome c and apoptosis inducing factor (AIF) from the mitochondria (Elmore, 2007). The cytochrome c binds with the apoptotic protease activating factor-1 (Apaf-1), pro-caspase-9, and ATP to form an apoptosome which cleaves and activates caspase-9, consequently activating caspases-3/7 resulting in apoptotic cell death (Figure 2.9) (Elmore, 2007).

The anti-apoptotic molecule, BCL-2 maintains the integrity of the mitochondrial membrane by inhibiting cellular free radical formation, cytochrome c release, and caspase activation; thereby, preventing apoptosis (Elmore, 2007). Following apoptotic stimuli, the BH3-domain-only molecule, BIM translocates to the mitochondria where it interacts with BCL-2 to antagonize its anti-apoptotic activity and promote apoptosis (Elmore, 2007).

#### **2.8.2.2. The Extrinsic Apoptotic Pathway**

In the extrinsic apoptotic pathway, death ligands such as tumor necrosis factor alpha (TNF- $\alpha$ ), tumor necrosis factor related apoptosis inducing ligand (TRAIL) and Fas ligand (FasL) bind to death receptors on the cell's surface, type 1 TNF receptor (TNFR1), death receptor 4/5 (DR4/5), and Fas receptor (FasR), respectively (Elmore, 2007). These death receptors have an

intracellular death domain that recruits adaptor proteins such as TNFR-associated death domain (TRADD) and Fas-associated death domain (FADD) resulting in the formation of a death inducing signaling complex (DISC). DISC is responsible for the assembly and auto-catalytic activation of pro-caspase-8 to caspase-8 (Elmore, 2007). Caspase-8 activates caspases-3/7 leading to apoptotic cell death (Figure 2.9).

The activation of the extrinsic apoptotic pathway can initiate activation of the intrinsic apoptotic pathway via the BH3-domain-only molecule, Bid (Elmore, 2007). The activation of caspase-8, via the extrinsic apoptotic pathway, cleaves cytosolic p22 Bid at the amino-terminus leading to the formation of a p15 carboxy-terminal fragment of Bid known as truncated p15 Bid (tBid). tBid translocates to the mitochondria and directly activates pro-apoptotic proteins to induce mitochondrial membrane permeabilization causing the release of cytochrome c and activation of the intrinsic apoptotic cascade (Figure 2.9) (Elmore, 2007).

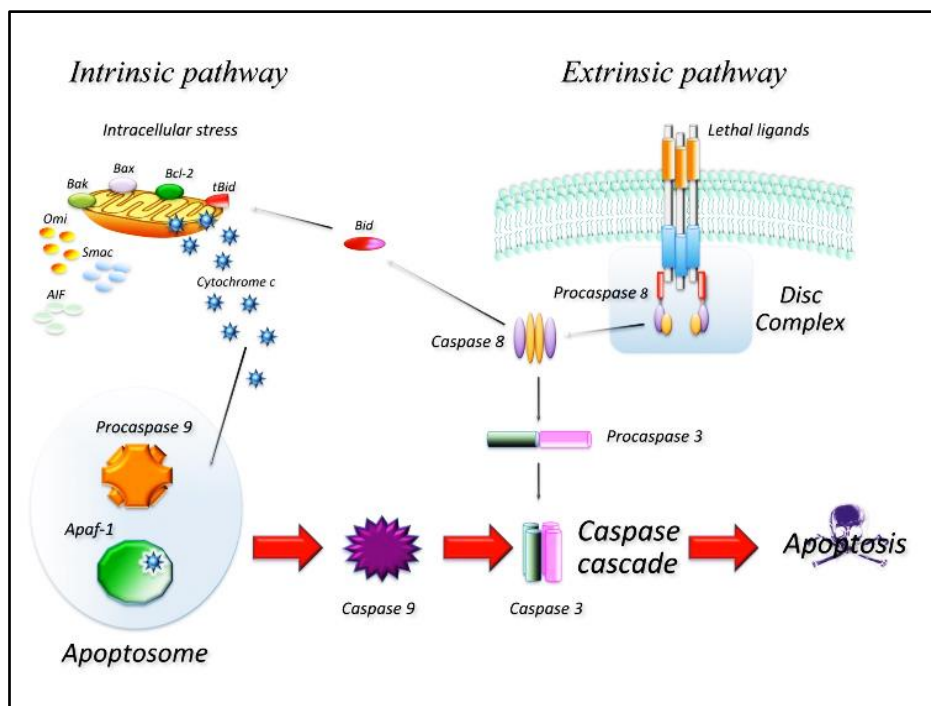


**Figure 2.9** Intrinsic and extrinsic pathways of apoptosis (Favaloro et al., 2012)

## 2.9. The p53 Tumor Suppressor Protein

The tumor suppressor protein, p53 often referred to as the guardian of the genome is a transcription factor involved in regulating the expression of genes critical for cell cycle arrest and apoptosis (Laptenko and Prives, 2006, Prives and Hall, 1999). It is encoded by one of the most frequently mutated genes in human cancers and over 50% of cancers have been reported to contain mutated or inactive p53 (Liu et al., 2013).

p53 is the central regulator of several cell signaling pathways and its major activators include DNA damage, excessive oncogene activation, hypoxia and oxidative stress (Figure 2.10) (Liu et al., 2013). Once activated, p53 acts as a critical regulator of cell proliferation by functioning as a checkpoint protein to monitor DNA damage, arrest the cell cycle, and initiate DNA repair (Figure 2.10) (Kruiswijk et al., 2015, Vousden and Prives, 2009). In the event of irreparable DNA damage, p53 induces apoptosis preventing the propagation of cells with damaged DNA and tumor formation (Liu et al., 2013). p53 also functions to recruit core transcriptional machinery to its target promoters enabling the transcription of genes such as MDM2, p21, and BAX which are involved in regulating cell proliferation and apoptosis (Kruiswijk et al., 2015, Vousden and Prives, 2009). p53 also has a major role in metabolic pathways by regulating glycolysis (Budanov, 2014, Liu et al., 2018), fatty acid oxidation (Liu et al., 2018), and autophagy (Jin, 2005). It enhances the antioxidant response and prevents oxidative damage to cellular macromolecules (Budanov, 2014).

Dysregulation in the expression of p53 has been linked with several cellular abnormalities and diseases such as neurodegenerative disorders (Chang et al., 2012, Szybińska and Leśniak, 2017) and cancer (Spafford et al., 1996). It has been shown to affect metabolic pathways contributing to the metabolic changes characteristic of the cancer phenotype (Liu et al., 2018). Previously, *p53* knockout mice displayed excessive DNA damage and inhibition of apoptosis and are extremely susceptible to early tumor development (Donehower et al., 1992).

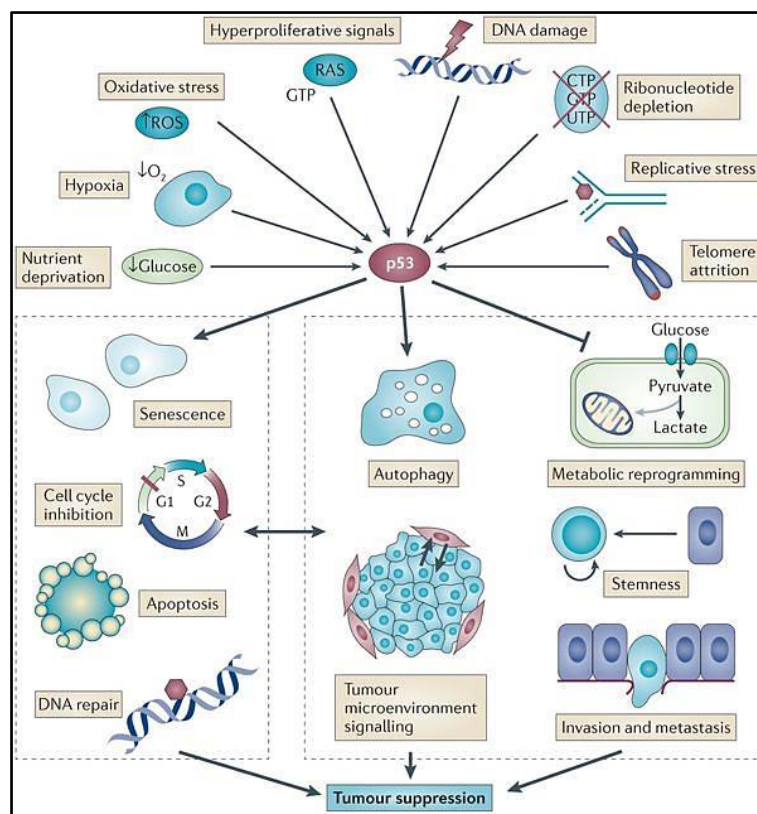


**Figure 2.10** Activation and functions of p53 (Bieging et al., 2014)

### 2.9.1. Regulation of p53

The tight regulation of p53 function is essential for maintaining normal cell growth and preventing tumourigenesis (Brooks and Gu, 2003). p53 is subjected to a variety of post-translational modifications that regulate its function as a tumor suppressor protein (Brooks and Gu, 2003). The role of post-translational modifications such as phosphorylation, acetylation, and ubiquitination in regulating the stability and activity of p53 has been extensively studied (Barlev et al., 2001, Shieh et al., 1997, Tang et al., 2008); and our previous work showed that FA has the ability to induce genotoxic and cytotoxic effects in human liver (HepG2) cells by post-translationally increasing the stability and activity of p53 (Ghazi et al., 2017) (Addendum A). However, p53 is also regulated at the transcriptional and post-transcriptional level by promoter methylation and N6-methyladenosine (m6A) RNA methylation (Chmelarova et al., 2013, Kang et al., 2001, Uddin et al., 2019).

#### 2.9.1.1. Promoter Methylation of p53

The methylation of CpG dinucleotides within the p53 gene promoter is essential in regulating p53 transcription. The p53 gene contains a basal promoter region of approximately 85 base pairs

that is essential for its full promoter activity and the *p53* promoter has putative binding sites for transcription factors (Tuck and Crawford, 1989).

Alterations in *p53* promoter methylation have been linked with an array of *p53* mutations, loss in tumor suppressor function, and cancer progression (Mitsudomi et al., 1992). Previously, it was determined that promoter hypermethylation of *p53* inhibits the binding of transcription factors and reduces *p53* transcription whereas promoter hypomethylation enables access to transcription factors and increases *p53* expression (Chmelarova et al., 2013, Kang et al., 2001).

The epigenetic silencing of tumor suppressor genes is a frequent phenomenon of cancer cells, and studies conducted on glioma cell lines indicate that *p53* promoter methylation significantly affects *p53* expression contributing to tumorigenesis (Soto-Reyes and Recillas-Targa, 2010, Amatya et al., 2005). Similarly, single-site methylation of the *p53* gene promoter was associated with a significant reduction in wild-type *p53* and tumorigenesis *in vivo* (Pogribny et al., 2000).

#### 2.9.1.2. *m6A RNA Methylation*

Chemical modifications of RNA transcripts are involved in regulating RNA-protein and RNA-RNA interactions, thereby, regulating gene expression by modulating RNA processing, localization, translation, and decay (Meyer et al., 2015, Wang et al., 2014b, Xiao et al., 2016, Zheng et al., 2013). *m6A* RNA methylation is a predominant post-transcriptional modification of mammalian messenger RNA (mRNA) that occurs in an estimated 0.2-0.5% of adenines (Fu et al., 2014, Geula et al., 2015). It is found in the coding region, 3' untranslated region (UTR), and 5'UTR of mRNA where it plays an important role in gene expression regulation (Meyer et al., 2015, Wang et al., 2015, Wang et al., 2014b), animal development (Frye et al., 2018), and disease (Hsu et al., 2017).

*m6A* is deposited on mRNA co-transcriptionally by a methyltransferase complex which consists of methyltransferase-like 3 (METTL3), methyltransferase-like 14 (METTL14), and Wilms' tumor 1-associated protein (WTAP) (Figure 2.11) (Wang and He, 2014, Liu et al., 2014). METTL3 is catalytically active and regulates *m6A* levels by transferring a methyl group from SAM to the N-6 position of specific adenines on the target mRNA, METTL14 facilitates RNA binding and stabilizes METTL3, whereas WTAP binds to the METTL3-METTL14 complex and is required for substrate recruitment and nuclear localization (Liu et al., 2014, Shi et al., 2019). Adaptor proteins such as Vir-like *m6A* methyltransferase-associated (VIRMA), zinc finger CCCH-type-containing 13 (ZC3H13), and RNA binding motif protein 15 (RBM15) also form part of the methyltransferase complex where they act as cofactors to facilitate RNA

binding, nuclear localization, and m6A deposition (Shi et al., 2019). The demethylases, fat mass and obesity-associated protein (FTO) and ALKB homolog 5 (ALKBH5), are Fe<sup>2+</sup> and alpha-ketoglutarate-dependent and function by oxidizing N-methyl groups of m6A to a hydroxymethyl group (Figure 2.11) (Woo and Chambers, 2019, Jia et al., 2011). Previously, knockdown of *FTO* increased m6A levels on *myc* mRNA leading to mRNA decay and *myc* downregulation (Su et al., 2018). Knockdown of *FTO* also increased m6A levels on *USP7* mRNA leading to *USP7* degradation and decreased *USP7* expression in human lung cancer cell lines (Li et al., 2019). Additionally, knockdown of *METTL3* and *METTL14* reduced m6A-*p21* levels and decreased *p21* mRNA and protein expression in HELA cells (Li et al., 2017a).

M6A is enriched on several RNA transcripts where it affects RNA processing by recruiting specific reader proteins: YT521-B homology domain containing proteins 1 and 2 (YTHDC1 and YTHDC2) and the YT521-B homology domain family proteins 1, 2, and 3 (YTHDF1, YTHDF2, and YTHDF3) (Meyer et al., 2015, Wang et al., 2015, Wang et al., 2014b, Xiao et al., 2016, Zheng et al., 2013). YTHDF1, YTHDF3, and YTHDC2 regulate mRNA translation by interacting with translation machinery and enhancing translation efficiency (Meyer et al., 2015, Wang et al., 2015), YTHDF1 induces mRNA degradation by recruiting the CCR4-NOT deadenylation complex (Wang et al., 2014b), and YTHDC1 regulates cellular localization and mRNA splicing by recruiting the pre-mRNA splicing factor, SRSF3 (Figure 2.11) (Xiao et al., 2016, Zheng et al., 2013).

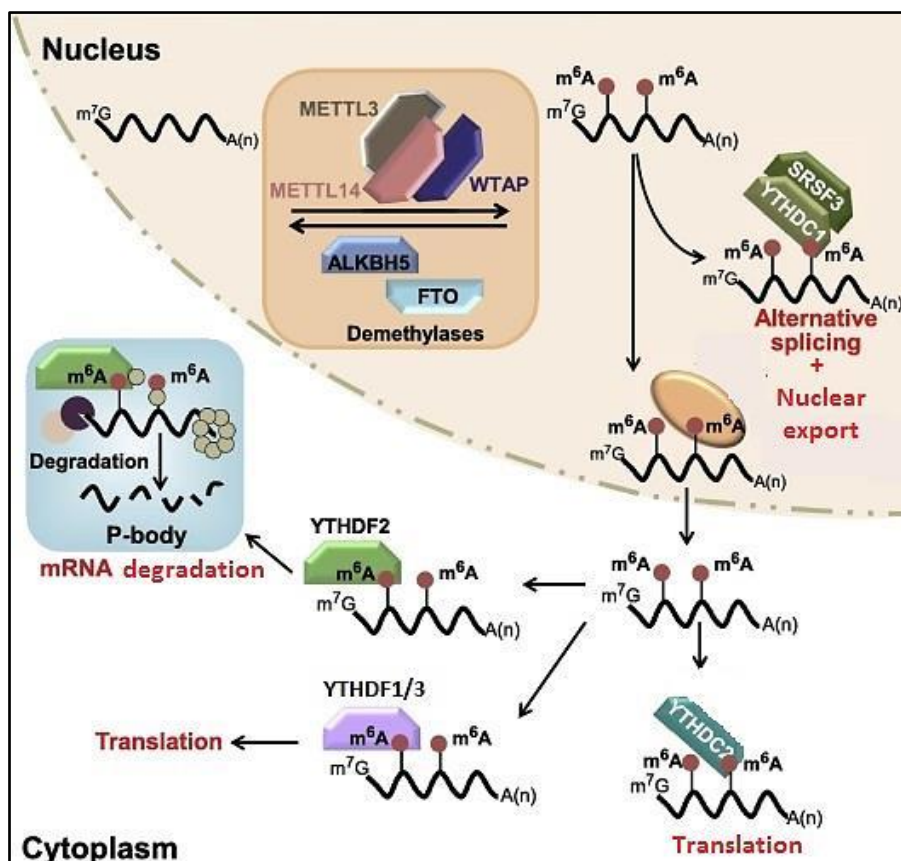


**Figure 2.11** Regulation and function of m<sup>6</sup>A RNA methylation (Liao et al., 2018)

M<sup>6</sup>A-containing genes are enriched in important cellular processes, and a subset of m<sup>6</sup>A sites appear in response to stimuli and stress (Dominissini et al., 2015, Meyer et al., 2015). Previously, dietary factors have also been found to affect m<sup>6</sup>A levels on RNA transcripts (Li et al., 2016, Lu et al., 2018) suggesting a possible effect of FA on the m<sup>6</sup>A levels and regulation of the stress response protein, p53. Studies on m<sup>6</sup>A and p53 have indicated that m<sup>6</sup>A at the point mutated codon 273 of *p53* pre-mRNA promotes the expression of p53 R273H mutant protein and drug resistance of cancer cells (Uddin et al., 2019). Similarly, alterations in m<sup>6</sup>A have been strongly associated with a reduction in wild type p53 and the presence of *p53* mutations in patients with acute myeloid leukemia (Kwok et al., 2017).

## 2.10. MicroRNAs

MicroRNAs (miRNAs) are endogenously expressed small (20-23 nucleotides) non-coding RNA molecules that control both physiological and pathological processes by post-transcriptionally regulating gene expression (Winter et al., 2009). This process occurs in a sequence specific manner and involves binding of the miRNA to the 3'UTR of mRNA and negatively regulating the processing, stability, and translation of the mRNA (Winter et al., 2009).

MiRNAs are critical for normal development and are involved in various biological processes such as cell cycle and apoptosis (Winter et al., 2009, O'Brien et al., 2018). While a single miRNA can regulate several target mRNAs, several miRNAs can also target a single mRNA; and dysregulation in the expression and regulatory functions of miRNAs have been implicated in the pathogenesis of several human diseases (Winter et al., 2009, O'Brien et al., 2018). MiRNAs are known to be aberrantly expressed in cancer where they are capable of acting as either tumor suppressors or oncogenes depending on their expression and cellular targets (Winter et al., 2009, O'Brien et al., 2018). MiRNAs also serve as cell signaling molecules to mediate cell-cell communication and aberrant levels of extracellular miRNAs have been identified as potential biomarkers for cancer and other human diseases (Weiland et al., 2012, Chen et al., 2008, Kim, 2015, Wang et al., 2014a, Ha, 2011).

### ***2.10.1. Biogenesis of MiRNAs***

The biogenesis of miRNAs occurs via two pathways: a canonical pathway and a non-canonical pathway (O'Brien et al., 2018). The canonical pathway is mediated by RNA polymerase II and III and is the dominant pathway by which mammalian miRNAs are generated (Winter et al., 2009, O'Brien et al., 2018). In this pathway, miRNA biogenesis begins in the nucleus where the RNA polymerase II and RNA polymerase III dependent transcription of miRNA genes generates a long primary miRNA (pri-miRNA) transcript that can fold into a hairpin structure (Winter et al., 2009, O'Brien et al., 2018). These pri-miRNAs are cleaved into short 70 nucleotide precursor miRNAs (pre-miRNAs) by the micro-processor complex which is comprised of the RNase III enzyme, Drosha and its cofactor, DGCR8 (DiGeorge Syndrome Critical Region 8) (O'Brien et al., 2018). DGCR8 binds to double-stranded RNA and positions Drosha approximately 11 base pairs away from the base of the hairpin stem where its two RNase domains cleaves the 5' and 3' arms of the pri-miRNA hairpin (Winter et al., 2009). The resultant pre-miRNAs are then exported out of the nucleus to the cytoplasm by the Ran-GTP-dependent transporter, exportin-5 where it is cleaved by the RNase III enzyme, Dicer and its double-stranded RNA binding cofactor, trans-activation response (TAR) RNA-binding protein (TRBP) to yield mature double-stranded miRNA duplexes that are approximately 20-23 nucleotides in length (Winter et al., 2009). These mature miRNAs are then loaded together with Argonaute (Ago2) proteins into the RNA-induced silencing complex (RISC) leading to unwinding of the miRNA duplex and the generation of mature single-stranded miRNAs (Winter et al., 2009). The passenger strand is degraded and the mature miRNA binds, via complementary base pairing, to target mRNAs leading to the degradation, inhibition of translation, and deadenylation of the mRNA (Figure 2.12) (Winter et al., 2009).

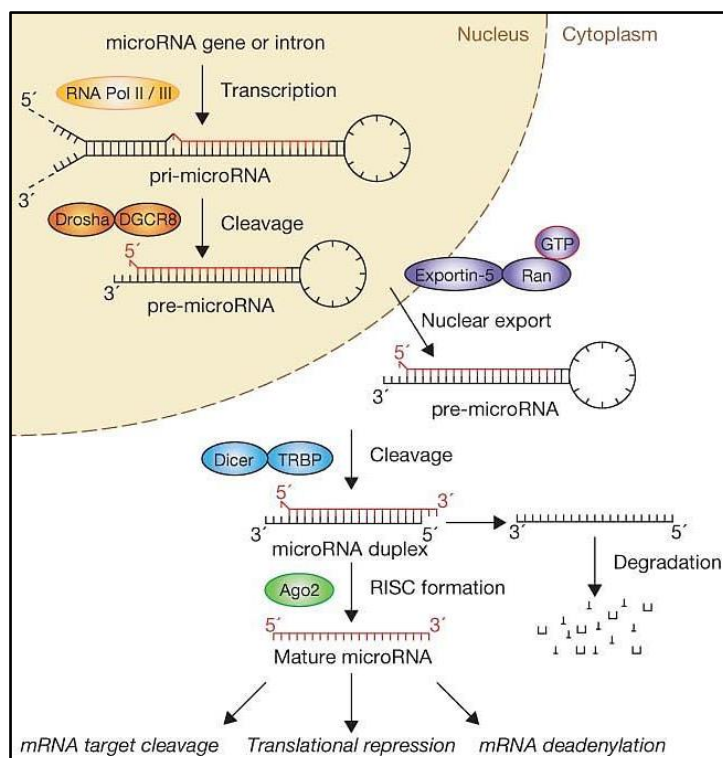


**Figure 2.12** The canonical pathway of microRNA biogenesis (Winter et al., 2009)

The non-canonical pathway of miRNA biogenesis is also referred to as the Drosha-DGCR8-independent and Dicer-TRBP-independent pathways (O'Brien et al., 2018). In this pathway, mirtrons (pre-miRNAs produced from the introns of mRNAs during splicing) and 7-methylguanosine-capped pre-miRNAs are produced independent of Drosha and directly exported into the cytoplasm where, independent of Dicer-TRBP cleavage, it is loaded onto Ago2 proteins and further processed by RISC into mature miRNAs (O'Brien et al., 2018).

### 2.10.2. MiRNAs and DNA Methylation

DNA methylation in miRNA gene promoters has been reported as a mechanism that may cause dysregulation of mature miRNAs and consequently impact gene expression (Moore et al., 2013). Previously, the loss of *DNMT1* and *DNMT3B* revealed that approximately 10% of miRNAs are regulated by DNA methylation (Han et al., 2007); and the hypo- and hypermethylation of miRNA gene promoters causes an increase and decrease in miRNA expression, respectively (Ortiz et al., 2018). Additionally, miRNAs can regulate DNA methylation patterns by altering the expression of *DNMTs* (Fabbri et al., 2007, Garzon et al., 2009).

MiR-29b, a member of the miR-29 family that consists of miR-29a, miR-29b, and miR-29c, displays sequence complementarity to the 3'UTRs of *DNMT3A* and *DNMT3B* (Garzon et al.,

2009, Fabbri et al., 2007). The expression of miR-29b is inversely correlated with the expression of *DNMT3A* and *DNMT3B* in lung cancer tissues and miR-29b was shown to directly target both *DNMT3A* and *DNMT3B* (Fabbri et al., 2007). MiR-29b was also found to regulate the expression of *DNMT1* in an indirect mechanism that involves the direct targeting and repression of the transcriptional activator, *Sp1* (Fabbri et al., 2007, Garzon et al., 2009). Additionally, the expression of miR-29b is itself regulated by DNA methylation and enforced expression of miR-29b was shown to decrease the expression of *DNMT1*, *DNMT3A*, and *DNMT3B* leading to DNA hypomethylation in acute myeloid leukemia cells (Garzon et al., 2009).

### **2.10.3. MiRNAs and Histone Methylation**

MiRNAs have been reported to control chromatin structure and histone methylation by post-transcriptionally regulating the expression of chromatin-modifying enzymes such as histone methyltransferases and demethylases (Moore et al., 2013).

MiR-200a is a member of the miR-200 family (miR-200a, miR-200b, miR-200c, miR-429, and miR-141) that has been shown to play a significant role in regulating histone methylation (Eades et al., 2011). MiR-200a modulates H3K9me3 by directly targeting *Sirt1* and decreasing the activity and expression of the histone methyltransferase, SUV39H1 (Eades et al., 2011, Bosch-Presegué et al., 2011, Vaquero et al., 2007). MiR-200a was also found to directly target *SUV39H2* and reduce H3K9me3 in CD4+ T cells (Quiroz et al., 2019). Additionally, histone methylation on miRNA gene promoters can influence the expression of miRNAs. H3K9me3 on the promoter of miR-200a decreased miR-200a expression and led to epithelial to mesenchymal transition in glioma cells (Bian et al., 2019).

## **2.11. The Role of Epigenetics in Mycotoxicology**

The chronic consumption of mycotoxin-contaminated commodities is long known to cause harmful effects in humans and animals. In the body, mycotoxins are bio-transformed into highly toxic metabolites that interact with various biomolecules such as DNA and RNA affecting their normal functions with adverse cellular outcomes (Dai et al., 2017). To date, the majority of the information available on mycotoxins indicate that they are unlikely to act via a single well-defined mechanism; and recently, epigenetic studies on mycotoxins have provided insights into their mechanisms of toxicity (Bbosa et al., 2013, Marin-Kuan et al., 2008, Chaturgoon et al., 2014a, Chaturgoon et al., 2014b, Dai et al., 2017, Demirel et al., 2015, Zhu et al., 2016, Zhu et al., 2014, Sancak and Ozden, 2015, Han et al., 2016).

AFB<sub>1</sub> is a mycotoxin produced by fungi of the genus *Aspergillus* that was shown to induce hepatocellular carcinoma by altering global DNA methylation (Hernandez-Vargas et al., 2015) and inducing promoter hypermethylation of genes (*MGMT*, *RASSF1A*, and *p16*) involved in DNA repair and cell cycle control (Zhang et al., 2003, Zhang et al., 2002).

OTA, a mycotoxin produced by some *Aspergillus* and *Penicillium* species, induced cytotoxicity by decreasing global DNA methylation *in vitro* (Li et al., 2015), and OTA-induced nephrotoxicity occurred via modulation of DNMT1 and alterations in global DNA methylation *in vivo* (Li et al., 2015). OTA-induced promoter hypermethylation of cell adhesion-related genes, *E-cadherin* and *N-cadherin* activated the Wnt and PI3K/AKT signaling pathways leading to nephrotoxicity (Li et al., 2015).

The *Fusarium* mycotoxins, FB<sub>1</sub>, zearalenone, T2-toxin, and DON were also shown to have epigenetic effects *in vitro* and *in vivo*. FB<sub>1</sub> induced chromatin instability and liver tumorigenesis by inducing global DNA hypomethylation and histone methylation in human liver cells (Chuturgoon et al., 2014a). FB<sub>1</sub> inhibited miR-27b, increased cytochrome P450 1B1, and altered promoter methylation of tumor suppressor genes (*c-myc*, *p15*, *p16*, and *e-cadherin*) leading to hepatic neoplastic transformation (Chuturgoon et al., 2014b, Demirel et al., 2015). FB<sub>1</sub>-induced increase in H3K9me2/3 and decrease in H3K9Ac and H4K20me3 also provided a mechanism for carcinogenesis in rat kidney cells (Sancak and Ozden, 2015).

Zearalenone induced global DNA hypomethylation (So et al., 2014), and decreased H3K9me3, H3K4me2, and H4K20me1/2/3 leading to a reduction in cell viability (Zhu et al., 2014). In contrast, other *Fusarium* mycotoxins such as DON and T2-toxin induced autophagy and apoptosis by increasing both global DNA methylation and histone methylation (Han et al., 2016, Zhu et al., 2016).

These studies provide evidence for the role of epigenetic mechanisms in regulating mycotoxin-induced toxicities, and suggest that alterations in epigenetic modifications may be a crucial underlying mechanism of their toxicities.

## 2.12. References

Abdul NS, Nagiah S, Chaturgoon AA. (2016). Fusaric acid induces mitochondrial stress in human hepatocellular carcinoma (HepG2) cells. *Toxicon*, 119, 336-344.

Abdul NS, Nagiah S, Chaturgoon AA. (2019). Fusaric acid induces NRF2 as a cytoprotective response to prevent NLRP3 activation in the liver derived HepG2 cell line. *Toxicology In Vitro*, 55, 151-159.

Amatya VJ, Naumann U, Weller M, Ohgaki H. (2005). TP53 promoter methylation in human gliomas. *Acta Neuropathologica*, 110, 178-184.

Bacon C, Porter J, Norred W, Leslie J. (1996). Production of fusaric acid by *Fusarium* species. *Applied and Environmental Microbiology*, 62, 4039-4043.

Bacon CW, Porter JK, Norred WP. (1995). Toxic interaction of fumonisin B1 and fusaric acid measured by injection into fertile chicken egg. *Mycopathologia*, 129, 29-35.

Barlev NA, Liu L, Chehab NH, Mansfield K, Harris KG, Halazonetis TD, Berger SL. (2001). Acetylation of p53 activates transcription through recruitment of coactivators/histone acetyltransferases. *Molecular Cell*, 8, 1243-1254.

Bassing CH, Chua KF, Sekiguchi J, Suh H, Whitlow SR, Fleming JC, Monroe BC, Ciccone DN, Yan C, Vlasakova K. (2002). Increased ionizing radiation sensitivity and genomic instability in the absence of histone H2AX. *Proceedings of the National Academy of Sciences*, 99, 8173-8178.

Bbosa GS, Kitya D, Odda J, Ogwal-okeng J. (2013). Aflatoxins metabolism, effects on epigenetic mechanisms and their role in carcinogenesis. *Health*, 5, 720-726.

Bennett J, Klich M. (2003). Mycotoxins. *Clinical Microbiological Reviews*, 16, 497-516.

Bian E, Chen X, Xu Y, Ji X, Cheng M, Wang H, Fang Z, Zhao B. (2019). A central role for MeCP2 in the epigenetic repression of miR-200c during epithelial-to-mesenchymal transition of glioma. *Journal of Experimental and Clinical Cancer Research*, 38, 1-15.

Biegging KT, Mello SS, Attardi LD. (2014). Unravelling mechanisms of p53-mediated tumour suppression. *Nature Reviews Cancer*, 14, 359-370.

Bochner BR, Huang HC, Schieven GL, Ames BN. (1980). Positive selection for loss of tetracycline resistance. *Journal of Bacteriology*, 143, 926-933.

Bosch-Presegué L, Raurell-Vila H, Marazuela-Duque A, Kane-Goldsmith N, Valle A, Oliver J, Serrano L, Vaquero A. (2011). Stabilization of Suv39H1 by SirT1 is part of oxidative stress response and ensures genome protection. *Molecular Cell*, 42, 210-223.

Brooks CL, Gu W. (2003). Ubiquitination, phosphorylation and acetylation: the molecular basis for p53 regulation. *Current Opinion in Cell Biology*, 15, 164-171.

Budanov AV. (2014). The role of tumor suppressor p53 in the antioxidant defense and metabolism. *Subcellular Biochemistry*, 85, 337-358.

Cedar H, Bergman Y. (2009). Linking DNA methylation and histone modification: patterns and paradigms. *Nature Reviews Genetics*, 10, 295-304.

Celeste A, Difilippantonio S, Difilippantonio MJ, Fernandez-Capetillo O, Pilch DR, Sedelnikova OA, Eckhaus M, Ried T, Bonner WM, Nussenzweig A. (2003). H2AX haploinsufficiency modifies genomic stability and tumor susceptibility. *Cell*, 114, 371-383.

Chang JR, Ghafouri M, Mukerjee R, Bagashev A, Chabrashvili T, Sawaya BE. (2012). Role of p53 in neurodegenerative diseases. *Neurodegenerative Diseases*, 9, 68-80.

Cheishvili D, Chik F, Li CC, Bhattacharya B, Suderman M, Arakelian A, Hallett M, Rabbani SA, Szyf M. (2014). Synergistic effects of combined DNA methyltransferase inhibition and MBD2 depletion on breast cancer cells; MBD2 depletion blocks 5-aza-2'-deoxycytidine-triggered invasiveness. *Carcinogenesis*, 35, 2436-2446.

Chen J, Zhang YC, Huang C, Shen H, Sun B, Cheng X, Zhang YJ, Yang YG, Shu Q, Yang Y. (2019). m6A Regulates Neurogenesis and Neuronal Development by Modulating Histone Methyltransferase Ezh2. *Genomics, Proteomics and Bioinformatics*, 17, 154-168.

Chen TT, Wu SM, Ho SC, Chuang HC, Liu CY, Chan YF, Kuo LW, Feng PH, Li WT, Chen KY. (2017a). SUV39H1 reduction is implicated in abnormal inflammation in COPD. *Scientific Reports*, 7, 46667-46924.

Chen X, Ba Y, Ma L, Cai X, Yin Y, Wang K, Guo L, Zhang Y, Chen L, Guo X. (2008). Characterization of microRNAs in serum: a novel class of biomarkers for diagnosis of cancer and other diseases. *Cell Research*, 18, 997-1006.

Chen Z, Luo Q, Wang M, Chen B. (2017b). A rapid method with UPLC for the determination of fusaric acid in fusarium strains and commercial food and feed products. *Indian Journal of Microbiology*, 57, 68-74.

- Cheng J, Yang H, Fang J, Ma L, Gong R, Wang P, Li Z, Xu Y. (2015). Molecular mechanism for USP7-mediated DNMT1 stabilization by acetylation. *Nature Communications*, 6, 7023-7033.
- Cheng L, Tang Y, Chen X, Zhao L, Liu S, Ma Y, Wang N, Zhou K, Zhou J, Zhou M. (2018). Deletion of MBD2 inhibits proliferation of chronic myeloid leukaemia blast phase cells. *Cancer Biology and Therapy*, 19, 676-686.
- Cheng X, Blumenthal RM. (2008). Mammalian DNA methyltransferases: a structural perspective. *Structure*, 16, 341-350.
- Chiba T, Saito T, Yuki K, Zen Y, Koide S, Kanogawa N, Motoyama T, Ogasawara S, Suzuki E, Ooka Y. (2015). Histone lysine methyltransferase SUV39H1 is a potent target for epigenetic therapy of hepatocellular carcinoma. *International Journal of Cancer*, 136, 289-298.
- Chmelarova M, Krepinska E, Spacek J, Laco J, Beranek M, Palicka V. (2013). Methylation in the p53 promoter in epithelial ovarian cancer. *Clinical and Translational Oncology*, 15, 160-163.
- Chuturgoon A, Phulukdaree A, Moodley D. (2014a). Fumonisin B1 induces global DNA hypomethylation in HepG2 cells—An alternative mechanism of action. *Toxicology*, 315, 65-69.
- Chuturgoon AA, phulukdaree A, Moodley D. (2014b). Fumonisin B1 modulates expression of human cytochrome P450 1b1 in human hepatoma (Hepg2) cells by repressing Mir-27b. *Toxicology Letters*, 227, 50-55.
- Dabrowski MJ, Wojtas B. (2019). Global DNA methylation patterns in human gliomas and their interplay with other epigenetic modifications. *International Journal of Molecular Sciences*, 20, 3478-3494.
- Dai Y, Huang K, Zhang B, Zhu L, Xu W. (2017). Aflatoxin B1-induced epigenetic alterations: an overview. *Food and Chemical Toxicology*, 109, 683-689.
- D'alton A, Etherton B. (1984). Effects of fusaric acid on tomato root hair membrane potentials and ATP levels. *Plant Physiology*, 74, 39-42.
- Demirel G, Alpertunga B, Ozden S. (2015). Role of fumonisin B1 on DNA methylation changes in rat kidney and liver cells. *Pharmaceutical Biology*, 53, 1302-1310.

- Denis H, Ndlovu MN, Fuks F. (2011). Regulation of mammalian DNA methyltransferases: a route to new mechanisms. *EMBO Reports*, 12, 647-656.
- Detich N, Theberge J, Szyf M. (2002). Promoter-specific activation and demethylation by MBD2/demethylase. *Journal of Biological Chemistry*, 277, 35791-35794.
- Devaraja S, Girish KS, Santhosh MS, Hemshekhar M, Nayaka SC, Kemparaju K. (2013). Fusaric acid, a mycotoxin, and its influence on blood coagulation and platelet function. *Blood Coagulation and Fibrinolysis*, 24, 419-423.
- Devnarain N, Tiloke C, Nagiah S, Chuturgoon AA. (2017). Fusaric acid induces oxidative stress and apoptosis in human cancerous oesophageal SNO cells. *Toxicon*, 126, 4-11.
- Dhani S, Nagiah S, Naidoo DB, Chuturgoon AA. (2017). Fusaric Acid immunotoxicity and MAPK activation in normal peripheral blood mononuclear cells and Thp-1 cells. *Scientific Reports*, 7, 3051-3060.
- Diniz S, Oliveira R. (2009). Effects of fusaric acid on *Zea mays* L. seedlings. *Phyton (Buenos Aires)*, 78, 155-160.
- Diringer MN, Kramarcy NR, Brown JW, Thurmond JB. (1982). Effect of fusaric acid on aggression, motor activity, and brain monoamines in mice. *Pharmacology Biochemistry and Behavior*, 16, 73-79.
- Dodge JE, Okano M, Dick F, Tsujimoto N, Chen T, Wang S, Ueda Y, Dyson N, Li E. (2005). Inactivation of Dnmt3b in mouse embryonic fibroblasts results in DNA hypomethylation, chromosomal instability, and spontaneous immortalization. *Journal of Biological Chemistry*, 280, 17986-17991.
- Dominissini D, Moshitch-Moshkovitz S, Amariglio N, Rechavi G. (2015). Transcriptome-wide mapping of N6-methyladenosine by m6A-Seq. *Methods in Enzymology*, 560, 131-147.
- Donehower LA, Harvey M, Slagle BL, McArthur MJ, Montgomery Jr CA, Butel JS, Bradley A. (1992). Mice deficient for p53 are developmentally normal but susceptible to spontaneous tumours. *Nature*, 356, 215-221.
- Dong C, Wu Y, Wang Y, Wang C, Kang T, Rychahou PG, Chi YI, Evers BM, Zhou BP. (2013). Interaction with Suv39H1 is critical for Snail-mediated E-cadherin repression in breast cancer. *Oncogene*, 32, 1351-1362.

- Dowd PF. (1988). Toxicological and biochemical interactions of the fungal metabolites fusaric acid and kojic acid with xenobiotics in *Heliothis zea* (F.) and *Spodoptera frugiperda*. *Pesticide Biochemistry and Physiology*, 32, 123-134.
- Du Q, Luu PL, Stirzaker C, Clark SJ. (2015). Methyl-CpG-binding domain proteins: readers of the epigenome. *Epigenomics*, 7, 1051-1073.
- Eades G, Yao Y, Yang M, Zhang Y, Chumsri S, Zhou Q. (2011). MiR-200a regulates SIRT1 expression and epithelial to mesenchymal transition (EMT)-like transformation in mammary epithelial cells. *Journal of Biological Chemistry*, 286, 25992-26002.
- Eads CA, Danenberg KD, Kawakami K, Saltz LB, Danenberg PV, Laird PW. (1999). CpG island hypermethylation in human colorectal tumors is not associated with DNA methyltransferase overexpression. *Cancer Research*, 59, 2302-2306.
- Elmore S. (2007). Apoptosis: a review of programmed cell death. *Toxicologic Pathology*, 35, 495-516.
- Engel M, Eggert C, Kaplick PM, Eder M, Röh S, Tietze L, Namendorf C, Arloth J, Weber P, Rex-Haffner M. (2018). The role of m<sup>6</sup>A/m-RNA methylation in stress response regulation. *Neuron*, 99, 389-403.
- Espada J, Ballestar E, Fraga MF, Villar-Garea A, Juarranz A, Stockert JC, Robertson KD, Fuks F, Esteller M. (2004). Human DNA methyltransferase 1 is required for maintenance of the histone H3 modification pattern. *Journal of Biological Chemistry*, 279, 37175-37184.
- Estève PO, Chin HG, Smallwood A, Feehery GR, Gangisetty O, Karpf AR, Carey MF, Pradhan S. (2006). Direct interaction between DNMT1 and G9a coordinates DNA and histone methylation during replication. *Genes and Development*, 20, 3089-3103.
- Fabbri M, Garzon R, Cimmino A, Liu Z, Zanesi N, Callegari E, Liu S, Alder H, Costinean S, Fernandez-Cymering C. (2007). MicroRNA-29 family reverts aberrant methylation in lung cancer by targeting DNA methyltransferases 3A and 3B. *Proceedings of the National Academy of Sciences*, 104, 15805-15810.
- Fairchild A, Grimes J, Porter J, Croom Jr W, Daniel L, Hagler Jr W. (2005). Effects of diacetoxyscirpenol and fusaric acid on poult: Individual and combined effects of dietary diacetoxyscirpenol and fusaric acid on turkey poult performance. *International Journal of Poultry Science*, 4, 350-355.

- Favaloro B, Allocati N, Graziano V, Di Ilio C, De Laurenzi V. (2012). Role of apoptosis in disease. *Aging (Albany NY)*, 4, 330-349.
- Fernandez-Pol J, Klos D, Hamilton P. (1993). Cytotoxic activity of fusaric acid on human adenocarcinoma cells in tissue culture. *Anticancer Research*, 13, 57-64.
- Fernandez-Pol JA. (1998). Antiviral agent. Google patents number: EP0869789A4.
- Firestein R, Cui X, Huie P, Cleary ML. (2000). SET domain-dependent regulation of transcriptional silencing and growth control by SUV39H1, a mammalian ortholog of *Drosophila* Su (var) 3-9. *Molecular and Cellular Biology*, 20, 4900-4909.
- Frye M, Harada BT, Behm M, He C. (2018). RNA modifications modulate gene expression during development. *Science*, 361, 1346-1349.
- Fu Y, Dominissini D, Rechavi G, He C. (2014). Gene expression regulation mediated through reversible m<sup>6</sup>A RNA methylation. *Nature Reviews Genetics*, 15, 293-306.
- Fukz F, Hurd PJ, Wolf D, Nan X, Bird AP, Kouzarides T. (2003). The methyl-CpG-binding protein MeCP2 links DNA methylation to histone methylation. *Journal of Biological Chemistry*, 278, 4035-4040.
- García-Cao M, O'sullivan R, Peters AH, Jenuwein T, Blasco MA. (2004). Epigenetic regulation of telomere length in mammalian cells by the Suv39h1 and Suv39h2 histone methyltransferases. *Nature Genetics*, 36, 94-99.
- Garzon R, Liu S, Fabbri M, Liu Z, Heaphy CE, Callegari E, Schwind S, Pang J, Yu J, Muthusamy N. (2009). MicroRNA-29b induces global DNA hypomethylation and tumor suppressor gene reexpression in acute myeloid leukemia by targeting directly DNMT3A and 3B and indirectly DNMT1. *Blood*, 113, 6411-6418.
- Geula S, Moshitch-Moshkovitz S, Dominissini D, Mansour AA, Kol N, Salmon-Divon M, Hershkovitz V, Peer E, Mor N, Manor YS. (2015). m<sup>6</sup>A mRNA methylation facilitates resolution of naïve pluripotency toward differentiation. *Science*, 347, 1002-1006.
- Ghazi T, Nagiah S, Tiloke C, Abdul NS, Chuturgoon AA. (2017). Fusaric acid induces DNA damage and post-translational modifications of p53 in human hepatocellular carcinoma (HepG2) cells. *Journal of Cellular Biochemistry*, 118, 3866-3874.

- Girault I, Tozlu S, Lidereau R, Bièche I. (2003). Expression analysis of DNA methyltransferases 1, 3A, and 3B in sporadic breast carcinomas. *Clinical Cancer Research*, 9, 4415-4422.
- Gopalakrishnan S, Van Emburgh BO, Robertson KD. (2008). DNA methylation in development and human disease. *Mutation Research*, 647, 30-38.
- Grant R, Coggan S, Smythe G. (2009). The physiological action of picolinic acid in the human brain. *International Journal of Tryptophan Research*, 2, 71-79.
- Ha TY. (2011). MicroRNAs in human diseases: from cancer to cardiovascular disease. *Immune Network*, 11, 135-154.
- Han J, Wang QC, Zhu CC, Liu J, Zhang Y, Cui XS, Kim NH, Sun SC. (2016). Deoxynivalenol exposure induces autophagy/apoptosis and epigenetic modification changes during porcine oocyte maturation. *Toxicology and Applied Pharmacology*, 300, 70-76.
- Han L, Witmer PDW, Casey E, Valle D, Sukumar S. (2007). DNA methylation regulates microRNA expression. *Cancer Biology and Therapy*, 6, 1290-1294.
- Handy DE, Castro R, Loscalzo J. (2011). Epigenetic modifications: basic mechanisms and role in cardiovascular disease. *Circulation*, 123, 2145-2156.
- Hendrich B, Guy J, Ramsahoye B, Wilson VA, Bird A. (2001). Closely related proteins MBD2 and MBD3 play distinctive but interacting roles in mouse development. *Genes and Development*, 15, 710-723.
- Hendrich B, Hardeland U, Ng HH, Jiricny J, Bird A. (1999). The thymine glycosylase MBD4 can bind to the product of deamination at methylated CpG sites. *Nature*, 401, 301-304.
- Hengartner MO. (2000). The biochemistry of apoptosis. *Nature*, 407, 685-700.
- Hernandez-Vargas H, Castelino J, Silver MJ, Dominguez-Salas P, Cros MP, Durand G, Calvez-Kelm FL, Prentice AM, Wild CP, Moore SE. (2015). Exposure to aflatoxin B1 in utero is associated with DNA methylation in white blood cells of infants in Gambia. *International Journal of Epidemiology*, 44, 1238-1248.
- Hervouet E, Peixoto P, Delage-Mourroux R, Boyer-Guittaut M, Cartron PF. (2018). Specific or not specific recruitment of DNMTs for DNA methylation, an epigenetic dilemma. *Clinical Epigenetics*, 10, 17-34.

- Hidaka H, Nagatsu T, Takeya K, Takeuchi T, Suda H, Kojiri K, Matsuzaki M, Umezawa H. (1969). Fusaric acid, a hypotensive agent produced by fungi. *The Journal of Antibiotics*, 22, 228-230.
- Hsu PJ, Shi H, He C. (2017). Epitranscriptomic influences on development and disease. *Genome Biology*, 18, 197-205.
- Iraola-Guzán S, Estivill X, Rabionet R. (2011). DNA methylation in neurodegenerative disorders: a missing link between genome and environment? *Clinical Genetics*, 80, 1-14.
- Jeltsch A, Jurkowska RZ. (2016). Allosteric control of mammalian DNA methyltransferases—a new regulatory paradigm. *Nucleic Acids Research*, 44, 8556-8575.
- Jia G, Fu Y, Zhao X, Dai Q, Zheng G, Yang Y, Yi C, Lindahl T, Pan T, Yang YG. (2011). N6-methyladenosine in nuclear RNA is a major substrate of the obesity-associated FTO. *Nature Chemical Biology*, 7, 885-887.
- Jia Y, Li P, Fang L, Zhu H, Xu L, Cheng H, Zhang J, Li F, Feng Y, Li Y. (2016). Negative regulation of DNMT3A de novo DNA methylation by frequently overexpressed UHRF family proteins as a mechanism for widespread DNA hypomethylation in cancer. *Cell Discovery*, 2, 16007-16026.
- Jin B, Li Y, Robertson KD. (2011). DNA methylation: superior or subordinate in the epigenetic hierarchy? *Genes and Cancer*, 2, 607-617.
- Jin S. (2005). p53, autophagy and tumor suppression. *Autophagy*, 1, 171-173.
- Kang JH, Kim SJ, Noh DY, Park IA, Choe KJ, Yoo OJ, Kang HS. (2001). Methylation in the p53 promoter is a supplementary route to breast carcinogenesis: correlation between CpG methylation in the p53 promoter and the mutation of the p53 gene in the progression from ductal carcinoma in situ to invasive ductal carcinoma. *Laboratory Investigation*, 81, 573-579.
- Kerr JF, Winterford CM, Harmon BV. (1994). Apoptosis its significance in cancer and cancer therapy. *Cancer*, 73, 2013-2026.
- Kerr JF, Wyllie AH, Currie AR. (1972). Apoptosis: a basic biological phenomenon with wideranging implications in tissue kinetics. *British Journal of Cancer*, 26, 239-257.
- Kim H, Kwon YM, Kin JS, Han J, Shim YM, Park J, Kim DH. (2006). Elevated mRNA levels of DNA methyltransferase-1 as an independent prognostic factor in primary nonsmall cell lung

cancer. *Cancer: Interdisciplinary International Journal of the American Cancer Society*, 107, 1042-1049.

Kim YK. (2015). Extracellular microRNAs as biomarkers in human disease. *Chonnam Medical Journal*, 51, 51-57.

Kobayashi H, Sakurai T, Imai M, Takahashi N, Fukuda A, Yayoi O, Sato S, Nakabayashi K, Hata K, Sotomaru Y. (2012). Contribution of intragenic DNA methylation in mouse gametic DNA methylomes to establish oocyte-specific heritable marks. *PLoS Genetics*, 8, 1002440-1002454.

Köhler K, Bentrup FW. (1983). The effect of fusaric acid upon electrical membrane properties and ATP level in photoautotrophic cell suspension cultures of *Chenopodium rubrum* L. *Zeitschrift für Pflanzenphysiologie*, 109, 355-361.

Kruiswijk F, Labuschagne CF, Vousden KH. (2015). p53 in survival, death and metabolic health: a lifeguard with a licence to kill. *Nature Reviews Molecular Cell Biology*, 16, 393-405.

Kuźniak E. (2001). Effects of fusaric acid on reactive oxygen species and antioxidants in tomato cell cultures. *Journal of Phytopathology*, 149, 575-582.

Kwok CT, Marshall AD, Rasko JE, Wong JJ. (2017). Genetic alterations of m6A regulators predict poorer survival in acute myeloid leukemia. *Journal of Hematology and Oncology*, 10, 39-44.

Lai W, Jia J, Yan B, Jiang Y, Shi Y, Chen L, Mao C, Liu X, Tang H, Gao M. (2018). Baicalin hydrate inhibits cancer progression in nasopharyngeal carcinoma by affecting genome instability and splicing. *Oncotarget*, 9, 901-914.

Laptenko O, Prives C. (2006). Transcriptional regulation by p53: one protein, many possibilities. *Cell Death and Differentiation*, 13, 951-961.

Li C, Zuo C, Deng G, Kuang R, Yang Q, Hu C, Sheng O, Zhang S, Ma L, Wei Y. (2013). Contamination of bananas with beauvericin and fusaric acid produced by *Fusarium oxysporum* f. sp. *cubense*. *PLoS One*, 8, 70226-70236.

Li J, Han Y, Zhang H, Qian Z, Jia W, Gao Y, Zheng H, Li B. (2019). The m6A demethylase FTO promotes the growth of lung cancer cells by regulating the m6A level of USP7 mRNA. *Biochemical and Biophysical Research Communications*, 512, 479-485.

- Li M, Zhao X, Wang W, Shi H, Pan Q, Lu Z, Perez SP, Suganthan R, He C, Bjørås M. (2018). Ythdf2-mediated m6A mRNA clearance modulates neural development in mice. *Genome Biology*, 19, 69-84.
- Li Q, Li X, Tang H, Jiang B, Dou Y, Gorospe M, Wang W. (2017a). NSUN2-mediated m5C methylation and METTL3/METTL14-mediated m6A methylation cooperatively enhance p21 translation. *Journal of Cellular Biochemistry*, 118, 2587-2598.
- Li X, Gao J, Huang K, Qi X, Dai Q, Mei X, Xu W. (2015). Dynamic changes of global DNA methylation and hypermethylation of cell adhesion-related genes in rat kidneys in response to ochratoxin A. *World Mycotoxin Journal*, 8, 465-476.
- Li X, Yang J, Zhu Y, Liu Y, Shi XE, Yang G. (2016). Mouse maternal high-fat intake dynamically programmed mRNA m6A modifications in adipose and skeletal muscle tissues in offspring. *International Journal of Molecular Sciences*, 17, 1336-1344.
- Li X, Zhang ZL, Wang HF. (2017b). Fusaric acid (FA) protects heart failure induced by isoproterenol (ISP) in mice through fibrosis prevention via TGF- $\beta$ 1/SMADs and PI3K/AKT signaling pathways. *Biomedicine and Pharmacotherapy*, 93, 130-145.
- Liao S, Sun H, Xu C. (2018). YTH domain: a family of N6-methyladenosine (m6A) readers. *Genomics, Proteomics and Bioinformatics*, 16, 99-107.
- Lin RK, Wang YC. (2014). Dysregulated transcriptional and post-translational control of DNA methyltransferases in cancer. *Cell and Bioscience*, 4, 1-11.
- Liu C, Teng ZQ, Santistevan NJ, Szulwach KE, Guo W, Jin P, Zhao X. (2010). Epigenetic regulation of miR-184 by MBD1 governs neural stem cell proliferation and differentiation. *Cell Stem Cell*, 6, 433-444.
- Liu J, Yue Y, Han D, Wang X, Fu Y, Zhang L, Jia G, Yu M, Lu Z, Deng X. (2014). A METTL3-METTL14 complex mediates mammalian nuclear RNA N6-adenosine methylation. *Nature Chemical Biology*, 10, 93-95.
- Liu J, Zhang C, Feng Z. (2013). Tumor suppressor p53 and its gain-of-function mutants in cancer. *Acta Biochimica et Biophysica Sinica*, 46, 170-179.
- Liu J, Zhang C, Hu W, Feng Z. (2018). Tumor suppressor p53 and metabolism. *Journal of Molecular Cell Biology*, 11, 284-292.

- Liu W, Wang N, Lu M, Du XJ, Xing BC. (2016). MBD2 as a novel marker associated with poor survival of patients with hepatocellular carcinoma after hepatic resection. *Molecular Medicine Reports*, 14, 1617-1623.
- Lu N, Li X, Yu J, Li Y, Wang C, Zhang L, Wang T, Zhong X. (2018). Curcumin attenuates lipopolysaccharide-induced hepatic lipid metabolism disorder by modification of m6A RNA methylation in piglets. *Lipids*, 53, 53-63.
- Magdinier F, Wolffe AP. (2001). Selective association of the methyl-CpG binding protein MBD2 with the silent p14/p16 locus in human neoplasia. *Proceedings of the National Academy of Sciences*, 98, 4990-4995.
- Mamur S, Ünal F, Yilmaz S, Erikel E, Yüzbaşıoğlu D. (2018). Evaluation of the cytotoxic and genotoxic effects of mycotoxin fusaric acid. *Drug and Chemical Toxicology*, 1-9.
- Marin-Kuan M, Cavin C, Delatour T, Schilter B. (2008). Ochratoxin A carcinogenicity involves a complex network of epigenetic mechanisms. *Toxicol*, 52, 195-202.
- Marin ML, Murtha J, Dong W, Pestka JJ. (1996). Effects of mycotoxins on cytokine production and proliferation in EL-4 thymoma cells. *Journal of Toxicology and Environmental Health*, 48, 379-396.
- May HD, Wu Q, Blake CK. (2000). Effects of the *Fusarium* spp. mycotoxins fusaric acid and deoxynivalenol on the growth of *Ruminococcus albus* and *Methanobrevibacter ruminantium*. *Canadian Journal of Microbiology*, 46, 692-699.
- Melcher M, Schmid M, Aagaard L, Selenko P, Laible G, Jenuwein T. (2000). Structure-function analysis of SUV39H1 reveals a dominant role in heterochromatin organization, chromosome segregation, and mitotic progression. *Molecular and Cellular Biology*, 20, 3728-3741.
- Meyer H, Skhosana ZD, Motlanthe M, Louw W, Rohwer E. (2019). Long term monitoring (2014–2018) of multi-mycotoxins in South African commercial maize and wheat with a locally developed and validated LC-MS/MS method. *Toxins*, 11, 271-291.
- Meyer KD, Patil DP, Zhou J, Zinoviev A, Skabkin MA, Elemento O, Pestova TV, Qian SB, Jaffrey SR. (2015). 5' UTR m6A promotes cap-independent translation. *Cell*, 163, 999-1010.
- Miranda-Gonçalves V, Lameirinhas A, Henrique R, Jeronimo C. (2018). Metabolism and epigenetic interplay in cancer: Regulation and putative therapeutic targets. *Frontiers in Genetics*, 9, 1-21.

- Mitsudomi T, Steinberg SM, Nau MM, Carbone D, D'amico D, Bodner S, Oie HK, Linnoila RI, Mulshine JL, Minna JD. (1992). p53 gene mutations in non-small-cell lung cancer cell lines and their correlation with the presence of ras mutations and clinical features. *Oncogene*, 7, 171-180.
- Moarii M, Boeva V, Vert JP, Reyal F. (2015). Changes in correlation between promoter methylation and gene expression in cancer. *BMC Genomics*, 16, 873-886.
- Moore LD, Le T, Fan G. (2013). DNA methylation and its basic function. *Neuropsychopharmacology*, 38, 23-38.
- Morales S, Monzo M, Navarro A. (2017). Epigenetic regulation mechanisms of microRNA expression. *Biomolecular Concepts*, 8, 203-212.
- Naghitorabi M, Asl JM, Sadeghi HMM, Rabbani M, Jafarian-Dehkordi A, Javanmard HS. (2013). Quantitative evaluation of DNMT3B promoter methylation in breast cancer patients using differential high resolution melting analysis. *Research in Pharmaceutical Sciences*, 8, 167-175.
- Nicetto D, Donahue G, Jain T, Peng T, Sidoli S, Sheng L, Montavon T, Becker JS, Grindheim JM, Blahnik K. (2019). H3K9me3-heterochromatin loss at protein-coding genes enables developmental lineage specification. *Science*, 363, 294-297.
- Novakovic B, Wong NC, Sibson M, Ng HK, Morley R, Manuelpillai U, Down T, Rakyan VK, Beck S, Hiendleder S. (2010). DNA methylation-mediated down-regulation of DNA methyltransferase-1 (DNMT1) is coincident with, but not essential for, global hypomethylation in human placenta. *Journal of Biological Chemistry*, 285, 9583-9593.
- O'brien J, Hayder H, Zayed Y, Peng C. (2018). Overview of microRNA biogenesis, mechanisms of actions, and circulation. *Frontiers in Endocrinology*, 9, 1-12.
- Ogata S, Inoue K, Iwata K, Okumura K, Taguchi H. (2001). Apoptosis induced by picolinic acid-related compounds in HL-60 cells. *Bioscience, Biotechnology, and Biochemistry*, 65, 2337-2339.
- Ogunbo S, Broomhead J, Ledoux D, Bermudez A, Rottinghaus G. (2007). The individual and combined effects of fusaric acid and T-2 toxin in broilers and turkeys. *International Journal of Poultry Science*, 6, 484-488.
- Okano M, Bell DW, Haber DA, Li E. (1999). DNA methyltransferases Dnmt3a and Dnmt3b are essential for de novo methylation and mammalian development. *Cell*, 99, 247-257.

- Omotayo OP, Omotayo AO, Mwanza M, Babalola OO. (2019). Prevalence of mycotoxins and their consequences on Human health. *Toxicological Research*, 35, 1-7.
- Ooi SK, Qiu C, Bernstein E, Li K, Jia D, Yang Z, Erdjument-Bromage H, Tempst P, Lin SP, Allis CD. (2007). DNMT3L connects unmethylated lysine 4 of histone H3 to de novo methylation of DNA. *Nature*, 448, 714-717.
- Ortiz IMDP, Barros-Filho MC, Dos Reis MB, Beltrami CM, Marchi FA, Kuasne H, Do Canto LM, De Mello JBH, Abildgaard C, Pinto CAL. (2018). Loss of DNA methylation is related to increased expression of miR-21 and miR-146b in papillary thyroid carcinoma. *Clinical Epigenetics*, 10, 144-156.
- Osumi Y, Takaori S, Fujiwara M. (1973). Preventive effect of fusaric acid, a dopamine  $\beta$ -hydroxylase inhibitor, on the gastric ulceration induced by water-immersion stress in rats. *Japanese Journal of Pharmacology*, 23, 904-906.
- Park JA, Kim AJ, Kang Y, Jung YJ, Kim HK, Kim KC. (2011). Deacetylation and methylation at histone H3 lysine 9 (H3K9) coordinate chromosome condensation during cell cycle progression. *Molecules and Cells*, 31, 343-349.
- Patra SK, Patra A, Zhao H, Dahiya R. (2002). DNA methyltransferase and demethylase in human prostate cancer. *Molecular Carcinogenesis*, 33, 163-171.
- Pavlovkin J, Mistrik I, Prokop M. (2004). Some aspects of the phytotoxic action of fusaric acid on primary Ricinus roots. *Plant Soil and Environment*, 50, 397-401.
- Peng L, Yuan Z, Ling H, Fukasawa K, Robertson K, Olashaw N, Koomen J, Chen J, Lane WS, Seto E. (2011). SIRT1 deacetylates the DNA methyltransferase 1 (DNMT1) protein and alters its activities. *Molecular and Cellular Biology*, 31, 4720-4734.
- Peters AH, O'carroll D, Scherthan H, Mechtler K, Sauer S, Schöfer C, Weipoltshammer K, Paganì M, Lachner M, Kohlmaier A. (2001). Loss of the Suv39h histone methyltransferases impairs mammalian heterochromatin and genome stability. *Cell*, 107, 323-337.
- Pieterman C, Conemans E, Dreijerink K, De Laat J, Timmers HTM, Vriens M, Valk G. (2014). Thoracic and duodenopancreatic neuroendocrine tumors in multiple endocrine neoplasia type 1: natural history and function of menin in tumorigenesis. *Endocrine-Related Cancer*, 21, 121-142.

- Placinta C, D'mello J, Macdonald A. (1999). A review of worldwide contamination of cereal grains and animal feed with *Fusarium* mycotoxins. *Animal Feed Science and Technology*, 78, 21-37.
- Podhorecka M, Skladanowski A, Bozko P. (2010). H2AX phosphorylation: its role in DNA damage response and cancer therapy. *Journal of Nucleic Acids*, 2010, 1-9.
- Pogribny IP, Pogribna M, Christman JK, James SJ. (2000). Single-site methylation within the p53 promoter region reduces gene expression in a reporter gene construct: possible in vivo relevance during tumorigenesis. *Cancer Research*, 60, 588-594.
- Porter JK, Bacon CW, Wray EM, Hagler Jr WM. (1995). Fusaric acid in *Fusarium moniliforme* cultures, corn, and feeds toxic to livestock and the neurochemical effects in the brain and pineal gland of rats. *Natural Toxins*, 3, 91-100.
- Pozuelo J. (1978). Method of pharmacologically treating drug addiction with fusaric acid. Google patents number: US4124715A.
- Prives C, Hall PA. (1999). The p53 pathway. *Journal of Pathology*, 187, 112-126.
- Quiroz EN, Quiroz RN, Lugo LP, Martínez GA, Escorcía LG, Torres HG, Bonfanti AC, Del CMM, Sanchez E, Camacho JLV. (2019). Integrated analysis of microRNA regulation and its interaction with mechanisms of epigenetic regulation in the etiology of systemic lupus erythematosus. *PloS One*, 14, 1-13.
- Rajendran G, Shanmuganandam K, Bendre A, Mujumdar D, Goel A, Shiras A. (2011). Epigenetic regulation of DNA methyltransferases: DNMT1 and DNMT3B in gliomas. *Journal of Neuro-Oncology*, 104, 483-494.
- Reddy R, Larson C, Brimer G, Frappier B, Reddy C. (1996). Developmental toxic effects of fusaric acid in CD1 mice. *Bulletin of Environmental Contamination and Toxicology*, 57, 354-360.
- Reimann M, Lee S, Loddenkemper C, Dörr JR, Tabor V, Aichele P, Stein H, Dörken B, Jenuwein T, Schmitt CA. (2010). Tumor stroma-derived TGF- $\beta$  limits myc-driven lymphomagenesis via Suv39h1-dependent senescence. *Cancer Cell*, 17, 262-272.
- Rose NR, Klose RJ. (2014). Understanding the relationship between DNA methylation and histone lysine methylation. *Biochimica et Biophysica Acta (BBA)-Gene Regulatory Mechanisms*, 1839, 1362-1372.

- Rosenfeld CS. (2010). Animal models to study environmental epigenetics. *Biology of Reproduction*, 82, 473-488.
- Ruoß M, Damm G, Vosough M, Ehret L, Grom-Baumgarten C, Petkov M, Naddalin S, Ladurner R, Seehofer D, Nussler A, Sajadian S. (2019). Epigenetic modifications of the liver tumour cell line HepG2 increase their drug metabolic capacity. *International Journal of Molecular Sciences*, 20, 347-362.
- Saito Y, Kanai Y, Nakagawa T, Sakamoto M, Saito H, Ishii H, Hirohashi S. (2003). Increased protein expression of DNA methyltransferase (DNMT) 1 is significantly correlated with the malignant potential and poor prognosis of human hepatocellular carcinomas. *International Journal of Cancer*, 105, 527-532.
- Sancak D, Ozden S. (2015). Global histone modifications in fumonisin B1 exposure in rat kidney epithelial cells. *Toxicology In Vitro*, 29, 1809-1815.
- Sapko O, Utarbaeva AS, Makulbek S. (2011). Effect of fusaric acid on prooxidant and antioxidant properties of the potato cell suspension culture. *Russian Journal of Plant Physiology*, 58, 828-835.
- Scott A, Song J, Ewing R, Wang Z. (2014). Regulation of protein stability of DNA methyltransferase 1 by post-translational modifications. *Acta Biochimica et Biophysica Sinica*, 46, 199-203.
- Shi H, Wei J, He C. (2019). Where, when, and how: context-dependent functions of RNA methylation writers, readers, and erasers. *Molecular Cell*, 74, 640-650.
- Shieh SY, Ikeda M, Taya Y, Prives C. (1997). DNA damage-induced phosphorylation of p53 alleviates inhibition by MDM2. *Cell*, 91, 325-334.
- Shimshoni J, Cuneah O, Sulyok M, Krska R, Galon N, Sharir B, Shlosberg A. (2013). Mycotoxins in corn and wheat silage in Israel. *Food Additives and Contaminants: Part A*, 30, 1614-1625.
- Singh VK, Singh HB, Upadhyay RS. (2017). Role of fusaric acid in the development of fusarium wilt symptoms in tomato: Physiological, biochemical and proteomic perspectives. *Plant Physiology and Biochemistry*, 118, 320-332.
- Smith MC, Madec S, Coton E, Hymery N. (2016). Natural co-occurrence of mycotoxins in foods and feeds and their in vitro combined toxicological effects. *Toxins*, 8, 94-129.

- Smith T, Macdonald E. (1991). Effect of fusaric acid on brain regional neurochemistry and vomiting behavior in swine. *Journal of Animal Science*, 69, 2044-2049.
- Smith TK, McMillan EG, Castillo JB. (1997). Effect of feeding blends of fusarium mycotoxin-contaminated grains containing deoxynivalenol and fusaric acid on growth and feed consumption of immature swine. *Journal of Animal Science*, 75, 2184-2191.
- Smith TK, Sousadias MG. (1993). Fusaric acid content of swine feedstuffs. *Journal of Agricultural and Food Chemistry*, 41, 2296-2298.
- So MY, Tian Z, Phoon YS, Sha S, Antoniou MN, Zhang J, Wu RS, Tan-Un KC. (2014). Gene expression profile and toxic effects in human bronchial epithelial cells exposed to zearalenone. *PLoS One*, 9, 1-19.
- Soto-Reyes E, Recillas-Targa F. (2010). Epigenetic regulation of the human p53 gene promoter by the CTCF transcription factor in transformed cell lines. *Oncogene*, 29, 2217-2227.
- Spafford MF, Koeppe J, Pan Z, Archer PG, Meyers AD, Franklin WA. (1996). Correlation of tumor markers p53, bcl-2, CD34, CD44H, CD44v6, and Ki-67 with survival and metastasis in laryngeal squamous cell carcinoma. *Archives of Otolaryngology—Head & Neck Surgery*, 122, 627-632.
- Šrobárová A, Eged Š, Da Silva JT, Ritieni A, Santini A. (2009). The use of *Bacillus subtilis* for screening fusaric acid production by *Fusarium* spp. *Czech Journal of Food Sciences*, 27, 203-209.
- Stack Jr BC, Hansen JP, Ruda JM, Jaglowski J, Shvidler J, Hollenbeak CS. (2004). Fusaric acid: a novel agent and mechanism to treat HNSCC. *Otolaryngology—Head and Neck Surgery*, 131, 54-60.
- Streit E, Schwab C, Sulyok M, Naehrer K, Krska R, Schatzmayr G. (2013). Multi-mycotoxin screening reveals the occurrence of 139 different secondary metabolites in feed and feed ingredients. *Toxins*, 5, 504-523.
- Su R, Dong L, Li C, Nachtergaele S, Wunderlich M, Qing Y, Deng X, Wang Y, Weng X, Hu C. (2018). R-2HG exhibits anti-tumor activity by targeting FTO/m6A/MYC/CEBPA signaling. *Cell*, 172, 90-105.
- Szybińska A, Leśniak W. (2017). P53 dysfunction in neurodegenerative diseases-the cause or effect of pathological changes? *Aging and disease*, 8, 506-518.

- Tang Y, Zhao W, Chen Y, Zhao Y, Gu W. (2008). Acetylation is indispensable for p53 activation. *Cell*, 133, 612-626.
- Telles-Pupulin AR, Diniz S, Bracht A, Ishii-Iwamoto E. (1996). Effects of fusaric acid on respiration in maize root mitochondria. *Biologia Plantarum*, 38, 421-429.
- Terasawa F, Kameyama M. (1971). The clinical trial of a new hypotensive agent, fusaric acid (5-butylpicolinic acid): the preliminary report. *Japanese Circulation Journal*, 35, 339-357.
- Thankam FG, Boosani CS, Dilisio MF, Agrawal DK. (2019). Epigenetic mechanisms and implications in tendon inflammation. *International Journal of Molecular Medicine*, 43, 3-14.
- Toshiharu N, Hiroyoshi H, Hiroshi K, Kazumi T, Hamao U, Tomio T, Hiroyuki S. (1970). Inhibition of dopamine  $\beta$ -hydroxylase by fusaric acid (5-butylpicolinic acid) in vitro and in vivo. *Biochemical Pharmacology*, 19, 35-44.
- Tuck SP, Crawford L. (1989). Characterization of the human p53 gene promoter. *Molecular and Cellular Biology*, 9, 2163-2172.
- Uddin MB, Roy KR, Hosain SB, Khiste SK, Hill RA, Jois SD, Zhao Y, Tackett AJ, Liu YY. (2019). An N6-methyladenosine at the transited codon 273 of p53 pre-mRNA promotes the expression of R273H mutant protein and drug resistance of cancer cells. *Biochemical Pharmacology*, 160, 134-145.
- Vaquero A, Scher M, Erdjument-Bromage H, Tempst P, Serrano L, Reinberg D. (2007). SIRT1 regulates the histone methyl-transferase SUV39H1 during heterochromatin formation. *Nature*, 450, 440-444.
- Voss K, Porter J, Bacon C, Meredith F, Norred W. (1999). Fusaric acid and modification of the subchronic toxicity to rats of fumonisins in *F. moniliforme* culture material. *Food and Chemical Toxicology*, 37, 853-861.
- Vousden KH, Prives C. (2009). Blinded by the light: the growing complexity of p53. *Cell*, 137, 413-431.
- Wang J, Zhang KY, Liu SM, Sen S. (2014a). Tumor-associated circulating microRNAs as biomarkers of cancer. *Molecules*, 19, 1912-1938.

- Wang T, Xu C, Liu Y, Fan K, Li Z, Sun X, Ouyang H, Zhang X, Zhang J, Li Y. (2012). Crystal structure of the human SUV39H1 chromodomain and its recognition of histone H3K9me2/3. *PloS One*, 7, 1-7.
- Wang X, He C. (2014). Dynamic RNA modifications in post-transcriptional regulation. *Molecular Cell*, 56, 5-12.
- Wang X, Lu Z, Gomez A, Hon GC, Yue Y, Han D, Fu Y, Parisien M, Dai Q, Jia G. (2014b). N6-methyladenosine-dependent regulation of messenger RNA stability. *Nature*, 505, 117-120.
- Wang X, Zhao BS, Roundtree IA, Lu Z, Han D, Ma H, Weng X, Chen K, Shi H, He C. (2015). N6-methyladenosine modulates messenger RNA translation efficiency. *Cell*, 161, 1388-1399.
- Wang Y, Li Y, Yue M, Wang J, Kumar S, Wechsler-Reya RJ, Zhang Z, Ogawa Y, Kellis M, Duester G. (2018). N6-methyladenosine RNA modification regulates embryonic neural stem cell self-renewal through histone modifications. *Nature Neuroscience*, 21, 195-206.
- Watson G, Wickramasekara S, Palomera-Sanchez Z, Black C, Maier C, Williams D, Dashwood R, Ho E. (2014). SUV39H1/H3K9me3 attenuates sulforaphane-induced apoptotic signaling in PC3 prostate cancer cells. *Oncogenesis*, 3, 1-9.
- Webster KE, O'bryan MK, Fletcher S, Crewther PE, Aapola U, Craig J, Harrison DK, Aung H, Phutikanit N, Lyle R. (2005). Meiotic and epigenetic defects in Dnmt3L-knockout mouse spermatogenesis. *Proceedings of the National Academy of Sciences*, 102, 4068-4073.
- Weiland M, Gao XH, Zhou L, Mi QS. (2012). Small RNAs have a large impact: circulating microRNAs as biomarkers for human diseases. *RNA Biology*, 9, 850-859.
- Winter J, Jung S, Keller S, Gregory RI, Diederichs S. (2009). Many roads to maturity: microRNA biogenesis pathways and their regulation. *Nature Cell Biology*, 11, 228-234.
- Woo HH, Chambers SK. (2019). Human ALKBH3-induced m1A demethylation increases the CSF-1 mRNA stability in breast and ovarian cancer cells. *Biochimica et Biophysica Acta (BBA)-Gene Regulatory Mechanisms*, 1862, 35-46.
- Xiao W, Adhikari S, Dahal U, Chen YS, Hao YJ, Sun BF, Sun HY, Li A, Ping XL, Lai WY. (2016). Nuclear m6A reader YTHDC1 regulates mRNA splicing. *Molecular Cell*, 61, 507-519.

- Yarychivska O, Shahabuddin Z, Comfort N, Boulard M, Bestor TH. (2018). BAH domains and a histone-like motif in DNA methyltransferase 1 (DNMT1) regulate de novo and maintenance methylation in vivo. *Journal of Biological Chemistry*, 293, 19466-19475.
- Ye J, Montero M, Stack Jr BC. (2013). Effects of fusaric acid treatment on HEP2 and docetaxel-resistant HEP2 laryngeal squamous cell carcinoma. *Chemotherapy*, 59, 121-128.
- Yiannikouris A, Jouany JP. (2002). Mycotoxins in feeds and their fate in animals: a review. *Animal Research*, 51, 81-99.
- Yin ES, Rakhmankulova M, Kucera K, De Sena Filho JG, Portero CE, Narváez-Trujillo A, Holley SA, Strobel SA. (2015). Fusaric acid induces a notochord malformation in zebrafish via copper chelation. *BioMetals*, 28, 783-789.
- Zain ME. (2011). Impact of mycotoxins on humans and animals. *Journal of Saudi Chemical Society*, 15, 129-144.
- Zamudio NM, Scott HS, Wolski K, Lo CY, Law C, Leong D, Kinkel SA, Chong S, Jolley D, Smyth GK. (2011). DNMT3L is a regulator of X chromosome compaction and post-meiotic gene transcription. *PLoS One*, 6, 1-12.
- Zhang B, Chen J, Cheng AS, Ko BC. (2014). Depletion of sirtuin 1 (SIRT1) leads to epigenetic modifications of telomerase (TERT) gene in hepatocellular carcinoma cells. *PLoS One*, 9, 84931-84937.
- Zhang YJ, Ahsan H, Chen Y, Lunn RM, Wang LY, Chen SY, Lee PH, Chen CJ, Santella RM. (2002). High frequency of promoter hypermethylation of RASSF1A and p16 and its relationship to aflatoxin B1-DNA adduct levels in human hepatocellular carcinoma. *Molecular Carcinogenesis*, 35, 85-92.
- Zhang YJ, Chen Y, Ahsan H, Lunn RM, Lee PH, Chen CJ, Santella RM. (2003). Inactivation of the DNA repair gene O6-methylguanine-DNA methyltransferase by promoter hypermethylation and its relationship to aflatoxin B1-DNA adducts and p53 mutation in hepatocellular carcinoma. *International Journal of Cancer*, 103, 440-444.
- Zheng G, Dahl JA, Niu Y, Fedorcsak P, Huang CM, Li CJ, Vågbø CB, Shi Y, Wang WL, Song SH. (2013). ALKBH5 is a mammalian RNA demethylase that impacts RNA metabolism and mouse fertility. *Molecular Cell*, 49, 18-29.

Zheng H, Chen L, Pledger WJ, Fang J, Chen J. (2014). p53 promotes repair of heterochromatin DNA by regulating JMJD2b and SUV39H1 expression. *Oncogene*, 33, 734-744.

Zhu CC, Hou YJ, Han J, Cui XS, Kim NH, Sun SC. (2014). Zearalenone exposure affects epigenetic modifications of mouse eggs. *Mutagenesis*, 29, 489-495.

Zhu CC, Zhang Y, Duan X, Han J, Sun SC. (2016). Toxic effects of HT-2 toxin on mouse oocytes and its possible mechanisms. *Archives of Toxicology*, 90, 1495-1505.

## CHAPTER 3

### **Fusaric acid-induced promoter methylation of DNA methyltransferases triggers DNA hypomethylation in human hepatocellular carcinoma (HepG2) cells**

Terisha Ghazi, Savania Nagiah, Pragalathan Naidoo, and Anil A. Chuturgoon\*

Discipline of Medical Biochemistry and Chemical Pathology, School of Laboratory Medicine and Medical Science, College of Health Sciences, Howard College Campus, University of Kwa-Zulu Natal, Durban 4041, South Africa

\*Corresponding author: Professor Anil A. Chuturgoon, Discipline of Medical Biochemistry and Chemical Pathology, School of Laboratory Medicine and Medical Science, College of Health Sciences, Howard College Campus, University of Kwa-Zulu Natal, Durban 4041, South Africa. Telephone: +27 31 260 4404; Fax: +27 31 260 4785; Email: [CHUTUR@ukzn.ac.za](mailto:CHUTUR@ukzn.ac.za)

#### **Author Email Addresses:**

Terisha Ghazi: [terishaghazi@gmail.com](mailto:terishaghazi@gmail.com)

Savania Nagiah: [nagiah.savania@gmail.com](mailto:nagiah.savania@gmail.com)

Pragalathan Naidoo: [pragalathan.naidoo@gmail.com](mailto:pragalathan.naidoo@gmail.com)

Anil A. Chuturgoon: [CHUTUR@ukzn.ac.za](mailto:CHUTUR@ukzn.ac.za)

**Epigenetics 14 (8): 804-817 (2019)**

**DOI: 10.1080/15592294.2019.1615358**

## ABSTRACT

Fusaric acid (FA), a mycotoxin contaminant of maize, displays toxicity in plants and animals; however, its epigenetic mechanism is unknown. DNA methylation, an epigenetic modification that regulates gene expression, is mediated by DNA methyltransferases (DNMTs; DNMT1, DNMT3A, and DNMT3B) and demethylases (MBD2). The expression of DNMTs and demethylases are regulated by promoter methylation, microRNAs (miR-29b), and post-translational modifications (ubiquitination). Alterations in these DNA methylation modifying enzymes affect DNA methylation patterns and offer novel mechanisms of FA toxicity. We determined the effect of FA on global DNA methylation as well as a mechanism of FA-induced changes in DNA methylation by transcriptional (promoter methylation), post-transcriptional (miR-29b), and post-translational (ubiquitination) regulation of DNMTs and MBD2 in the human hepatocellular carcinoma (HepG2) cell line. FA induced global DNA hypomethylation ( $p < 0.0001$ ) in HepG2 cells. FA decreased the mRNA and protein expression of DNMT1 ( $p < 0.0001$ ), DNMT3A ( $p < 0.0001$ ), and DNMT3B ( $p < 0.0001$ ) by upregulating miR-29b ( $p < 0.0001$ ) and inducing promoter hypermethylation of *DNMT1* ( $p < 0.0001$ ) and *DNMT3B* ( $p < 0.0001$ ). FA decreased the ubiquitination of DNMT1 ( $p = 0.0753$ ), DNMT3A ( $p = 0.0008$ ), and DNMT3B ( $p < 0.0001$ ) by decreasing *UHRF1* ( $p < 0.0001$ ) and *USP7* ( $p < 0.0001$ ). FA also induced *MBD2* promoter hypomethylation ( $p < 0.0001$ ) and increased MBD2 expression ( $p < 0.0001$ ). Together these results indicate that FA induces global DNA hypomethylation by altering *DNMT* promoter methylation, upregulating miR-29b, and increasing MBD2 in HepG2 cells.

**KEYWORDS:** Fusaric acid; global DNA hypomethylation; promoter methylation; DNA methyltransferases; miR-29b; DNMT ubiquitination; MBD2

## Introduction

Fusaric acid (FA; 5-butylpicolinic acid), a ubiquitous mycotoxin and secondary metabolite produced by pathogenic fungi of the genus *Fusarium*, contaminates agricultural foods and exhibits low to moderate toxicity [1]. Previously, feed samples were reported to contain an average of 643 µg/kg FA [2] and approximately 2.5 to 18 µg/kg FA were reported to contaminate commercial foods and feeds [3]. These foods, especially maize, form an essential part of the human and animal diet; and the consumption of FA-contaminated commodities may have serious health implications. Studies evaluating the effects of FA are limited and understanding the molecular and epigenetic effects of FA exposure is important in decreasing FA contamination and lowering the risk of FA-related adverse health outcomes.

FA is phytotoxic to several plants by inhibiting root and leaf cell function [4] and has been implicated in the pathogenesis of wilt diseases [4, 5, 6, 7]; it is a highly lipophilic toxin that traverses cellular membranes and induces toxicity by altering various biochemical processes. Known mechanisms of FA toxicity include alterations in membrane permeability [5, 7], oxidative stress [8, 9], mitochondrial dysfunction [6, 10, 11], DNA damage [12, 13], and apoptosis [10, 12, 14, 15]. It is also immuno-toxic to peripheral blood mononuclear cells (PBMCs) and human monocytic (THP-1) cells [14]. FA has tumouristatic and tumouricidal effects in several mammalian tumor cell lines, thereby, displaying anti-cancer activity [13, 16]. It has neurochemical effects in mice brain and reduced aggressive behavior and motor activity [17]. FA also attenuates isoproterenol induced heart failure by preventing the development of cardiac hypertrophy and fibrosis [18].

FA is a chelating agent and the removal of essential divalent cations such as calcium affects bone ossification [19] and blood coagulation [20]; it also chelates copper causing hypotension [21, 22] and notochord malformation [23]. The toxicity of FA may also be attributed to synergistic interactions with other co-occurring mycotoxins such as fumonisin B<sub>1</sub> (FB<sub>1</sub>) [24], deoxynivalenol (DON) [25], and 4,15-diacetoxyscirpenol (DAS) [26].

DNA methylation is a common epigenetic modification that regulates gene expression and plays a major role in cell signaling pathways that are essential in the normal growth and development of higher organisms. Dysregulation in the DNA methylation pattern has been observed in several human diseases such as cancer [27] and neurodegeneration [28]. DNA methylation is catalyzed by DNA methyltransferases (DNMTs) such as DNMT1, DNMT3A, and DNMT3B. DNMT1 is a maintenance DNMT that binds specifically to hemi-methylated DNA and is responsible for conserving the methylation pattern from one generation to the next [29].

DNMT3A and DNMT3B are *de novo* DNMTs that target unmethylated cytosine bases to initiate methylation [29]. DNMTs are the major regulators of DNA methylation and alterations in their expression and activity affects DNA methylation patterns and cellular function. The activity and stability of DNMTs are regulated by promoter methylation, microRNAs, and post-translational modifications (PTMs).

Promoter methylation, methylation of CpG islands within the promoter region of specific genes, is important in regulating gene transcription; promoter hypermethylation prevents binding of transcription factors and inhibits gene transcription, whereas promoter hypomethylation activates gene transcription.

MicroRNAs are small non-coding RNA molecules that post-transcriptionally regulate gene expression by binding to the 3' untranslated region (3'UTR) of the target messenger RNA (mRNA) and negatively regulating the processing, stability, and translation of the mRNA [30]. MiR-29 plays a major role in cell proliferation, differentiation, and apoptosis [31, 32]. The miR-29 family consists of two clusters: cluster 1, located on chromosome 7q32.3, consists of miR-29a and miR-29b-1; and cluster 2, located on chromosome 1q32.2, consists of miR-29b-2 and miR-29c. MiR-29b-1 and miR-29b-2 have identical mature sequences and are collectively referred to as miR-29b. Several effects of miR-29b have been identified such as activating the tumor suppressor protein, p53 and regulating cell proliferation, and apoptosis by targeting *p85α* and the *cell division cycle 42 (CDC42)* [31, 32]. It prevents liver fibrosis by targeting the PI3K/AKT signaling pathway [33], and targets *AKT2* and *AKT3* to regulate the Warburg effect in ovarian cancer cells [34]. MiR-29b can also regulate the DNA methylation status of the cell in a negative feedback loop by directly targeting *DNMT3A* and *DNMT3B* [35, 36]. Furthermore, the expression of miR-29b is itself epigenetically regulated and thus inversely correlated with the DNA methylation status of the cell.

PTMs also regulate the expression and activity of DNMTs. These modifications occur in the N- and C-terminal regions of the protein and include acetylation and ubiquitination [29]. The acetylation of DNMTs is regulated by the acetyltransferase, Tip60 and the deacetylases, HDAC1 and HDAC2 [29, 37, 38]. The ubiquitination of DNMTs is triggered by DNMT acetylation and is regulated by the E3 ligase, ubiquitin-like and ring finger domain 1 (UHRF1), and the deubiquitylating enzyme, ubiquitin specific peptidase 7 (USP7) [29, 37, 38]. The ubiquitination of DNMTs play a major role in inhibiting DNMT stability and promoting proteasomal degradation.

DNA methylation forms a platform for several methyl binding proteins. Methyl-CpG binding domain proteins (MBDs) are a family of nuclear proteins that play an important role in regulating DNA methylation and gene transcription by recruiting chromatin remodeling complexes to regions of methylated DNA. Several MBDs have been identified (MBD1-6); however, MBD2 is the major MBD that binds specifically to methylated CpG islands and acts as a methylation-dependent transcriptional repressor and DNA demethylase [39].

Although several effects of FA have been described, the effect of FA on epigenetic regulation has not been determined. This study aimed to determine an epigenetic effect of FA in the human hepatocellular carcinoma (HepG2) cell line, as a mechanism of FA-induced toxicity. The effect of FA on global DNA methylation as well as the mechanism of FA-induced changes in DNA methylation by transcriptional (promoter methylation), post-transcriptional (miR-29b), and post-translational (ubiquitination) regulation of DNMTs and MBD2 was determined.

## **Results**

### ***Fusaric acid induced global DNA hypomethylation in HepG2 cells***

We first determined the effect of FA on global DNA methylation in liver (HepG2) cells. 5-methylcytosine, a common marker of global DNA methylation, was quantified using a commercialized kit (Abcam, ab117128) and 5-aza-2-DC was used as a negative control. The percentage of 5-methylcytosine in the 5-aza-2-DC and FA-treated HepG2 cells were decreased compared to the control ( $p < 0.0001$ ; Figure 3.1). This suggested that FA induced a dose-dependent decrease in global DNA methylation in HepG2 cells.

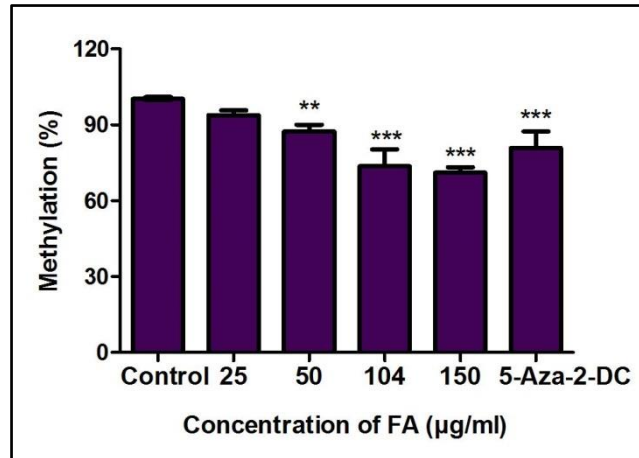


**Figure 3.1 Fusaric acid induced global DNA hypomethylation in HepG2 cells.** DNA isolated from control and FA-treated HepG2 cells were assayed for global DNA methylation by quantifying 5-methylcytosine using a Colorimetric Methylated DNA Quantification Kit. Fusaric acid decreased the percentage of 5-methylcytosine in HepG2 cells compared to the control. Results are represented as mean fold-change  $\pm$  SD (n = 3). Statistical significance was determined by one-way ANOVA with the Bonferroni multiple comparisons test (\*\* $p < 0.005$ , \*\*\* $p < 0.0001$ ).

***Fusaric acid decreased the expression of DNMT1, DNMT3A, and DNMT3B in HepG2 cells***

The DNMTs, DNMT1, DNMT3A, and DNMT3B, play a major role in initiating and maintaining DNA methylation patterns. Due to the FA-induced global DNA hypomethylation in the HepG2 cells, we evaluated the mRNA and protein expressions of DNMT1, DNMT3A, and DNMT3B. FA significantly decreased the mRNA expression of *DNMT1* ( $p < 0.0001$ ; Figure 3.2A), *DNMT3A* ( $p < 0.0001$ ; Figure 3.2A), and *DNMT3B* ( $p < 0.0001$ ; Figure 3.2A) in HepG2 cells compared to the control. The protein expression of DNMT1 ( $p < 0.0001$ ; Figure 3.2B), DNMT3A ( $p < 0.0001$ ; Figure 3.2B), and DNMT3B ( $p < 0.0001$ ; Figure 3.2B) was also significantly decreased in the FA-treated HepG2 cells compared to the control.

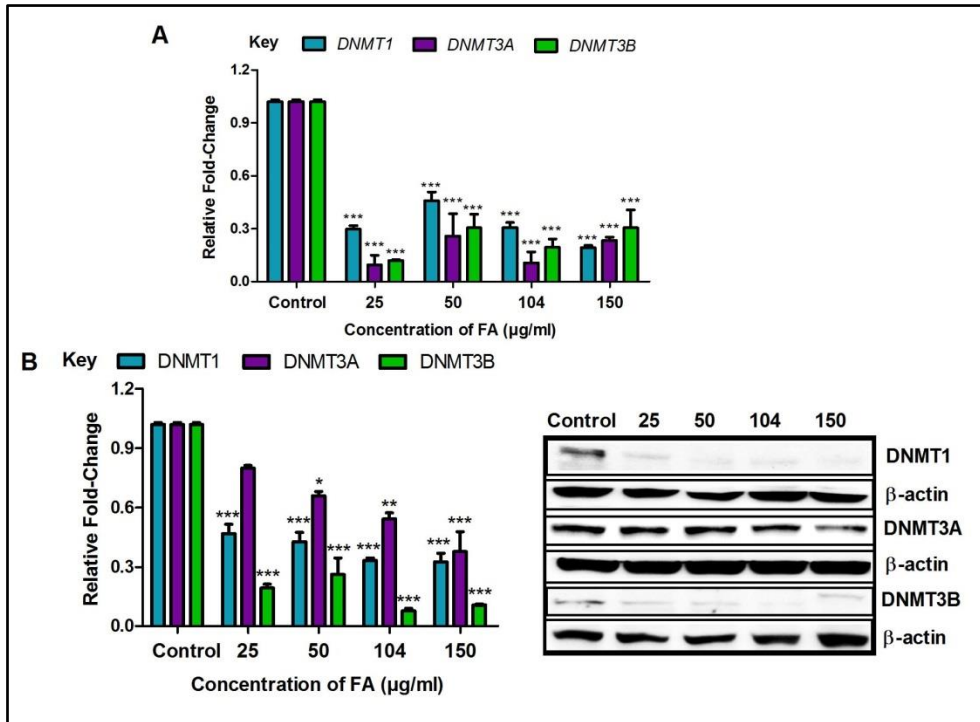


**Figure 3.2** The effect of FA on DNA methyltransferases in HepG2 cells. (A) RNA isolated from control and FA-treated HepG2 cells were reverse transcribed into cDNA and analyzed by qPCR. Fusaric acid significantly decreased the mRNA expression of *DNMT1*, *DNMT3A*, and *DNMT3B* in HepG2 cells. (B) Protein expression of DNMT1, DNMT3A, and DNMT3B were determined by western blot. Fusaric acid decreased the protein expression of DNMT1, DNMT3A, and DNMT3B in HepG2 cells. Results are represented as mean fold-change  $\pm$  SD ( $n = 3$ ). Statistical significance was determined by one-way ANOVA with the Bonferroni multiple comparisons test (\* $p < 0.05$ , \*\* $p < 0.005$ , \*\*\* $p < 0.0001$ ).

### *Fusaric acid altered DNMT promoter methylation in HepG2 cells*

The methylation of gene promoters plays a major role in determining transcriptional activity and gene expression. We determined if the decrease in the mRNA expression of *DNMT1*, *DNMT3A*, and *DNMT3B* observed in the FA-treated HepG2 cells were a result of promoter methylation. FA significantly increased promoter methylation of *DNMT1* ( $p < 0.0001$ ; Figure 3.3) and *DNMT3B* ( $p < 0.0001$ ; Figure 3.3) in HepG2 cells compared to the control; however, the promoter methylation of *DNMT3A* was decreased in the lower FA concentrations (25, 50, and 104 µg/ml) and increased in the higher FA concentration (150 µg/ml) ( $p < 0.0001$ ; Figure 3.3).

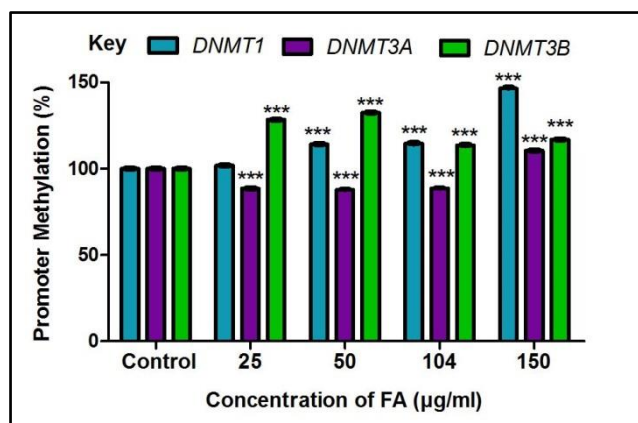


**Figure 3.3** The effect of FA on the promoter methylation of *DNMT1*, *DNMT3A*, and *DNMT3B* in HepG2 cells. DNA isolated from control and FA-treated HepG2 cells were assayed for *DNMT* promoter methylation using the OneStep qMethyl Kit. Fusaric acid induced promoter hypermethylation of *DNMT1* and *DNMT3B*, and altered promoter methylation of *DNMT3A* in HepG2 cells. Results are represented as mean fold-change  $\pm$  SD (n = 3). Statistical significance was determined by one-way ANOVA with the Bonferroni multiple comparisons test (\*\*\*)  $p < 0.0001$ .

***Fusaric acid decreased miR-29b promoter methylation, upregulated miR-29b, and decreased the expression of Sp1 in HepG2 cells***

The expression of miR-29b is regulated by DNA methylation; miR-29b is silenced by DNA hypermethylation whereas DNA hypomethylation is known to upregulate miR-29b [36]. Since FA induced DNA hypomethylation in HepG2 cells, we determined the effect of FA on the promoter methylation and expression of miR-29b. FA significantly decreased the promoter methylation of miR-29b ( $p < 0.0001$ ; Figure 3.4A) and increased the expression of miR-29b ( $p < 0.0001$ ; Figure 3.4B) in HepG2 cells compared to the control. The expression of miR-29b was also significantly increased by 5-aza-2-DC ( $p < 0.0001$ ; Figure 3.4B).

MiR-29b is also a known regulator of *DNMT* expression. MiR-29b was previously shown to directly target *DNMT3A* and *DNMT3B* and indirectly target *DNMT1* via repression of the transcriptional activator, *Sp1* [35, 36, 40]. This was confirmed using the bioinformatics prediction algorithm software, TargetScan version 7.1. MiR-29b was found to have complementary base pairs with *DNMT3A* at positions 862 – 868, 1305 – 1311 and 5559 – 5565; *DNMT3B* at position 1202 – 1209; and *Sp1* at position 3584 – 3591 (Figure 3.4C). *DNMT1* was not a direct target of miR-29b. Due to the increase in miR-29b and decrease in *DNMT* expression by FA, we then determined the effect of FA on the mRNA expression of *Sp1*. FA significantly decreased the expression of *Sp1* ( $p < 0.0001$ ; Figure 3.4D) in HepG2 cells

compared to the control. These data suggest that the decrease in the mRNA expression of *DNMT1*, *DNMT3A*, and *DNMT3B* may be influenced by miR-29b.

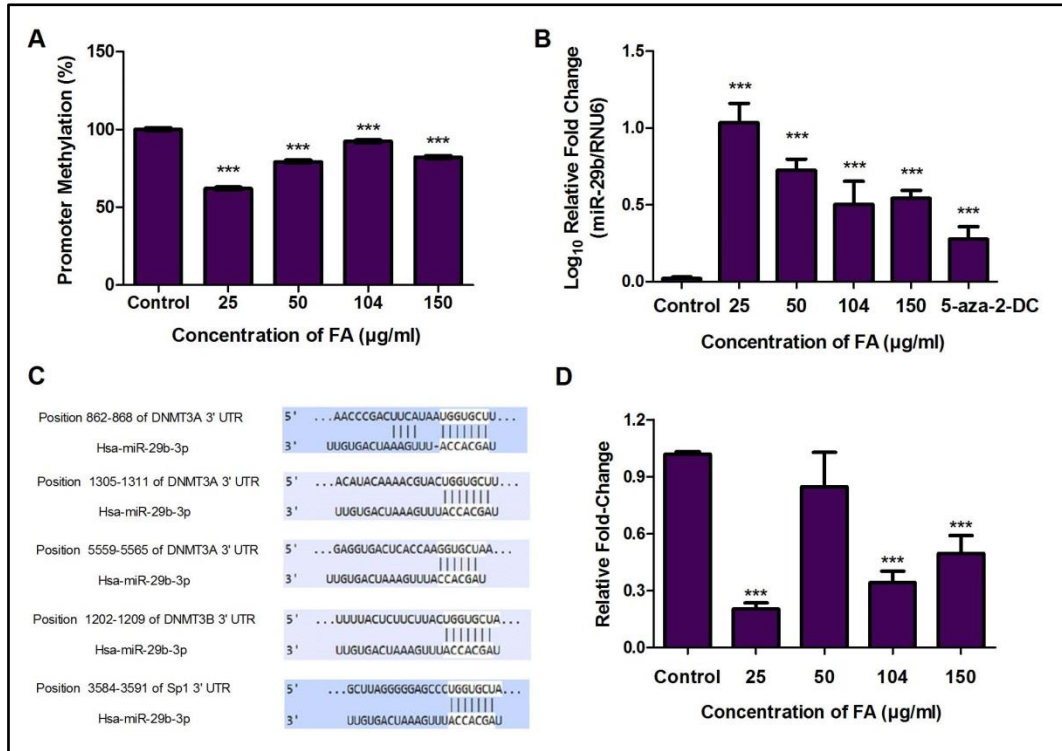


**Figure 3.4** The effect of FA on miR-29b and *Sp1* in HepG2 cells. (A) DNA isolated from control and FA-treated HepG2 cells were assayed for miR-29b promoter methylation using the OneStep qMethyl Kit. Fusaric acid induced promoter hypomethylation of miR-29b in HepG2 cells. (B) RNA isolated from control and FA-treated HepG2 cells were reverse transcribed into cDNA and analyzed by qPCR. Fusaric acid significantly increased the expression of miR-29b in HepG2 cells. (C) TargetScan analysis of miR-29b to the 3'UTRs of *DNMT3A*, *DNMT3B*, and *Sp1*. (D) RNA isolated from control and FA-treated HepG2 cells were reverse transcribed into cDNA and analyzed for *Sp1* expression by qPCR. Fusaric acid decreased the mRNA expression of *Sp1* in HepG2 cells. Results are represented as mean fold-change  $\pm$  SD (n = 3). Statistical significance was determined by one-way ANOVA with the Bonferroni multiple comparisons test (\*\*\*)  $p < 0.0001$ .

***Fusaric acid decreased the ubiquitination of DNMT1, DNMT3A, and DNMT3B by decreasing the expression of UHRF1 and USP7 in HepG2 cells***

PTMs such as acetylation and ubiquitination regulate the activity and expression of DNMTs. The acetylation of DNMTs triggers the ubiquitination of DNMTs leading to proteasomal degradation. We determined if the decrease in the protein expression of DNMT1, DNMT3A,

and DNMT3B in the FA treatments were a result of the ubiquitination and proteasomal degradation of the DNMTs. FA significantly decreased the ubiquitination of DNMT1 ( $p = 0.0753$ ; Figure 3.5A), DNMT3A ( $p = 0.0008$ ; Figure 3.5A), and DNMT3B ( $p < 0.0001$ ; Figure 3.5A) in HepG2 cells compared to the control. However, at 150  $\mu\text{g/ml}$  FA the ubiquitination of DNMT1 and DNMT3B were increased.

The ubiquitination regulators, UHRF1 and USP7, are the major enzymes responsible for ubiquitinating and deubiquitinating DNMTs, respectively. The FA-induced decrease in the ubiquitination of DNMT1, DNMT3A, and DNMT3B led to the assessment of *UHRF1* and *USP7*. FA significantly decreased the mRNA expression of *UHRF1* ( $p < 0.0001$ ; Figure 3.5B) and *USP7* ( $p < 0.0001$ ; Figure 3.5B) in HepG2 cells compared to the control. These results indicate that the decrease in the protein expression of DNMT1, DNMT3A, and DNMT3B observed in the FA-treated cells is not due to the ubiquitination and proteasomal degradation of DNMTs.

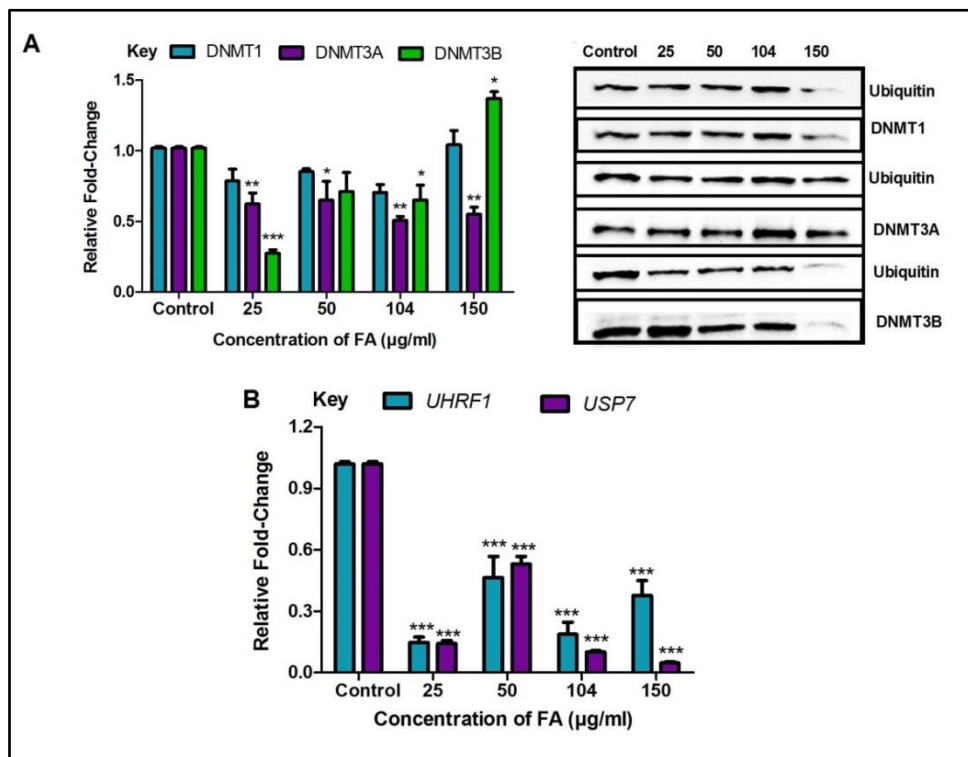


**Figure 3.5 The effect of FA on the ubiquitination of DNMT1, DNMT3A, and DNMT3B in HepG2 cells. (A)** The ubiquitination of DNMT1, DNMT3A, and DNMT3B were detected by immuno-precipitation and western blot. Fusaric acid altered the ubiquitination of DNMT1, DNMT3A, and DNMT3B in HepG2 cells. **(B)** RNA isolated from control and FA-treated HepG2 cells were reverse transcribed into cDNA and analyzed by qPCR. Fusaric acid significantly decreased the expression of *UHRF1* and *USP7* in HepG2 cells. Results are

represented as mean fold-change  $\pm$  SD ( $n = 3$ ). Statistical significance was determined by one-way ANOVA with the Bonferroni multiple comparisons test ( $*p < 0.05$ ,  $**p < 0.005$ ,  $***p < 0.0001$ ).

### ***Fusaric acid induced MBD2 promoter hypomethylation and increased the expression of MBD2 in HepG2 cells***

Methyl CpG binding domain protein 2 (MBD2), a major MBD, promotes global DNA hypomethylation by binding specifically to methylated DNA and functioning as a methylation-dependent transcriptional repressor and DNA demethylase. We determined if the FA-induced decrease in global DNA methylation occurred as a result of MBD2. FA significantly decreased *MBD2* promoter methylation ( $p < 0.0001$ ; Figure 3.6A) and increased the protein expression of MBD2 ( $p < 0.0001$ ; Figure 3.6B) in HepG2 cells compared to the control. The mRNA expression of *MBD2* ( $p < 0.0001$ ), and other MBDs such as *MBD1* ( $p < 0.0001$ ), *MBD3* ( $p < 0.0001$ ), *MBD4* ( $p < 0.0001$ ), *MBD5* ( $p < 0.0001$ ), and *MBD6* ( $p < 0.0001$ ) were significantly decreased in the FA-treated cells compared to the control (Supplementary Table S3.1).

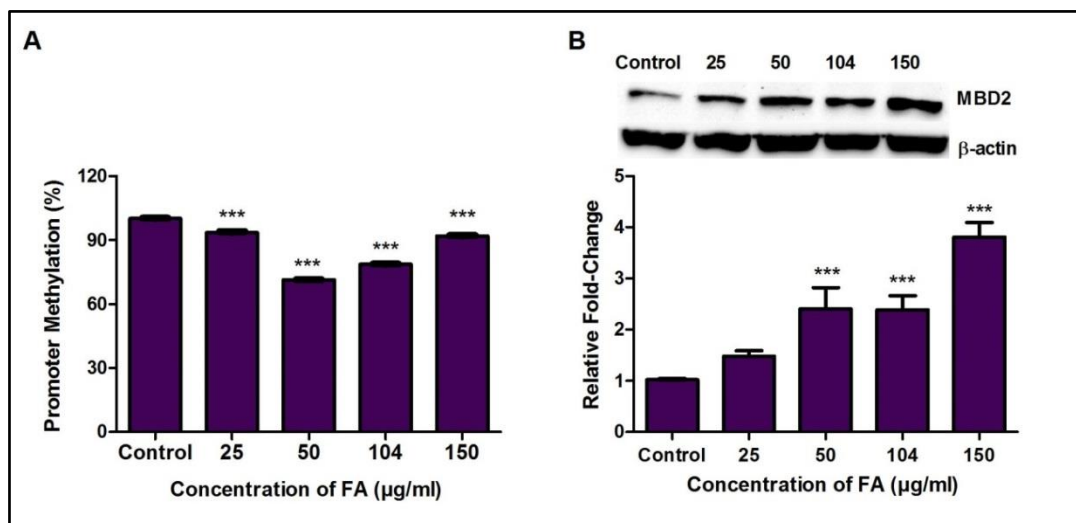


**Figure 3.6** The effect of FA on *MBD2* promoter methylation and MBD2 expression in HepG2 cells. (A) DNA isolated from control and FA-treated HepG2 cells were assayed for *MBD2* promoter methylation using the OneStep qMethyl Kit. Fusaric acid significantly induced promoter hypomethylation of *MBD2* in HepG2 cells. (B) Protein expression of MBD2 was determined by western blot. Fusaric acid significantly increased the protein expression of MBD2 in HepG2 cells. Results are represented as mean fold-change  $\pm$  SD ( $n = 3$ ). Statistical significance was determined by one-way ANOVA with the Bonferroni multiple comparisons test ( $***p < 0.0001$ ).

## Discussion

FA, a neglected mycotoxin found in agricultural foods, alters biological pathways causing toxicity in various plant and animal models. To date several mechanisms of FA toxicity have been described [10, 12, 14, 15, 20, 21, 23]; however, the effect of FA on epigenetic modifications is unknown. DNA methylation is an important epigenetic modification that regulates chromatin structure and alters gene expression and thus may play a crucial role in FA toxicity. In this study, we provide evidence that FA alters global DNA methylation in HepG2 cells by modulating the expression of DNMTs and demethylases in a mechanism that involves alterations in promoter methylation and miR-29b expression, but not the ubiquitination of DNMTs.

FA induced global DNA hypomethylation in HepG2 cells as evidenced by the significant decrease in 5-methylcytosine content (Figure 3.1); this global DNA hypomethylation is due to a concomitant decrease in the expression of the *de novo* methyltransferases, DNMT3A and DNMT3B, and the maintenance methyltransferase, DNMT1 (Figure 3.2A and Figure 3.2B) as well as an increase in the demethylase, MBD2 (Figure 3.6B). Furthermore, FA altered the mRNA expression of *DNMT1* and *DNMT3B* by inducing promoter hypermethylation (Figure 3.3). This is in agreement with previous studies in which promoter hypermethylation of *DNMT1* and *DNMT3B* decreased the mRNA expression of *DNMT1* and *DNMT3B*, respectively [41, 42]. Although promoter hypomethylation of *DNMT3A* is associated with an increase in the transcription of *DNMT3A*, the decrease in *DNMT3A* mRNA transcript levels observed in the FA-treated HepG2 cells suggests possible regulation at the post-transcriptional level.

MicroRNAs regulate gene expression at the post-transcriptional level. This occurs in a sequence specific manner and leads to either the degradation of the target mRNA or inhibition of translation. MiR-29b, regulated by DNA methylation, was previously shown to repress DNA methylation by directly targeting *DNMT3A* and *DNMT3B*, and indirectly targeting *DNMT1* by inhibiting the transcriptional activator, *Sp1* [35, 36]. This was further confirmed using TargetScan version 7.1 (Figure 3.4C). FA significantly upregulated the expression of miR-29b in HepG2 cells (Figure 3.4B) and the expression of miR-29b was inversely correlated with the DNA methylation status in the FA-treated HepG2 cells, as evidenced by the significant decrease in miR-29b promoter methylation (Figure 3.4A). The upregulation of miR-29b also corresponds with the decrease in the mRNA expression of *Sp1*, *DNMT1*, *DNMT3A*, and *DNMT3B* in the FA-treated cells. This is in agreement with previous studies where overexpression of miR-29b was found to downregulate the expression of *DNMT3A* and *DNMT3B*, and induce global DNA

hypomethylation in acute myeloid leukemia (AML) and lung cancer cells [35, 36]. Overexpression of miR-29b in AML was also shown to downregulate the expression of *Sp1* causing a subsequent decrease in *DNMT1* expression and global DNA hypomethylation [35, 40]. Therefore, these results indicate that the FA-induced increase in miR-29b expression may be an alternative mechanism for the reduced *DNMT3A* mRNA expression and an additional mechanism for the reduced *DNMT1* and *DNMT3B* mRNA expressions.

The protein expression of DNMT1, DNMT3A, and DNMT3B were also significantly decreased in the FA-treated HepG2 cells (Figure 3.2B). PTMs such as acetylation and ubiquitination play a major role in influencing the catalytic activity, stability, and protein-protein interactions of DNMTs. The acetylation of DNMTs is mediated by Tip60 and primes DNMTs for UHRF1-mediated ubiquitination and proteasomal degradation [29, 37, 38]. The DNMTs are deacetylated by HDAC1 and HDAC2, and deubiquitinated by USP7.

The role of acetylation and ubiquitination on the regulation of DNMT1 is well understood. The acetylation of DNMT1 on lysine (K) residues, K1349 and K1415, in the catalytic domain decreases DNMT1 activity whereas the acetylation of K1111, K1113, K1115, and K1117 in the lysine-glycine rich (KG)-repeat increases the transcriptional repressor activity of DNMT1 [43]. The acetylation of lysine residues in the KG-repeat also increases the DNMT1-UHRF1 interaction and impairs the DNMT1-USP7 interaction, thereby, promoting the ubiquitination and degradation of DNMT1 [44, 45]. The overexpression of UHRF1 was also shown to increase the ubiquitination of DNMT1 and decrease DNMT1 expression [44]. Previous studies also indicate that UHRF1 physically interacts with DNMT3A and DNMT3B, thereby, inhibiting the activity of both DNMT3A and DNMT3B and promoting proteasomal degradation [46].

The decrease in the protein expression of DNMT1, DNMT3A, and DNMT3B in the FA-treated HepG2 cells suggested that FA may also decrease the protein expression of DNMTs by ubiquitination and proteasomal degradation. In fact, FA actually decreased the ubiquitination of DNMT1, DNMT3A, and DNMT3B in HepG2 cells (Figure 3.5A). The expression of *UHRF1* and *USP7* was also significantly decreased in the FA-treated cells (Figure 3.5B), suggesting that the decrease in the ubiquitination of DNMT1, DNMT3A, and DNMT3B was a result of *UHRF1* and *USP7*. Thus, the FA-induced decrease in the protein expression of DNMT1, DNMT3A, and DNMT3B was due to the increased *DNMT* promoter methylation and/or miR-29b expression and a subsequent inhibition of translation, and not the ubiquitination and proteasomal degradation of the DNMT protein.

UHRF1 also contains a methyl DNA-binding domain, SRA (SET and RING associated) domain, that binds preferentially to hemi-methylated DNA and functions to recruit DNMT1 to hemi-methylated CpG islands to facilitate maintenance of DNA methylation [47]. The observed decrease in global DNA methylation in the FA-treated HepG2 cells may also occur as a result of the decrease in UHRF1 and DNMT1 leading to a loss in the maintenance of DNA methylation.

In addition to alterations in the expression of DNMTs and UHRF1, FA may also induce global DNA hypomethylation by targeting the transcriptional repressor and demethylase, MBD2. MBD2 plays an essential role in hypomethylation and was previously shown to activate gene expression by promoting demethylation of several target genes. Our results indicate that FA induced *MBD2* promoter hypomethylation (Figure 3.6A) and increased the protein expression of MBD2 (Figure 3.6B) in HepG2 cells. This occurred despite the significant decrease in the mRNA expression of *MBD2* (Supplementary Table S3.1), and suggests that the FA-induced expression of MBD2 may contribute to global DNA hypomethylation. Previous studies indicate *MBD2* promoter hypomethylation to be associated with active gene transcription and an increase in *MBD2* expression. Although MBD2 is associated with gene activation, overexpression of MBD2 and global DNA hypomethylation leads to genomic instability in several human cancers [48, 49].

Global DNA hypomethylation is considered a hallmark of cancer as it leads to genomic instability and increases the frequency of mutations [50]. Global DNA hypomethylation also inhibits cellular differentiation [51] and induces apoptosis [51, 52, 53, 54]. Previously, FB<sub>1</sub>, a *Fusarium* derived mycotoxin often co-produced with FA, was shown to induce global DNA hypomethylation (by modulating the expression of DNMTs and MBD2) and histone demethylation, possibly leading to chromatin instability and liver tumourigenesis [55]. FB<sub>1</sub> also alters promoter methylation of tumor suppressor genes (*c-myc*, *p15*, *p16*, and *e-cadherin*) [56, 57], inhibits miR-27b and increases cytochrome P450 1B1 [58] leading to hepatic neoplastic transformation. Zearalenone also induces global DNA hypomethylation and reduces the viability of human bronchial epithelial cells via DNA damage, cell cycle arrest, and apoptosis [59]. In contrary, other *Fusarium* produced mycotoxins such as deoxynivalenol and T2 toxin induce global DNA hypermethylation and histone demethylation [60, 61]. The toxicity of FA has been mainly attributed to oxidative stress, DNA damage, and apoptosis [10, 12, 13, 14, 15, 62], and the FA-induced global DNA hypomethylation may provide an alternative mechanism by which FA induces its genotoxic and cytotoxic effects.

In conclusion, this study provides an alternative mechanism of FA-induced genotoxicity and cytotoxicity at the epigenetic level. The results indicate that FA induces global DNA

hypomethylation in HepG2 cells by decreasing the expression of DNMT1, DNMT3A, and DNMT3B and increasing the expression of MBD2 (Figure 3.7). The results further indicate that FA decreases the expression of DNMT1, DNMT3A, DNMT3B, and MBD2 proteins by increasing promoter methylation and/or by upregulating miR-29b. It has also been shown that miR-29b itself can be regulated by DNA methylation, and that reduced methylation as seen globally following treatment with FA may lead to increased expression of miR-29b. These findings suggest that FA-induced changes in DNA methylation may potentially be used as a biomarker for FA exposure and toxicity. Finally, targeting the DNA methylation pathway via epigenetic modulation of DNMTs and miR-29b may provide a therapeutic intervention against FA toxicity; this is particularly important in poverty stricken areas where maize forms a staple diet and the risk of FA contamination is high.

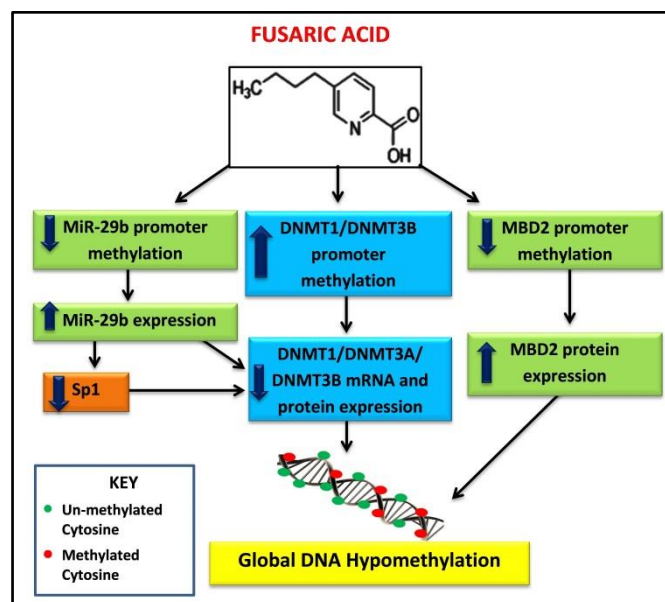


**Figure 3.7 Proposed mechanism of FA-induced global DNA hypomethylation in HepG2 cells.** FA induces global DNA hypomethylation by decreasing the mRNA and protein expression of DNMT1, DNMT3A, and DNMT3B. The decrease in DNMTs is caused by promoter hypermethylation of *DNMT1* and *DNMT3B*, and promoter hypomethylation and upregulation of miR-29b. MiR-29b negatively regulates the mRNA expression of *DNMT1*, *DNMT3A*, and *DNMT3B*. In addition, FA may also induce global DNA hypomethylation by causing promoter hypomethylation and upregulation of MBD2.

## **Materials and Methods**

### ***Materials***

FA (*Gibberella fujikuroi*, F6513) and the DNA methylation inhibitor, 5-aza-2-deoxycytidine (5-aza-2-DC; A3653) were purchased from Sigma-Aldrich. The HepG2 cell line was purchased from Highveld Biologicals. Cell culture consumables were obtained from Lonza Biotechnology. Western Blot reagents were purchased from Bio-Rad. All other reagents were purchased from Merck.

### ***Cell culture and treatment***

HepG2 cells ( $1.5 \times 10^6$ ) were cultured (37°C, 5% CO<sub>2</sub>) in complete culture media (CCM; Eagle's Minimum Essentials Medium (EMEM) containing 10% fetal calf serum, 1% penicillin-streptomycin fungizone, and 1% L-glutamine), until 90% confluent. Stocks of FA (1 mg/ml) were prepared in 0.1 M PBS and the cells were incubated (37°C, 5% CO<sub>2</sub>, 24 h) with various concentrations of FA (25, 50, 104, and 150 µg/ml). These FA concentrations were obtained from literature [10] and represented 90%, 75%, 50%, and 40% cell viabilities, respectively. The 5-aza-2-DC (50 mM) stock was prepared in 100% DMSO. The concentration of 5-aza-2-DC (10 µM, 24 h) inducing DNA hypomethylation in HepG2 cells was obtained from literature [63] and used as a negative control. An untreated control (CCM only) was also prepared. Cell viability was determined using the trypan blue cell exclusion method. All results were verified by performing two independent experiments in triplicate.

### ***DNA isolation and quantification of DNA methylation***

Genomic DNA was isolated from control and FA-treated HepG2 cells. Briefly, HepG2 cells were incubated in cell lysis buffer (600 µl, 15 min, RT; 0.5 M EDTA (pH 8.0), 1 M Tris-Cl (pH 7.6), 0.1% SDS) and potassium acetate buffer (600 µl, 8 min, RT; 5 M potassium acetate, glacial acetic acid) before centrifugation (13,000xg, 5 min, 24°C). The supernatant containing genomic DNA was transferred into fresh 1.5 ml micro-centrifuge tubes and 100% isopropanol (600 µl) was added to precipitate the DNA which was recovered by centrifugation (13,000xg, 5 min, 24°C). The DNA was washed in 100% ethanol (300 µl) and centrifuged (13,000xg, 5 min, 24°C). The DNA pellets were air dried (30 min, RT), re-suspended in DNA hydration buffer (40 µl; 10 mM EDTA (pH 8.0), 100 mM Tris-Cl (pH 7.4)), and heated (65°C, 15 min). DNA concentration was determined using the Nanodrop2000 spectrophotometer (Thermo-Fischer

Scientific) and standardized to 100 ng/μl. DNA purity was assessed using the A260/A280 absorbance ratios.

The DNA was used to quantify global DNA methylation using the Colorimetric Methylated DNA Quantification Kit (Abcam, ab117128), as per manufacturer's instructions. The percentage 5-methylcytosine (5-mC) content was calculated using the supplied formula (Supplementary Information) and represented as fold-change relative to the control.

### ***Promoter methylation of miR-29b, DNMTs, and MBD2***

Genomic DNA was isolated from control and FA-treated HepG2 cells using the Quick-g-DNA MiniPrep Kit (Zymo Research, D3007), as per manufacturer's instructions. The isolated DNA was then eluted in nuclease-free water and purified using the DNA Clean and Concentrator™-5 Kit (Zymo Research, D4003), as per manufacturer's instructions. The DNA was quantified using the Nanodrop2000 spectrophotometer and standardized to 4 ng/μl. The promoter methylation of *DNMT1*, *DNMT3A*, *DNMT3B*, *MBD2*, and miR-29b was assessed using the OneStep qMethyl Kit (Zymo Research, 5310), as per manufacturer's instructions. Briefly, 20 ng DNA was subject to a test and reference reaction containing specific primers (Supplementary Table S3.2). Cycling conditions were as follows: digestion by methyl sensitive restriction enzymes (AccII, HpaII, and HpyCH4IV) (37°C, 2 h), initial denaturation (95°C, 10 min), followed by 45 cycles of denaturation (95°C, 30 s), annealing (Supplementary Table S3.2, 60 s), extension (72°C, 60 s), final extension (72°C, 60 s), and a hold at 4°C. The percentage methylation was calculated using the supplied formula (Supplementary Information) and represented as fold-change relative to the control.

### ***RNA isolation and quantitative polymerase chain reaction (qPCR)***

Total RNA was extracted from control and FA-treated HepG2 cells using Qiazol Reagent (Qiagen, 79306). Briefly, HepG2 cells were rinsed in 0.1 M PBS and incubated (5 min, RT) in 500 μl Qiazol and 500 μl 0.1 M PBS before extraction with a cell scraper. Cellular lysates were incubated overnight (-80°C). Thereafter, chloroform (100 μl) was added and centrifuged (12,000xg, 4°C, 15 min). The aqueous phase containing RNA was transferred to fresh 1.5 ml micro-centrifuge tubes and 100% cold isopropanol (250 μl) was added to each sample before overnight incubation (-80°C). Samples were centrifuged (12,000xg, 4°C, 20 min) and the RNA pellets were washed in 75% cold ethanol (500 μl). Finally, samples were centrifuged (7,400xg, 4°C, 15 min), RNA pellets were air dried (30 min, RT), re-suspended in nuclease-free water (15 μl), and incubated (3 min, RT). The RNA was quantified using the Nanodrop2000

spectrophotometer and standardized to 1,000 ng/μl. The A260/A280 absorbance ratio was used to assess RNA purity.

The RNA was used to prepare cDNA using the miScript II RT Kit (Qiagen, 218161), as per manufacturer's instructions. The expression of miR-29b was analyzed using the miScript SYBR Green PCR Kit (Qiagen, 218073) and specific 10X miScript primer assay [Hs\_miR-29b\_1, Qiagen, MS00006566], as per manufacturer's instructions. Human RNU6 (Qiagen, MS000033740) was used as the housekeeping gene to normalize microRNA expression.

For mRNA expression, cDNA was synthesized using the iScript cDNA Synthesis Kit (Bio-Rad, 1708891), as per manufacturer's instructions. The expression of *DNMT1*, *DNMT3A*, *DNMT3B*, *MBD1-MBD6*, *Sp1*, *UHRF1*, and *USP7* were determined using the Sso Advanced™ Universal SYBR Green Supermix (Bio-Rad, 1725270), as per manufacturer's instructions. *GAPDH* was used as the housekeeping gene to normalise mRNA expression. Primer sequences and annealing temperatures are listed in Supplementary Table S3.2. All qPCR experiments were conducted using the CFX96 Real Time PCR System (Bio-Rad) and analyzed using the Bio-Rad CFX Manager™ Software version 3.1. The comparative threshold cycle (Ct) method was used to determine relative changes in expression [64].

### ***Protein isolation and Western blot***

The protein expression of DNMT1, DNMT3A, DNMT3B, and MBD2 was determined using Western blot. Briefly, crude protein extracts were isolated from control and FA-treated HepG2 cells using cytotbuster reagent (200 μl; Novagen, 71009) supplemented with protease and phosphatase inhibitors (Roche; 05892791001 and 04906837001, respectively). The protein was quantified using the bicinchoninic acid (BCA) assay, standardized to 1 mg/ml and boiled (100°C, 5 min) in a 1:1 dilution with 1X Laemmli buffer [dH<sub>2</sub>O, 0.5 M Tris-HCl (pH 6.8), glycerol, 10% SDS, 5% β-mercaptoethanol, 1% bromophenol blue]. Thereafter, the proteins were separated using sodium dodecyl sulphate polyacrylamide gel electrophoresis (10% resolving gel, 4% stacking gel; 1 h, 150V) and transferred onto nitrocellulose membranes using the Bio-Rad Trans-Blot® Turbo Transfer System (20V, 30 min). Following transfer, the membranes were blocked in 5% BSA in Tris buffered saline with 0.05% Tween 20 [TTBS; 150 mM NaCl, 3 mM KCl, 25 mM Tris, 0.05% Tween 20, dH<sub>2</sub>O, pH 7.5; 1 h, RT] and probed overnight (4°C) with primary antibody [DNMT1 (Cell Signaling Technology, #5032S; 1:250), DNMT3A (Cell Signaling Technology, #3598S; 1:500), DNMT3B (Santa Cruz, sc-130740; 1:250), and MBD2 (Santa Cruz, sc-271562; 1:500)]. The membranes were rinsed five times with TTBS (10 min, RT) and probed with a horse-radish peroxidase (HRP)-conjugated

secondary antibody [goat anti-rabbit (Cell Signaling Technology, #7074S; 1:10,000) and goat anti-mouse (Cell Signaling Technology, #7076P2; 1:5,000); 1 h, RT]. The membranes were rinsed five times in TTBS (10 min, RT). The Clarity™ Western ECL Substrate Kit (Bio-Rad, #170-5060) was used to detect specific protein bands and the images were captured using the ChemiDoc™ XRS+ Molecular Imaging System (Bio-Rad). The membranes were then quenched in hydrogen peroxide (5%, 37°C, 30 min), rinsed once in TTBS (10 min, RT) and probed with the housekeeping protein, anti-β-actin (Sigma-Aldrich, A3854; 1:5,000; 30 min, RT) to normalise protein expression. Densitometric analysis was performed using the Bio-Rad Image Lab Software version 5.1 and the results were represented as a fold-change in band density (RBD) relative to the control.

### ***Immuno-precipitation***

Immuno-precipitation was used to determine ubiquitinated DNMT1, DNMT3A, and DNMT3B levels. Briefly, crude protein extracts were isolated from control and FA-treated HepG2 cells using 1X cell lysis buffer [500 µl; 20 mM Tris (pH 7.5), 150 mM NaCl, 1 mM EDTA, 10% glycerol, 1% Triton X-100]. The protein was quantified using the BCA assay and standardized to 1.5 mg/ml. Thereafter, the protein lysates (200 µl) were incubated with primary antibody [DNMT1 (Cell Signaling Technology, #5032S); DNMT3A (Cell Signaling Technology, #3598S); and DNMT3B (Santa Cruz, sc-130740); 1:100] overnight (4°C) and the antigen-antibody complex was precipitated using protein A beads (20 µl 50% bead slurry; Cell Signaling Technology, #9863) for 1-3 h at 4°C. The immuno-precipitates were recovered by centrifugation (14,000xg, 4°C, 30 s), washed five times in 1X cell lysis buffer (500 µl), re-suspended in 3X Laemmli buffer (20 µl), and boiled (100°C, 5 min). The samples were then analyzed by Western blotting using the following antibodies: primary antibody [ubiquitin (BD BioSciences, BD550944; 1:1,000), DNMT1 (Cell Signaling Technology, #5032S; 1:1,000), DNMT3A (Cell Signaling Technology, #3598S; 1:1,000), and DNMT3B (Santa Cruz, sc-130740; 1:500)] and secondary antibody [goat anti-rabbit (Cell Signaling Technology, #7074S) and goat anti-mouse (Cell Signaling Technology, #7076P2); 1:5,000]. The protein expression of ubiquitin was divided by the total protein expressed to determine the ratio of ubiquitinated protein.

### ***Statistical analysis***

GraphPad Prism version 5.0 (GraphPad Prism Software Inc.) was used to perform all statistical analyses. The one way analysis of variance (ANOVA) with the Bonferroni multiple comparisons test was used to analyze the data. The results were expressed as the mean fold-

change  $\pm$  standard deviation (SD) ( $n = 3$ ), unless otherwise indicated. Statistical significance was considered at  $p < 0.05$ .

### **Author contributions**

TG, SN, PN, and AC conceptualized and designed the study. TG conducted all laboratory experiments, analyzed the data, and wrote the manuscript. PN assisted in conducting laboratory experiments. SN, PN, and AC revised the manuscript. All authors have read the manuscript prior to submission.

### **Disclosure statement**

No potential conflict of interest was reported by the authors.

### **Funding**

This work was supported by the National Research Foundation Innovation Doctoral Scholarship (Grant no.: SFH160703175722) and the College of Health Sciences (University of Kwa-Zulu Natal; Grant no.: 570869).

### **Data availability**

All datasets generated in this study are available in Supplementary Information and from the corresponding author on reasonable request.

### **ORCID**

Terisha Ghazi: <http://orcid.org/0000-0002-0179-213X>

Savana Nagiah: <http://orcid.org/0000-0002-7614-8226>

Pragalathan Naidoo: <http://orcid.org/0000-0002-8905-5926>

Anil A. Chuturgoon: <http://orcid.org/0000-0003-4649-4133>

## Supplementary Information

### Quantification of DNA methylation formula:

$$\text{5-Methylcytosine (ng)} = (\text{Sample OD} - \text{Negative Control OD}) / (\text{Slope} \times 2)$$

$$\text{5-Methylcytosine (\%)} = (5 - \text{Methylcytosine (ng)} / (\text{Input DNA (ng)}) \times 100\%$$

### Quantification of promoter methylation formula:

$$\text{Methylation (\%)} = 100 \times 2^{-\Delta\text{Ct}}, \text{ where } \Delta\text{Ct} = \text{Ct (test)} - \text{Ct (reference)}$$

**Supplementary Table S3.1: The effect of FA on the mRNA expression of *MBD1*, *MBD2*, *MBD3*, *MBD4*, *MBD5*, and *MBD6* in HepG2 cells**

Gene	Concentration of Fusaric Acid ( $\mu\text{g/ml}$ )					<i>p</i> value
	0	25	50	104	150	
<i>MBD1</i>	1.02 $\pm$ 0.01	0.38 $\pm$ 0.03***	0.42 $\pm$ 0.08***	0.18 $\pm$ 0.03***	0.48 $\pm$ 0.03***	<0.0001
<i>MBD2</i>	1.02 $\pm$ 0.01	0.17 $\pm$ 0.01***	0.64 $\pm$ 0.08***	0.14 $\pm$ 0.01***	0.09 $\pm$ 0.01***	<0.0001
<i>MBD3</i>	1.02 $\pm$ 0.01	0.40 $\pm$ 0.05***	0.31 $\pm$ 0.02***	0.34 $\pm$ 0.08***	0.34 $\pm$ 0.03***	<0.0001
<i>MBD4</i>	1.02 $\pm$ 0.01	0.14 $\pm$ 0.01***	0.67 $\pm$ 0.09***	0.20 $\pm$ 0.04***	0.22 $\pm$ 0.04***	<0.0001
<i>MBD5</i>	1.02 $\pm$ 0.01	0.16 $\pm$ 0.11***	0.31 $\pm$ 0.13***	0.28 $\pm$ 0.04***	0.13 $\pm$ 0.07***	<0.0001
<i>MBD6</i>	1.02 $\pm$ 0.01	0.18 $\pm$ 0.01***	0.15 $\pm$ 0.02***	0.18 $\pm$ 0.03***	0.72 $\pm$ 0.06***	<0.0001

RNA isolated from control and FA-treated HepG2 cells were reverse transcribed into cDNA and analyzed for *MBD1*-*MBD6* expression by qPCR. Results are represented as mean relative fold-change  $\pm$  SD (n = 3). **Key:** \*\*\**p* < 0.0001, denotes statistical significance, one-way ANOVA with the Bonferroni multiple comparisons test.

Supplementary Table S3.2: qPCR primer sequences and annealing temperatures

Gene	GenBank Accession no.	Sense Primer (5'→3')	Anti-Sense Primer (5'→3')	Annealing Temperature (°C)
<i>Promoter Methylation</i>				
<i>DNMT1</i>	NM_00113 0823	ACCGCTTCTACTTCCTCG AGGCCTA	GTTGCAGTCCTCTGTGA ACACTGTGG	60
<i>DNMT3A</i>	NM_17562 9	GGGACGTCCGCAGCGT CACAC	CAGGGTTGGACTCGAG AAATCGC	58
<i>DNMT3B</i>	NM_00689 2	CCTGCTGAATTACTCAC GCCCC	GTCTGTGTAGTGCACAG GAAAGCC	58
<i>MBD2</i>	NM_00392 7	AGGTAGCAATGATGAGA CCCTTTTA	TAAGCCAAACAGCAGG GTTCTT	60
<i>miR-29b</i>	-	TCCGTATGCTGGTTACT CAC	ATTCTGATAAAACCACC AACT	54
<i>Gene Expression</i>				
<i>DNMT1</i>	NM_00113 0823	ACCGCTTCTACTTCCTCG AGGCCTA	GTTGCAGTCCTCTGTGA ACACTGTGG	60
<i>DNMT3A</i>	NM_17562 9	GGGACGTCCGCAGCGT CACAC	CAGGGTTGGACTCGAG AAATCGC	58
<i>DNMT3B</i>	NM_00689 2	CCTGCTGAATTACTCAC GCCCC	GTCTGTGTAGTGCACAG GAAAGCC	58
<i>Sp1</i>	NM_13847 3	CTTGGTATCATCACAAG CCAGTT	TCCCTGATGATCCACTG GTAGTA	56
<i>UHRF1</i>	NM_00104 8201	GCCATACCCTCTTCGAC TACG	GCCCCAATTCGGTCTCA TCC	58
<i>USP7</i>	NM_00347 0	GGAAGCGGGAGATACA GATGA	AAGGACCGACTCACTC AGTCT	58
<i>MBD1</i>	NM_01584 6	AAGTCTTTCGCAAGTCA GGGG	TCAGTCAACTTTGCTT CGGA	58
<i>MBD2</i>	NM_00392 7	AGGTAGCAATGATGAGA CCCTTTTA	TAAGCCAAACAGCAGG GTTCTT	60
<i>MBD3</i>	NM_00128 1453	CAGCCGGTGACCAAGAT TACC	CTCCTCAGCAATGTCGA AGG	58

<b><i>MBD4</i></b>	NM_00392 5	TCTAGTGAGCGCCTAGT CCCAG	TTCCAATTCCATAGCAA CATCTTCT	60
<b><i>MBD5</i></b>	NM_01832 8	GGTCTTCCAGCTATAACA AGTTCC	ACCTGCTCCAAGCAAG ATAAC	56
<b><i>MBD6</i></b>	NM_05289 7	GGAGTGTCCACTTAATG TCCCC	GTTGCACAGCTTGGTCA TGTC	58



**Supplementary Figure S3.1 CpG islands within the *DNMT1*, *DNMT3A*, *DNMT3B*, and *MBD2* promoter regions obtained using the MethPrimer software version 2.0. [65].**

## References

- [1] Bacon C, Porter J, Norred W, et al. Production of fusaric acid by *Fusarium* species. *Appl Environ Microbiol.* 1996 Nov;62:4039-4043. PubMed PMID: 8899996.
- [2] Streit E, Schwab C, Sulyok M, et al. Multi-mycotoxin screening reveals the occurrence of 139 different secondary metabolites in feed and feed ingredients. *Toxins.* 2013 Mar;5:504-523. PubMed PMID: 23529186.
- [3] Chen Z, Luo Q, Wang M, et al. A Rapid Method with UPLC for the Determination of Fusaric Acid in *Fusarium* Strains and Commercial Food and Feed Products. *Indian J Microbiol.* 2016 Aug;57:68-74. PubMed Central PMCID: PMC5243244.
- [4] Singh VK, Singh HB, Upadhyay RS. Role of fusaric acid in the development of *Fusarium* wilt symptoms in tomato: Physiological, biochemical and proteomic perspectives. *Plant Physiol Biochem.* 2017 Sept;118:320-332. PubMed PMID: 28683401.
- [5] D'Alton A, Etherton B. Effects of fusaric acid on tomato root hair membrane potentials and ATP levels. *Plant Physiol.* 1984 Jan;74:39-42. PubMed PMID: 16663382.
- [6] Diniz S, Oliveira R. Effects of fusaric acid on *Zea mays* L. seedlings. *Phyton Int J Exp Bot.* 2009 Jan;78:155-160.
- [7] Pavlovkin J, Mistrik I, Prokop M. Some aspects of the phytotoxic action of fusaric acid on primary *Ricinus* roots. *Plant Soil Environ.* 2004 Sept;50:397-401.
- [8] Singh VK, Upadhyay RS. Fusaric acid induced cell death and changes in oxidative metabolism of *Solanum lycopersicum* L. *Bot Stud.* 2014 Dec;55:66-76. PubMed PMID: 28510945.
- [9] Sapko O, Utarbaeva AS, Makulbek S. Effect of fusaric acid on prooxidant and antioxidant properties of the potato cell suspension culture. *Russian J Plant Physiol.* 2011 Sept;58:828-835.
- [10] Abdul NS, Nagiah S, Chuturgoon AA. Fusaric acid induces mitochondrial stress in human hepatocellular carcinoma (HepG2) cells. *Toxicon.* 2016 Sept;119:336-344. PubMed PMID: 27390038.

- [11] Köhler K, Bentrup FW. The effect of fusaric acid upon electrical membrane properties and ATP level in photoautotrophic cell suspension cultures of *Chenopodium rubrum* L. *Z Pflanzenphysiol.* 1983 Mar;109:355-361.
- [12] Ghazi T, Nagiah S, Tiloke C, et al. Fusaric acid induces DNA damage and post-translational modifications of p53 in human hepatocellular carcinoma (HepG2) cells. *J Cell Biochem.* 2017 Nov;118:3866-3874. PubMed PMID: 28387973.
- [13] Stack BC Jr, Hansen JP, Ruda JM, et al. Fusaric acid: a novel agent and mechanism to treat HNSCC. *Otolaryngol Head Neck Surg.* 2004 Jul;131:54-60. PubMed PMID: 15243558.
- [14] Dhani S, Nagiah S, Naidoo DB, et al. Fusaric acid immunotoxicity and MAPK activation in normal peripheral blood mononuclear cells and Thp-1 cells. *Sci Rep.* 2017 Jun;7:3051-3060. PubMed PMID: 28596589.
- [15] Ogata S, Inoue K, Iwata K, et al. Apoptosis induced by picolinic acid-related compounds in HL-60 cells. *Biosci Biotechnol Biochem.* 2001 Oct;65:2337-2339. PubMed PMID: 11758936.
- [16] Fernandez-Pol J, Klos D, Hamilton P. Cytotoxic activity of fusaric acid on human adenocarcinoma cells in tissue culture. *Anticancer Res.* 1993 Jan;13:57-64. PubMed PMID: 8476229.
- [17] Diringer MN, Kramarcy NR, Brown JW, et al. Effect of fusaric acid on aggression, motor activity, and brain monoamines in mice. *Pharmacol Biochem Behav.* 1982 Jan;16:73-79. PubMed PMID: 6173886.
- [18] Li X, Zhang Z-L, Wang HF. Fusaric acid (FA) protects heart failure induced by isoproterenol (ISP) in mice through fibrosis prevention via TGF- $\beta$ 1/SMADs and PI3K/AKT signaling pathways. *Biomed Pharmacother.* 2017 Sept;93:130-145. PubMed PMID: 28624424.
- [19] Reddy R, Larson C, Brimer G, et al. Developmental toxic effects of fusaric acid in CD1 mice. *Bull Environ Contam Toxicol.* 1996 Sept;57:354-360. PubMed PMID: 8672059.
- [20] Devaraja S, Girish KS, Santhosh MS, et al. Fusaric acid, a mycotoxin, and its influence on blood coagulation and platelet function. *Blood Coagul Fibrinolysis.* 2013 Jun;24:419-423. PubMed PMID: 23343693.
- [21] Hidaka H, Nagatsu T, Takeya K, et al. Fusaric acid, a hypotensive agent produced by fungi. *J Antibiot.* 1969 May;22:228-230. PubMed PMID: 5811396.

- [22] Terasawa F, Kameyama M. The clinical trial of a new hypotensive agent, fusaric acid (5-butylpicolinic acid): the preliminary report. *Circ J.* 1971 Mar;35:339-357. PubMed PMID: 4932992.
- [23] Yin ES, Rakhmankulova M, Kucera K, et al. Fusaric acid induces a notochord malformation in zebrafish via copper chelation. *Biometals.* 2015 Aug;28:783-789. PubMed PMID: 25913293.
- [24] Bacon CW, Porter JK, Norred WP. Toxic interaction of fumonisin B1 and fusaric acid measured by injection into fertile chicken egg. *Mycopathologia.* 1995 Jan;129:29-35. PubMed PMID: 7617015.
- [25] Smith T, MacDonald E. Effect of fusaric acid on brain regional neurochemistry and vomiting behavior in swine. *J Anim Sci.* 1991 May;69:2044-2049. PubMed PMID: 1712354.
- [26] Fairchild AS, Grimes JL, Porter JK, et al. Effects of diacetoxyscirpenol and fusaric acid on poult: Individual and combined effects of dietary diacetoxyscirpenol and fusaric acid on turkey poult performance. *Int J Poult Sci.* 2005;4(3):350-355.
- [27] Gopalakrishnan S, Van Emburgh BO, Robertson KD. DNA methylation in development and human disease. *Mutat Res.* 2008 Dec;647:30-38. PubMed PMID: 18778722.
- [28] Iraola-Guzmán S, Estivill X, Rabionet R. DNA methylation in neurodegenerative disorders: a missing link between genome and environment? *Clin Genet.* 2011 Jul;80:1-14. PubMed PMID: 21542837.
- [29] Lin R-K, Wang Y-C. Dysregulated transcriptional and post-translational control of DNA methyltransferases in cancer. *Cell Biosci.* 2014 Aug;4:46-56. PubMed PMID: 25949795.
- [30] Winter J, Jung S, Keller S, et al. Many roads to maturity: microRNA biogenesis pathways and their regulation. *Nat Cell Biol.* 2009 Mar;11:228-234. PubMed PMID: 19255566.
- [31] Park SY, Lee JH, Ha M, et al. miR-29 miRNAs activate p53 by targeting p85 alpha and CDC42. *Nat Struct Mol Biol.* 2009 Jan;16:23-29. PubMed PMID: 19079265.
- [32] Wei W, He HB, Zhang WY, et al. miR-29 targets Akt3 to reduce proliferation and facilitate differentiation of myoblasts in skeletal muscle development. *Cell Death Dis.* 2013 Jun;4:e668-e678. PubMed PMID: 23764849.

- [33] Wang J, Chu ESH, Chen H-Y, et al. microRNA-29b prevents liver fibrosis by attenuating hepatic stellate cell activation and inducing apoptosis through targeting PI3K/AKT pathway. *Oncotarget*. 2015 Mar;6:7325-7338. PubMed PMID: 25356754.
- [34] Teng Y, Zhang Y, Qu K, et al. MicroRNA-29B (mir-29b) regulates the Warburg effect in ovarian cancer by targeting AKT2 and AKT3. *Oncotarget*. 2015 Dec;6:40799-40814. PubMed PMID: 26512921.
- [35] Garzon R, Liu S, Fabbri M, et al. MicroRNA-29b induces global DNA hypomethylation and tumor suppressor gene reexpression in acute myeloid leukemia by targeting directly DNMT3A and 3B and indirectly DNMT1. *Blood*. 2009 Jun;113:6411-6418. PubMed PMID: 19211935.
- [36] Fabbri M, Garzon R, Cimmino A, et al. MicroRNA-29 family reverts aberrant methylation in lung cancer by targeting DNA methyltransferases 3A and 3B. *Proc Natl Acad Sci USA*. 2007 Oct;104:15805-15810. PubMed PMID: 17890317.
- [37] Scott A, Song J, Ewing R, et al. Regulation of protein stability of DNA methyltransferase 1 by post-translational modifications. *Acta Biochim Biophys Sin*. 2014 Mar;46:199-203. PubMed PMID: 24389641.
- [38] Denis H, Ndlovu MN, Fuks F. Regulation of mammalian DNA methyltransferases: a route to new mechanisms. *EMBO Rep*. 2011 Jul;12:647-656. PubMed PMID: 21660058.
- [39] Detich N, Theberge J, Szyf M. Promoter-specific activation and demethylation by MBD2/demethylase. *J Biol Chem*. 2002 Sept;277:35791-35794. PubMed PMID: 12177048.
- [40] Qin H, Zhu X, Liang J, et al. MicroRNA-29b contributes to DNA hypomethylation of CD4+ T cells in systemic lupus erythematosus by indirectly targeting DNA methyltransferase 1. *J Dermatol Sci*. 2013 Jan;69:61-67. PubMed PMID: 23142053.
- [41] Novakovic B, Wong NC, Sibson M, et al. DNA methylation-mediated down-regulation of DNA methyltransferase-1 (DNMT1), is coincident with, but not essential for, global hypomethylation in human placenta. *J Biol Chem*. 2010 Mar;285:9583-9593. PubMed PMID: 20071334.
- [42] Naghitorabi M, Asl JM, Sadeghi HMM, et al. Quantitative evaluation of DNMT3B promoter methylation in breast cancer patients using differential high resolution melting analysis. *Res Pharm Sci*. 2013 Jul;8:167-175. PubMed PMID: 24019826.

- [43] Peng L, Yuan Z, Ling H, et al. SIRT1 deacetylates the DNA methyltransferase 1 (DNMT1) protein and alters its activities. *Mol Cell Biol*. 2011 Dec;31:4720-4734. PubMed PMID: 21947282.
- [44] Du Z, Song J, Wang Y, et al. DNMT1 stability is regulated by proteins coordinating deubiquitination and acetylation-driven ubiquitination. *Sci Signal*. 2010 Nov;3:ra80-ra101. PubMed PMID: 21045206.
- [45] Cheng J, Yang H, Fang J, et al. Molecular mechanism for USP7-mediated DNMT1 stabilization by acetylation. *Nat Commun*. 2015 May;6:7023-7033. PubMed PMID: 25960197.
- [46] Jia Y, Li P, Fang L, et al. Negative regulation of DNMT3A de novo DNA methylation by frequently overexpressed UHRF family proteins as a mechanism for widespread DNA hypomethylation in cancer. *Cell Discov*. 2016 Apr;2:16007-16026. PubMed PMID: 27462454.
- [47] Bostick M, Kim JK, Estève PO, et al. UHRF1 plays a role in maintaining DNA methylation in mammalian cells. *Science*. 2007 Sept;317:1760-1764. PubMed PMID: 17673620.
- [48] Yuan K, Xie K, Fox J, et al. Decreased levels of miR-224 and the passenger strand of miR-221 increase MBD2, suppressing maspin and promoting colorectal tumor growth and metastasis in mice. *Gastroenterology*. 2013 Oct;145:853-864. PubMed PMID: 23770133.
- [49] Stirzaker C, Song JZ, Ng W, et al. Methyl-CpG-binding protein MBD2 plays a key role in maintenance and spread of DNA methylation at CpG islands and shores in cancer. *Oncogene*. 2017 Mar;36:1328-1338. PubMed PMID: 27593931.
- [50] Fazio C, Covre A, Cutaia O, et al. Immunomodulatory properties of DNA hypomethylating agents: selecting the optimal epigenetic partner for cancer immunotherapy. *Front Pharmacol*. 2018 Dec;9:1443-1456. PubMed PMID: 30581389.
- [51] Jackson M, Krassowska A, Gilbert N, et al. Severe global DNA hypomethylation blocks differentiation and induces histone hyperacetylation in embryonic stem cells. *Mol Cell Biol*. 2004 Oct;24:8862-8871. PubMed PMID: 15456861.
- [52] Rodriguez J, Frigola J, Vendrell E, et al. Chromosomal instability correlates with genome-wide DNA demethylation in human primary colorectal cancers. *Cancer Res*. 2006 Sept;66:8462-9468. PubMed PMID: 16951157.

- [53] Dodge JE, Okano M, Dick F, et al. Inactivation of Dnmt3b in mouse embryonic fibroblasts results in DNA hypomethylation, chromosomal instability, and spontaneous immortalization. *J Biol Chem*. 2005 May;280:17986-17991. PubMed PMID: 15757890.
- [54] Jackson-Grusby L, Beard C, Possemato R, et al. Loss of genomic methylation causes p53-dependent apoptosis and epigenetic deregulation. *Nat Genet*. 2001 Jan;27:31-39. PubMed PMID: 11137995.
- [55] Chuturgoon A, Phulukdaree A, Moodley D. Fumonisin B1 induces global DNA hypomethylation in HepG2 cells – An alternative mechanism of action. *Toxicology*. 2014 Jan;315:65-69. PubMed PMID: 24280379.
- [56] Demirel G, Alpertunga B, Ozden S. Role of fumonisin B1 on DNA methylation changes in rat kidney and liver cells. *Pharm Biol*. 2015 Apr;53:1302-1310. PubMed PMID: 25858139.
- [57] Sancak D, Ozden S. Global histone modifications in fumonisin B1 exposure in rat kidney epithelial cells. *Toxicol In Vitro*. 2015 Oct;29:1809-1815. PubMed PMID: 26208285.
- [58] Chuturgoon AA, Phulukdaree A, Moodley D. Fumonisin B1 modulates expression of human cytochrome P450 1b1 in human hepatoma (Hepg2) cells by repressing Mir-27b. *Toxicol Lett*. 2014 May;227:50-55. PubMed PMID: 24614526.
- [59] So MY, Tian Z, Phoon YS, et al. Gene expression profile and toxic effects in human bronchial epithelial cells exposed to zearalenone. *PLoS One*. 2014 May;9:e96404-e96422. PubMed PMID: 24788721.
- [60] Lan M, Han J, Pan MH, et al. Melatonin protects against defects induced by deoxynivalenol during mouse oocyte maturation. *J Pineal Res*. 2018 Aug;65:e12477-e12487. PubMed PMID: 29453798.
- [61] Zhu C-C, Zhang Y, Duan X, et al. Toxic effects of HT-2 toxin on mouse oocytes and its possible mechanisms. *Arch Toxicol*. 2016 Jun;90:1495-1505. PubMed PMID: 26138683.
- [62] Mamur S, Ünal F, Yılmaz S, et al. Evaluation of the cytotoxic and genotoxic effects of mycotoxin fusaric acid. *Drug Chem Toxicol*. 2018 Sept;11:1-9. PubMed PMID: 30204001.
- [63] Ahn EY, Kim JS, Kim GJ, et al. RASSF1A-mediated regulation of AREG via the Hippo pathway in hepatocellular carcinoma. *Mol Cancer Res*. 2013 Jul;11:748-758. PubMed PMID: 23594797.

[64] Livak KJ, Schmittgen TD. Analysis of relative gene expression data using real-time quantitative PCR and the  $2^{-\Delta\Delta CT}$  method. *Methods*. 2001 Dec;25:402-408. PubMed PMID: 11846609.

[65] Li LC, Dahiya R. MethPrimer: designing primers for methylation PCRs. *Bioinformatics*. 2002 Nov;18:1427-1431. PubMed PMID: 12424112.

## CHAPTER 4

### **Fusaric acid-induced epigenetic modulation of hepatic H3K9me3 triggers apoptosis *in vitro* and *in vivo***

Terisha Ghazi, Savania Nagiah, Shanel Dhani, and Anil A. Chuturgoon\*

Discipline of Medical Biochemistry and Chemical Pathology, School of Laboratory Medicine and Medical Science, College of Health Sciences, Howard College Campus, University of KwaZulu-Natal, Durban 4041, South Africa

\*Corresponding author: Professor Anil A. Chuturgoon, Discipline of Medical Biochemistry and Chemical Pathology, School of Laboratory Medicine and Medical Science, College of Health Sciences, Howard College Campus, University of KwaZulu-Natal, Durban 4041, South Africa. Telephone: +27 31 260 4404; Fax: +27 31 260 4785; Email: [CHUTUR@ukzn.ac.za](mailto:CHUTUR@ukzn.ac.za)

#### **Author Email Addresses:**

Terisha Ghazi: [terishaghazi@gmail.com](mailto:terishaghazi@gmail.com)

Savania Nagiah: [nagiah.savania@gmail.com](mailto:nagiah.savania@gmail.com)

Shanel Dhani: [dhanishanel@gmail.com](mailto:dhanishanel@gmail.com)

Anil A. Chuturgoon: [CHUTUR@ukzn.ac.za](mailto:CHUTUR@ukzn.ac.za)

**Running title:** Fusaric acid and SUV39H1-mediated H3K9me3

**Future Medicine: Epigenomics (*In Review*)**

**Manuscript ID: EPI-2019-0284**

## Abstract

**Background:** Fusaric acid (FA), a food-borne mycotoxin, may cause toxicity via epigenetic mechanisms such as microRNAs (miRs) and histone methylation. Sirt1, a target of miR-200a, maintains H3K9me3 by interacting with SUV39H1. **Aim:** To determine the effect of FA on miR-200a, SUV39H1-mediated H3K9me3, genome integrity, and apoptosis in HepG2 cells and C57BL/6 mice livers. **Methods:** HepG2 cells (0, 25, 50, 104, and 150 µg/ml; 24 h) and C57BL/6 mice (0 and 50 mg/kg; 24 h) were treated with FA, and DNA, RNA, and protein was isolated. The expression of miR-200a, Sirt1, SUV39H1, MDM2, H3K9me1/3, KDM4B, and p-S139-H2Ax was quantified using qPCR and/or western blot. Immuno-precipitation was used to determine SUV39H1 ubiquitination. Genome integrity was assessed using DNA electrophoresis. Cell viability and apoptosis was determined using the crystal violet and luminometry assays, respectively. **Results:** FA upregulated miR-200a and decreased Sirt1 expression in HepG2 cells and mice livers; decreased expression of SUV39H1 and *KDM4B*, thus decreasing H3K9me3 and increasing H3K9me1; increased cell mortality via apoptosis. **Conclusion:** FA induced apoptosis by upregulating miR-200a and decreasing SUV39H1-mediated H3K9me3 in HepG2 cells and mice livers. This indicates that FA is toxic via epigenetic mechanisms which may serve as potential biomarkers for determining FA exposure and toxicity. This is important in poverty stricken areas where mycotoxin-contaminated commodities form an integral part of the staple diet.

**Keywords:** Fusaric Acid, MiR-200a, Sirt1, SUV39H1, H3K9me3, Apoptosis

## Introduction

The contamination of foods and feeds with pathogenic fungi and mycotoxins is a serious problem that occurs globally; and exposure to mycotoxin-contaminated commodities has been associated with harmful effects in humans and animals [1]. Epigenetic modifications play a key role in mycotoxin-induced health effects and understanding the molecular and epigenetic mechanisms of mycotoxins will help decrease mycotoxin exposure and lower the risk of mycotoxin-related adverse health effects.

Fusaric acid (FA; 5-butylpicolinic acid) is a mycotoxin produced by fungi of the genus *Fusarium* that contaminates agricultural foods and feeds. Previously other studies have indicated feed samples to be contaminated with approximately 643 µg/kg FA [2] whereas commercial foods and feeds were contaminated with 2.5-18 µg/kg FA [3]. These foods are an essential part of both human and animal diets and the regular consumption of FA-contaminated commodities may lead to adverse health effects.

To date, little is known on the toxic effects of FA on human and animal health. Recently, we showed that FA induces DNA hypomethylation as an epigenetic mechanism of FA-induced genotoxicity and cytotoxicity in HepG2 cells [4], and this may possibly lead to liver cancer in humans and animals.

FA is a non-specific mycotoxin known to affect multiple biochemical pathways, and acts synergistically with other co-produced *Fusarium* mycotoxins [5-7]. FA is phytotoxic to several plants and has been implicated in the pathogenesis of wilt diseases by damaging plant photosynthetic machinery and inhibiting root and leaf cell function [8]. FA is also toxic to human liver cells by inducing oxidative stress [9], mitochondrial dysfunction [9], DNA damage [10], and apoptosis [9, 10]. It is immuno-toxic to peripheral blood mononuclear cells (PBMCs) and human monocytic (THP-1) cells by altering the MAPK signaling pathway [11]. FA also prevents cardiac hypertrophy and fibrosis by inactivating the TGF-β1/SMADs and PI3K/AKT signaling pathways [12].

FA is a chelator of divalent cations; its chelation of calcium affects bone ossification [13] and platelet aggregation [14] whereas copper chelation inhibits the enzymes dopamine β-hydroxylase and lysyl oxidase that leads to hypotension [15-17] and notochord malformation [18].

Epigenetic modifications such as DNA methylation, histone modifications and microRNAs are important in regulating many cellular processes, and may constitute a mechanism of FA-induced toxicity.

MicroRNAs (miRs) are small non-coding RNA molecules that regulate gene expression at the post-transcriptional level by negatively regulating the processing, stability, and translation of the target messenger RNA (mRNA) [19]. The miR-200 family plays a major role in maintaining cellular motility and is implicated in tumorigenesis and metastasis [20]. This family comprises of two clusters: cluster 1, located on chromosome 1, consists of miR-200b, miR-200a, and miR-429; and cluster 2, located on chromosome 12, consists of miR-200c and miR-141. MiR-200a is highly expressed in epithelial cells and has high sequence homology with miR-141 [20, 21]. Several effects of miR-200a have been described such as modulating the oxidative stress response by targeting p38 $\alpha$  [21] and the NRF-2 regulator, Kelch-like ECH-associated protein 1 (Keap1) [22]. It prevents renal fibrogenesis by repressing transforming growth factor beta 2 (TGF- $\beta$ 2) [23], and targets phospholipase C-gamma 1 (PLC- $\gamma$ 1) to regulate cell proliferation and epithelial growth factor (EGF)-mediated invasion in breast cancer [24]. MiR-200a also regulates epithelial to mesenchymal transition by targeting the zinc finger E-box binding proteins, ZEB1 and ZEB2 [25-27],  $\beta$ -catenin [28-30], and Sirtuin 1 (Sirt1) [20].

Sirt1, a class III histone deacetylase, regulates chromatin structure and gene expression through modification of chromatin-associated histones [31]. Sirt1 promotes heterochromatin formation by deacetylating histones, H4K16Ac, H3K9Ac, and H1K26Ac [32]; recruits DNA methyltransferases to gene promoter regions and facilitates transcriptional repression of tumor suppressor genes by modulating the histone methyltransferase, suppressor of variegation 3-9 homolog 1 (SUV39H1) [20, 33].

SUV39H1 is a key enzyme responsible for the trimethylation of histone 3 on lysine (K) 9 (H3K9me3) [32-35]. SUV39H1-mediated H3K9me3 is essential for maintaining genome integrity [36], heterochromatin organization [37], chromosome condensation [38] and mitosis [39]; and the inhibition of SUV39H1 was previously associated with a reduction in cell viability [40], genome instability [33, 36], inhibition of cell growth [41] and apoptosis [35].

The interaction between Sirt1 and SUV39H1 helps maintain the H3K9me3 repressive mark [32, 33]. SUV39H1 is subject to post-translational modifications (PTMs) such as acetylation and ubiquitination that regulate its activity and expression [33]. The acetylation of SUV39H1 on K266 in the catalytic domain decreases SUV39H1 activity [33], and enables the E3 ubiquitin ligase, murine double minute 2 (MDM2) to polyubiquitinate SUV39H1 on K87 mediating its

proteasomal degradation [33]. Sirt1 directly interacts with, recruits and deacetylates SUV39H1 on K266 thereby increasing its catalytic activity and inhibiting its MDM2-mediated polyubiquitination and proteasomal degradation [32, 33]. Sirt1 also maintains H3K9me3 by directly deacetylating H3K9Ac to enable trimethylation by SUV39H1 [33].

Although several effects of FA have recently been described, there are currently no studies evaluating the effect of FA on epigenetic modifications such as microRNAs and histone methylation. This study aimed to determine an epigenetic mechanism of FA-induced toxicity by specifically investigating the effect of FA on miR-200a, SUV39H1-mediated H3K9me3, genome integrity, and apoptosis in human liver (HepG2) cells and C57BL/6 mice livers.

## **Materials and methods**

### **Materials**

FA (*Gibberella fujikuroi*, F6513) was purchased from Sigma-Aldrich (St. Louis, MO, USA). The miR-200a mimic (Syn-hsa-miR-200a-3p; MSY0000682) and miR-200a inhibitor (Anti-hsa-miR-200a-3p; MIN0000682) were purchased from Qiagen (Hilden, Germany). The HepG2 cell line (HB-8065) was purchased from the American Type Culture Collection (ATCC; Johannesburg, SA). Cell culture consumables were purchased from Lonza Biotechnology (Basel, Switzerland). Western Blot reagents were purchased from Bio-Rad (Hercules, CA, USA). All other reagents were purchased from Merck (Darmstadt, Germany).

### **Cell culture and treatment**

HepG2 cells ( $1.5 \times 10^6$ , passage 3) were seeded and maintained (37°C, 5% CO<sub>2</sub>, humidified incubator) in 25 cm<sup>3</sup> sterile cell culture flasks containing complete culture media (CCM; Eagle's Minimum Essentials Medium (EMEM) supplemented with 10% fetal calf serum, 1% penicillin-streptomycin-fungizone, and 1% L-glutamine), until 90% confluent. A stock solution of 1 mg/ml FA was prepared in 0.1 M phosphate buffered saline (PBS) and the cells were incubated (37°C, 5% CO<sub>2</sub>, 24 h) with various concentrations of FA (25, 50, 104, and 150 µg/ml) [4]. An untreated control (CCM only) was also prepared. All experiments were repeated two independent times and in triplicate for reproducibility of results.

### **Transfection of HepG2 cells with the miR-200a mimic and miR-200a inhibitor**

To assess the effect of miR-200a on Sirt1 mRNA and protein levels, HepG2 cells were transfected with the miR-200a mimic (Syn-hsa-miR-200a-3p; MSY0000682) and miR-200a

inhibitor (Anti-hsa-miR-200a-3p; MIN0000682) [42]. Briefly, HepG2 cells were grown (37°C, 5% CO<sub>2</sub>) to 90% confluency in 25 cm<sup>3</sup> cell culture flasks. The lyophilized microRNA mimic and inhibitor (1 nmol) were reconstituted in nuclease-free water to a concentration of 20 μM. The transfection complex consisting of 15 μl microRNA mimic or inhibitor, 72 μl serum-free media and 3 μl attractene was prepared and incubated (15 min, RT). Thereafter, the CCM was removed from the cells and 2,910 μl fresh CCM was added to yield a final concentration of 100 nM mimic and inhibitor. The transfection complex was added in a dropwise manner with gentle swirling to allow even distribution. The cells were incubated (37°C, 5% CO<sub>2</sub>, 24 h) before isolating protein and RNA.

### **Animal treatment**

Six-to-eight-week-old C57BL/6 male mice were obtained from the Africa Health Research Institute (AHRI) at the University of KwaZulu-Natal, Durban, South Africa. The mice were maintained according to the ARRIVE guidelines and the rules and regulations of the University of KwaZulu-Natal Animal Research Ethics Committee (Ethics approval number: AREC/079/016). Mice with a mean body weight of 20 ± 2.99 g were randomly divided into two groups, control and FA, with each group consisting of four mice. The mice were housed under standard laboratory conditions (temperature = 25°C, humidity = 40-60%, 12 hr light/dark cycle) and fed a commercially available mice pellet diet and normal drinking water *ad libitum* for the duration of the experiment. The mice were orally administered either with 0.1 M PBS (control group) or 50 mg/kg FA (FA group) [13] at a rate of 0.25 ml/23 g once for a period of 24 h. Following treatment, the mice were euthanized using Isofor (halothane anesthesia) and the livers were harvested. The livers were rinsed three times in 0.1 M PBS and stored in cytobuster reagent (500 μl; Novagen, 71009) and Qiazol reagent (500 μl; Qiagen, 79306) for protein and RNA isolation, respectively.

### **RNA isolation and quantitative polymerase chain reaction (qPCR)**

Total RNA was isolated from control, FA-treated HepG2 cells, and mice livers using Qiazol Reagent (Qiagen, 79306), as previously described [4]. The RNA was quantified using the Nanodrop2000 spectrophotometer (Thermo-Fisher Scientific) and standardized to 1,000 ng/μl. The purity of the RNA was assessed using the A260/A280 absorbance ratio.

The RNA was reverse transcribed into complementary DNA (cDNA) using the miScript II RT Kit (Qiagen, 218161), as per manufacturer's instructions. The expression of miR-200a and miR-141 was analyzed using the miScript SYBR Green PCR Kit (Qiagen, 218073) and 10X miScript

primer assays (Hs-miR-200a\_1, Qiagen, MS00003738; Mm-miR-200a\_1, Qiagen, MS00001813; Hs-miR-141\_1, Qiagen, MS00003507; Mm-miR-141\_1, Qiagen, MS00001610), as per manufacturer's instructions. RNU6 (Qiagen, MS00033740) was used as the internal control to normalise microRNA expression.

For mRNA expression, cDNA was synthesized using the iScript cDNA Synthesis Kit (Bio-Rad, 1708891), as per manufacturer's instructions. The expression of *Sirt1*, *SUV39H1*, and *KDM4B* was determined using the Sso Advanced™ Universal SYBR Green Supermix (Bio-Rad, 1725270), as per manufacturer's instructions. *GAPDH* was used as the housekeeping gene to normalise mRNA expression. Primer sequences and annealing temperatures are listed in Supplementary Table S4.1. All qPCR experiments were performed using the CFX96 Real Time PCR System and analyzed using the Bio-Rad CFX Manager™ Software version 3.1. Data was analyzed using the comparative threshold cycle (Ct) method and represented as a mean fold-change relative to the control [43].

### **Protein isolation and western blot**

Western blots were used to determine the protein expression of Sirt1, MDM2, SUV39H1, H3K9me3, H3K9me1, p-S139-H2Ax, cleaved-Asp175-caspase-3, caspase-3, cleaved-Asp330-caspase-9, and caspase-9 [44]. Briefly, protein was isolated from control, FA-treated HepG2 cells, and mice livers using cytotbuster reagent (Novagen, 71009) supplemented with protease and phosphatase inhibitors (Roche; 05892791001 and 04906837001, respectively). The protein samples were quantified using the bicinchoninic acid (BCA) assay and standardized to 1 mg/ml (HepG2 cells) and 5 mg/ml (mice livers). The samples were then boiled (100°C, 5 min) in a 1:1 dilution with Laemmli buffer [dH<sub>2</sub>O, 0.5 M Tris-HCl (pH 6.8), glycerol, 10% SDS, 5% β-mercaptoethanol and 1% bromophenol blue] and electrophoresed (1 hr, 150 V) in sodium dodecyl sulphate polyacrylamide gels (10% resolving gel, 4% stacking gel) using the Bio-Rad compact power supply. The separated proteins were transferred onto nitrocellulose membranes using the Bio-Rad Trans-Blot® Turbo Transfer System (20 V, 30 min). Non-specific binding was blocked by incubating the membranes in 5% BSA in Tris buffered saline with 0.05% Tween 20 [TTBS; 150 mM NaCl, 3 mM KCl, 25 mM Tris, 0.05% Tween 20, dH<sub>2</sub>O, pH 7.5] for 1 hr at RT. Thereafter, the membranes were probed with primary antibody (Sirt1 [Cell Signaling Technology, #2496], MDM2 [Sigma-Aldrich, M4308], SUV39H1 [Abcam, ab155164], H3K9me3 [Abcam, ab8898], H3K9me1 [Cell Signaling Technology, #7538S], p-S139-H2Ax [Abcam, ab131385], cleaved-Asp175-caspase-3 [Cell Signaling Technology, #9664P], caspase-3 [Cell Signaling Technology, #9662P], cleaved-Asp330-caspase-9 [Cell Signaling Technology,

#7273P], caspase-9 [Cell Signaling Technology, #9504; 1:1,000) for 1 hr at RT and then overnight at 4°C. The membranes were washed five times with TTBS (10 min, RT) and probed with a horse-radish peroxidase (HRP)-conjugated secondary antibody (goat anti-rabbit [Cell Signaling Technology, #7074S] and goat anti-mouse [Cell Signaling Technology, #7076P2]; 1:5,000) for 1 hr at RT. The membranes were washed five times in TTBS (10 min, RT). Protein bands were visualized using the Clarity™ Western ECL Substrate Kit (Bio-Rad, #170-5060) and the images were captured using the ChemiDoc™ XRS+ Molecular Imaging System (Bio-Rad). Following detection, the membranes were incubated in hydrogen peroxide (5%, 37°C, 30 min), washed once in TTBS (10 min, RT), blocked in 5% BSA (1 hr, RT) and probed with the housekeeping protein, anti-β-actin (Sigma-Aldrich, A3854; 1:5,000; 30 min, RT). The Image Lab Software version 5.1 (Bio-Rad) was used to analyze protein expression and the results were represented as a mean fold-change in band density (RBD) relative to the control. Protein expression was normalized against the housekeeping protein, β-actin.

### **Immuno-precipitation**

Immuno-precipitation was used to determine ubiquitinated SUV39H1 levels [4]. Briefly, crude protein was harvested from control and FA-treated HepG2 cells using 1X cell lysis buffer [20 mM Tris (pH 7.5), 150 mM NaCl, 1 mM EDTA, 10% glycerol, and 1% Triton X-100]. The protein was quantified using the BCA assay and standardized to 1.5 mg/ml. Thereafter, the protein lysates (200 μl) were incubated with primary antibody [SUV39H1 (Abcam, ab155164); 1:100] overnight (4°C) and then with Protein A beads (20 μl 50% bead slurry; Cell Signaling Technology, #9863) for 1-3 h at 4°C. The samples were centrifuged (14,000 x g, 4°C, 30 s); the immuno-precipitates were washed five times in 1X cell lysis buffer (500 μl) and re-suspended in 3X Laemmli buffer (20 μl) before boiling (100°C) for 5 min. The samples were then analyzed by western blotting using the following antibodies: primary antibody [SUV39H1 (Abcam, ab155164; 1:1,000) and ubiquitin (BD BioSciences, BD550944; 1:1,000)] and secondary antibody [goat anti-rabbit (Cell Signaling Technology, #7074S; 1:5,000) and goat anti-mouse (Cell Signaling Technology, #7076P2; 1:5,000)]. The protein expression of ubiquitin was divided by the protein expression of total SUV39H1 to determine the ratio of ubiquitinated SUV39H1.

### **Extraction of nuclear and cytoplasmic protein fractions**

The nuclear and cytoplasmic protein fractions were isolated from control and FA-treated HepG2 cells using the ReadyPrep™ Protein Extraction Kit (Cytoplasmic/Nuclear) (Bio-Rad, #163-2089), as per manufacturer's instructions [45]. Briefly, control and FA-treated HepG2 cells

were incubated (30 min, 4°C) in cytoplasmic protein extraction buffer (500 µl) supplemented with protease (Roche, 05892791001) and phosphatase (Roche, 04906837001) inhibitors before passing through a needle (21 gauge/ 20 strokes). Cell lysates were centrifuged (1,000 x g, 4°C, 10 min) and the supernatant containing the cytoplasmic protein fraction was transferred to fresh 1.5 ml micro-centrifuge tubes. The remaining nuclear pellet was re-suspended in protein solubilization buffer (500 µl) and vortexed (4-5 times, 60 s). The samples were centrifuged (16,000 x g, 4°C, 20 min) and the supernatant containing the nuclear protein fraction was transferred to 1.5 ml micro-centrifuge tubes. The nuclear and cytoplasmic protein fractions were quantified using the Nanodrop2000 spectrophotometer and standardized to a concentration of 0.3 mg/ml. Thereafter, Laemmli buffer [dH<sub>2</sub>O, 0.5 M Tris-HCl (pH 6.8), glycerol, 10% SDS, 5% β-mercaptoethanol and 1% bromophenol blue] was added and the samples were boiled (100°C) for 5 min. The protein expression of SUV39H1 was determined in both the nuclear and cytoplasmic fractions using western blotting as mentioned above. Antibodies used were as follows: primary antibody [SUV39H1 (Abcam, ab155164); 1:1,000] and secondary antibody [goat anti-rabbit (Cell Signaling Technology, #7074S); 1:5,000]. The cytoplasmic protein expression was normalized against β-actin (Sigma-Aldrich, A3854; 1:5,000) whereas the nuclear protein expression was normalized against laminin B<sub>1</sub> (Sigma-Aldrich, SAB2101352; 1:500). Results are represented as a mean fold-change in band density relative to the control.

### **DNA isolation and DNA electrophoresis**

DNA electrophoresis was used to determine the effect of FA on genome stability in HepG2 cells [46]. Briefly, control and FA-treated HepG2 cells were incubated (15 min, RT) in cell lysis buffer (600 µl; 0.5 M EDTA (pH 8.0), 1 M Tris-Cl (pH 7.6), and 0.1% SDS). Thereafter, potassium acetate buffer (600 µl; 5 M potassium acetate and glacial acetic acid) was added to the samples (8 min, RT) and centrifuged (13,000 x g, 5 min, 24°C). The supernatant containing genomic DNA was transferred into fresh 1.5 ml micro-centrifuge tubes and 100% isopropanol (600 µl) was added to the samples to precipitate the DNA. The DNA was recovered by centrifugation (13,000 x g, 5 min, 24°C), washed once in 100% ethanol (300 µl), and centrifuged (13,000 x g, 5 min, 24°C). The DNA pellets were air dried (30 min, RT), re-suspended in DNA hydration buffer (40 µl; 10 mM EDTA (pH 8.0) and 100 mM Tris-Cl (pH 7.4)), and heated (65°C, 15 min). The DNA was quantified using the Nanodrop2000 spectrophotometer, standardized to 100 ng/µl and prepared in a 1:1 ratio with loading dye [3.7 mM bromophenol blue, 1.2 M sucrose]. The DNA was then electrophoresed (120 V, 25 min) in a 1.8% agarose gel containing 2 µl GelRed and visualized using the ChemiDoc™ XRS+

Molecular Imaging System (Bio-Rad). A 500 bp DNA ladder and 5  $\mu$ M Camptothecin was used as a positive control to determine DNA damage/fragmentation.

### **Crystal violet cell viability assay**

The crystal violet assay was used to determine the effect of FA on HepG2 cell viability [47]. Briefly, HepG2 cells (20,000 cells/well) were seeded in a 96-well microtiter plate and allowed to adhere overnight (37°C, 5% CO<sub>2</sub>), before incubation with FA (37°C, 5% CO<sub>2</sub>, 24 h). Following treatment, the cells were rinsed twice in dH<sub>2</sub>O and incubated with 0.5% crystal violet staining solution (50  $\mu$ l/well; 20 min, RT). The cells were washed four times in dH<sub>2</sub>O and allowed to air dry overnight. Methanol (200  $\mu$ l) was added to each well and the cells were incubated (20 min, RT). The absorbance was then measured at 570 nm using the Biotek uQuant spectrophotometer and the percentage cell viability in each FA treatment was determined relative to the control.

### **Luminometry**

The activities of caspases -8, -9, and -3/7 were assessed using the Caspase-Glo® luminometry assays (Promega) [9]. Briefly, control and FA-treated HepG2 cells (20,000 cells/well in 50  $\mu$ l PBS) were seeded into an opaque 96-well microtiter plate in triplicate. Thereafter, 20  $\mu$ l of Caspase-Glo® Reagent was added to each well and the plate was incubated (30 min, RT) in the dark. Luminescence was measured using the Modulus™ microplate luminometer (Turner Biosystems) and the results were expressed as relative light units (RLU).

### **Statistical analysis**

All statistical analyses were performed using GraphPad Prism version 5.0 (GraphPad Prism Software Inc.). Normality was determined using the D'Agostino and Pearson tests. Data from the HepG2 cells were analyzed using the one-way Analysis of Variance (ANOVA) with the Bonferroni multiple comparisons test and the results were represented as the mean fold-change  $\pm$  standard deviation (SD) (n = 3). Data from the mice livers were analyzed using the unpaired t-test with Welch's correction and the results were represented as the mean fold-change  $\pm$  standard error of the mean (SEM) (n = 3 (qPCR assays) / n = 4 (western blot assays)). Statistical significance was considered at  $p < 0.05$ .

## Results

### Fusaric acid upregulates miR-200a in HepG2 cells and mice livers

The expression of miR-200a was assessed in control, FA-treated HepG2 cells, and mice livers using qPCR. The HepG2 cells were also treated with a miR-200a mimic (positive control) and miR-200a inhibitor (negative control). The expression of miR-200a was increased by FA in HepG2 cells ( $p < 0.0001$ ; Figure 4.1A) and mice livers ( $p = 0.0055$ ; Figure 4.1B) compared to the controls. The expression of miR-200a in HepG2 cells by the mimic and inhibitor were increased and decreased ( $p < 0.0001$ ; Figure 4.1A), respectively. Since, miR-200a and miR-141 have high sequence homology [20, 21], the effect of FA on miR-141 expression was assessed; miR-141 expression was significantly increased by FA in HepG2 cells ( $p < 0.0001$ ; Supplementary Figure S4.1A) but decreased in the mice livers ( $p < 0.0001$ ; Supplementary Figure S4.1B) compared to the controls.

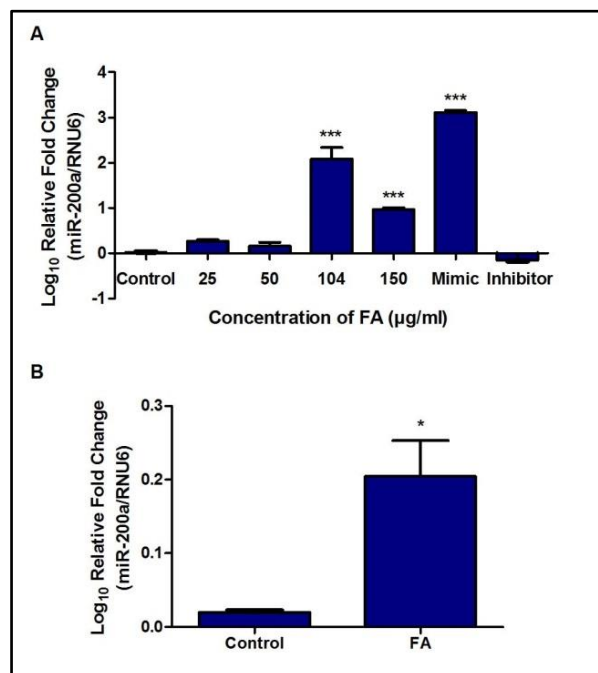


**Figure 4.1 FA upregulates miR-200a in HepG2 cells and mice livers.** qPCR analysis of miR-200a expression in HepG2 cells and mice livers. (A) FA increased the expression of miR-200a in HepG2 cells. The expression of miR-200a in the mimic and inhibitor was significantly increased and decreased, respectively. Results are represented as mean fold-change  $\pm$  SD,  $n = 3$  (\*\*\*)  $p < 0.0001$ ; one way ANOVA with the Bonferroni multiple comparisons test). (B) FA increased the expression of miR-200a in mice livers. Results are represented as mean fold-change  $\pm$  SEM,  $n = 3$  (\*)  $p < 0.05$ ; unpaired t-test with Welch's correction). FA: Fusaric acid.

## **Fusaric acid decreases Sirt1 expression in HepG2 cells and mice livers**

MiR-200a and miR-141 were previously shown to directly target *Sirt1* [20]. This was further confirmed using the bioinformatics prediction algorithm software, TargetScan (version 7.1), where miR-200a and miR-141 were found to have complementary base pairs with *Sirt1* at positions 1728 - 1734 in humans (Figure 4.2A and Supplementary Figure S4.2A) and positions 1562 - 1568 in mice (Figure 4.2B and Supplementary Figure S4.2B). Due to the increased expression of miR-200a by FA, we next determined the effect of FA on Sirt1 mRNA and protein expression levels in HepG2 cells and mice livers. FA decreased Sirt1 mRNA (HepG2 cells:  $p < 0.0001$ , Figure 4.2C; mice livers:  $p = 0.0006$ , Figure 4.2D) and protein (HepG2 cells:  $p < 0.0001$ , Figure 4.2E; mice livers:  $p = 0.0231$ , Figure 4.2F) expression levels compared to the controls. Treatment of HepG2 cells with the miR-200a mimic and inhibitor resulted in a decrease and increase, respectively in Sirt1 mRNA (Figure 4.2C) and protein levels (Figure 4.2E). This further validates that *Sirt1* is a target of miR-200a in the liver.

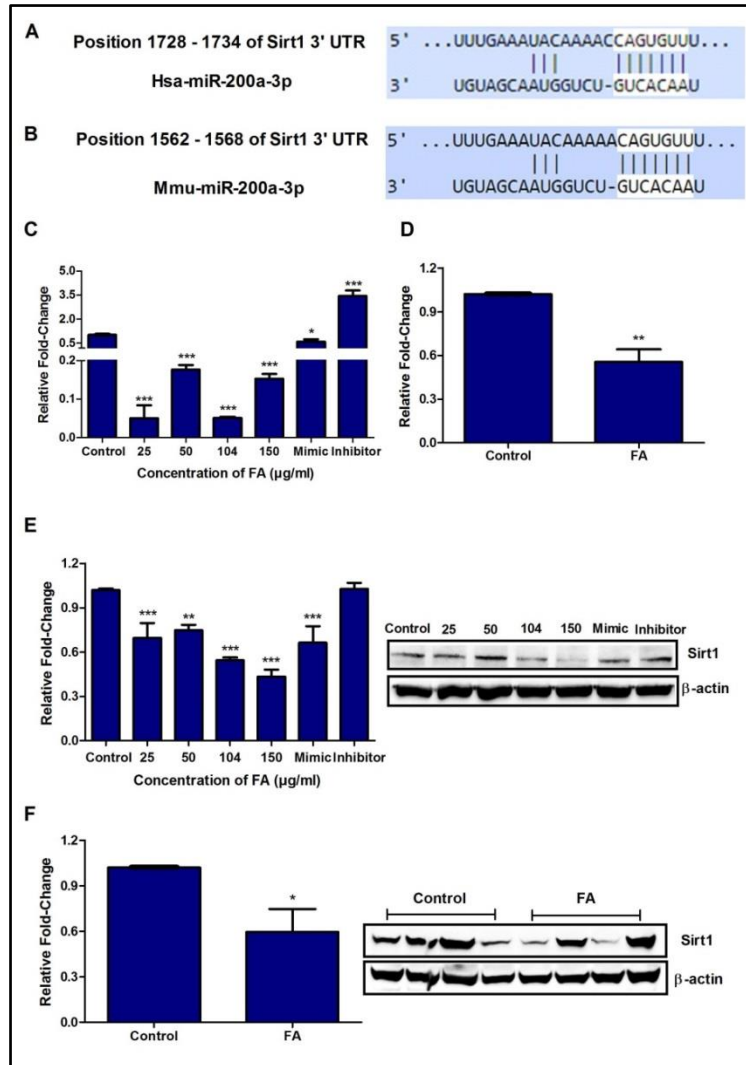


**Figure 4.2 FA decreases *Sirt1* mRNA and protein expression in HepG2 cells and mice livers.** qPCR and western blot analysis of *Sirt1* in HepG2 cells and mice livers. **(A)** TargetScan analysis of miR-200a to the 3'UTR of *Sirt1* in humans. **(B)** TargetScan analysis of miR-200a to the 3'UTR of *Sirt1* in mice. **(C)** FA decreased *Sirt1* expression in HepG2 cells. The expression of *Sirt1* in the miR-200a mimic and inhibitor was decreased and increased, respectively. Results are represented as mean fold-change  $\pm$  SD,  $n = 3$  (\* $p < 0.05$ , \*\*\* $p < 0.0001$ ; one-way ANOVA with the Bonferroni multiple comparisons test). **(D)** FA decreased *Sirt1* expression in mice livers. Results are represented as mean fold-change  $\pm$  SEM,  $n = 3$  (\*\* $p < 0.005$ ; unpaired t-test with Welch's correction). **(E)** FA decreased *Sirt1* protein expression in HepG2 cells. The expression of *Sirt1* in the miR-200a mimic and inhibitor was decreased and increased, respectively. Results are represented as mean fold-change  $\pm$  SD,  $n = 3$  (\*\* $p < 0.005$ , \*\*\* $p < 0.0001$ ; one-way ANOVA with the Bonferroni multiple comparisons test). **(F)** FA decreased *Sirt1* protein expression in mice livers. Results are represented as mean fold-change  $\pm$  SEM,  $n = 4$  (\* $p < 0.05$ ; unpaired t-test with Welch's correction). FA: Fusaric acid; *Sirt1*: Sirtuin 1.

### Fusaric acid alters SUV39H1 ubiquitination in HepG2 Cells

SUV39H1 is subject to PTMs that regulate its expression and activity. Acetylation of K266 was associated with an inhibition in catalytic activity [37] and ubiquitination of K87 was shown to promote proteosomal degradation [33]. Sirt1 regulates SUV39H1 ubiquitination by directly interacting with and deacetylating SUV39H1 thereby, preventing its ubiquitination and degradation. Due to the FA-induced decrease in Sirt1 expression, we evaluated the effect of FA on the ubiquitination of SUV39H1 in HepG2 cells using immuno-precipitation. The expression of ubiquitinated SUV39H1 was significantly decreased in the 25, 50, and 150  $\mu\text{g/ml}$  FA treatments; however, at 104  $\mu\text{g/ml}$  FA the ubiquitination of SUV39H1 was significantly increased compared to the control ( $p < 0.0001$ ; Figure 4.3A).

The E3 ubiquitin ligase, MDM2, is the main regulator of SUV39H1 ubiquitination [33, 48]. Therefore, we determined the effect of FA on the protein expression of MDM2. FA increased the expression of MDM2 in HepG2 cells compared to the control ( $p < 0.0001$ ; Figure 4.3B).

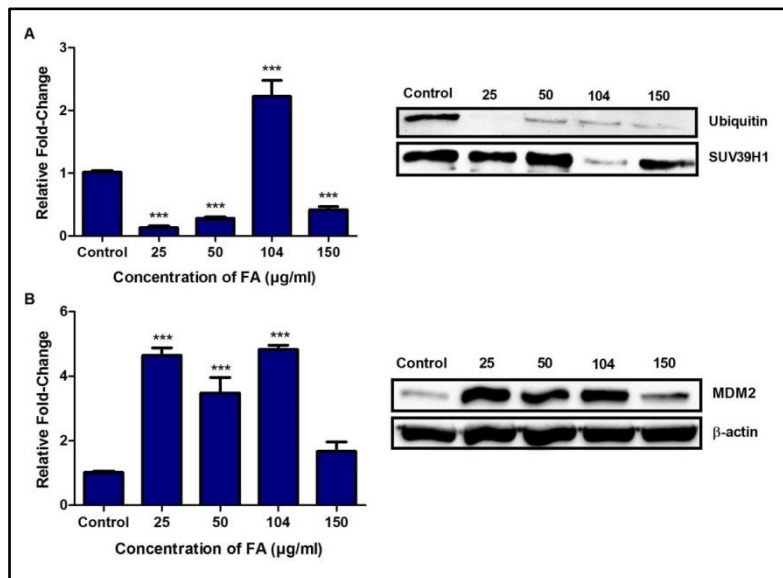


**Figure 4.3 FA alters SUV39H1 ubiquitination and increases MDM2 expression in HepG2 cells.** (A) The ubiquitination of SUV39H1 in HepG2 cells was determined by immuno-precipitation and western blot. FA altered SUV39H1 ubiquitination in HepG2 cells. Results are represented as mean fold-change  $\pm$  SD,  $n = 3$  ( $***p < 0.0001$ ; one-way ANOVA with the Bonferroni multiple comparisons test). (B) Western blot analysis of MDM2 in HepG2 cells. FA increased the protein expression of MDM2 in HepG2 cells. Results are represented as mean fold-change  $\pm$  SD,  $n = 3$  ( $***p < 0.0001$ ; one-way ANOVA with the Bonferroni multiple comparisons test). FA: Fusaric acid; SUV39H1: suppressor of variegation 3-9 homolog 1; MDM2: murine double minute 2.

## Fusaric acid alters SUV39H1 nuclear and cytoplasmic levels in HepG2 cells

PTMs of SUV39H1 are associated with changes in cellular localization. Mobile or free SUV39H1 is usually ubiquitinated and found in the cytoplasm where it is targeted for proteasomal degradation, however, chromatin-associated SUV39H1 is found in the nucleus where it functions to trimethylate H3K9. Due to the changes in SUV39H1 ubiquitination, we determined the effect of FA on the protein expression of nuclear and cytoplasmic SUV39H1. FA significantly altered the expression of SUV39H1 nuclear levels ( $p < 0.0001$ ; Figure 4.4) and increased its cytoplasmic levels ( $p < 0.0001$ ; Figure 4.4) in HepG2 cells relative to the control.

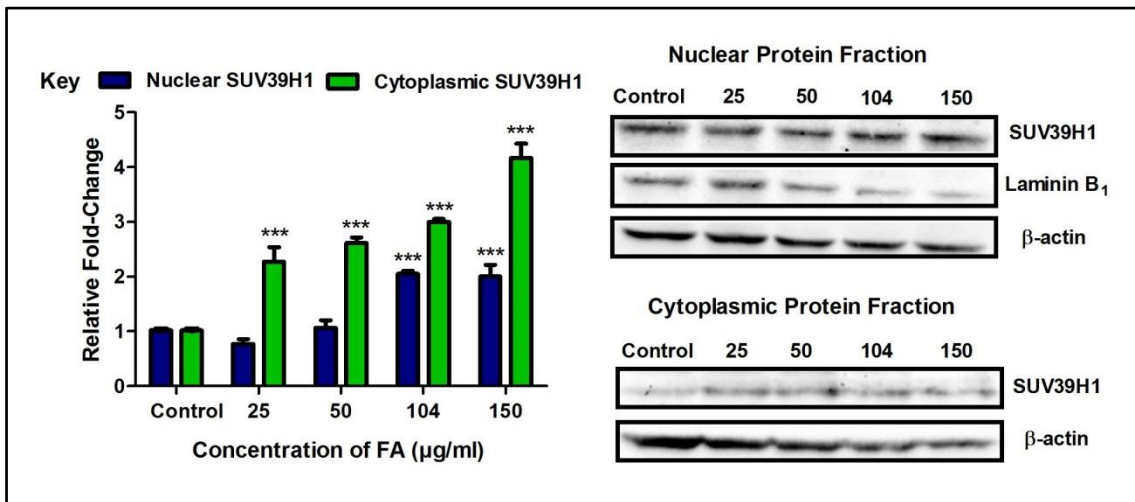


**Figure 4.4** FA alters expression levels of nuclear and cytoplasmic SUV39H1 in HepG2 cells. Western blot analyses of SUV39H1 in the nuclear and cytoplasmic protein fractions. FA altered SUV39H1 nuclear levels and increased SUV39H1 cytoplasmic levels in HepG2 cells. Results are represented as mean fold-change  $\pm$  SD,  $n = 3$  (\*\*\*)  $p < 0.0001$ ; one-way ANOVA with the Bonferroni multiple comparisons test). FA: Fusaric acid; SUV39H1: suppressor of variegation 3-9 homolog 1.

## Fusaric acid decreases the expression of SUV39H1 in HepG2 cells and mice livers

SUV39H1 ubiquitination as well as changes in cellular localization is known to affect SUV39H1 stability and expression [33, 37, 48]; hence, we determined the effect of FA on the expression of SUV39H1 mRNA and protein levels. FA significantly decreased SUV39H1 mRNA ( $p < 0.0001$ ; Figure 4.5A) and protein ( $p < 0.0001$ ; Figure 4.5B) levels in HepG2 cells compared to the control. The expression of SUV39H1 mRNA ( $p = 0.0110$ ; Figure 4.5C) and protein ( $p < 0.0001$ ; Figure 4.5D) levels were significantly increased and decreased in the FA-treated mice livers, respectively.

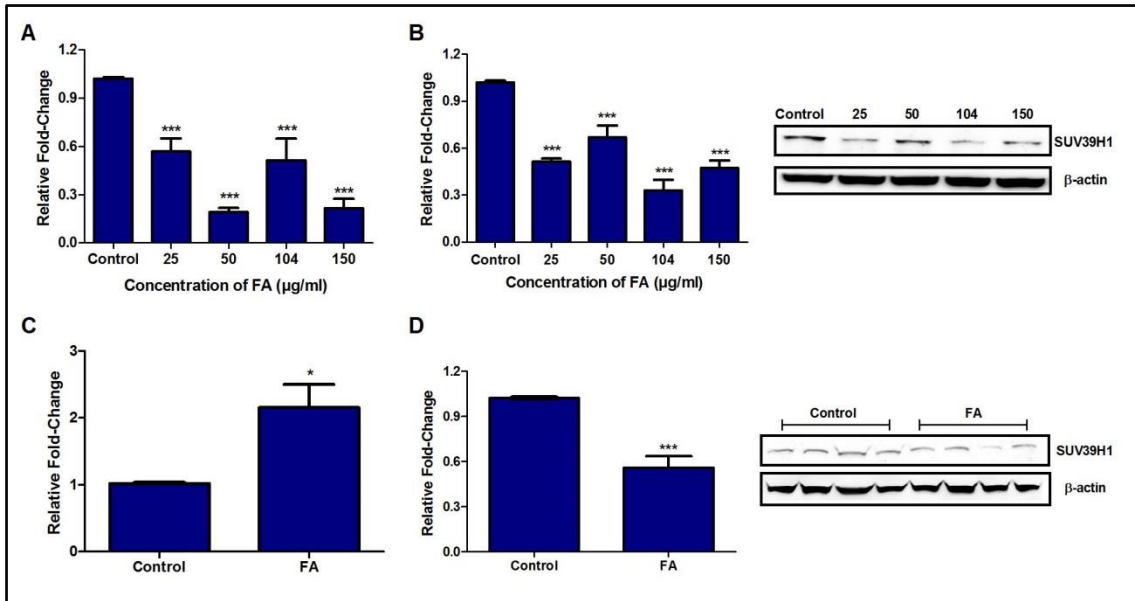


**Figure 4.5 FA alters SUV39H1 mRNA and protein expression in HepG2 cells and mice livers.** qPCR and western blot analysis of SUV39H1 in HepG2 cells and mice livers. **(A)** FA significantly decreased *SUV39H1* mRNA expression in HepG2 cells. Results are represented as mean fold-change  $\pm$  SD,  $n = 3$  (\*\* $p < 0.0001$ ; one-way ANOVA with the Bonferroni multiple comparisons test). **(B)** FA significantly decreased SUV39H1 protein expression in HepG2 cells. Results are represented as mean fold-change  $\pm$  SD,  $n = 3$  (\*\* $p < 0.0001$ ; one-way ANOVA with the Bonferroni multiple comparisons test). **(C)** FA significantly increased *SUV39H1* mRNA expression in mice livers. Results are represented as mean fold-change  $\pm$  SEM,  $n = 3$  ( $*p < 0.05$ ; unpaired t-test with Welch's correction). **(D)** FA significantly decreased SUV39H1 protein expression in mice livers. Results are represented as mean fold-change  $\pm$  SEM,  $n = 4$  (\*\* $p < 0.0001$ ; unpaired t-test with Welch's correction). FA: Fusaric acid; SUV39H1: suppressor of variegation 3-9 homolog 1.

### Fusaric acid decreases H3K9me3 and increases H3K9me1 in HepG2 cells and mice livers

SUV39H1 is the key regulator of H3K9me3, and an inhibition or depletion in SUV39H1 may result in alterations in H3K9me3. Since FA decreased the expression of SUV39H1, we determined if FA effects H3K9me3 in HepG2 cells and mice livers. The expression of H3K9me3 was significantly decreased in the FA-treated HepG2 cells ( $p < 0.0001$ ; Figure 4.6A) and mice livers ( $p = 0.0194$ ; Figure 4.6B) compared to the controls.

The lysine demethylase, KDM4B is responsible for specifically demethylating H3K9me3 by converting H3K9me3 to its mono-methylated state (H3K9me1) which then forms a substrate for

SUV39H1-mediated trimethylation. Due to FA decreasing H3K9me3, we next evaluated the effect of FA on H3K9me1 and the mRNA expression of the lysine demethylase, *KDM4B*. FA increased the expression of H3K9me1 in HepG2 cells ( $p < 0.0001$ ; Figure 4.6A) and mice livers ( $p = 0.1292$ ; Figure 4.6B) compared to the controls. FA decreased the expression of *KDM4B* in HepG2 cells ( $p < 0.0001$ ; Figure 4.6C) and mice livers ( $p = 0.5076$ ; Figure 4.6D) compared to their respective controls.

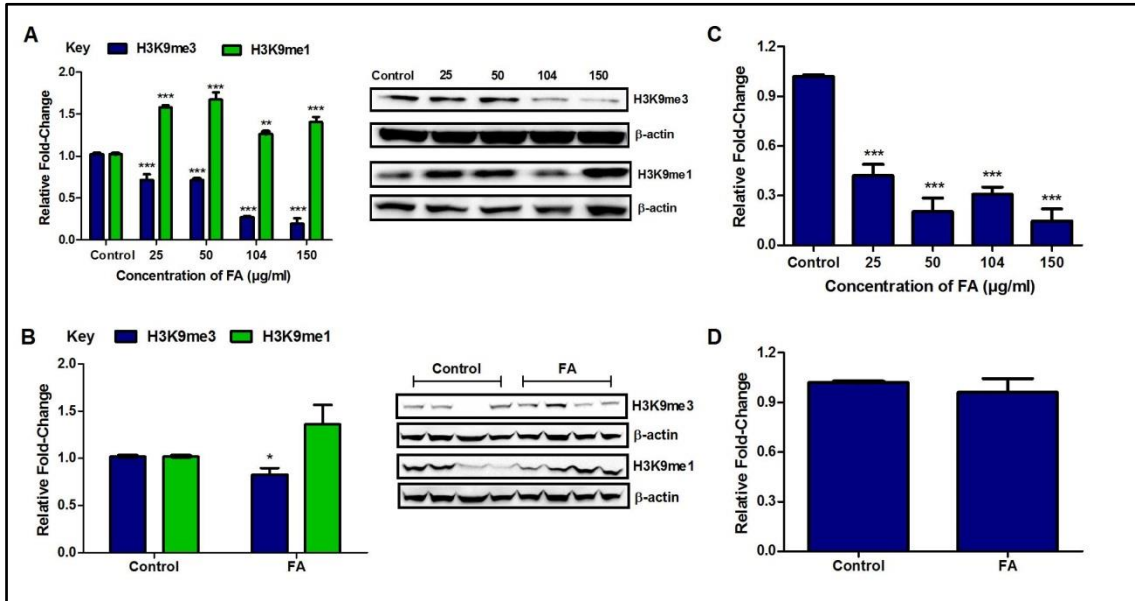


**Figure 4.6 FA decreases H3K9me3 and increases H3K9me1 in HepG2 cells and mice livers.** Western blot analyses of H3K9me3 and H3K9me1 expression, and qPCR analysis of *KDM4B* expression in HepG2 cells and mice livers. (A) FA significantly decreased H3K9me3 and increased H3K9me1 in HepG2 cells. Results are represented as mean fold-change  $\pm$  SD,  $n = 3$  (\*\* $p < 0.005$ , \*\*\* $p < 0.0001$ ; one-way ANOVA with the Bonferroni multiple comparisons test). (B) FA decreased H3K9me3 and increased H3K9me1 in mice livers. Results are represented as mean fold-change  $\pm$  SEM,  $n = 4$  (\* $p < 0.05$ ; unpaired t-test with Welch's correction). (C) FA significantly decreased *KDM4B* mRNA expression in HepG2 cells. Results are represented as mean fold-change  $\pm$  SD,  $n = 3$  (\*\*\*) $p < 0.0001$ ; one-way ANOVA with the Bonferroni multiple comparisons test). (D) FA decreased *KDM4B* mRNA expression in mice livers. Results are represented as mean fold-change  $\pm$  SEM,  $n = 3$  (non-significant; unpaired t-test with Welch's correction). FA: Fusaric acid; H3K9me3: histone 3 lysine 9 trimethylation; H3K9me1: histone 3 lysine 9 mono-methylation.

## **Fusaric acid induces genome instability and alters p-S139-H2Ax in HepG2 cells and mice livers**

PTMs of histones influence chromatin structure and thus have a crucial role in regulating gene transcription and genome integrity [33, 36]. H3K9me3 plays a major role in maintaining heterochromatin; and a decrease in H3K9me3 was previously shown to lead to a loss in heterochromatin formation and genome instability [33]. We determined if the loss in H3K9me3 observed in the FA treatments led to genome instability by using DNA electrophoresis. The effect of FA on phosphorylated serine 139 Histone H2Ax (p-S139-H2Ax), a marker of DNA double-strand breaks and indicator of DNA damage, was also determined. Analysis of DNA isolated from the FA-treated HepG2 cells revealed a significant amount of DNA smearing as compared to the controls (Figure 4.7A). The expression of p-S139-H2Ax by FA was significantly decreased at 25, 50, and 104 µg/ml, however, at 150 µg/ml FA its expression was significantly increased ( $p < 0.0001$ ; Figure 4.7B). The expression of p-S139-H2Ax in the FA-treated mice livers was also decreased compared to the control ( $p = 0.2207$ ; Figure 4.7C).

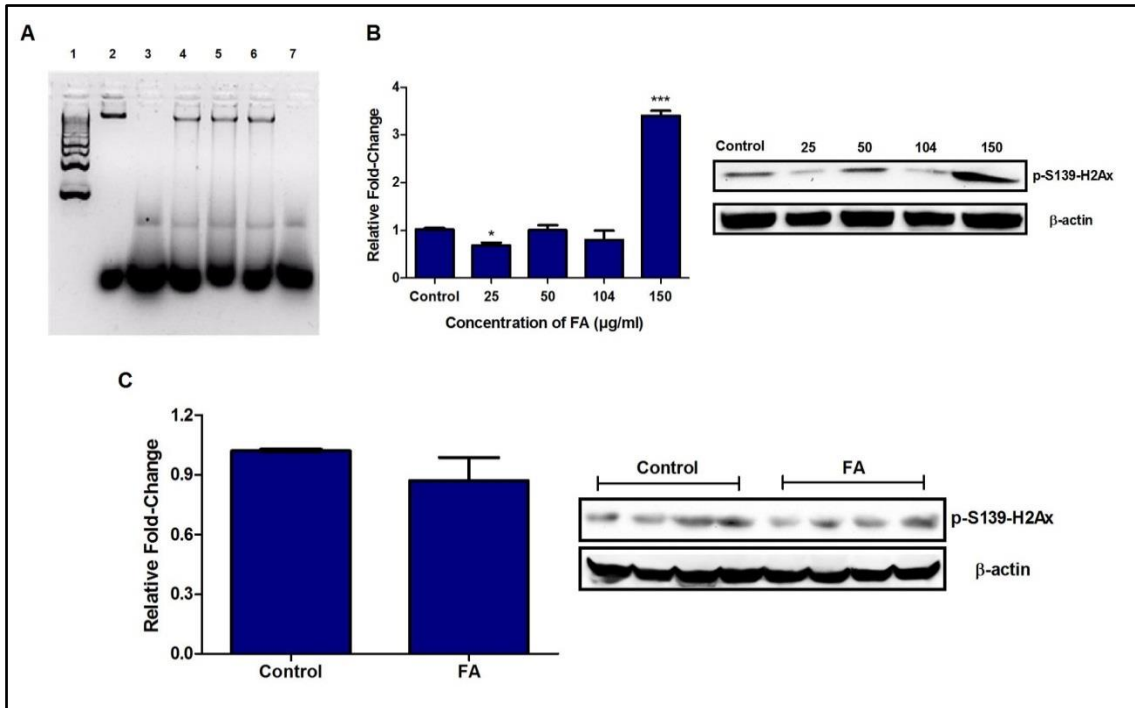


**Figure 4.7 FA induces genome instability and alters p-S139-H2Ax in HepG2 cells and mice livers.** (A) Electrophoresis of DNA isolated from control and FA-treated HepG2 cells. FA induced DNA fragmentation in HepG2 cells (Lane 1: DNA ladder, lane 2: control, lane 3: 25 µg/ml FA, lane 4: 50 µg/ml FA, lane 5: 104 µg/ml FA, lane 6: 150 µg/ml FA, lane 7: 5 µM Camptothecin). (B) Western blot analysis of p-S139-H2Ax in HepG2 cells. FA altered the expression of p-S139-H2Ax in HepG2 cells. Results are represented as mean fold-change ± SD, n = 3 (\* $p < 0.05$ , \*\*\* $p < 0.0001$ ; one-way ANOVA with the Bonferroni multiple comparisons test). (C) Western blot analysis of p-S139-H2Ax in mice livers. FA decreased p-S139-H2Ax in mice livers. Results are represented as mean fold-change ± SEM, n = 4 (non-significant; unpaired t-test with Welch's correction). FA: Fusaric acid; p-S139-H2Ax: phosphorylated serine 139 of histone H2Ax.

### Fusaric acid induces apoptosis in HepG2 cells and mice livers

Since a loss in H3K9me3 is known to affect cell proliferation by regulating apoptotic cell death, we determined if FA induced apoptosis by assessing the activity of the caspases -8, -9, and -3/7. The crystal violet cell viability assay and the Caspase-Glo luminometry assays were used to determine the effect of FA on cell viability and apoptosis in HepG2 cells, respectively. Apoptosis in the mice livers was determined by assessing the expression of total and cleaved caspases -3 and -9 via western blot. In HepG2 cells, FA significantly decreased cell viability ( $p < 0.0001$ ; Figure 4.8A), increased the activity of caspase-3/7 ( $p < 0.0001$ ; Figure 4.8B), and

significantly decreased the activity of caspase-8 as compared to the controls ( $p < 0.0001$ ; Supplementary Figure S4.3A). FA also decreased caspase-9 activity at 25, 50, and 104  $\mu\text{g/ml}$  treatments, but increased caspase-9 activity at 150  $\mu\text{g/ml}$  treatment in HepG2 cells ( $p < 0.0001$ ; Supplementary Figure S4.3B). The expression of cleaved-Asp175-caspase-3 (active caspase-3) was significantly increased in the FA-treated mice livers (19 kDa:  $p = 0.0372$  and 17 kDa:  $p = 0.0004$ ; Figure 4.8C), however, the expression of total caspase-3 was decreased ( $p = 0.1601$ ; Figure 4.8C). The expression of total and cleaved-Asp330-caspase-9 was significantly decreased in the FA-treated mice livers ( $p = 0.0032$  and  $p = 0.0013$ , respectively; Supplementary Figure S4.3C). This suggests that FA decreases cell viability and induces apoptosis in HepG2 cells and mice livers.

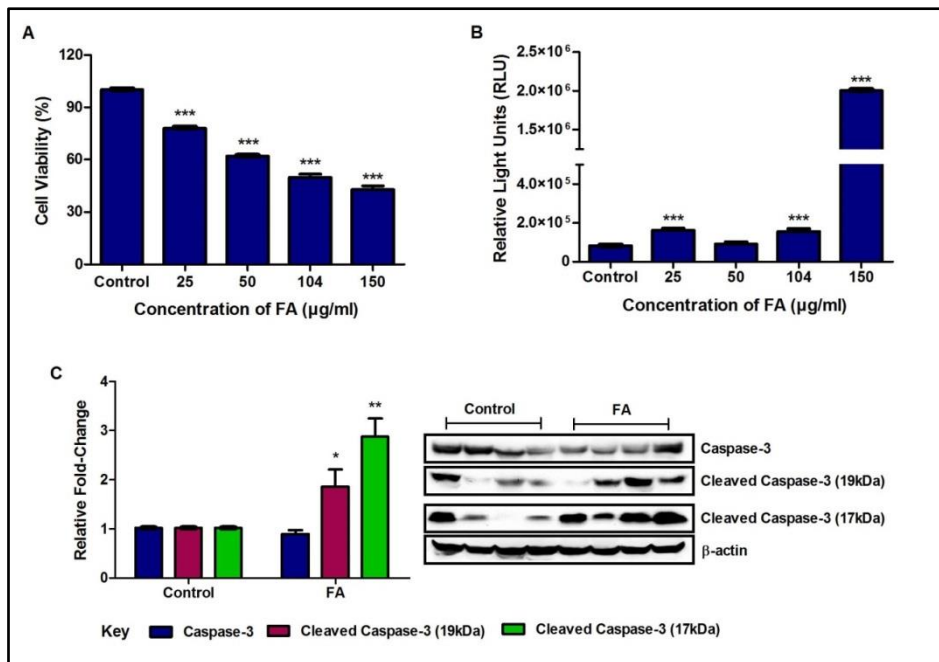


**Figure 4.8 FA decreases cell viability and increases caspase-3/7 activity in HepG2 cells and mice livers.** (A) Cell viability was determined using the Crystal Violet Assay. FA significantly decreased HepG2 cell viability in a dose-dependent manner. Results are represented as a mean percentage in cell viability  $\pm$  SD,  $n = 3$  (\*\*\*) $p < 0.0001$ ; one-way ANOVA with the Bonferroni multiple comparisons test). (B) Luminometric analysis of caspase-3/7 activity in HepG2 cells. FA increased the activity of caspase-3/7 in HepG2 cells. Results are represented as mean  $\pm$  SD,  $n = 3$  (\*\*\*) $p < 0.0001$ ; one-way ANOVA with the Bonferroni multiple comparisons test). (C) Western blot analysis of total caspase-3 and cleaved-Asp175-caspase-3 expressions in mice livers. FA decreased the expression of total caspase-3 and increased the expression of cleaved-Asp175-caspase-3 in mice livers. Results are represented as mean fold-change  $\pm$  SEM,  $n = 4$  (\* $p < 0.05$ , \*\* $p < 0.005$ ; unpaired t-test with Welch's correction). FA: Fusaric acid.

## Discussion

The food-borne mycotoxin, FA causes toxicity by altering cell signaling pathways in both plants and animals [10-12, 15, 18]. Currently, only a few studies have elucidated the effects of FA in human cells, with sparse information on its mechanisms of toxicity. Recently, epigenetic studies on mycotoxins have provided insights into their mechanisms of toxicity. Fumonisin B<sub>1</sub> (FB<sub>1</sub>), a *Fusarium*-produced mycotoxin often co-produced with FA, was shown to cause chromatin instability and liver tumorigenesis by inducing global DNA hypomethylation and histone demethylation [44]. FB<sub>1</sub> inhibits miR-27b, increases cytochrome P450 1B1, and alters promoter methylation of tumor suppressor genes (*c-myc*, *p15*, *p16*, and *e-cadherin*) possibly leading to hepatic neoplastic transformation [49, 50]. FB<sub>1</sub> also alters the expression of H3K9me2/3, H3K9Ac, and H4K20me3 [51]. Similarly, zearalenone induced global DNA hypomethylation [52], and decreased H3K9me3, H3K4me2, and H4K20me1/2/3 [53].

FA was recently shown to exert its genotoxic and cytotoxic effects by inducing global DNA hypomethylation in HepG2 cells [4]; however, there are currently no studies evaluating the effects of FA on histone modifications both *in vitro* and *in vivo*. In this study, we provide evidence for an epigenetic mechanism of FA-induced apoptosis by altering miR-200a and SUV39H1-mediated H3K9me3 in an *in vitro* (HepG2 cells) and *in vivo* (mouse liver) model.

MicroRNA expression and histone methylation are epigenetic modifications that regulate cell signaling pathways by altering chromatin structure and gene transcription. These processes can be modified by exogenous agents and alterations in the epigenetic machinery of the cell may provide an important mechanism of FA-induced toxicity.

Our results indicate that FA significantly upregulated miR-200a in HepG2 cells and mice livers (Figure 4.1); however, the expression of miR-141 was significantly upregulated in the FA-treated HepG2 cells (Supplementary Figure S4.1A) but downregulated in the mice livers (Supplementary Figure S4.1B). The expression of miR-200a and miR-141 is regulated by DNA methylation [20], oxidative stress [21, 54], and p53 expression [54]. DNA hypermethylation downregulates miR-200a and miR-141, whereas DNA hypomethylation upregulates them both [20]. We recently reported that FA induced DNA hypomethylation in HepG2 cells by decreasing the expression of the DNA methyltransferases, DNMT1, DNMT3A, and DNMT3B, whilst increasing the expression of the DNA demethylase, MBD2 [4]. Therefore, the increase in miR-200a and miR-141 observed in the HepG2 cells and mice livers may be due to the FA-induced DNA hypomethylation. Further, the expression of miR-200a and miR-141 is stimulated by an increase in oxidative stress [21, 54]. Previously, FA was shown to induce oxidative stress

in various human cell lines [9, 11, 55], and this may then lead to the increased expressions of miR-200a and miR-141 observed in the HepG2 cells and mice livers. MiR-200a and miR-141 also contain p53-binding sites that enable p53 to bind to miR-200a/miR-141 promoters and activate their transcription [54]. Previously, we showed that FA decreased p53 expression in HepG2 cells [10] and this may have resulted in the decreased expression of miR-141 observed in the FA-treated mice livers.

MiR-200a and miR-141 were previously shown to directly target *Sirt1* [20] and this was further confirmed using TargetScan version 7.1 (Figure 4.2A-B and Supplementary Figure S4.2). FA significantly decreased the mRNA and protein expressions of *Sirt1* in HepG2 cells (Figure 4.2C and Figure 4.2E) and mice livers (Figure 4.2D and Figure 4.2F). These results are in agreement with previous studies where upregulation of miR-200a and miR-141 was found to downregulate *Sirt1* expression at both the protein and transcript levels [20, 56].

*Sirt1* is an NAD<sup>+</sup>-dependent lysine deacetylase that regulates gene transcription via its interaction with chromatin-associated proteins such as histones [31-33]. *Sirt1* also maintains genome stability and is involved in regulating heterochromatin formation [32] by direct deacetylation of histones, recruitment of histone H1, and alterations in the chromatin modifying enzymes, histone methyltransferases and histone acetyltransferases [57].

SUV39H1 is a SET-domain containing histone methyltransferase responsible for catalyzing H3K9me3 [33-35, 37, 39]. SUV39H1 is involved in heterochromatin organization and genome stability via its association with heterochromatin protein 1 (HP1), and a loss in SUV39H1 and H3K9me3 causes delocalization of HP1 and a reduction in heterochromatin levels [33, 37, 57].

PTMs such as acetylation and ubiquitination regulate SUV39H1 activity and expression [33, 37, 48, 58]. The acetylation of SUV39H1 on K266 in the catalytic SET-domain reduces its enzymatic activity [33] and enables MDM2 to polyubiquitinate SUV39H1 on K87 thereby, targeting it for proteasomal degradation [37]. *Sirt1* regulates SUV39H1 activity and expression. Previously, *Sirt1* was shown to interact with the N-terminal chromo-domain of SUV39H1 causing deacetylation of K266 and an increase in its histone methyltransferase activity [33, 37]. *Sirt1* also regulates SUV39H1 protein levels by inhibiting MDM2-mediated polyubiquitination of K87 in the SUV39H1 chromo-domain thereby, preventing its proteasomal degradation and increasing its half-life by nearly four times [33]. This was further confirmed in cervical cancer (HELA) cells, where an increase in *Sirt1* expression correlated with an increase in SUV39H1 protein levels [33]. The decrease in the expression of *Sirt1* by FA in HepG2 cells and mice livers suggests that FA may decrease SUV39H1 expression by ubiquitination. FA significantly

altered SUV39H1 ubiquitination (Figure 4.3A) and increased the expression of MDM2 in HepG2 cells (Figure 4.3B). The ubiquitin specific peptidase 7 (USP7) is a deubiquitinating enzyme that regulates SUV39H1 stability by protecting it from MDM2-mediated polyubiquitination and degradation [48]. Mechanistically, USP7 interacts with MDM2 and forms a trimeric protein complex with SUV39H1 [48]. This protein complex is independent of DNA and occurs only in the presence of MDM2, indicating that the interaction between USP7, MDM2 and SUV39H1 is essential for USP7 to deubiquitinate SUV39H1 as well as for MDM2 to ubiquitinate SUV39H1 [48]. Previously, FA was shown to decrease *USP7* expression in HepG2 cells [4] and this decrease in *USP7* may inhibit the USP7-MDM2-SUV39H1 complex leading to the alterations in ubiquitinated SUV39H1 observed in the FA-treated HepG2 cells.

PTMs of SUV39H1 are often associated with changes in sub-cellular localization. The ubiquitination of SUV39H1 causes SUV39H1 to translocate from the nucleus to the cytoplasm where it is degraded by the proteasome. The expression of nuclear SUV39H1 was decreased in the lower (25 µg/ml) FA concentration and increased in the higher (50, 104, and 150 µg/ml) FA concentrations (Figure 4.4). FA significantly increased cytoplasmic SUV39H1 levels in HepG2 cells (Figure 4.4); however, the expression of SUV39H1 mRNA (Figure 4.5A) and protein (Figure 4.5B) was significantly decreased in the FA-treated HepG2 cells. The expression of SUV39H1 mRNA (Figure 4.5C) and protein (Figure 4.5D) was increased and decreased, respectively, in the FA-treated mice livers. The activation of p53 reduces *SUV39H1* at the transcriptional level by inducing p21 and repressing E2F activity [59]. FA was previously shown to activate p53 in HepG2 cells [10]; hence the decrease in *SUV39H1* transcript levels may occur due to the FA-induced p53 activation in HepG2 cells. Further, the decrease in SUV39H1 protein expression observed by FA in the HepG2 cells may result from a combined decrease in SUV39H1 transcription and translation. The decrease in SUV39H1 ubiquitination suggests that the FA-induced decrease in SUV39H1 protein expression may not necessarily occur due to proteasomal degradation, albeit an increase in SUV39H1 cytoplasmic levels. The increase in *SUV39H1* mRNA expression and decrease in SUV39H1 protein expression observed in the FA-treated mice livers may have occurred due to possible MDM2-mediated ubiquitination of SUV39H1 and proteasomal degradation.

Sirt1 deficiency is known to inhibit SUV39H1 deacetylation and enzymatic activity [33, 37]. Therefore, although FA upregulated SUV39H1 nuclear levels, it may not necessarily be active as a decrease in H3K9me3 was observed (Figure 6A-B).

The methylation of lysine residues on the amino-terminal tails of histone proteins is a dynamic epigenetic modification that regulates chromatin structure and gene expression. H3K9me3

maintains heterochromatin formation and plays a crucial role in preserving genome stability and gene silencing [36, 37]. H3K9me3 is regulated by SUV39H1 and KDM4B. KDM4B decreases chromosomal H3K9me3 by catalyzing the removal of H3K9 di- and tri- methyl marks resulting in H3K9me1, which then forms a substrate for trimethylation by SUV39H1 [59]. FA significantly increased the expression of H3K9me1 (Figure 4.6A-B) and decreased the mRNA expression of *KDM4B* in HepG2 cells and mice livers (Figure 4.6C-D). The decrease in SUV39H1 expression and *KDM4B* mRNA expression as well as the increase in H3K9me1 observed in the FA-treated HepG2 cells and mice livers, suggests that the decrease in H3K9me3 was due to the decrease in SUV39H1 and not *KDM4B*.

Since Sirt1 also regulates H3K9me3 by directly interacting with and deacetylating H3K9Ac to enable trimethylation by SUV39H1, the loss in Sirt1 expression may also be responsible for the decrease in H3K9me3 observed in the FA-treated HepG2 cells and mice livers.

DNA damage can also indirectly regulate H3K9me3 by promoting SET7/9-mediated methylation of SUV39H1 [58]. SET7/9 interacts with and methylates SUV39H1 at K105 and K123 resulting in a decrease in SUV39H1 activity and a loss in H3K9me3 [58].

The loss in H3K9me3 was previously associated with genome instability [36], inhibition of cell proliferation [40, 41] and apoptosis [35]. Analysis of DNA integrity using DNA electrophoresis revealed that FA induced a loss in genome stability/DNA integrity in HepG2 cells (Figure 4.7A). This is in agreement with previous studies in which FA induced DNA damage in several human cell lines [10, 60-63].

P-S139-H2Ax is an early response to the induction of DNA double-strand breaks and important molecular indicator of DNA damage. During DNA damage, H2Ax is rapidly phosphorylated on serine 139 by the phosphatidylinositol 3-kinase (PIKK) family of proteins, ataxia telangiectasia mutated (ATM), DNA-dependent protein kinase, and ATM and RAD3-related protein (ATR), causing a conformational change in the DNA-H2Ax complex. This enables DNA repair proteins such as poly (ADP-ribose) polymerase 1 (PARP1) to be recruited to sites of DNA double-strand breaks initiating the repair of the damaged DNA. FA decreased the expression of p-S139-H2Ax in HepG2 cells and mice livers (Figure 4.7B-C). H3K9me3 maintains genome stability by controlling ATM signaling and promoting the repair of DNA double-strand breaks. The ATM protein kinase is activated in response to DNA damage and functions to promote the phosphorylation of proteins involved in checkpoint activation and DNA repair [64]. The acetyltransferase, Tip60 acetylates and activates ATM by interacting with H3K9me3 [64]. Depletion of intracellular H3K9me3 prevents ATM activation and impairs the repair of DNA

double-strand breaks resulting in genome instability. The decrease in p-S139-H2Ax observed in the FA-treated HepG2 cells and mice livers may have resulted from a decrease in H3K9me3 and inactivation of ATM.

Sirt1 also functions in DNA damage response by relocating to sites of genomic instability and enabling the efficient repair of DNA double-strand breaks [57]. Therefore, FA induced genome instability by decreasing Sirt1 expression and H3K9me3 in HepG2 cells and mice livers.

The loss in H3K9me3 and subsequent increase in genomic instability induced by FA in HepG2 cells and mice livers suggests it may decrease cell viability by apoptotic signaling. Caspases form a major part of the apoptotic machinery and are responsible for both the initiation and execution of apoptosis [65]. Initiator caspases such as caspase -8 and -9 are the apical caspases in apoptosis and their activation is required for the cleavage and activation of the downstream executioner caspases -3 and -7. FA decreased HepG2 cell viability (Figure 4.8A) and induced apoptotic cell death as shown by the increase in the activity of caspase-3/7 (Figure 4.8B). The expression of cleaved-Asp175-caspase-3 was significantly increased in the FA-treated mice livers (Figure 4.8C). This is in keeping with previous studies where FA was shown to cause apoptosis by activating p53 [10] and caspase-3/7 [9] in HepG2 cells. FA also induced apoptosis in human promyelocytic leukemia (HL-60) cells [60] and human esophageal cancer (SNO) cells [66].

## **Conclusion**

This study provides a novel insight into an epigenetic mechanism of FA-induced apoptosis in the liver via modulation of the Sirt1/SUV39H1/H3K9me3 pathway. The results indicate that FA upregulates miR-200a and decreases H3K9me3 by downregulating Sirt1 expression and decreasing SUV39H1 ultimately leading to a loss in genome stability and apoptosis of HepG2 cells and mice livers. The results further suggest that FA-induced changes in miR-200a and SUV39H1-mediated H3K9me3 may serve as a potential biomarker for determining FA exposure and toxicity; this is particularly important in developing countries and poverty stricken areas where maize is a staple diet and the risk of exposure to FA is high.

## **Future perspective**

MicroRNAs and histone methylation are epigenetic mechanisms that regulate gene expression and play a crucial role in cell signaling pathways; however, the effect of mycotoxins on epigenetic mechanisms is limited. This study provided evidence for the role of miR-200a and

H3K9me3 in regulating genome integrity and apoptotic cell death following exposure to the food-borne mycotoxin, Fusaric acid (FA); and paves the way for future research on histone modifications and microRNAs in mycotoxicology. It also suggests that FA may have an effect on other essential histone modifications and microRNAs that contribute to its toxicity and studies targeting these modifications may provide insight into possible therapeutic interventions against FA toxicity. Furthermore, this study indicates a possible role for histone-modifying compounds such as histone deacetylase inhibitors in reversing FA-induced toxicity.

### **Executive summary**

- Fusaric acid (FA) is a *Fusarium* produced mycotoxin that commonly contaminates agricultural foods intended for human and animal consumption.
- FA displays various toxicological effects in plants and animals; however, its epigenetic effects are unclear.
- This study investigated the ability of FA to regulate genome integrity and apoptotic cell death via epigenetic mechanisms such as miR-200a and H3K9me3 *in vitro* and *in vivo*.
- FA upregulates miR-200a and downregulates Sirt1 expression.
- FA increases MDM2 expression and alters the ubiquitination of SUV39H1.
- FA alters nuclear and cytoplasmic SUV39H1 levels.
- FA decreases SUV39H1-mediated H3K9me3.
- FA induces genome instability/damage.
- FA induces apoptotic cell death.
- Results from this study provide evidence for alternative mechanisms of FA-induced genotoxicity and cytotoxicity at the epigenetic level.

### **Author contributions**

TG, SN, and AC conceptualized and designed the study. SD was involved in the sacrifice and collection of the mice tissue. TG conducted all laboratory experiments, analyzed the data and wrote the manuscript. AC revised the manuscript. All authors have read the manuscript prior to submission.

### **Acknowledgments**

We thank the Africa Health Research Institute (AHRI) for allowing us to use their animal housing facilities. We also thank Dr Sanil D. Singh and Dr Sooraj Baijnath for their role in maintaining, treating, and sacrificing the mice.

**Financial disclosure**

This work was supported by the National Research Foundation (Grant no.: SFH160703175722) and the University of KwaZulu-Natal College of Health Sciences (Grant no.: 570869). No external writing assistance was utilized in the production of this manuscript.

**Conflict of interest**

The authors declare that they have no conflict of interest.

**Ethical disclosure**

All procedures involving the mice were performed according to the ARRIVE guidelines and rules and regulations of the University of KwaZulu-Natal Animal Research Ethics Committee (Ethics approval number: AREC/079/016).

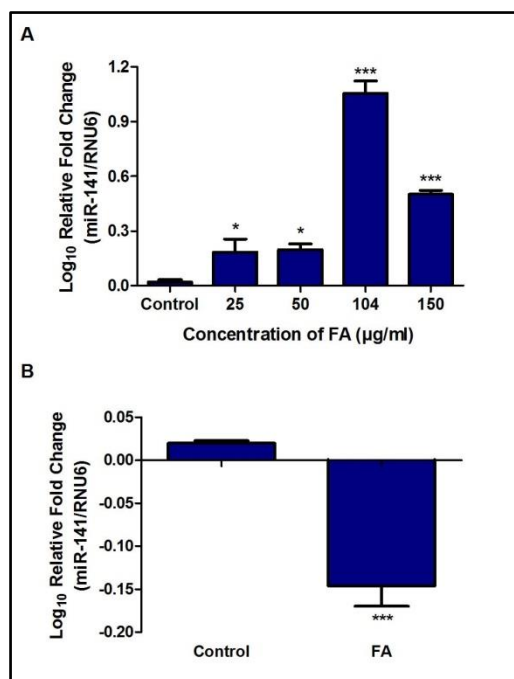
**Data availability**

All datasets generated in this study are available in Supplementary Information and from the corresponding author on reasonable request.

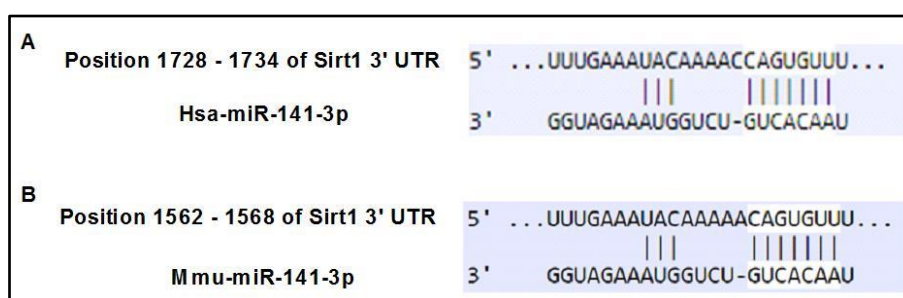
## Supplementary Information

**Supplementary Table S4.1: qPCR primer sequences and annealing temperatures**

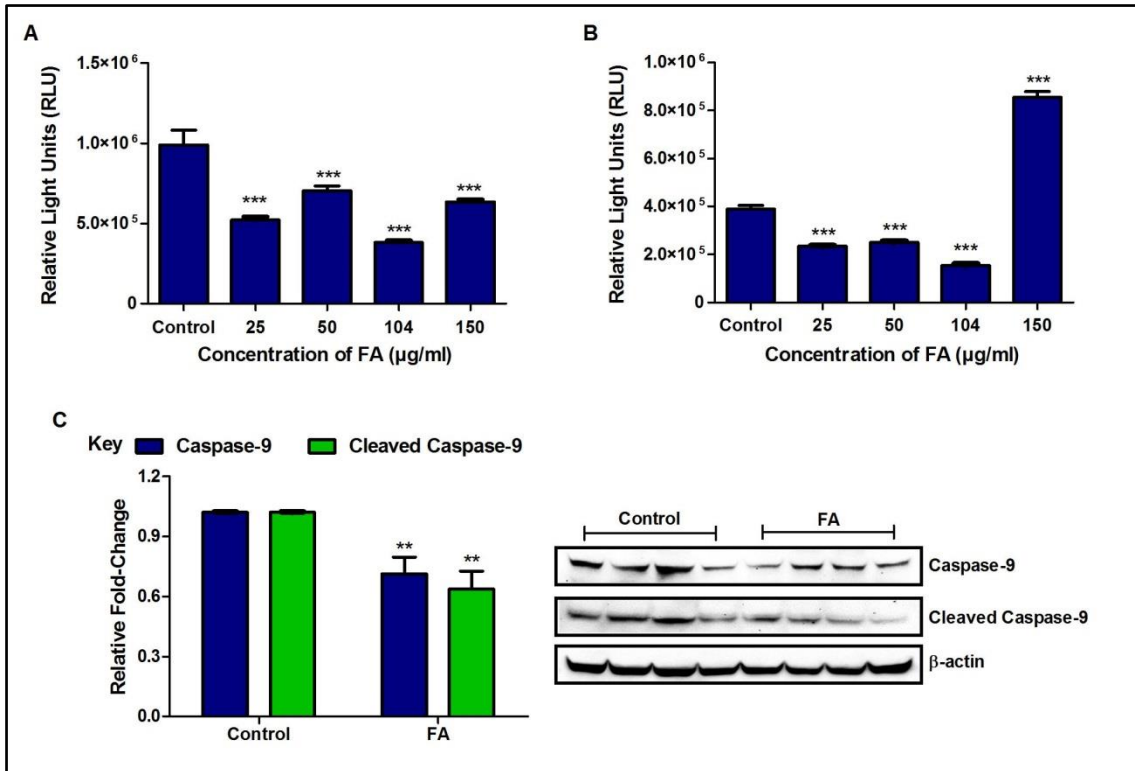
<b>Gene</b>	<b>GenBank Accession no.</b>	<b>Sense Primer 5'→3'</b>	<b>Anti-sense Primer 5'→3'</b>	<b>Annealing Temperature (°C)</b>
<i>Sirt1</i> (human)	NM_0122 38	AGGACATCGAGGAAC TACCTG	GATCTTCCAGATCCT CAAGCG	57
<i>SUV39H</i> <i>1</i> (human)	NM_0012 82166	ATATCCAGACTCAGA GAGCACC	CAGCTCCCTTTCTAA GTCCTTG	57
<i>KDM4B</i> (human)	NM_0150 15	GTCATCACCAAGAAC CGCAACG	CAGTCCCTACTCGT GATGCTC	60
<i>GAPDH</i> (human)	NM_0020 46	TCCACCACCCTGTTG CTGTA	ACCACAGTCCATGC CATCAC	Same as gene of interest
<i>Sirt1</i> (mouse)	NM_0198 12	CAGCCGTCTCTGTGT CACAAA	GCACCGAGGAACTA CCTGAT	58
<i>SUV39H</i> <i>1</i> (mouse)	NM_0115 14	GAGAGCTTGTCCGAC GACAC	CTTCTGCACCAGGT AATTGGC	60
<i>KDM4B</i> (mouse)	NM_1721 32	TCCAAGCCGAGAGGA AGTTCA	AGAAGAGGGTACAG ATGGCAC	60
<i>GAPDH</i> (mouse)	NM_0012 90631	AATGGATTTGGACGC ATTGGT	TTTGCACTGGTACGT GTTGAT	Same as gene of interest



**Supplementary Figure S4.1 FA alters miR-141 expression in HepG2 cells and mice livers.** qPCR analysis of miR-141 in HepG2 cells and mice livers. **(A)** FA increased the expression of miR-141 in HepG2 cells. Results are represented as mean fold-change  $\pm$  SD,  $n = 3$  ( $*p < 0.05$ ,  $***p < 0.0001$ ; one-way ANOVA with the Bonferroni multiple comparisons test). **(B)** FA decreased the expression of miR-141 in mice livers. Results are represented as mean fold-change  $\pm$  SEM,  $n = 3$  ( $***p < 0.0001$ ; unpaired t-test with Welch's correction). FA: Fusaric acid.



**Supplementary Figure S4.2 TargetScan analyses of miR-141 to the 3' UTR of *Sirt1* in humans and mice.** **(A)** MiR-141 has complementary base pairs with the 3' UTR of *Sirt1* at positions 1728-1734 in humans. **(B)** MiR-141 has complementary base pairs with the 3' UTR of *Sirt1* at positions 1562-1568 in mice.



**Supplementary Figure S4.3 FA decreased caspase -8 and -9 activities in HepG2 cells and mice livers.** (A) Luminometric analysis of caspase-8 activity in HepG2 cells. FA significantly decreased the activity of caspase-8 in HepG2 cells. Results are represented as mean  $\pm$  SD,  $n = 3$  (\*\*\*)  $p < 0.0001$ ; one-way ANOVA with the Bonferroni multiple comparisons test). (B) Luminometric analysis of caspase-9 activity in HepG2 cells. FA significantly altered the activity of caspase-9 in HepG2 cells. Results are represented as mean  $\pm$  SD,  $n = 3$  (\*\*\*)  $p < 0.0001$ ; one-way ANOVA with the Bonferroni multiple comparisons test). (C) Western blot analysis of total caspase-9 and cleaved-Asp330-caspase-9 expressions in mice livers. FA decreased the expression of total caspase-9 and cleaved-Asp330-caspase-9 in mice livers. Results are represented as mean fold-change  $\pm$  SEM,  $n = 4$  (\*\*\*)  $p < 0.005$ ; unpaired t-test with Welch's correction). FA: Fusaric acid.

## References

Papers of special note have been highlighted as: \*of interest; \*\*of considerable interest.

1. Zain ME. Impact of mycotoxins on humans and animals. *J. Saudi Chem. Soc.* 15(2), 129-144 (2011).
2. Streit E, Schwab C, Sulyok M, Naehrer K, Krska R, Schatzmayr G. Multi-mycotoxin screening reveals the occurrence of 139 different secondary metabolites in feed and feed ingredients. *Toxins* 5(3), 504-523 (2013).
3. Chen Z, Luo Q, Wang M, Chen B. A rapid method with UPLC for the determination of fusaric acid in *Fusarium* strains and commercial food and feed products. *Indian J. Med. Microbiol.* 57(1), 68-74 (2017).
4. Ghazi T, Nagiah S, Naidoo P, Chuturgoon AA. Fusaric acid induced promoter methylation of DNA methyltransferases triggers DNA hypomethylation in human hepatocellular carcinoma (HepG2) cells. *Epigenetics* 14(8), 804-817 (2019).  
  
\*\*First publication indicating Fusaric acid has epigenetic properties in human liver cells.
5. Bacon CW, Porter JK, Norred WP. Toxic interaction of fumonisin B1 and fusaric acid measured by injection into fertile chicken egg. *Mycopathologia* 129(1), 29-35 (1995).
6. Fairchild A, Grimes J, Porter J, Croom Jr W, Daniel L, Hagler Jr W. Effects of diacetoxyscirpenol and fusaric acid on poult: Individual and combined effects of dietary diacetoxyscirpenol and fusaric acid on turkey poult performance. *Int. J. Poult. Sci.* 4(3), 350-355 (2005).
7. Smith TK, McMillan EG, Castillo JB. Effect of feeding blends of *Fusarium* mycotoxin-contaminated grains containing deoxynivalenol and fusaric acid on growth and feed consumption of immature swine. *J. Anim. Sci.* 75(8), 2184-2191 (1997).
8. Singh VK, Singh HB, Upadhyay RS. Role of fusaric acid in the development of 'Fusarium wilt' symptoms in tomato: Physiological, biochemical and proteomic perspectives. *Plant Physiol. Biochem.* 118, 320-332 (2017).
9. Abdul NS, Nagiah S, Chuturgoon AA. Fusaric acid induces mitochondrial stress in human hepatocellular carcinoma (HepG2) cells. *Toxicon* 119, 336-344 (2016).

10. Ghazi T, Nagiah S, Tiloke C, Abdul NS, Chaturgoon AA. Fusaric acid induces DNA damage and post-translational modifications of p53 in human hepatocellular carcinoma (HepG2) cells. *J. Cell. Biochem.* 118(11), 3866-3874 (2017).

\*\*Preliminary results providing evidence that Fusaric acid has genotoxic effects in human liver cells.

11. Dhani S, Nagiah S, Naidoo DB, Chaturgoon AA. Fusaric acid immunotoxicity and MAPK activation in normal peripheral blood mononuclear cells and Thp-1 cells. *Sci. Rep.* 7(3051), 1-10 (2017).

12. Li X, Zhang ZL, Wang HF. Fusaric acid (FA) protects heart failure induced by isoproterenol (ISP) in mice through fibrosis prevention via TGF- $\beta$ 1/SMADs and PI3K/AKT signaling pathways. *Biomed. Pharmacother.* 93, 130-145 (2017).

13. Reddy R, Larson C, Brimer G, Frappier B, Reddy C. Developmental toxic effects of fusaric acid in CD1 mice. *Bull. Environ. Contam. Toxicol.* 57(3), 354-360 (1996).

14. Devaraja S, Girish KS, Santhosh MS, Hemshekhar M, Nayaka SC, Kemparaju K. Fusaric acid, a mycotoxin, and its influence on blood coagulation and platelet function. *Blood Coagul. Fibrinolysis* 24(4), 419-423 (2013).

15. Hidaka H, Nagatsu, T, Takeya K *et al.* Fusaric acid, a hypotensive agent produced by fungi. *J. Antibiot.* 22(5), 228-230 (1969).

16. Terasawa F, Kameyama M. The clinical trial of a new hypotensive agent, "fusaric acid (5-butylicpicolinic acid)": the preliminary report. *Japanese Circ. J.* 35(3), 339-357 (1971).

17. Smith T, MacDonald E. Effect of fusaric acid on brain regional neurochemistry and vomiting behavior in swine. *J. Anim. Sci.* 69(5), 2044-2049 (1991).

18. Yin ES, Rakhmankulova M, Kucera K *et al.* Fusaric acid induces a notochord malformation in zebrafish via copper chelation. *Biomaterials* 28(4), 783-789 (2015).

19. Winter J, Jung S, Keller S, Gregory RI, Diederichs S. Many roads to maturity: microRNA biogenesis pathways and their regulation. *Nat. Cell Biol.* 11(3), 228-234 (2009).

20. Eades G, Yao Y, Yang M, Zhang Y, Chumsri S, Zhou Q. MiR-200a regulates SIRT1 expression and epithelial to mesenchymal transition (EMT)-like transformation in mammary epithelial cells. *J. Biol. Chem.* 286(29), 25992-26002 (2011).

\*\*Provides evidence that miR-200a negatively regulates Sirt1 expression.

21. Mateescu B, Batista L, Cardon M *et al.* MiR-141 and miR-200a act on ovarian tumorigenesis by controlling oxidative stress response. *Nat. Med.* 17(12), 1627-1636 (2011).
22. Eades G, Yang M, Yao Y, Zhang Y, Zhou Q. MiR-200a regulates Nrf2 activation by targeting Keap1 mRNA in breast cancer cells. *J. Biol. Chem.* 286(47), 40725-40733 (2011).
23. Wang B, Koh P, Winbanks C *et al.* MiR-200a prevents renal fibrogenesis through repression of TGF- $\beta$ 2 expression. *Diabetes* 60(1), 280-287 (2011).
24. Uhlmann S, Zhang J, Schwäger A *et al.* MiR-200bc/429 cluster targets PLC $\gamma$ 1 and differentially regulates proliferation and EGF-driven invasion than miR-200a/141 in breast cancer. *Oncogene* 29(30), 4297-4306 (2010).
25. Gregory PA, Bert AG, Paterson EL *et al.* The miR-200 family and miR-205 regulate epithelial to mesenchymal transition by targeting ZEB1 and SIP1. *Nat. Cell Biol.* 10(5), 593-601 (2008).
26. Korpala M, Lee ES, Hu G, Kang Y. The miR-200 family inhibits epithelial-mesenchymal transition and cancer cell migration by direct targeting of E-cadherin transcriptional repressors ZEB1 and ZEB2. *J. Biol. Chem.* 283(22), 14910-14914 (2008).
27. Li A, Omura N, Hong SM *et al.* Pancreatic cancers epigenetically silence SIP1 and hypomethylate and overexpress miR-200a/200b in association with elevated circulating miR-200a and miR-200b levels. *Cancer Res.* 70(13), 5226-5237 (2010).
28. Xia H, Ng SS, Jiang S *et al.* MiR-200a-mediated downregulation of ZEB2 and CTNNB1 differentially inhibits nasopharyngeal carcinoma cell growth, migration and invasion. *Biochem. Biophys. Res. Commun.* 391(1), 535-541 (2010).
29. Saydam O, Shen Y, Würdinger T *et al.* Downregulated microRNA-200a in meningiomas promotes tumor growth by reducing E-cadherin and activating the Wnt/ $\beta$ -catenin signaling pathway. *Mol. Cell Biol.* 29(21), 5923-5940 (2009).
30. Cong N, Du P, Zhang A *et al.* Downregulated microRNA-200a promotes EMT and tumor growth through the wnt/ $\beta$ -catenin pathway by targeting the E-cadherin repressors ZEB1/ZEB2 in gastric adenocarcinoma. *Oncol. Rep.* 29(4), 1579-1587 (2013).

31. Zhang T, Berrocal JG, Frizzell KM *et al.* Enzymes in the NAD<sup>+</sup> salvage pathway regulate SIRT1 activity at target gene promoters. *J. Biol. Chem.* 284(30), 20408-20417 (2009).

32. Vaquero A, Scher M, Lee D, Erdjument-Bromage H, Tempst P, Reinberg D. Human SirT1 interacts with histone H1 and promotes formation of facultative heterochromatin. *Mol. Cell* 16(1), 93-105 (2004).

33. Bosch-Presegué L, Raurell-Vila H, Marazuela-Duque A *et al.* Stabilization of Suv39H1 by SirT1 is part of oxidative stress response and ensures genome protection. *Mol. Cell* 42(2), 210-223 (2011).

\*\*Provides evidence that Sirt1 regulates SUV39H1.

34. Vaute O, Nicolas E, Vandell L, Trouche D. Functional and physical interaction between the histone methyl transferase Suv39H1 and histone deacetylases. *Nucleic Acids Res.* 30(2), 475-481 (2002).

35. Watson G, Wickramasekara S, Palomera-Sanchez Z *et al.* SUV39H1/H3K9me3 attenuates sulforaphane-induced apoptotic signaling in PC3 prostate cancer cells. *Oncogenesis* 3(12), 1-9 (2014).

36. Peters AH, O'carroll D, Scherthan H *et al.* Loss of the Suv39h histone methyltransferases impairs mammalian heterochromatin and genome stability. *Cell* 107(3), 323-337 (2001).

37. Vaquero A, Scher M, Erdjument-Bromage H, Tempst P, Serrano L, Reinberg D. SIRT1 regulates the histone methyl-transferase SUV39H1 during heterochromatin formation. *Nature* 450(7168), 440-444 (2007).

\*\*Provides evidence that Sirt1 regulates SUV39H1.

38. Park JA, Kim AJ, Kang Y, Jung YJ, Kim HK, Kim KC. Deacetylation and methylation at histone H3 lysine 9 (H3K9) coordinate chromosome condensation during cell cycle progression. *Mol. Cell* 31(4), 343-349 (2011).

39. Melcher M, Schmid M, Aagaard L, Selenko P, Laible G, Jenuwein T. Structure-function analysis of SUV39H1 reveals a dominant role in heterochromatin organization, chromosome segregation, and mitotic progression. *Mol. Cell. Biol.* 20(10), 3728-3741 (2000).

40. Reimann M, Lee S, Loddenkemper C *et al.* Tumor stroma-derived TGF- $\beta$  limits myc-driven lymphomagenesis via Suv39h1-dependent senescence. *Cancer Cell* 17(3), 262-272 (2010).

41. Chiba T, Saito T, Yuki K *et al.* Histone lysine methyltransferase SUV39H1 is a potent target for epigenetic therapy of hepatocellular carcinoma. *Int. J. Cancer* 136(2), 289-298 (2015).
42. Phulukdaree A, Moodley D, Khan S, Chuturgoon AA. Atorvastatin increases miR-124a expression: a mechanism of Gamt modulation in liver cells. *J Cell Biochem* 116(11), 2620-2627 (2015).
43. Livak KJ, Schmittgen TD. Analysis of relative gene expression data using real-time quantitative PCR and the  $2^{-\Delta\Delta CT}$  method. *Methods* 25(4), 402-408 (2001).
44. Chuturgoon A, Phulukdaree A, Moodley D. Fumonisin B1 induces global DNA hypomethylation in HepG2 cells—An alternative mechanism of action. *Toxicology* 315, 65-69 (2014).
45. Attwood K, Fleyshman D, Prendergast L *et al.* Prognostic value of histone chaperone FACT subunits expression in breast cancer. *Breast Cancer* 2017(9), 301-311 (2017).
46. Bailly C, Lansiaux A, Dassonneville L *et al.* Homocamptothecin, an E-ring-modified camptothecin analogue, generates new topoisomerase I-mediated DNA breaks. *Biochemistry* 38(47), 15556-15563 (1999).
47. Feoktistova M, Geserick P, Leverkus M. Crystal violet assay for determining viability of cultured cells. *Cold Spring Harb. Protoc.* 2016(4), 343-346 (2016).
48. Mungamuri SK, Qiao RF, Yao S, Manfredi JJ, Gu W, Aaronson SA. USP7 enforces heterochromatinization of p53 target promoters by protecting SUV39H1 from MDM2-mediated degradation. *Cell Rep.* 14(11), 2528-2537 (2016).
49. Chuturgoon AA, Phulukdaree A, Moodley D. Fumonisin B1 modulates expression of human cytochrome P450 1b1 in human hepatoma (Hepg2) cells by repressing Mir-27b. *Toxicol. Lett.* 227(1), 50-55 (2014).
50. Demirel G, Alpertunga B, Ozden S. Role of fumonisin B1 on DNA methylation changes in rat kidney and liver cells. *Pharm. Biol.* 53(9), 1302-1310 (2015).
51. Sancak D, Ozden S. Global histone modifications in fumonisin B1 exposure in rat kidney epithelial cells. *Toxicol. In Vitro* 29(7), 1809-1815 (2015).
52. So MY, Tian Z, Phoon YS *et al.* Gene expression profile and toxic effects in human bronchial epithelial cells exposed to zearalenone. *PLoS One* 9(5), e96404-e96422 (2014).

53. Zhu CC, Hou YJ, Han J *et al.* Zearalenone exposure affects epigenetic modifications of mouse eggs. *Mutagenesis* 29(6), 489-495 (2014).
54. Xiao Y, Yan W, Lu L *et al.* p38/p53/miR-200a-3p feedback loop promotes oxidative stress-mediated liver cell death. *Cell Cycle* 14(10), 1548-1558 (2015).
55. Sapko O, Utarbaeva AS, Makulbek S. Effect of fusaric acid on prooxidant and antioxidant properties of the potato cell suspension culture. *Russ. J. Plant Physiol.* 2011. 58(5): p. 828-835 (2011).
56. Yang JJ, Tao H, Liu LP, Hu W, Deng ZY, Li J. MiR-200a controls hepatic stellate cell activation and fibrosis via SIRT1/Notch1 signal pathway. *Inflamm. Res.* 66(4), 341-352 (2017).
57. Bosch-Presegué L, Vaquero A. Sirtuin-dependent epigenetic regulation in the maintenance of genome integrity. *FEBS J.* 282(9), 1745-1767 (2015).
58. Wang D, Zhou J, Liu X *et al.* Methylation of SUV39H1 by SET7/9 results in heterochromatin relaxation and genome instability. *Proc. Natl. Acad. Sci. USA* 110(14), 5516-5521 (2013).
59. Zheng H, Chen L, Pledger WJ, Fang J, Chen J. p53 promotes repair of heterochromatin DNA by regulating JMJD2b and SUV39H1 expression. *Oncogene* 33(6), 734-744 (2014).
60. Ogata S, Inoue K, Iwata K, Okumura K, Taguchi H. Apoptosis induced by picolinic acid-related compounds in HL-60 cells. *Biosci. Biotechnol. Biochem.* 65(10), 2337-2339 (2001).
61. Stack Jr BC, Hansen JP, Ruda JM, Jaglowski J, Shvidler J, Hollenbeak CS. Fusaric acid: a novel agent and mechanism to treat HNSCC. *Otolaryngol. Head Neck Surg.* 131(1), 54-60 (2004).
62. Fernandez-Pol J, Klos D, Hamilton P. Cytotoxic activity of fusaric acid on human adenocarcinoma cells in tissue culture. *Anticancer Res.* 13(1), 57-64 (1993).
63. Mamur S, Ünal F, Yilmaz S, Erikel E, Yüzbaşıoğlu D. Evaluation of the cytotoxic and genotoxic effects of mycotoxin fusaric acid. *Drug Chem. Toxicol.* 1-9 (2018).
64. Sun Y, Jiang X, Price BD. Tip60: connecting chromatin to DNA damage signaling. *Cell Cycle* 9(5), 930-936 (2010).
65. Hengartner MO. The biochemistry of apoptosis. *Nature* 407(6805), 770-776 (2000).

66. Devnarain N, Tiloke C, Nagiah S, Chaturgoon AA. Fusaric acid induces oxidative stress and apoptosis in human cancerous oesophageal SNO cells. *Toxicon* 126, 4-11 (2017).

## CHAPTER 5

### **Fusaric acid regulates p53 expression via promoter methylation and m6A RNA methylation *in vitro* and *in vivo***

Terisha Ghazi, Savania Nagiah, and Anil A. Chuturgoon\*

Discipline of Medical Biochemistry and Chemical Pathology, School of Laboratory Medicine and Medical Science, College of Health Sciences, Howard College Campus, University of KwaZulu-Natal, Durban 4041, South Africa

\*Corresponding author: Professor Anil A. Chuturgoon, Discipline of Medical Biochemistry and Chemical Pathology, School of Laboratory Medicine and Medical Science, College of Health Sciences, Howard College Campus, University of KwaZulu-Natal, Durban 4041, South Africa, Telephone: +27 260 4404, Fax: +27 260 4785, Email: [CHUTUR@ukzn.ac.za](mailto:CHUTUR@ukzn.ac.za)

#### **Author email addresses:**

Terisha Ghazi: [terishaghazi@gmail.com](mailto:terishaghazi@gmail.com)

Savania Nagiah: [nagiah.savania@gmail.com](mailto:nagiah.savania@gmail.com)

Anil A. Chuturgoon: [CHUTUR@ukzn.ac.za](mailto:CHUTUR@ukzn.ac.za)

**Word count (excluding abstract, methods, references, and figure legends): 3,795 words**

**Scientific Reports (*In Review*)**

**Manuscript ID: SREP-19-40805**

## Abstract

Fusaric acid (FA), a food-borne mycotoxin, mediates toxicity with sparse information on its epigenetic mechanisms. The tumor suppressor protein, p53 is activated in response to cellular stress and regulates cell cycle arrest and apoptotic cell death. The expression of p53 is regulated at the transcriptional and post-transcriptional level by promoter methylation and N-6-methyladenosine (m6A) RNA methylation, respectively; and alterations in p53 may provide an alternative mechanism of FA-induced toxicity. We investigated the effect of FA on p53 expression and its epigenetic regulation via promoter methylation and m6A RNA methylation *in vitro* and *in vivo*. *In vitro*, FA induced *p53* promoter hypermethylation and decreased *p53* expression. FA decreased m6A-*p53* levels by decreasing *METTL3* and *METTL14*; and suppressed expression of *YTHDF1*, *YTHDF3*, and *YTHDC2* that ultimately reduced p53 translation. *In vivo*, FA induced *p53* promoter hypomethylation and increased *p53* expression. FA increased m6A-*p53* levels by increasing the expression of *METTL3* and *METTL14*; and upregulated expressions of *YTHDF1*, *YTHDF3*, and *YTHDC2*, thus increasing p53 translation. FA differentially induces epigenetic regulation of p53 expression via promoter methylation and m6A RNA methylation in HepG2 cells and C57BL/6 mice livers. These results provide evidence for an alternative mechanism of FA toxicity at the epigenetic level.

## Introduction

Fusaric acid (FA; 5-butylpicolinic acid) is a mycotoxin produced by the *Fusarium* species that parasitize agricultural foods and feeds and impacts on human and animal health. To date, little is known on the toxic and epigenetic effects of FA in humans and animals and understanding the molecular and epigenetic mechanisms of toxicity is important in decreasing FA contamination and lowering the risk of FA-related adverse health effects. Thus far, the only epigenetic study on FA showed induction of DNA hypomethylation that led to genotoxicity and cytotoxicity in an *in vitro* model<sup>1</sup>.

FA has diverse toxicological effects in plants<sup>2-5</sup> and animals<sup>6-9</sup>; it exhibits phytotoxicity by causing necrosis and wilt disease symptoms in various plants<sup>5</sup>. FA is also toxic to human and animal cells by inducing oxidative stress<sup>10</sup>, mitochondrial dysfunction<sup>11</sup>, DNA damage<sup>12,13</sup>, and apoptotic cell death<sup>10-12,14,15</sup>. It has neurochemical effects in mice<sup>16</sup>, rats<sup>17</sup> and pigs<sup>18,19</sup>; and reduced aggressive behavior and motor activity<sup>16</sup>. Additionally, the toxicity of FA was associated with alterations in platelet function<sup>20</sup>, delayed bone ossification<sup>21</sup>, hypotension<sup>7,22</sup>, and notochord malformation<sup>8</sup>. Synergism between FA and other *Fusarium*-produced mycotoxins such as deoxynivalenol (DON)<sup>23</sup>, Fumonisin B<sub>1</sub> (FB<sub>1</sub>)<sup>24</sup>, and 4,15-diacetoxyscirpenol (DAS)<sup>25</sup> have also been demonstrated.

The tumor suppressor protein, p53 is a transcription factor that is activated in response to cellular stress<sup>26</sup>. The most common p53 activating stressors include oxidative stress, DNA damage, excessive oncogene activation, and hypoxia<sup>26,27</sup>. Once activated, p53 recruits core transcriptional machinery to its target promoters, enabling the transcription of genes, with cellular outcomes such as cell cycle arrest and apoptosis<sup>28,29</sup>. Dysregulation in p53 expression has been associated with several human diseases including neurodegenerative diseases<sup>30,31</sup> and cancer<sup>32</sup>.

Although previous studies have indicated that p53 is regulated at the post-translational level by ubiquitination, phosphorylation, and acetylation<sup>33-35</sup>, the expression of p53 is also regulated epigenetically at the transcriptional and post-transcriptional levels by promoter methylation and N-6-methyladenosine (m6A) RNA methylation.

Promoter methylation, methylation of CpG islands within the promoter regions of specific genes, is crucial in regulating gene transcription. The *p53* promoter region was sequenced and basal promoter activity was localized to an 85bp region (nucleotides 760-844) that is indispensable for its full promoter activity<sup>36</sup>, and the *p53* promoter has putative binding sites for

transcription factors. Alterations in *p53* promoter methylation have been linked with an array of *p53* mutations, loss in tumor suppressor function, and cancer progression<sup>32</sup>. Previously, it was shown that promoter hypermethylation of *p53* prevents binding of transcription factors and is associated with a reduction in *p53* expression whereas promoter hypomethylation increases *p53* expression<sup>37,38</sup>.

Post-transcriptional regulation of messenger RNA (mRNA) expression involves RNA-protein and RNA-RNA interactions<sup>39</sup>. m6A RNA methylation occurs in approximately 0.2-0.5% of adenines and is the most abundant post-transcriptional modification of mammalian mRNA<sup>40,41</sup>. m6A is commonly found in the coding region and 3' untranslated region (UTR) of mRNA and is involved in regulating cellular processes including mRNA translation<sup>42,43</sup>, degradation<sup>44</sup>, splicing<sup>45</sup>, and cellular localization<sup>46</sup>. Dysregulation in the m6A methylation pattern has been associated with developmental abnormalities<sup>46-48</sup>, obesity<sup>49,50</sup>, type 2 diabetes<sup>51</sup>, cancer<sup>52-54</sup>, and other human diseases<sup>55</sup>.

m6A is catalyzed by the methyltransferase complex which consists of methyltransferase-like 3 (METTL3), methyltransferase-like 14 (METTL14), and Wilm's tumor 1-associated protein (WTAP)<sup>56,57</sup>. METTL3 is catalytically active and regulates m6A levels by binding to S-adenosyl methionine and catalyzing the transfer of a methyl group to the N-6 position of specific adenines on the target mRNA, METTL14 functions to maintain structure and substrate recognition by interacting with and stabilizing METTL3, whereas WTAP is catalytically inactive and facilitates RNA binding and m6A deposition by coordinating the localization of the METTL3-METTL14 complex<sup>57</sup>. The m6A demethylases, fat mass and obesity-associated protein (FTO) and ALKB homolog 5 (ALKBH5) are Fe<sup>2+</sup> and alpha-ketoglutarate-dependent and function by oxidizing N-methyl groups of m6A to a hydroxymethyl group<sup>39,58</sup>.

Chemical modifications of RNA transcripts alter the charge, base-pairing, secondary structure, and RNA-protein interactions, thereby, regulating gene expression by modulating RNA processing, localization, translation, and decay<sup>42,44-46</sup>. Similarly, m6A also affects RNA processing by recruiting specific reader proteins. The m6A readers such as the YTHDC1-B homology domain containing proteins 1 and 2 (YTHDC1 and YTHDC2) and the YTHDC1-B homology domain family proteins 1, 2, and 3 (YTHDF1, YTHDF2, and YTHDF3) specifically recognize m6A modified RNAs and regulate the expression and function of specific mRNAs and proteins. YTHDF1, YTHDF3, and YTHDC2 regulate mRNA translation<sup>42,43</sup>, YTHDF2 regulates mRNA degradation<sup>44</sup>, and YTHDC1 regulates mRNA splicing and cellular localization<sup>45,46</sup>.

Previously, we evaluated the effect of FA on cell proliferation, DNA damage, and apoptosis in HepG2 cells <sup>12</sup>; however, the mechanism underlying these effects is not well understood. p53 plays a crucial role in regulating these pathways and may provide an important mechanism of FA-induced toxicity.

Thus far, little is known on the effect of FA on p53 expression and its epigenetic regulation *in vitro* and *in vivo*. This study aimed to determine the effect of FA on p53 expression and its epigenetic regulation at the transcriptional and post-transcriptional level by promoter methylation and m6A RNA methylation in human liver (HepG2) cells and C57BL/6 mice livers as an alternative mechanism of FA-induced toxicity. Here we show that FA regulates the mRNA and protein expression of p53 via changes in promoter methylation and m6A RNA methylation *in vitro* and *in vivo*; however, contrasting results were observed between the *in vitro* and *in vivo* models. *In vivo* models, due to their complexity, multicellularity, and absence of disease, are more reliable models for epigenetic and toxicity testing compared to an *in vitro* model which consists of a single cell type in either a cancerous or transformed cell line that has a substantially abnormal function.

## Results

### Fusaric acid alters p53 expression in HepG2 cells and mice livers

The tumor suppressor protein, p53 is activated during cellular stress and functions in cell cycle control and apoptosis <sup>27</sup>. Previously, we showed that FA activates p53 via phosphorylation and acetylation in HepG2 cells <sup>12</sup>; however, its effect on p53 mRNA and protein expression is not well understood. This study determined the effect of FA on p53 mRNA and protein expression in HepG2 cells and mice livers using qPCR and western blot, respectively. FA significantly decreased p53 mRNA ( $p < 0.0001$ ; Fig. 5.1a) and protein ( $p < 0.0001$ ; Fig. 5.1b) expression in HepG2 cells compared to the control; however, the expression of p53 mRNA ( $p = 0.0262$ ; Fig. 5.1c) and protein ( $p = 0.0003$ ; Fig. 5.1d) was significantly increased in the FA-treated mice livers compared to the control.

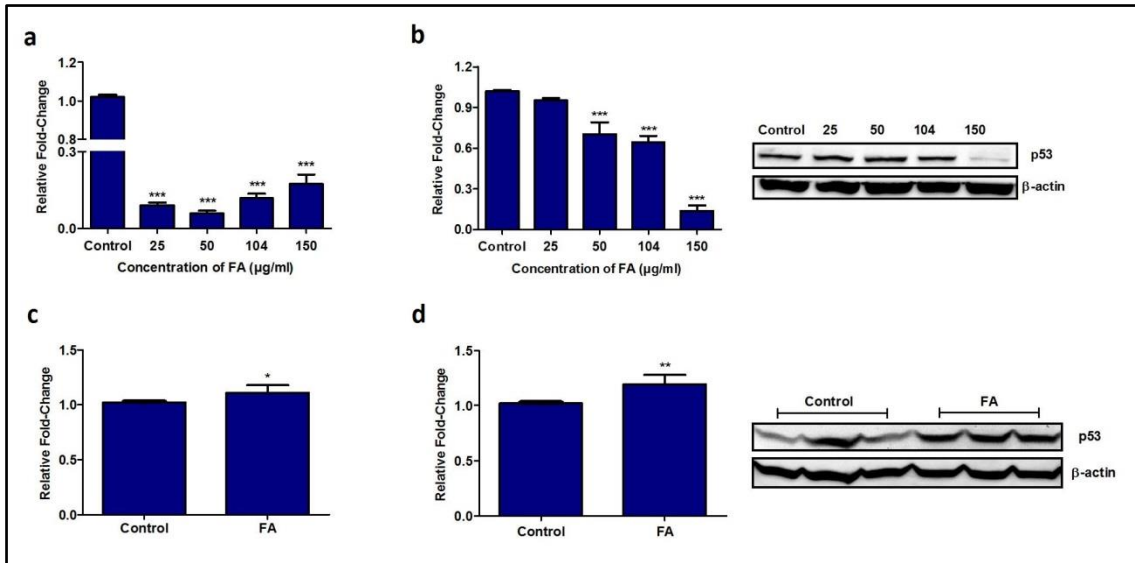


**Figure 5.1 FA alters p53 expression in HepG2 cells and mice livers.** p53 mRNA and protein expression was detected in HepG2 cells and mice livers using qPCR and western blot, respectively. **(a)** FA significantly decreased *p53* mRNA expression in HepG2 cells. **(b)** FA significantly decreased p53 protein expression in HepG2 cells. Blot images were derived from the same gel; a single membrane was first probed for p53 and then re-probed for  $\beta$ -actin. Full length blots are presented in Supplementary Fig. S5.1. **(c)** FA significantly increased *p53* mRNA expression in mice livers. **(d)** FA significantly increased p53 protein expression in mice livers. Blot images were derived from the same gel; a single membrane was first probed for p53 and then re-probed for  $\beta$ -actin. Full length blots are presented in Supplementary Fig. S5.2. Densitometric analysis was performed using Image Lab Software (Bio-Rad). Results are represented as mean fold-change  $\pm$  SD,  $n = 3$ . Statistical significance was determined using the one-way ANOVA with the Bonferroni multiple comparisons test (HepG2 cells) and the unpaired t-test with Welch's correction (mice livers) (\* $p < 0.05$ , \*\* $p < 0.005$ , \*\*\* $p < 0.0001$ ).

### Fusaric acid alters *p53* promoter methylation in HepG2 cells and mice livers

The promoter methylation of genes is essential in regulating transcriptional activity and gene expression. Previously, *p53* promoter hypomethylation was shown to increase *p53* expression<sup>59,60</sup> whereas *p53* promoter hypermethylation was shown to decrease *p53* expression<sup>37,38</sup>. We determined if the decrease and increase in *p53* mRNA expression observed in the FA-treated HepG2 cells and mice livers, respectively, were a result of alterations in *p53* promoter methylation. FA significantly increased *p53* promoter methylation in the 25, 104, and 150  $\mu\text{g/ml}$  FA treatments; however, the promoter methylation of *p53* was significantly decreased by the 50  $\mu\text{g/ml}$  FA in HepG2 cells ( $p < 0.0001$ ; Fig. 5.2a). The promoter methylation of *p53* in the FA-

treated mice livers was significantly decreased compared to the control ( $p = 0.0026$ ; Fig. 5.2b). This suggests that FA may alter p53 transcript levels via promoter methylation *in vitro* and *in vivo*.

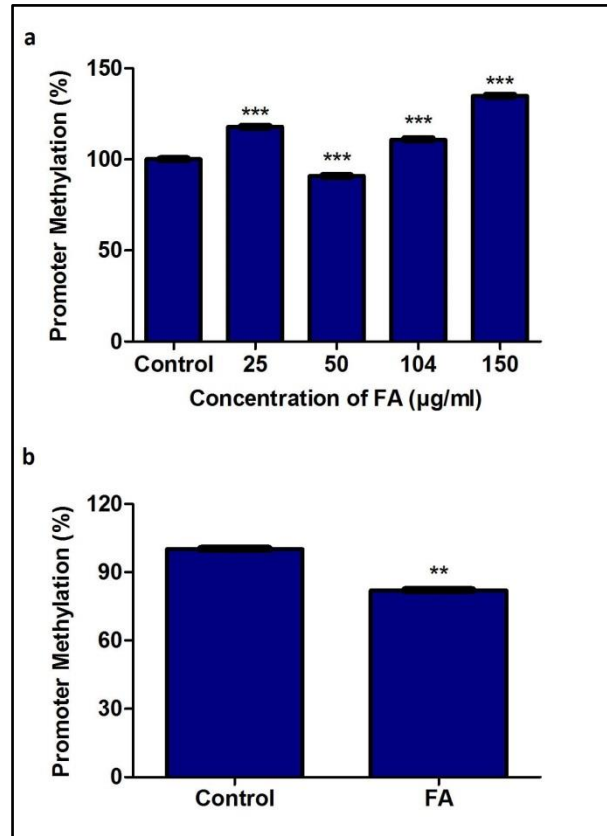


**Figure 5.2 FA alters p53 promoter methylation in HepG2 cells and mice livers.** DNA isolated from controls, FA-treated HepG2 cells, and mice livers were assayed for p53 promoter methylation using the OneStep qMethyl Kit. (a) FA significantly altered p53 promoter methylation in HepG2 cells. (b) FA significantly decreased p53 promoter methylation in mice livers. Results are represented as mean fold-change  $\pm$  SD,  $n = 3$ . Statistical significance was determined using the one-way ANOVA with the Bonferroni multiple comparisons test (HepG2 cells) and the unpaired t-test with Welch's correction (mice livers) (\*\* $p < 0.005$ , \*\*\* $p < 0.0001$ ).

### Fusaric acid alters m6A-p53 levels in HepG2 cells and mice livers

M6A, an abundant and dynamic post-transcriptional modification of mRNA, regulates mRNA degradation and translation<sup>42-44</sup>. Due to the FA-induced changes in p53 expression at both the transcript and protein levels, we determined the effect of FA on m6A-p53 levels in HepG2 cells and mice livers using RNA immuno-precipitation. FA significantly decreased m6A-p53

expression in HepG2 cells ( $p < 0.0001$ ; Fig. 5.3a) compared to the control. In the mice livers, FA significantly increased m6A-*p53* expression levels compared to the control mice ( $p = 0.0382$ ; Fig. 5.3b).

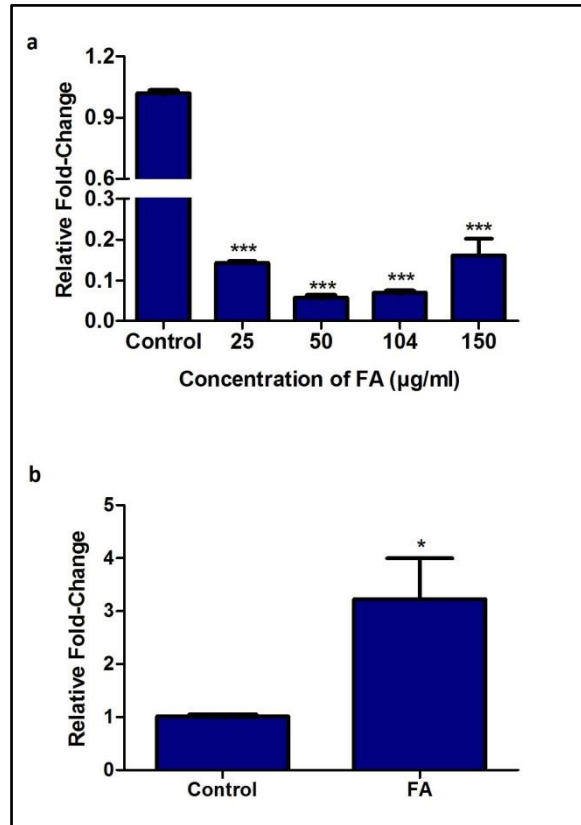


**Figure 5.3 FA alters m6A-*p53* levels in HepG2 cells and mice livers.** RNA immunoprecipitation using m6A antibody and quantification of *p53* mRNA levels in HepG2 cells and mice livers. **(a)** FA decreased m6A-*p53* levels in HepG2 cells. **(b)** FA increased m6A-*p53* levels in mice livers. Results are represented as mean fold-change  $\pm$  SD,  $n = 3$ . Statistical significance was determined using the one-way ANOVA with the Bonferroni multiple comparisons test (HepG2 cells) and the unpaired t-test with Welch's correction (mice livers) (\* $p < 0.05$ , \*\*\* $p < 0.0001$ ).

### **Fusaric acid alters the expression of m6A methyltransferases and demethylases in HepG2 cells and mice livers**

The m6A levels of RNA transcripts are regulated by the methyltransferases, METTL3 and METTL14, and the demethylases, FTO and ALKBH5. Due to the FA-induced changes in m6A-*p53* levels observed in the FA-treated HepG2 cells and mice livers; we determined the effect of FA on the mRNA expression of *METTL3*, *METTL14*, *FTO*, and *ALKBH5*. FA significantly

decreased the expression of *METTL3* ( $p < 0.0001$ ; Fig. 5.4a), *METTL14* ( $p < 0.0001$ ; Fig. 5.4a), *FTO* ( $p < 0.0001$ ; Fig. 5.4b), and *ALKBH5* ( $p < 0.0001$ ; Fig. 5.4b) in HepG2 cells compared to the control. The expression of *METTL3* ( $p = 0.0007$ ; Fig. 5.4c), *METTL14* ( $p = 0.0041$ ; Fig. 5.4c), *FTO* ( $p = 0.0017$ ; Fig. 5.4d), and *ALKBH5* ( $p = 0.0018$ ; Fig. 5.4d) in the FA-treated mice livers was increased compared to the control. This suggests that FA may alter m6A-*p53* levels by modulating the expression of the m6A methyltransferases in HepG2 cells and mice livers.

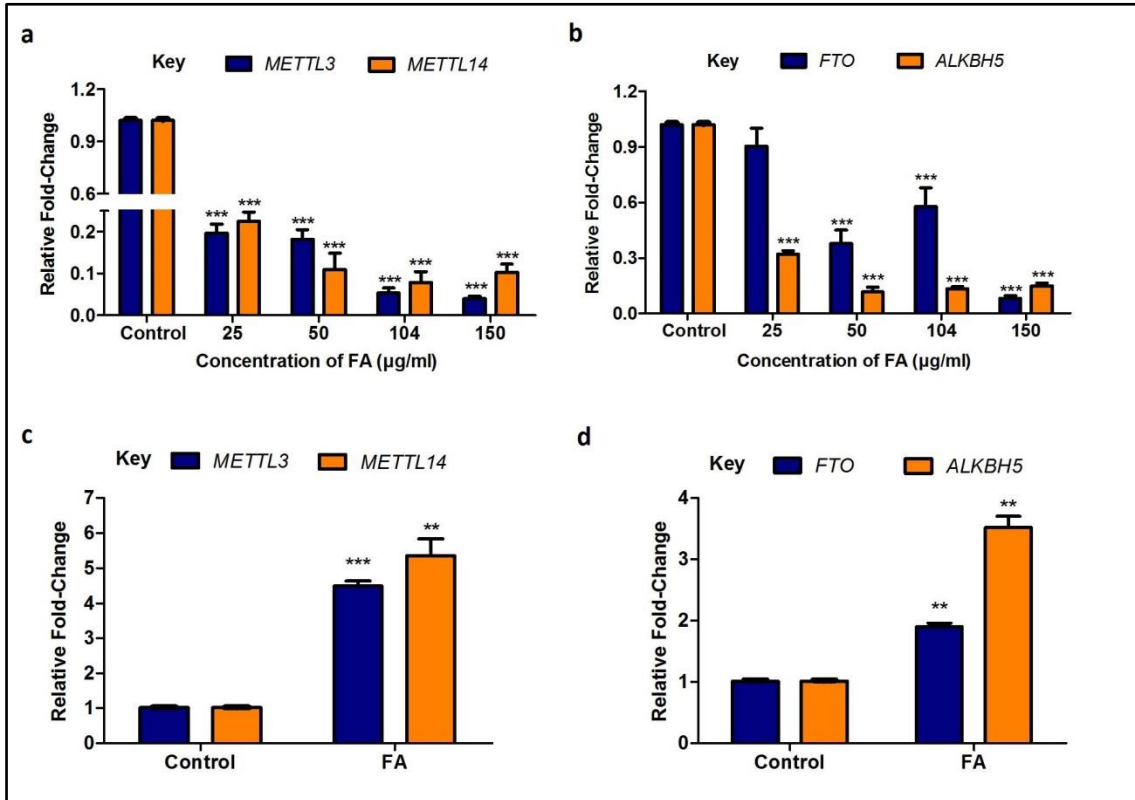


**Figure 5.4 FA alters the expression of m6A methyltransferases and demethylases in HepG2 cells and mice livers.** qPCR analysis of m6A methyltransferases and demethylases in HepG2 cells and mice livers. (a) FA significantly decreased the expression of *METTL3* and *METTL14* in HepG2 cells. (b) FA significantly decreased the expression of *FTO* and *ALKBH5* in HepG2 cells. (c) FA significantly increased the expression of *METTL3* and *METTL14* in mice livers. (d) FA significantly increased the expression of *FTO* and *ALKBH5* in mice livers. Results are represented as mean fold-change  $\pm$  SD,  $n = 3$ . Statistical significance was determined using the one-way ANOVA with the Bonferroni multiple comparisons test (HepG2 cells) and the unpaired t-test with Welch's correction (mice livers) (\*\* $p < 0.005$ , \*\*\* $p < 0.0001$ ).

## Fusaric acid alters the expression of m6A readers in HepG2 cells and mice livers

M6A plays a major role in RNA processing by recruiting specific readers which recognize m6A modified RNAs and regulate the expression of the target mRNA and protein<sup>55</sup>. The m6A readers, YTHDF1, YTHDF3, and YTHDC2 have been shown to regulate mRNA translation/protein expression<sup>42</sup> whereas YTHDF2 was shown to regulate mRNA expression<sup>44</sup>. Due to the FA-induced decrease and increase in p53 mRNA and protein expression observed in the FA-treated HepG2 cells and mice livers, respectively as well as the FA-induced changes in m6A-p53 levels, we determined the effect of FA on the mRNA expression of *YTHDF1*, *YTHDF2*, *YTHDF3*, and *YTHDC2*. FA significantly decreased the expression of *YTHDF1* ( $p < 0.0001$ ; Fig. 5.5a), *YTHDF2* ( $p < 0.0001$ ; Fig. 5.5a), *YTHDF3* ( $p < 0.0001$ ; Fig. 5.5a), and *YTHDC2* ( $p < 0.0001$ ; Fig. 5.5a) in HepG2 cells compared to the control; however, the expression of *YTHDF1* ( $p = 0.0136$ ; Fig. 5.5b), *YTHDF2* ( $p = 0.0062$ ; Fig. 5.5b), *YTHDF3* ( $p = 0.0060$ ; Fig. 5.5b), and *YTHDC2* ( $p = 0.0039$ ; Fig. 5.5b) was significantly upregulated in the FA-treated mice livers compared to the control mice.

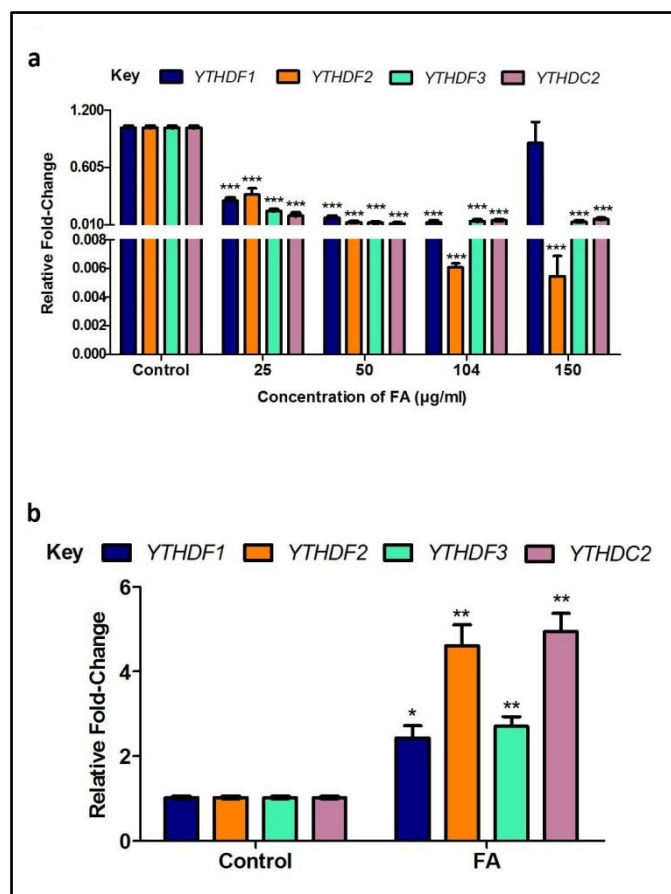


**Figure 5.5 FA alters the expression of m6A readers in HepG2 cells and mice livers.** qPCR analysis of m6A readers in HepG2 cells and mice livers. **(a)** FA significantly decreased the expression of *YTHDF1*, *YTHDF2*, *YTHDF3*, and *YTHDC2* in HepG2 cells. **(b)** FA significantly increased the expression of *YTHDF1*, *YTHDF2*, *YTHDF3*, and *YTHDC2* in mice livers. Results are represented as mean fold-change  $\pm$  SD, n = 3. Statistical significance was determined using the one-way ANOVA with the Bonferroni multiple comparisons test (HepG2 cells) and the unpaired t-test with Welch's correction (mice livers) (\* $p$  < 0.05, \*\* $p$  < 0.005, \*\*\* $p$  < 0.0001).

## Discussion

Exposure to mycotoxins causes harmful/adverse effects in humans and animals. FA is a common food-borne mycotoxin and chelator of divalent cations that alters cellular pathways causing toxicity in plants and animals<sup>3,5,7,8,61</sup>; however, its epigenetic mechanisms of toxicity are unclear. Recently, FA was shown to induce global DNA hypomethylation as an epigenetic mechanism of genotoxicity and cytotoxicity in liver cells<sup>1</sup>. Similarly, Fumonisin B<sub>1</sub> (a common mycotoxin found in corn) caused chromatin instability and liver tumorigenesis by inducing global DNA hypomethylation and histone demethylation<sup>62</sup>. Zearalenone (a myco-estrogen) also reduced cell viability and caused apoptotic cell death by inducing global DNA hypomethylation

<sup>63</sup> and decreasing histone methylation <sup>64</sup>. Despite several studies indicating the genotoxic and cytotoxic effects of mycotoxins, no studies have been conducted on mycotoxins and its effect on the epigenetic regulation of p53 expression at the transcriptional and post-transcriptional level *in vitro* and *in vivo*.

Previously, FA was shown to inhibit cell proliferation and induce apoptosis in HepG2 cells by post-translational modifications of p53 <sup>12</sup>; however, the effect of FA on p53 expression and its epigenetic regulation is not well understood. In addition to post-translational regulation of p53 protein stability and activity, the expression of p53 is also regulated at the transcriptional and post-transcriptional level by promoter methylation and m6A RNA methylation. In this study, we provide evidence for an epigenetic mechanism of FA-induced changes in p53 expression at both the transcript and protein levels by altering *p53* promoter methylation and m6A RNA methylation in human liver (HepG2) cells and C57BL/6 mice livers.

Our results indicate that FA significantly decreased p53 mRNA (Fig. 5.1a) and protein (Fig. 5.1b) expression by inducing *p53* promoter hypermethylation (Fig. 5.2a) and decreasing m6A-*p53* expression levels (Fig. 5.3a) in HepG2 cells; however, in the mice livers, FA significantly increased p53 mRNA (Fig. 5.1c) and protein (Fig. 5.1d) expression by inducing *p53* promoter hypomethylation (Fig. 5.2b) and increasing m6A-*p53* levels (Fig. 5.3b). This is in agreement with previous studies in which *p53* promoter hypermethylation was associated with a decrease in *p53* transcript levels <sup>37,38</sup> and *p53* promoter hypomethylation was associated with an increase in *p53* expression levels both *in vitro* and *in vivo* <sup>59,60</sup>.

Chemical modifications of RNA transcripts regulate gene and protein expression by modulating RNA processing, translation, and degradation <sup>65</sup>. As an epi-transcriptomic marker, m6A is the most abundant post-transcriptional modification of internal mRNA that occurs predominantly at the 3' UTRs of mRNA <sup>43,66,67</sup>. M6A, regulated by the methyltransferases, METTL3, METTL14 and WTAP, and the demethylases, FTO and ALKBH5 <sup>39,57,58</sup>, promotes translation efficiency and mRNA degradation by recruiting specific readers capable of recognizing m6A modified mRNAs.

Previous studies have shown that the aberrant regulation of m6A RNA transcripts affect many biological processes, including circadian rhythm and lipid metabolism <sup>68</sup>, adipogenesis <sup>49</sup>, cell differentiation <sup>41</sup>, and embryonic stem cell renewal <sup>47</sup>. Additionally, modulation of m6A RNAs were associated with various cancers such as acute myeloid leukemia <sup>69,70</sup>, breast cancer <sup>71</sup>, liver cancer <sup>72</sup>, and lung cancer <sup>67</sup>.

Previous studies have shown dietary factors to affect RNA m6A levels<sup>73,74</sup>, and studies on *p53* and m6A have indicated that m6A at the point mutated codon 273 of *p53* pre-mRNA promotes the expression of *p53* R273H mutant protein and drug resistance of cancer cells<sup>75</sup>.

In our study, we found that FA decreased m6A-*p53* levels in HepG2 cells (Fig. 5.3a). This occurred despite the significant decrease in both m6A methyltransferases (*METTL3* and *METTL14*; Fig. 5.4a) and demethylases (*FTO* and *ALKBH5*; Fig. 5.4b) in the FA-treated HepG2 cells. The FA-induced decrease in *FTO* and *ALKBH5* suggests that it may not necessarily be responsible for the decrease in m6A-*p53* levels in the HepG2 cells, and that the decrease in m6A-*p53* levels is rather a consequence of the FA-induced decrease in *METTL3* and *METTL14*. In contrast, FA significantly increased m6A-*p53* levels (Fig. 5.3b) in mice livers despite significantly increasing the expression of both methyltransferases (*METTL3* and *METTL14*; Fig. 5.4c) and demethylases (*FTO* and *ALKBH5*; Fig. 5.4d). This suggests that the increased m6A-*p53* levels in the mice livers may result from the increase in *METTL3* and *METTL14*. This is in agreement with previous studies in which knockdown of *METTL3* or *METTL14* was associated with a substantial decrease in m6A mRNA levels<sup>57</sup> whereas overexpression of *METTL3* or *METTL14* was associated with an increase in m6A mRNA levels<sup>68</sup>. Interestingly, although *ALKBH5* and *FTO* have been recognized as m6A demethylases, it was shown that *FTO* is highly co-expressed with the m6A methyltransferases *in vitro* and *in vivo*<sup>76</sup>, and this may account for the positive correlation between *FTO* and *METTL3* and *METTL14* expression in the FA-treated HepG2 cells and mice livers.

On a global level, m6A is highly conserved between humans and mice<sup>66</sup>; however, transcriptome wide analysis of the m6A methylome of different tissue types in humans and mice indicated that the overlap between m6A containing genes is grouped by species rather than tissue types<sup>76</sup> and this may account for the differences in m6A-*p53* expression levels observed between the FA-treated HepG2 cells and mice livers. Furthermore, the differences in m6A-*p53* expression levels *in vitro* and *in vivo* may occur due to the fact that *in vivo* FA acts in the entire animal and the liver consists of various cell types (hepatocytes, stellate cells, kupffer cells, and endothelial cells) with each cell type having its own m6A methylation pattern as opposed to the *in vitro* model which consists of a single cell type and thus a single m6A methylation pattern. This can affect the overall average m6A methylation pattern in liver tissue versus an *in vitro* model. A previous study indicated a similar trend in the DNA methylation pattern of human liver tissue where each individual cell type (stellate cells and kupffer cells) displayed a different DNA methylation pattern and thus affected the overall average DNA methylation pattern of the liver tissue<sup>77</sup>. Additionally, functional heterogeneity among the individual cell types including

hepatocytes, stellate cells, kupffer cells, and endothelial cells in liver tissue may contribute to cell-cell variations in methylation<sup>77</sup>.

YTHDF1, YTHDF2, YTHDF3, and YTHDC2 specifically recognize m6A modified mRNAs and regulate mRNA degradation<sup>44</sup> and translation<sup>42,43</sup>. In HepG2 cells, the FA-induced decrease in m6A-*p53* levels led to a decrease in the expression of *YTHDF1*, *YTHDF2*, *YTHDF3*, and *YTHDC2* (Fig. 5.5a). YTHDF2 plays a major role in mRNA degradation; the carboxy-terminal domain of YTHDF2 selectively binds to m6A-containing mRNA, whereas the amino-terminal domain is responsible for the localization of the YTHDF2-mRNA complex to RNA decay sites such as processing bodies<sup>44</sup>. The decrease in *YTHDF2* expression, decrease in *p53* mRNA expression, and increase in *p53* promoter methylation observed in the FA-treated HepG2 cells suggests that FA may decrease *p53* mRNA expression via promoter hypermethylation and inhibition in *p53* transcription, and not YTHDF2-mediated degradation of *p53* mRNA. YTHDF1, YTHDF3, and YTHDC2 function by interacting with translational machinery and actively promote protein synthesis to ensure effective protein production from dynamic transcripts that are marked by m6A<sup>43</sup>. Therefore, the FA-induced decrease in YTHDF1, YTHDF3, and YTHDC2 may be responsible for the decrease in *p53* protein expression observed in the HepG2 cells. Contrastingly in the mice livers, the FA-induced increase in m6A-*p53* levels led to an increase in the expression of *YTHDF1*, *YTHDF2*, *YTHDF3*, and *YTHDC2* (Fig. 5.5b). The increase in *YTHDF2*, increase in *p53* mRNA expression, and decrease in *p53* promoter methylation in the FA-treated mice livers indicates that FA increased *p53* mRNA expression via promoter hypomethylation and induction of *p53* transcription. Although YTHDF2 may play a role in degrading *p53* mRNA, the increase in *p53* mRNA expression suggests that the transcription of *p53* may be greater than that of its degradation. The FA-induced increase in *YTHDF1*, *YTHDF3*, and *YTHDC2* in the mice livers led to an increase in *p53* translation and increase in *p53* protein expression. These results are in agreement with the study by Wang et al (2015) in which ribosome profiling on *METTL3* knockdown cells showed that YTHDF1 promotes translation efficiency in an m6A-dependent manner, and knockdown of *YTHDF1* reduced ribosome occupancy and translation efficiency of m6A targeted transcripts<sup>43</sup>. Similarly, YTHDF3 and YTHDC2 promote protein synthesis in synergy with YTHDF1 by interacting with ribosomal proteins and unwinding the 5'UTR of mRNA<sup>78-80</sup>.

In conclusion, this study provides evidence for a possible mechanism of FA-induced *p53* expression at the epigenetic level. The results indicate that FA epigenetically regulates *p53* expression at both the transcript and protein levels by altering *p53* promoter methylation and

m6A RNA methylation in HepG2 cells and C57BL/6 mice livers. The results further indicate that the alterations in m6A-*p53* expression levels was mediated by alterations in the expression of the m6A methyltransferases, *METTL3* and *METTL14*, and occurred independently of the demethylases, *FTO* and *ALKBH5*. Although FA regulates *p53* transcript and protein expression at the epigenetic level, differences were observed between the epigenetic regulation of *p53* expression in the FA-treated HepG2 cells and mice livers. The *in vivo* model is a more reliable and representative model for determining FA-induced toxicity and epigenetic regulation as its level of complexity, multicellularity, and health status is similar to that of the human system. Epigenetic modifications also vary based on the health status of the cells and changes in epigenetic patterns are often associated with various disease states, therefore, the difference between our results *in vitro* and *in vivo* may also occur due to the health status of the cells: our *in vivo* model comprised of healthy mice whereas our *in vitro* model was a cancerous cell line; this is important as majority of the population exposed to mycotoxins are healthy individuals. These findings suggest that the increase in *p53* expression, as shown in the mice livers, may provide an alternative mechanism of FA-induced genotoxicity and cytotoxicity in the liver.

## **Materials and methods**

### **Materials**

FA (*Gibberella fujikuroi*, F6513) was purchased from Sigma-Aldrich (St. Louis, MO, USA). The HepG2 cell line (HB-8065) was purchased from the American Type Culture Collection (ATCC; Johannesburg, SA). Cell culture reagents were purchased from Lonza Biotechnology (Basel, Switzerland). Western blot reagents were purchased from Bio-Rad (Hercules, CA, USA). All other reagents were purchased from Merck (Darmstadt, Germany).

### **Cell culture and treatment**

HepG2 cells ( $1.5 \times 10^6$ , passage 3) were cultured (37°C, 5% CO<sub>2</sub>, humidified incubator) to 90% confluency in 25 cm<sup>3</sup> cell culture flasks containing complete culture media (CCM; Eagle's Minimum Essentials Medium (EMEM) supplemented with 10% fetal calf serum, 1% penicillin-streptomycin fungizone, and 1% L-glutamine). A stock solution of 1 mg/ml FA in 0.1 M phosphate buffered saline (PBS) was prepared and the cells were incubated (37°C, 5% CO<sub>2</sub>, 24 h) with a range of FA concentrations (25, 50, 104, and 150 µg/ml)<sup>1</sup>. An untreated control (CCM only) was also prepared. The viability of the cells was assessed using the trypan blue cell exclusion method. All results were verified by performing two independent experiments in triplicate.

## **Animal treatment**

Six-to-eight-week-old C57BL/6 male mice were obtained from the Africa Health Research Institute (AHRI; University of KwaZulu-Natal, Durban, SA) and housed under standard laboratory conditions (temperature: 25°C, humidity: 40-60%, 12 h light/dark cycle) with *ad libitum* access to a commercial mice feed and normal drinking water. After one week acclimatization, mice with a mean body weight of  $20 \pm 2.99$  g were randomly divided into two groups, control and FA, with each group consisting of three mice. For the treatments, mice were orally administered with either 0.1 M PBS (control group) or 50 mg/kg FA <sup>21</sup> (FA group) at a rate of 0.25 ml/23 g once for a period of 24 h. Thereafter, the mice were euthanized using Isoflurane and the livers were harvested. The livers were rinsed three times in 0.1 M PBS, cut into 1 cm x 1 cm sections, and stored in Cytobuster reagent (500 µl; Novagen, 71009) and Qiazol reagent (500 µl; Qiagen, 79306) for protein and RNA isolation, respectively. All mice were maintained according to the ARRIVE guidelines and the rules and regulations of the University of KwaZulu-Natal Animal Research Ethics Committee (Ethics approval number: AREC/079/016).

## **RNA isolation and quantitative polymerase chain reaction (qPCR)**

Total RNA was extracted from controls, FA-treated HepG2 cells, and mice livers using Qiazol reagent (Qiagen, 79306), as previously described <sup>1</sup>. The RNA was quantified using the Nanodrop2000 spectrophotometer (Thermo-Fischer Scientific), standardized to 1,000 ng/µl, and reverse transcribed into complementary DNA (cDNA) using the Maxima H Minus First Strand cDNA Synthesis Kit (Thermo-Fischer Scientific, K1652). Thereafter, the mRNA expression of *p53*, *METTL3*, *METTL14*, *FTO*, *ALKBH5*, *YTHDC2*, *YTHDF1*, *YTHDF2*, and *YTHDF3* was determined using the PowerUp™ SYBR™ Green Master Mix (Thermo-Fischer Scientific, A25742) and the CFX96 Real Time PCR System (Bio-Rad) with the following cycling conditions: initial denaturation (95°C, 8 min), followed by 40 cycles of denaturation (95°C, 15 s), annealing (Supplementary Table S5.1, 40 s), and extension (72°C, 30 s). Primer sequences and annealing temperatures are listed in Supplementary Table S5.1. *GAPDH* was used as the internal control to normalise mRNA expression. The comparative threshold cycle (Ct) method was used to determine relative changes in expression <sup>81</sup>.

## **Protein isolation and western blot**

The protein expression of p53 was determined using western blot <sup>12</sup>. Briefly, crude protein was isolated from controls, FA-treated HepG2 cells, and mice livers using cytotbuster reagent (200 µl; Novagen, 71009) supplemented with protease and phosphatase inhibitors (Roche;

05892791001 and 04906837001, respectively). The Bicinchoninic Acid (BCA) Assay was used to quantify the proteins and the samples were subsequently standardized to 1 mg/ml (HepG2 cells) and 5 mg/ml (mice livers). The samples were then boiled (100°C, 5 min) in a 1:1 dilution with 1X Laemmli buffer [dH<sub>2</sub>O, 0.5 M Tris-HCl (pH 6.8), glycerol, 10% SDS, 5% β-mercaptoethanol, 1% bromophenol blue], separated in sodium dodecyl sulphate polyacrylamide gels (10% resolving gel, 4% stacking gel; 1 h, 150 V), and transferred onto nitrocellulose membranes using the Bio-Rad Trans-Blot® Turbo Transfer System (20 V, 30 min). The membranes were then blocked in 5% non-fat dry milk (NFD) in Tris buffered saline with 0.05% Tween 20 [TTBS; 150 mM NaCl, 3 mM KCl, 25 mM Tris, 0.05% Tween 20, dH<sub>2</sub>O, pH 7.5; 1 h, RT] and probed overnight (4°C) with primary antibody [p53 (1:500; Santa Cruz, sc-6243)]. Membranes were rinsed five times in TTBS (10 min, RT) and incubated with a horseradish peroxidase (HRP)-conjugated secondary antibody [goat anti-rabbit (1:5,000; Cell Signaling Technology, #7074S); 1 h, RT]. Membranes were rinsed five times in TTBS (10 min, RT). Immunoblots were visualized using the Clarity™ Western ECL Substrate Kit (Bio-Rad, #170-5060) and the images were captured using the ChemiDoc™ XRS+ Molecular Imaging System (Bio-Rad). Following detection, membranes were quenched in hydrogen peroxide (5%, 37°C, 30 min) and probed with the housekeeping protein, anti-β-actin (1:5,000, 30 min, RT; Sigma-Aldrich, A3854) to normalize protein expression. Protein expression was determined using the Image Lab Software version 5.1 (Bio-Rad) and the results were represented as a fold-change in band density (RBD) relative to the control.

### **Promoter methylation of *p53***

Genomic DNA was extracted from controls, FA-treated HepG2 cells, and mice livers using the Quick-g-DNA MiniPrep Kit (Zymo Research, D3007) and purified using the DNA Clean and Concentrator™-5 Kit (Zymo Research, D4003), as per manufacturer's instructions<sup>1</sup>. DNA concentration was determined using the Nanodrop2000 spectrophotometer and standardized to 4 ng/μl. The purity of the DNA was assessed using the A260/A280 absorbance ratio. The promoter methylation of *p53* was determined using the OneStep qMethyl Kit (Zymo Research, 5310) in which 20 ng DNA was subject to a test and reference reaction containing specific primers<sup>1</sup>. Primer sequences and annealing temperatures are listed in Supplementary Table S5.1. Cycling conditions were as follows: digestion by methyl sensitive restriction enzymes (37°C, 2 h), initial denaturation (95°C, 10 min), followed by 45 cycles of denaturation (95°C, 30 s), annealing (Supplementary Table S5.1, 60 s), extension (72°C, 60 s), final extension (72°C, 60 s), and a hold at 4°C. The percentage methylation was calculated using the supplied formula (Supplementary Information) and represented as a fold-change relative to the control.

## RNA immuno-precipitation

Quantification of m6A-*p53* levels were conducted using RNA immuno-precipitation [82]. Briefly, control, FA-treated HepG2 cells, and mice livers were incubated in nuclear isolation buffer [500  $\mu$ l; 1.28 M sucrose, 40 mM Tris-HCl (pH 7.5), 20 mM magnesium chloride, 4% Triton X-100; 4°C, 20 min] and centrifuged (2,500 x g, 4°C, 15 min). Nuclear pellets were re-suspended in RNA immuno-precipitation buffer [1 ml; 150 mM potassium chloride, 25 mM Tris-HCl (pH 7.4), 5 mM EDTA, 0.5 mM DTT, 0.5% IGEPAL, 100 U/ml SUPERase IN™ RNase Inhibitor (Thermo-Fisher Scientific, AM2694), protease inhibitors (Roche, 05892791001), phosphatase inhibitors (Roche, 04906837001)] and the chromatin was mechanically sheared using a needle (20 gauge/20 strokes). Thereafter, the nuclear pellet and debris were pelleted by centrifugation (13,000 x g, 4°C, 10 min). The supernatant was transferred into fresh 1.5 ml micro-centrifuge tubes and incubated with primary antibody [m6A (1:100; Abcam, ab208577)] overnight at 4°C. The RNA-antibody complex was precipitated using protein A beads [20  $\mu$ l 50% bead slurry (Cell Signaling Technology, #9863), 4°C, 3 h]. Thereafter, the immuno-precipitates were recovered by centrifugation (2,500 x g, 4°C, 60 s), washed three times in RNA immuno-precipitation buffer, followed by re-suspension in Qiazol reagent (500  $\mu$ l; Qiagen, 79306). RNA was isolated as previously described<sup>1</sup>. The RNA was quantified using the Nanodrop2000 spectrophotometer, standardized to 400 ng/ $\mu$ l, and reverse transcribed into cDNA using the Maxima H Minus First Strand cDNA Synthesis Kit (Thermo-Fischer Scientific, K1652). The expression of m6A-*p53* was then determined using qPCR as mentioned above. Primer sequences and annealing temperatures are listed in Supplementary Table S5.1.

## Statistical analysis

GraphPad Prism version 5.0 (GraphPad Prism Software Inc.) was used to perform all statistical analyses. The D'Agostino and Pearson tests were used to determine normality. Data from the HepG2 cells were analyzed using the one-way Analysis of Variance (ANOVA) followed by the Bonferroni multiple comparisons test. Data from the mice livers were analyzed using the unpaired t-test with Welch's correction. All results were represented as a mean fold-change  $\pm$  standard deviation (SD) (n = 3). Statistical significance was considered at  $p < 0.05$ .

## Acknowledgments

We thank the Africa Health Research Institute (AHRI) for allowing us to use their animal housing facilities. We thank Dr Sanil D. Singh and Dr Sooraj Baijnath for their role in

maintaining, treating, and sacrificing the mice. The authors are also grateful to Miss Shanel Dhani for her assistance in collecting the mice tissue. This work was supported by the National Research Foundation (Grant no.: SFH160703175722) and the University of KwaZulu-Natal College of Health Sciences (Grant no.: 570869).

### **Author contributions**

TG, SN, and AC conceptualized and designed the study. TG conducted all laboratory experiments, analyzed the data, and wrote the manuscript. SN and AC revised the manuscript. All authors have read the manuscript prior to submission.

### **Competing interests**

The authors declare no competing interests.

### **Data availability**

All datasets generated in this study are available in Supplementary Information and from the corresponding author on reasonable request.

### **ORCID**

Terisha Ghazi: <https://orcid.org/0000-0002-0179-213X>

Savania Nagiah: <https://orcid.org/0000-0002-7614-8226>

Anil A. Chuturgoon: <https://orcid.org/0000-0003-4649-4133>

## Supplementary Information

**Supplementary Table S5.1: qPCR primer sequences and annealing temperatures**

<b>Gene</b>	<b>GenBank Accession no.</b>	<b>Sense Primer 5'→3'</b>	<b>Anti-sense Primer 5'→3'</b>	<b>Annealing Temperature (°C)</b>
<b>qPCR</b>				
<i>p53</i> (human)	NM_0012 76760	GCCCAACAACACC AGCTCCT	CCTGGGCATCCTTG AGTTCC	56
<i>METTL3</i> (human)	NM_0198 52	TTGTCTCCAACCTT CCGTAGT	CCAGATCAGAGAG GTGGTGTAG	56
<i>METTL14</i> (human)	NM_0209 61	GAACACAGAGCTT AAATCCCCA	TGTCAGCTAAACCT ACATCCCTG	56
<i>FTO</i> (human)	NM_0010 80432	GCTGCTTATTTCGG GACCTG	AGCCTGGATTACC AATGAGGA	56
<i>ALKBH5</i> (human)	NM_0177 58	ATCCTCAGGAAGA CAAGATTAG	TTCTCTTCCTTGTC CATCTC	60
<i>YTHDF1</i> (human)	NM_0177 98	ATACCTCACCACC TACGGACA	GTGCTGATAGATGT TGTTCCCC	58
<i>YTHDF2</i> (human)	NM_0162 58	CCTTAGGTGGAGC CATGATTG	TCTGTGCTACCCAA CTTCAGT	56
<i>YTHDF3</i> (human)	NM_1527 58	TCAGAGTAACAGC TATCCACCA	GGTTGTCAGATATG GCATAGGCT	56

<i>YTHDC2</i> (human)	NM_0228 28	CAAAACATGCTGT TAGGAGCCT	CCACTTGTCTTGCT CATTCCC	60
<i>GAPDH</i> (human)	NM_0020 46	TCCACCACCCTGTT GCTGTA	ACCACAGTCCATG CCATCAC	Same as gene of interest
<i>p53</i> (mouse)	XM_0065 32900	GGGCCCGTGTGG TTCATCC	CCGCGAGACTCCT GGCACAA	60
<i>METTL3</i> (mouse)	NM_0197 21	CTGGGCACTTGGA TTTAAGGAA	TGAGAGGTGGTGT AGCAACTT	58
<i>METTL14</i> (mouse)	NM_2016 38	GACTGGCATCACT GCGAATGA	AGGTCCAATCCTTC CCCAGAA	60
<i>FTO</i> (mouse)	NM_0119 36	CCGTCCTGCGATG ATGAAGT	CCCATGCCGAAAT AGGGCTC	60
<i>ALKBH5</i> (mouse)	NM_1729 43	GCATACGGCCTCA GGACATTA	TTCCAATCGCGGTG CATCTAA	60
<i>YTHDF1</i> (mouse)	NM_1737 61	ACAGTTACCCCTC GATGAGTG	GGTAGTGAGATAC GGGATGGGA	58
<i>YTHDF2</i> (mouse)	NM_1453 93	ACAGGCAAGGCCG AATAATG	GGCTGTGTCACCTC CAGTAG	58
<i>YTHDF3</i> (mouse)	NM_1726 77	TACATGGGGAACA AGTGGATCT	TAGGTGGATAGCC GTAAGTGC	58
<i>YTHDC2</i> (mouse)	NM_0011 63013	GAAGATCGCCGTC AACATCG	GCTCTTCCGTA GGTCAAA	60
<i>GAPDH</i> (mouse)	NM_0012 89726	ATGTGTCCGTCGT GGATCTGAC	AGACAACCTGGTC CTCAGTGTAG	Same as gene of interest
<b>Promoter methylation</b>				

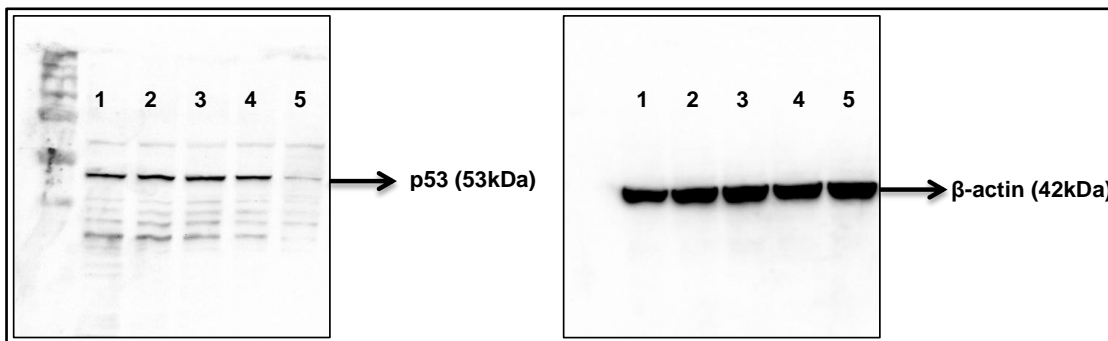
<i>p53</i> ( <i>human</i> )	XM_0244 50825	GTGGATATTACGG AAAGT	AAAATATCCCCGA AACC	54
<i>p53</i> ( <i>mouse</i> )	XM_0065 32900	CAGCTTTGTGCCA GGAGTCT	TAACTGTAGTCGCT ACCTAC	54
<b>RNA immuno-precipitation</b>				
<i>p53</i> ( <i>human</i> )	NM_0012 76760	GCCCAACAACACC AGCTCCT	CCTGGGCATCCTTG AGTTCC	56
<i>p53</i> ( <i>mouse</i> )	XM_0065 32900	GGGCCCGTGTTGG TTCATCC	CCGCGAGACTCCT GGCACAA	60

**Quantification of promoter methylation formula:**

Methylation (%) =  $100 \times 2^{-\Delta Ct}$ , where  $\Delta Ct = Ct (\text{test}) - Ct (\text{reference})$

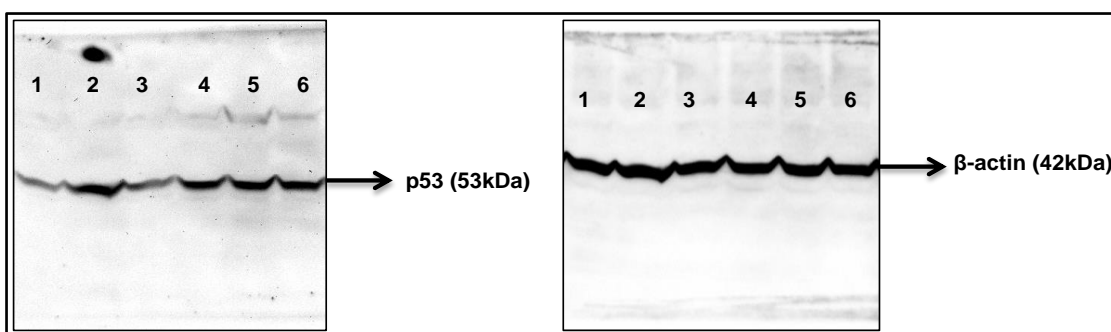
## Original western blot images

### Membrane 1 – HepG2 cells



**Supplementary Figure S5.1: Full size western blot images for Figure 5.1b.** Protein expression of p53 was determined by western blot. A single membrane was first probed for p53, and then the same membrane was re-probed for β-actin. Blots were developed using enhanced chemi-luminescence together with the Bio-Rad ChemiDoc™ XRS+ Molecular Imaging System. **Key:** 1 - Control; 2 – 25 µg/ml FA; 3 – 50 µg/ml FA; 4 – 104 µg/ml FA; 5 – 150 µg/ml FA.

### Membrane 2 – Mouse liver



**Supplementary Figure S5.2: Full size western blot images for Figure 5.1d.** Protein expression of p53 was determined by western blot. A single membrane was first probed for p53, and then the same membrane was re-probed for β-actin. Blots were developed using enhanced chemi-luminescence together with the Bio-Rad ChemiDoc™ XRS+ Molecular Imaging System. **Key:** 1 – 3 - Control; 4 - 6 – 50 mg/kg FA.

## References

1. Ghazi, T., Nagiah, S., Naidoo, P. & Chuturgoon, A.A. Fusaric acid-induced promoter methylation of DNA methyltransferases triggers DNA hypomethylation in human hepatocellular carcinoma (HepG2) cells. *Epigenetics* **14**, 804-817, <https://doi.org/10.1080/15592294.2019.1615358> (2019).
2. D'Alton, A. & Etherton, B. Effects of fusaric acid on tomato root hair membrane potentials and ATP levels. *Plant Physiol* **74**, 39-42, <https://doi.org/10.1104/pp.74.1.39> (1984).
3. Diniz, S. & Oliveira, R. Effects of fusaric acid on *Zea mays* L. seedlings. *Phyton (Buenos Aires)* **78**, 155-160 (2009).
4. Pavlovkin, J., Mistrik, I. & Prokop, M. Some aspects of the phytotoxic action of fusaric acid on primary Ricinus roots. *Plant Soil Environ* **50**, 397-401, <https://doi.org/10.17221/4050-PSE> (2004).
5. Singh, V. K., Singh, H. B. & Upadhyay, R. S. Role of fusaric acid in the development of 'fusarium wilt' symptoms in tomato: Physiological, biochemical and proteomic perspectives. *Plant Physiol Biochem* **118**, 320-332, <https://doi.org/10.1016/j.plaphy.2017.06.028> (2017).
6. Hidaka, H. & Asano, M. Relaxation of isolated rabbit arteries by fusaric (5-butylpicolinic) acid. *J Pharmacol Exp Ther* **199**, 620-629 (1976).
7. Hidaka, H. *et al.* Fusaric acid, a hypotensive agent produced by fungi. *J Antibiot* **22**, 228-230, <https://doi.org/10.7164/antibiotics.22.228> (1969).
8. Yin, E. S. *et al.* Fusaric acid induces a notochord malformation in zebrafish via copper chelation. *BioMetals* **28**, 783-789, <https://doi.org/10.1007/s10534-015-9855-7> (2015).
9. Bungo, T. *et al.* Induction of food intake by a noradrenergic system using clonidine and fusaric acid in the neonatal chick. *Brain Res* **826**, 313-316, [https://doi.org/10.1016/s0006-8993\(99\)01299-8](https://doi.org/10.1016/s0006-8993(99)01299-8) (1999).
10. Devnarain, N., Tiloke, C., Nagiah, S. & Chuturgoon, A. A. Fusaric acid induces oxidative stress and apoptosis in human cancerous oesophageal SNO cells. *Toxicon* **126**, 4-11, <https://doi.org/10.1016/j.toxicon.2016.12.006> (2017).

11. Abdul, N. S., Nagiah, S. & Chuturgoon, A. A. Fusaric acid induces mitochondrial stress in human hepatocellular carcinoma (HepG2) cells. *Toxicon* **119**, 336-344, <https://doi.org/10.1016/j.toxicon.2016.07.002> (2016).
12. Ghazi, T., Nagiah, S., Tiloke, C., Abdul, N.S. & Chuturgoon, A. A. Fusaric acid induces DNA damage and post-translational modifications of p53 in human hepatocellular carcinoma (HepG2) cells. *J Cell Biochem* **118**, 3866-3874, <https://doi.org/10.1002/jcb.26037> (2017).
13. Mamur, S., Ünal, F., Yilmaz, S., Erikel, E. & Yüzbaşıoğlu, D. Evaluation of the cytotoxic and genotoxic effects of mycotoxin fusaric acid. *Drug Chem Toxicol*, 1-9, <https://doi.org/10.1080/01480545.2018.1499772> (2018).
14. Dhani, S., Nagiah, S., Naidoo, D. B. & Chuturgoon, A. A. Fusaric acid immunotoxicity and MAPK activation in normal peripheral blood mononuclear cells and Thp-1 cells. *Sci Rep* **7**, 3051-3060, <https://doi.org/10.1038/s41598-017-03183-0> (2017).
15. Ogata, S., Inoue, K., Iwata, K., Okumura, K. & Taguchi, H. Apoptosis induced by picolinic acid-related compounds in HL-60 cells. *Biosci Biotechnol Biochem* **65**, 2337-2339, <https://doi.org/10.1271/bbb.65.2337> (2001).
16. Diringer, M. N., Kramarcy, N. R., Brown, J. W. & Thurmond, J. B. Effect of fusaric acid on aggression, motor activity, and brain monoamines in mice. *Pharmacol Biochem Behav* **16**, 73-79, [https://doi.org/10.1016/0091-3057\(82\)90016-8](https://doi.org/10.1016/0091-3057(82)90016-8) (1982).
17. Porter, J. K., Bacon, C. W., Wray, E. M. & Hagler Jr, W. M. Fusaric acid in fusarium moniliforme cultures, corn, and feeds toxic to livestock and the neurochemical effects in the brain and pineal gland of rats. *Nat Toxins* **3**, 91-100, <https://doi.org/10.1002/nt.2620030206> (1995).
18. Smith, T. & MacDonald, E. Effect of fusaric acid on brain regional neurochemistry and vomiting behavior in swine. *J Anim Sci* **69**, 2044-2049, <https://doi.org/10.2527/1991.6952044x> (1991).
19. Swamy, H., Smith, T., MacDonald, E., Boermans, H. & Squires, E. Effects of feeding a blend of grains naturally contaminated with Fusarium mycotoxins on swine performance, brain regional neurochemistry, and serum chemistry and the efficacy of a polymeric glucomannan mycotoxin adsorbent. *J Anim Sci* **80**, 3257-3267, <https://doi.org/10.2527/2002.80123257x> (2002).

20. Devaraja, S. *et al.* Fusaric acid, a mycotoxin, and its influence on blood coagulation and platelet function. *Blood Coagul Fibrinolysis* **24**, 419-423, <https://doi.org/10.1097/MBC.0b013e32835d548c> (2013).
21. Reddy, R., Larson, C., Brimer, G., Frappier, B. & Reddy, C. Developmental toxic effects of fusaric acid in CD1 mice. *Bull Environ Contam Toxicol* **57**, 354-360, <https://doi.org/10.1007/s001289900198> (1996).
22. Terasawa, F. & Kameyama, M. The clinical trial of a new hypotensive agent," fusaric acid (5-butylpicolinic acid)": the preliminary report. *Japanese Circ J* **35**, 339-357, <https://doi.org/10.1253/jcj.35.339> (1971).
23. Smith, T. K., McMillan, E. G. & Castillo, J. B. Effect of feeding blends of Fusarium mycotoxin-contaminated grains containing deoxynivalenol and fusaric acid on growth and feed consumption of immature swine. *J Anim Sci* **75**, 2184-2191, <https://doi.org/10.2527/1997.7582184x> (1997).
24. Bacon, C. W., Porter, J. K. & Norred, W. P. Toxic interaction of fumonisin B1 and fusaric acid measured by injection into fertile chicken egg. *Mycopathologia* **129**, 29-35, <https://doi.org/10.1007/bf01139334> (1995).
25. Fairchild, A. *et al.* Effects of diacetoxyscirpenol and fusaric acid on poults: Individual and combined effects of dietary diacetoxyscirpenol and fusaric acid on turkey poult performance. *Int J Poult Sci* **4**, 350-355 (2005).
26. Laptenko, O. & Prives, C. Transcriptional regulation by p53: one protein, many possibilities. *Cell Death Differ* **13**, 951-961, <https://doi.org/10.1038/sj.cdd.4401916> (2006).
27. Prives, C. & Hall, P. A. The p53 pathway. *J Pathol* **187**, 112-126, [https://doi.org/10.1002/\(SICI\)1096-9896\(199901\)187:1<112::AID-PATH250>3.0.CO;2-3](https://doi.org/10.1002/(SICI)1096-9896(199901)187:1<112::AID-PATH250>3.0.CO;2-3) (1999).
28. Kruiswijk, F., Labuschagne, C. F. & Vousden, K. H. p53 in survival, death and metabolic health: a lifeguard with a licence to kill. *Nat Rev Mol Cell Biol* **16**, 393-405, <https://doi.org/10.1038/nrm4007> (2015).
29. Vousden, K. H. & Prives, C. Blinded by the light: the growing complexity of p53. *Cell* **137**, 413-431, <https://doi.org/10.1016/j.cell.2009.04.037> (2009).

30. Chang, J. R. *et al.* Role of p53 in neurodegenerative diseases. *Neurodegener Dis* **9**, 68-80, <https://doi.org/10.1159/000329999> (2012).
31. Szybińska, A. & Leśniak, W. P53 dysfunction in neurodegenerative diseases-the cause or effect of pathological changes? *Aging Dis* **8**, 506-518, <https://doi.org/10.14336/AD.2016.1120> (2017).
32. Mitsudomi, T. *et al.* p53 gene mutations in non-small-cell lung cancer cell lines and their correlation with the presence of ras mutations and clinical features. *Oncogene* **7**, 171-180 (1992).
33. Barlev, N. A. *et al.* Acetylation of p53 activates transcription through recruitment of coactivators/histone acetyltransferases. *Mol Cell* **8**, 1243-1254, [https://doi.org/10.1016/S1097-2765\(01\)00414-2](https://doi.org/10.1016/S1097-2765(01)00414-2) (2001).
34. Shieh, S.Y., Ikeda, M., Taya, Y. & Prives, C. DNA damage-induced phosphorylation of p53 alleviates inhibition by MDM2. *Cell* **91**, 325-334, [https://doi.org/10.1016/s0092-8674\(00\)80416-x](https://doi.org/10.1016/s0092-8674(00)80416-x) (1997).
35. Tang, Y., Zhao, W., Chen, Y., Zhao, Y. & Gu, W. Acetylation is indispensable for p53 activation. *Cell* **133**, 612-626, <https://doi.org/10.1016/j.cell.2008.03.025> (2008).
36. Tuck, S. P. & Crawford, L. Characterization of the human p53 gene promoter. *Mol Cell Biol* **9**, 2163-2172, <https://doi.org/10.1128/MCB.9.5.2163> (1989).
37. Chmelarova, M. *et al.* Methylation in the p53 promoter in epithelial ovarian cancer. *Clin Transl Oncol* **15**, 160-163, <https://doi.org/10.1007/s12094-012-0894-z> (2013).
38. Kang, J. H. *et al.* Methylation in the p53 promoter is a supplementary route to breast carcinogenesis: correlation between CpG methylation in the p53 promoter and the mutation of the p53 gene in the progression from ductal carcinoma in situ to invasive ductal carcinoma. *Lab Invest* **81**, 573-579, <https://doi.org/10.1038/labinvest.3780266> (2001).
39. Woo, H. H. & Chambers, S. K. Human ALKBH3-induced m1A demethylation increases the CSF-1 mRNA stability in breast and ovarian cancer cells. *Biochim Biophys Acta Gene Regul Mech* **1862**, 35-46, <https://doi.org/10.1016/j.bbagr.2018.10.008> (2019).
40. Fu, Y., Dominissini, D., Rechavi, G. & He, C. Gene expression regulation mediated through reversible m6A RNA methylation. *Nat Rev Genet* **15**, 293-306, <https://doi.org/10.1038/nrg3724> (2014).

41. Geula, S. *et al.* m6A mRNA methylation facilitates resolution of naive pluripotency toward differentiation. *Science* **347**, 1002-1006, <https://doi.org/10.1126/science.1261417> (2015).
42. Meyer, K. D. *et al.* 5' UTR m6A promotes cap-independent translation. *Cell* **163**, 999-1010, <https://doi.org/10.1016/j.cell.2015.10.012> (2015).
43. Wang, X. *et al.* N6-methyladenosine modulates messenger RNA translation efficiency. *Cell* **161**, 1388-1399, <https://doi.org/10.1016/j.cell.2015.05.014> (2015).
44. Wang, X. *et al.* N6-methyladenosine-dependent regulation of messenger RNA stability. *Nature* **505**, 117-120, <https://doi.org/10.1038/nature12730> (2014).
45. Xiao, W. *et al.* Nuclear m(6)A reader YTHDC1 regulates mRNA splicing. *Mol Cell* **61**, 507-519, <https://doi.org/10.1016/j.molcel.2016.01.012> (2016).
46. Zheng, G. *et al.* ALKBH5 is a mammalian RNA demethylase that impacts RNA metabolism and mouse fertility. *Mol Cell* **49**, 18-29, <https://doi.org/10.1016/j.molcel.2012.10.015> (2013).
47. Batista, P. J. *et al.* M(6)A RNA modification controls cell fate transition in mammalian embryonic stem cells. *Cell Stem Cell* **15**, 707-719, <https://doi.org/10.1016/j.stem.2014.09.019> (2014).
48. Wang, C. X. *et al.* METTL3-mediated m6A modification is required for cerebellar development. *PLoS Biol* **16**, 1-29, <https://doi.org/10.1371/journal.pbio.2004880> (2018).
49. Wang, X., Zhu, L., Chen, J. & Wang, Y. mRNA m6A methylation downregulates adipogenesis in porcine adipocytes. *Biochem Biophys Res Commun* **459**, 201-207, <https://doi.org/10.1016/j.bbrc.2015.02.048> (2015).
50. Dina, C. *et al.* Variation in FTO contributes to childhood obesity and severe adult obesity. *Nat Genet* **39**, 724-726, <https://doi.org/10.1038/ng2048> (2007).
51. Yang, Y. *et al.* Glucose is involved in the dynamic regulation of m6A in patients with type 2 diabetes. *J Clin Endocrinol Metab* **104**, 665-673, <https://doi.org/10.1210/jc.2018-00619> (2018).
52. Lin, S., Choe, J., Du, P., Triboulet, R. & Gregory, R. I. The m(6)A methyltransferase METTL3 promotes translation in human cancer cells. *Mol Cell* **62**, 335-345, <https://doi.org/10.1016/j.molcel.2016.03.021> (2016).
53. Panneerdoss, S. *et al.* Cross-talk among writers, readers, and erasers of m6A regulates cancer growth and progression. *Sci Adv* **4**, 1-15, <https://doi.org/10.1126/sciadv.aar8263> (2018).

54. Dai, D., Wang, H., Zhu, L., Jin, H. & Wang, X. N6-methyladenosine links RNA metabolism to cancer progression. *Cell Death Dis* **9**, 124-136, <https://doi.org/10.1038/s41419-017-0129-x> (2018).
55. Wei, W., Ji, X., Guo, X. & Ji, S. Regulatory role of N6-methyladenosine (m6A) methylation in RNA processing and human diseases. *J Cell Biochem* **118**, 2534-2543, <https://doi.org/10.1002/jcb.25967> (2017).
56. Wang, X. & He, C. Dynamic RNA modifications in posttranscriptional regulation. *Mol Cell* **56**, 5-12, <https://doi.org/10.1016/j.molcel.2014.09.001> (2014).
57. Liu, J. *et al.* A METTL3–METTL14 complex mediates mammalian nuclear RNA N6-adenosine methylation. *Nat Chem Biol* **10**, 93-95, <https://doi.org/10.1038/nchembio.1432> (2014).
58. Jia, G. *et al.* N6-methyladenosine in nuclear RNA is a major substrate of the obesity-associated FTO. *Nat Chem Biol* **7**, 885-887, <https://doi.org/10.1038/nchembio.687> (2011).
59. Heo, S. H., Kwak, J. & Jang, K. L. All-trans retinoic acid induces p53-dependent apoptosis in human hepatocytes by activating p14 expression via promoter hypomethylation. *Cancer Lett* **362**, 139-148, <https://doi.org/10.1016/j.canlet.2015.03.036> (2015).
60. Qing, Y. *et al.* Berberine induces apoptosis in human multiple myeloma cell line U266 through hypomethylation of p53 promoter. *Cell Biol Int* **38**, 563-570, <https://doi.org/10.1002/cbin.10206> (2014).
61. Köhler, K. & Bentrup, F.W. The effect of fusaric acid upon electrical membrane properties and ATP level in photoautotrophic cell suspension cultures of *Chenopodium rubrum* L. *Zeitschrift für Pflanzenphysiologie* **109**, 355-361, [https://doi.org/10.1016/S0044-328X\(83\)80117-2](https://doi.org/10.1016/S0044-328X(83)80117-2) (1983).
62. Chuturgoon, A., Phulukdaree, A. & Moodley, D. Fumonisin B1 induces global DNA hypomethylation in HepG2 cells – an alternative mechanism of action. *Toxicology* **315**, 65-69, <https://doi.org/10.1016/j.tox.2013.11.004> (2014).
63. So, M. Y. *et al.* Gene expression profile and toxic effects in human bronchial epithelial cells exposed to zearalenone. *PLoS One* **9**, 65-69, <https://doi.org/10.1371/journal.pone.0096404> (2014).

64. Zhu, C. C. *et al.* Zearalenone exposure affects epigenetic modifications of mouse eggs. *Mutagenesis* **29**, 489-495, <https://doi.org/10.1093/mutage/geu033> (2014).
65. Yang, Y., Hsu, P. J., Chen, Y. S. & Yang, Y. G. Dynamic transcriptomic m6A decoration: writers, erasers, readers and functions in RNA metabolism. *Cell Res* **28**, 616-624, <https://doi.org/10.1038/s41422-018-0040-8> (2018).
66. Dominissini, D. *et al.* Topology of the human and mouse m6A RNA methylomes revealed by m6A-seq. *Nature* **485**, 201-206, <https://doi.org/10.1038/nature11112> (2012).
67. Li, J. *et al.* The m6A demethylase FTO promotes the growth of lung cancer cells by regulating the m6A level of USP7 mRNA. *Biochem Biophys Res Commun* **512**, 479-485, <https://doi.org/10.1016/j.bbrc.2019.03.093> (2019).
68. Zhong, X. *et al.* Circadian clock regulation of hepatic lipid metabolism by modulation of m6A mRNA methylation. *Cell Rep* **25**, 1816-1828, <https://doi.org/10.1016/j.celrep.2018.10.068> (2018).
69. Li, Z. *et al.* FTO plays an oncogenic role in acute myeloid leukemia as a N6-methyladenosine RNA demethylase. *Cancer Cell* **31**, 127-141, <https://doi.org/10.1016/j.ccell.2016.11.017> (2017).
70. Kwok, C. T., Marshall, A. D., Rasko, J. E. & Wong, J. J. Genetic alterations of m6A regulators predict poorer survival in acute myeloid leukemia. *J Hematol Oncol* **10**, 39-44, <https://doi.org/10.1186/s13045-017-0410-6> (2017).
71. Zhang, C. *et al.* Hypoxia induces the breast cancer stem cell phenotype by HIF-dependent and ALKBH5-mediated m6A-demethylation of NANOG mRNA. *Proc Natl Acad Sci* **113**, 2047-2056, <https://doi.org/10.1073/pnas.1602883113> (2016).
72. Chen, M. *et al.* RNA N6-methyladenosine methyltransferase-like 3 promotes liver cancer progression through YTHDF2-dependent posttranscriptional silencing of SOCS2. *Hepatology* **67**, 2254-2270, <https://doi.org/10.1002/hep.29683> (2018).
73. Li, X. *et al.* Mouse maternal high-fat intake dynamically programmed mRNA m6A modifications in adipose and skeletal muscle tissues in offspring. *Int J Mol Sci* **17**, 1336-1344, <https://doi.org/10.3390/ijms17081336> (2016).

74. Lu, N. *et al.* Curcumin attenuates lipopolysaccharide-induced hepatic lipid metabolism disorder by modification of m6A RNA methylation in piglets. *Lipids* **53**, 53-63, <https://doi.org/10.1002/lipd.12023> (2018).
75. Uddin, M. B. *et al.* An N6-methyladenosine at the transited codon 273 of p53 pre-mRNA promotes the expression of R273H mutant protein and drug resistance of cancer cells. *Biochem Pharmacol* **160**, 134-145, <https://doi.org/10.1016/j.bcp.2018.12.014> (2019).
76. Liu, J. E. *et al.* Landscape and regulation of m6A and m6Am methylome across human and mouse tissues. *Mol Cell*, 1-56, <https://doi.org/10.1101/632000> (2019).
77. Huse, S. M., Gruppuso, P. A., Boekelheide, K. & Sanders, J. A. Patterns of gene expression and DNA methylation in human fetal and adult liver. *BMC Genomics* **16**, 981-994, <https://doi.org/10.1186/s12864-015-2066-3> (2015).
78. Li, A. *et al.* Cytoplasmic m6A reader YTHDF3 promotes mRNA translation. *Cell Res* **27**, 444-447, <https://doi.org/10.1038/cr.2017.10> (2017).
79. Shi, H. *et al.* YTHDF3 facilitates translation and decay of N6-methyladenosine-modified RNA. *Cell Res* **27**, 315-328, <https://doi.org/10.1038/cr.2017.15> (2017).
80. Tanabe, A. *et al.* RNA helicase YTHDC2 promotes cancer metastasis via the enhancement of the efficiency by which HIF-1 $\alpha$  mRNA is translated. *Cancer Lett* **376**, 34-42, <https://doi.org/10.1016/j.canlet.2016.02.022> (2016).
81. Livak, K. J. & Schmittgen, T. D. Analysis of relative gene expression data using real-time quantitative PCR and the  $2^{-\Delta\Delta CT}$  method. *Methods* **25**, 402-408, <https://doi.org/10.1006/meth.2001.1262> (2001).
82. Rinn, J. L. *et al.* Functional demarcation of active and silent chromatin domains in human HOX loci by noncoding RNAs. *Cell* **129**, 1311-1323. <https://doi.org/10.1016/j.cell.2007.05.022> (2007).

## CHAPTER 6

### CONCLUSION

FA, a neglected food-borne mycotoxin, displays various toxic effects and increases the risk for the development of human and animal pathologies (Yin et al., 2015, Reddy et al., 1996, Hidaka et al., 1969, Abdul et al., 2016, Abdul et al., 2019, Devnarain et al., 2017, Dhani et al., 2017). Thus far, studies on FA have focused mainly on its toxic effects with limited information on its molecular and epigenetic mechanisms of action. The lack of knowledge on the molecular mechanisms of FA-mediated toxicities is of concern as it obscures the development of preventative and therapeutic measures, thereby, increasing human and animal susceptibility to FA exposure and adverse health effects.

Recently, several studies have postulated that FA possesses genotoxic properties and this may be crucial for adverse outcomes in mammals (Ghazi et al., 2017, Mamur et al., 2018, Stack Jr et al., 2004). Epigenetics, due to its close interaction with DNA and vital role in regulating cellular function, is particularly relevant in FA-mediated genotoxicity. Hence, elucidating the epigenetic mode of action of FA may form the basis for the development of diagnostic biomarkers and therapeutic interventions against FA toxicity.

This study, for the first time, shows that FA altered the epigenetic landscape in liver cells; and these epigenetic modifications may provide insight into alternative mechanisms of FA-induced hepatotoxicity.

FA induced global DNA hypomethylation in human liver (HepG2) cells by decreasing the expression of DNA methyltransferases (DNMT1, DNMT3A, and DNMT3B) and increasing the expression of the demethylase, MBD2. The decrease in the expression of *DNMT1*, *DNMT3A*, and *DNMT3B* occurred due to promoter hypermethylation and/or upregulation of miR-29b. Additionally, miR-29b was itself regulated by DNA methylation and the decrease in global DNA methylation coupled with a decrease in miR-29b promoter methylation by FA led to an increase in the expression of miR-29b.

The protein expressions of DNMT1, DNMT3A, and DNMT3B were also significantly decreased by FA and hence DNMT regulation via post-translational modifications such as ubiquitination was assessed. FA decreased the ubiquitination of DNMT1, DNMT3A, and DNMT3B by decreasing the expression of the ubiquitination regulators, *UHRF1* and *USP7*, and suggested that FA did not decrease DNMT protein expression via ubiquitination and proteasomal degradation; instead the decrease in DNMT protein expression observed by FA

may be a consequence of the FA-induced decrease in *DNMT* mRNA expressions and an inhibition of translation. FA also induced *MBD2* promoter hypomethylation and increased the protein expression of MBD2 contributing to the decrease in global DNA methylation observed in the HepG2 cells. These findings confirmed that FA induced epigenetic changes via global DNA hypomethylation and alterations in promoter DNA methylation, leading to genotoxicity and cytotoxicity in human liver cells.

In addition to DNA hypomethylation, a loss in H3K9me3 also disrupts chromatin structure leading to genome instability and/or DNA damage (Putiri and Robertson, 2011, Peters et al., 2001). Sirt1 expression is inversely regulated by miR-200a and post-translationally modifies both SUV39H1 and H3K9Ac to maintain H3K9me3 and genome integrity (Eades et al., 2011, Bosch-Presegué et al., 2011, Vaquero et al., 2007). Transfection of HepG2 cells with a miR-200a mimic and inhibitor proved, in addition to computational prediction software (TargetScan version 7.1), that Sirt1 is a target of miR-200a. FA upregulated miR-200a and decreased Sirt1 expression at both the transcript and protein level in HepG2 cells and C57BL/6 mice livers. The decrease in Sirt1 expression by FA led to changes in MDM2-mediated SUV39H1 ubiquitination, and nuclear and cytoplasmic SUV39H1 expression. This ultimately led to a decrease in total SUV39H1 expression in HepG2 cells and mice livers.

The FA-induced decrease in SUV39H1 and *KDM4B* decreased H3K9me3 and increased H3K9me1 in HepG2 cells and mice livers. The decrease in H3K9me3 by FA decreased genome stability/DNA integrity as shown via DNA electrophoresis. The decrease in H3K9me3 also decreased p-S139-H2Ax (a marker of DNA damage) by preventing ATM activation and inhibiting the repair of damaged DNA. Furthermore, the loss in H3K9me3 and subsequent decrease in genome integrity caused cell death via apoptotic signaling, as evidenced by the decrease in HepG2 cell viability and increase in the activity of the executioner caspase-3/7. These results indicated that FA has genotoxic and cytotoxic effects by upregulating miR-200a and decreasing SUV39H1-mediated H3K9me3 in HepG2 cells and mice livers.

DNA damage is a major activator of p53 which arrests the cell cycle to initiate DNA repair or apoptosis (Laptenko and Prives, 2006). In HepG2 cells, the FA-induced p53 promoter hypermethylation decreased *p53* expression which in turn decreased m6A-*p53* levels despite the decrease in both m6A methyltransferases (*METTL3* and *METTL14*) and demethylases (*FTO* and *ALKBH5*). The decreased m6A-*p53* levels by FA suppressed the m6A-dependent readers, *YTHDF1*, *YTHDF2*, *YTHDF3*, and *YTHDC2*, consequently decreasing p53 translation efficiency and reducing p53 protein expression. Contrastingly in the mice livers, the FA-induced *p53* promoter hypomethylation increased *p53* expression which subsequently increased

m6A-p53 levels despite an increase in both *METTL3* and *METTL14*, and *FTO* and *ALKBH5*. The increased m6A-p53 levels upregulated expressions of *YTHDF1*, *YTHDF2*, *YTHDF3*, and *YTHDC2*, consequently increasing p53 translation and protein expression. These results indicated that FA differentially regulates p53 expression at the epigenetic level via promoter methylation and m6A methylation, and these differences between the HepG2 cells and mice livers can be alluded to the fact that in the mice FA acts in the entire animal that has a greater degree of complexity, multicellularity, and absence of disease compared to the HepG2 cell line that consists of a single cell type that is either cancerous or transformed.

Taken together, this study indicates that FA induced epigenetic changes via global DNA hypomethylation, modulated miRNA expression, decreased H3K9me3, and altered m6A-mediated regulation of p53 expression *in vitro* and *in vivo*; these epigenetic modifications may provide evidence for alternative mechanisms of FA-induced genotoxicity and cytotoxicity that leads to apoptosis in the liver. It also provides evidence for the possible involvement of FA exposure in human diseases especially cancer where epigenetic changes are the underlying cause. This is extremely important in underprivileged areas where quantity outweighs quality due to an inadequate food supply and improper storage facilities (Bennett and Klich, 2003). However, while this study indicated novel mechanisms for FA-induced hepatotoxicity at the epigenetic level, it focused on an acute (24 h) FA exposure in both the *in vitro* and *in vivo* aspects; and chronic (greater than 24 h) exposure to FA may exhibit different patterns of epigenetic changes with different cellular outcomes. Hence this study provides insight for future epigenetic studies at a longer FA exposure time as well as to determine the effect of FA on other epigenetic modifications such as long non-coding RNAs.

## References

- Abdul NS, Nagiah S, Chaturgoon AA. (2016). Fusaric acid induces mitochondrial stress in human hepatocellular carcinoma (HepG2) cells. *Toxicon*, 119, 336-344.
- Abdul NS, Nagiah S, Chaturgoon AA. (2019). Fusaric acid induces NRF2 as a cytoprotective response to prevent NLRP3 activation in the liver derived HepG2 cell line. *Toxicology In Vitro*, 55, 151-159.
- Bennett J, Klich M. (2003). Mycotoxins. *Clinical Microbiological Reviews*, 16, 497-516.
- Bosch-Presegué L, Raurell-Vila H, Marazuela-Duque A, Kane-Goldsmith N, Valle A, Oliver J, Serrano L, Vaquero A. (2011). Stabilization of Suv39H1 by SirT1 is part of oxidative stress response and ensures genome protection. *Molecular Cell*, 42, 210-223.
- Devnarain N, Tiloke C, Nagiah S, Chaturgoon AA. (2017). Fusaric acid induces oxidative stress and apoptosis in human cancerous oesophageal SNO cells. *Toxicon*, 126, 4-11.
- Dhani S, Nagiah S, Naidoo DB, Chaturgoon AA. (2017). Fusaric Acid immunotoxicity and MAPK activation in normal peripheral blood mononuclear cells and Thp-1 cells. *Scientific Reports*, 7, 3051-3060.
- Eades G, Yao Y, Yang M, Zhang Y, Chumsri S, Zhou Q. (2011). MiR-200a regulates SIRT1 expression and epithelial to mesenchymal transition (EMT)-like transformation in mammary epithelial cells. *Journal of Biological Chemistry*, 286, 25992-26002.
- Ghazi T, Nagiah S, Tiloke C, Abdul NS, Chaturgoon AA. (2017). Fusaric acid induces DNA damage and post-translational modifications of p53 in human hepatocellular carcinoma (HepG2) cells. *Journal of Cellular Biochemistry*, 118, 3866-3874.
- Hidaka H, Nagatsu T, Takeya K, Takeuchi T, Suda H, Kojiri K, Matsuzaki M, Umezawa H. (1969). Fusaric acid, a hypotensive agent produced by fungi. *Journal of Antibiotics*, 22, 228-230.
- Laptenko O, Prives C. (2006). Transcriptional regulation by p53: one protein, many possibilities. *Cell Death and Differentiation*, 13, 951-961.
- Mamur S, Ünal F, Yilmaz S, Erikel E, Yüzbaşıoğlu D. (2018). Evaluation of the cytotoxic and genotoxic effects of mycotoxin fusaric acid. *Drug and Chemical Toxicology*, 1-9.

- Peters AH, O'carroll, Scherthan H, Mechtler K, Sauer S, Schöfer C, Weipoltshammer K, Pagani M, Lachner M, Kohlmaier A. (2001). Loss of the Suv39h histone methyltransferases impairs mammalian heterochromatin and genome stability. *Cell*, 107, 323-337.
- Putiri EL, Robertson KD. (2011). Epigenetic mechanisms and genome stability. *Clinical Epigenetics*, 2, 299-314.
- Reddy R, Larson C, Brimer G, Frappier B, Reddy C. (1996). Developmental toxic effects of fusaric acid in CD1 mice. *Bulletin of Environmental Contamination and Toxicology*, 57, 354-360.
- Stack Jr BC, Hansen JP, Ruda JM, Jaglowski J, Shvidler J, Hollenbeak CS. (2004). Fusaric acid: a novel agent and mechanism to treat HNSCC. *Otolaryngology—Head and Neck Surgery*, 131, 54-60.
- Vaquero A, Scher M, Erdjument-Bromage H, Tempst P, Serrano L, Reinberg D. (2007). SIRT1 regulates the histone methyl-transferase SUV39H1 during heterochromatin formation. *Nature*, 450, 440-444.
- Yin ES, Rakhmankulova M, Kucera K, De Sena Filho JG, Portero CE, Narváez-Trujillo A, Holley SA, Strobel SA. (2015). Fusaric acid induces a notochord malformation in zebrafish via copper chelation. *BioMetals*, 28, 783-789.

## **ADDENDUM A**

The following study titled, “**Fusaric acid induces DNA damage and post-translational modifications of p53 in human hepatocellular carcinoma (HepG2) cells**” set the foundation for this study.

**Journal of Cellular Biochemistry 118 (11): 3866-3874 (2017)**

**DOI: 10.1002/jcb.26037**

## Fusaric Acid Induces DNA Damage and Post-Translational Modifications of p53 in Human Hepatocellular Carcinoma (HepG<sub>2</sub>) Cells

Terisha Ghazi, Savania Nagiah, Charlette Tiloke, Naeem Sheik Abdul, and Anil A. Chuturgoon \*

Discipline of Medical Biochemistry and Chemical Pathology, School of Laboratory Medicine and Medical Science, College of Health Sciences, University of Kwa-Zulu Natal, Congella, Durban 4013, South Africa

### ABSTRACT

Fusaric acid (FA), a common fungal contaminant of maize, is known to mediate toxicity in plants and animals; however, its mechanism of action is unclear. p53 is a tumor suppressor protein that is activated in response to cellular stress. The function of p53 is regulated by post-translational modifications—ubiquitination, phosphorylation, and acetylation. This study investigated a possible mechanism of FA induced toxicity in the human hepatocellular carcinoma (HepG<sub>2</sub>) cell line. The effect of FA on DNA integrity and post-translational modifications of p53 were investigated. Methods included: (a) culture and treatment of HepG<sub>2</sub> cells with FA (IC<sub>50</sub>: 580.32 μM, 24 h); (b) comet assay (DNA damage); (c) Western blots (protein expression of p53, MDM2, p-Ser-15-p53, a-K382-p53, a-CBP (K1535)/p300 (K1499), HDAC1 and p-Ser-47-Sirt1); and (d) Hoechst 33342 assay (apoptosis analysis). FA caused DNA damage in HepG<sub>2</sub> cells relative to the control ( $P < 0.0001$ ). FA decreased the protein expression of p53 (0.24-fold,  $P = 0.0004$ ) and increased the expression of p-Ser-15-p53 (12.74-fold,  $P = 0.0126$ ) and a-K382-p53 (2.24-fold,  $P = 0.0096$ ). This occurred despite the significant decrease in the histone acetyltransferase, a-CBP (K1535)/p300 (K1499) (0.42-fold,  $P = 0.0023$ ) and increase in the histone deacetylase, p-Ser-47-Sirt1 (1.22-fold,  $P = 0.0020$ ). The expression of MDM2, a negative regulator of p53, was elevated in the FA treatment compared to the control (1.83-fold,  $P < 0.0001$ ). FA also inhibited cell proliferation and induced apoptosis in HepG<sub>2</sub> cells as evidenced by the Hoechst assay. Together, these results indicate that FA is genotoxic and post-translationally modified p53 leading to HepG<sub>2</sub> cell death. *J. Cell. Biochem.* 9999: 1–9, 2017. © 2017 Wiley Periodicals, Inc.

**KEY WORDS:** FUSARIC ACID; DNA DAMAGE; p53; POST-TRANSLATIONAL MODIFICATIONS; p-Ser-15-p53; a-K382-p53

Fusaric acid (FA; 5-butylpicolinic acid or 5-n-butyl-pyridine-2-carboxylic acid), a secondary metabolite, and mycotoxin produced by the *Fusarium* species, is a common contaminant of several food commodities especially, maize [Bacon et al., 1996]. These foods form an integral part of the human and animal diet; and the consumption of FA contaminated commodities may have a serious impact on human and animal health. Fusaric acid is known to affect both plants [D'Alton and Etherton, 1984; Diniz and Oliveira, 2009; Li et al., 2013] and animals [Hidaka et al., 1969; Dowd, 1988; Voss et al., 1999; Ogunbo et al., 2007]; however, its mechanism of action remains unclear. Fusaric acid is a well-known phytotoxin that causes wilt disease symptoms in a variety of plants [Wu et al., 2008; Diniz and Oliveira, 2009]. Other effects of FA on plants include alterations in membrane permeability [D'Alton and Etherton, 1984;

Pavlovkin et al., 2004], increased electrolyte leakage [D'Alton and Etherton, 1984] and inhibition of respiration [D'Alton and Etherton, 1984; Pavlovkin et al., 2004].

Fusaric acid is a membrane permeating weak acid and is therefore, potentially toxic as a proton conductor. It alters the mitochondrial membrane potential of cells and decreases ATP production [Diniz and Oliveira, 2009; Abdul et al., 2016; Devnarain et al., 2016]. Fusaric acid impairs mitochondrial function and biogenesis in HepG<sub>2</sub> cells [Abdul et al., 2016]; and induces apoptosis by increasing the activity of caspases-8, -9, and -3/7 [Abdul et al., 2016; Devnarain et al., 2016]. Fusaric acid also elevates oxidative stress [Sapko et al., 2011; Singh and Upadhyay, 2014; Abdul et al., 2016; Devnarain et al., 2016] by decreasing the activity of anti-oxidant enzymes: superoxide dismutase (SOD), catalase (CAT) and ascorbate

Conflict of interest: The authors declare no conflict of interest.

Grant sponsor: National Research Foundation; Grant sponsor: Inyuvesi Yakwazulu-Natali.

\*Correspondence to: Prof. Anil A. Chuturgoon, Discipline of Medical Biochemistry and Chemical Pathology, School of Laboratory Medicine and Medical Science, College of Health Sciences, University of Kwa-Zulu Natal, Private Bag 7, Congella, Durban 4013, South Africa. E-mail: chatur@ukzn.ac.za

Manuscript Received: 17 February 2017; Manuscript Accepted: 6 April 2017

Accepted manuscript online in Wiley Online Library (wileyonlinelibrary.com): 7 April 2017

DOI 10.1002/jcb.26037 • © 2017 Wiley Periodicals, Inc.

peroxidase; and increasing the production of reactive oxygen species (ROS) [Singh and Upadhyay, 2014].

Fusaric acid is a potent chelator of divalent cations. It inhibits metal-containing oxidative enzymes and increases cytokine production [Ye et al., 2013]. Fusaric acid has potent anti-proliferative and anti-tumor activity in several human cancer cell lines [Fernandez-Pol et al., 1993]. In particular, FA has anti-tumor activity against head and neck squamous cell carcinoma by increasing DNA damage and preventing its synthesis and repair [Stack et al., 2004]. This may occur from the chelation of divalent cations from catalytic DNA associated metalloproteins and inactivation of zinc finger proteins [Stack et al., 2004]. Fusaric acid also inhibits the proliferation of WI-38 fibroblasts and is a potent inhibitor of DNA synthesis in breast cancer (MDA-MB-468) cells and WI-38 fibroblasts [Fernandez-Pol et al., 1993]. Fusaric acid affects blood coagulation and platelet function by chelating calcium ions and altering the platelet aggregation process [Devaraja et al., 2013]. It has anti-hypertensive activity in cats, dogs, rabbits, and rats by inhibiting the copper-dependent enzyme dopamine  $\beta$ -hydroxylase, a key enzyme in the synthesis of the neurotransmitter norepinephrine [Hidaka et al., 1969; Terasawa and Kameyama, 1971]. Previous studies show FA to be toxic to mice by chelating calcium causing a delay in bone ossification and affecting the growth of foetuses [Reddy et al., 1996]. Fusaric acid was also shown to be toxic to zebrafish by chelating copper and inhibiting the enzyme lysyl oxidase resulting in notochord malformation [Yin et al., 2015]. Synergistic effects of FA with other mycotoxins produced by the *Fusarium* species such as Fumonisin B<sub>1</sub> [Bacon et al., 1995], Deoxynivalenol (DON) [Smith et al., 1997] and 4, 15-diacetoxy-scirpenol (DAS) [Dowd, 1988, Fairchild et al., 2005] have been reported.

The guardian of the genome, p53, is a tumour suppressor protein and transcription factor that is activated in response to cellular stress [Prives and Hall, 1999]. Several stressors can activate p53 such as DNA damage, excessive oncogene activation, hypoxia, and oxidative stress [Prives and Hall, 1999]. Once activated, p53 mediates a plethora of functions including cell growth arrest, DNA repair, senescence, and apoptosis [Barlev et al., 2001]. The function of p53 is regulated by a variety of post-translational modifications. These modifications occur in the N- and C-terminal regions of the protein and include ubiquitination, phosphorylation, and acetylation [Barlev et al., 2001; Tang et al., 2008]. The ubiquitination of p53 occurs in the absence of cellular stress and is mediated by the protein murine double minute 2 (MDM2). MDM2 is the predominant negative regulator of p53. It adds ubiquitin chains to the C-terminal lysine (K) residues (K370, K372, K373, K381, K382, and K386), targeting p53 for degradation by the 26S proteasome [Rodriguez et al., 2000]. In this way, MDM2 helps maintain low basal levels of p53.

p53 stabilization and transcriptional activation are crucial early events in a cell's battle against genotoxic stress. The p53 protein contains an array of serine and threonine residues that are phosphorylated in response to genotoxic stress. During DNA damage several protein kinases such as ataxia telangiectasia mutated (ATM), ataxia telangiectasia and Rad 3 related protein (ATR) and DNA-dependent protein kinase (DNA-PK) are triggered

[Sakaguchi et al., 1998; Shieh et al., 1997; Barlev et al., 2001; Loughery et al., 2014]. These protein kinases phosphorylate p53 on serine (Ser-15, Ser-20, Ser-33, Ser-37, and Ser-46) and threonine (Thr-18) residues leading to the stabilization of p53 [Shieh et al., 1997; Barlev et al., 2001].

Acetylation status also dictates p53 function. Several acetylation sites (K120, K320, K370, K372, K373, K381, K382, and K386) have been identified for p53 [Barlev et al., 2001]; however, K382 is the major lysine residue acetylated in response to genotoxic stress. The acetylation of p53 is important as it stimulates its transcriptional activity [Tang et al., 2008; Yi and Luo, 2010], promotes its ability to bind to DNA in a sequence-specific manner [Sakaguchi et al., 1998] and recruits transcriptional coactivators to specific p53 response elements [Barlev et al., 2001]. This enables p53 to transcribe genes such as MDM2, p21 and BAX, which are involved in regulating cell proliferation and apoptosis [Tang et al., 2008]. The acetylation of p53 is regulated by histone acetyltransferases such as CREB-binding protein (CBP) and p300 and histone deacetylases such as HDAC1 and Sirtuin (Sirt) 1.

The dearth of studies on FA toxicity in humans little is known on the relationship between FA and p53. This study investigated a possible mechanism of FA induced toxicity by determining the effect of FA on DNA integrity and post-translational modifications that is, phosphorylation and acetylation of p53 in the human hepatocellular carcinoma (HepG<sub>2</sub>) cell line.

## MATERIALS AND METHODS

### MATERIALS

Fusaric acid, isolated from the fungus *Gibberella fujikuroi* (F6513), was purchased from Sigma-Aldrich (St. Louis, MO). The MDM2 inhibitor, SP 141 [6-Methoxy-1-(1-naphthalenyl)-9H-pyrido [3, 4-b] indole], was purchased from Tocris BioSciences (MO). The HepG<sub>2</sub> cell line was purchased from Highveld Biologicals (Johannesburg, SA). Cell culture equipment and reagents were purchased from Lonza Biotechnology (Basel, Switzerland). Western Blot equipment and reagents were purchased from Bio-Rad (Hercules, CA). All other reagents were purchased from Merck (Darmstadt, Germany), unless otherwise stated.

### CELL CULTURE

HepG<sub>2</sub> cells were cultured (37°C, 5% CO<sub>2</sub>) in 25 cm<sup>3</sup> sterile cell culture flasks containing complete culture media (CCM; Eagle's Minimum Essentials Medium (EMEM) supplemented with 10% foetal calf serum, 1% penicillin-streptomycin-fungizone, and 1% L-glutamine). The cells were grown to 90% confluency before incubation (37°C, 5% CO<sub>2</sub>, 24 h) with FA and SP 141. Thereafter, the cells were counted using the trypan blue cell exclusion method and used for the relevant assays. All experiments were repeated three independent times and in triplicate to validate the results.

### PREPARATION OF TREATMENTS

Stocks of FA (5 mM) were prepared by dissolving FA in 0.1M PBS. An inhibitory concentration of 50% (IC<sub>50</sub>: 580.32  $\mu$ M FA; 24 h) was obtained from literature [Abdul et al., 2016] and used in all

subsequent assays. The SP 141 (5 mM) stock was prepared by dissolving SP 141 in 100% DMSO. The inhibitory concentration (5  $\mu$ M) of SP 141 on MDM2 was determined by Western blotting (supplementary material) and used as the negative control. An untreated control (CCM only) and a vehicle control (0.081% DMSO) were also prepared. Since, the percentage DMSO used was less than 1% and displayed similar results to the untreated control, the vehicle control was omitted from statistical analyses.

#### COMET ASSAY

The comet assay was used to determine DNA damage in HepG<sub>2</sub> cells. Following incubation of HepG<sub>2</sub> cells with FA for 24 h, the supernatants were removed. The cells were rinsed thrice in 0.1M PBS and detached by the use of trypsin. Cells were suspended in 0.1M PBS (20,000 cells in 25  $\mu$ l PBS). Three frosted slides per sample (control and FA) were prepared by adding three layers of low melting point agarose gel (LMPA, 37°C) with each layer being allowed to solidify (4°C, 10 min). The first layer consisted of 2% LMPA (700  $\mu$ l). A second layer of 25  $\mu$ l cell suspension, 0.5  $\mu$ l Gel Red (catalog no. 41003, Biotium Inc., Hayward, CA) and 175  $\mu$ l 1% LMPA was added to the solidified first layer. The third layer consisting of 1% LMPA (200  $\mu$ l) was subsequently added. Once solidified, all slides were immersed in freshly prepared cold lysing solution [2.5 M NaCl, 100 mM EDTA, 1% Triton X-100, 10 mM Tris (pH 10) and 10% DMSO] and incubated (1 h, 4°C). Following incubation, the slides were placed in electrophoresis buffer [300 mM NaOH, 1 mM Na<sub>2</sub>EDTA; pH 13] for 20 min at RT. The slides were then electrophoresed (25V (300 mA, approx. 0.74 V/cm), 35 min, RT) using the Bio-Rad compact power supply. Thereafter, the slides were washed three times with neutralisation buffer [0.4M Tris; pH 7.4] for 5 min each. Slides were viewed using the Olympus IX51 inverted fluorescent microscope with 510–560 nm excitation and 590 nm emission filters. Images of at least 50 cells and comets were captured per sample at 20 $\times$  magnification and the comet tail lengths were measured using the Soft Imaging System (Life Science–Olympus Soft Imaging Solutions version 5) and reported as micrometer.

#### WESTERN BLOT

Western blots were used to determine the protein expression of p53, MDM2, p-Ser-15-p53, a-K382-p53, a-CBP (K1535)/p300 (K1499), HDAC1, and p-Ser-47-Sirt1. HepG<sub>2</sub> cells were treated with FA and SP 141 for 24 h in 25 cm<sup>3</sup> cell culture flasks. The supernatants were removed from the flask and the cells were rinsed three times in 0.1M PBS. Thereafter, Cytobuster™ Reagent (200  $\mu$ l) (Novagen, San Diego, CA, catalogue no. 71009) supplemented with a cocktail of protease inhibitors (Roche, catalogue no. 05892791001) and phosphatase inhibitors (Roche, catalogue no. 04906837001) was added to the flask and the cells were kept on ice for 30 min before further lysing with a cell scraper. The lysed cells were transferred to 1.5 ml micro-centrifuge tubes and centrifuged (10,000g, 10 min, 4°C). The supernatants containing the crude protein extract was aspirated into fresh 1.5 ml micro-centrifuge tubes and kept on ice. The Bicinchoninic Acid (BCA) Assay was used to quantify the crude protein. The proteins were subsequently standardized to a concentration of 1.5 mg/ml and the standardized samples were

prepared in Laemmli buffer [dH<sub>2</sub>O, 0.5M Tris-HCl (pH 6.8), glycerol, 10% SDS, 5%  $\beta$ -mercaptoethanol, and 1% bromophenol blue] by boiling (100°C) for 5 min. The protein samples were then electrophoresed (1 h, 150V) in sodium dodecyl sulphate polyacrylamide gels (10% resolving gel, 4% stacking gel) using the Bio-Rad compact power supply. Thereafter, the separated proteins were electro-transferred to a nitrocellulose membrane using the Bio-Rad Trans-Blot™ Turbo Transfer System (20V, 30 min). Following transfer, the membranes were blocked in blocking buffer consisting of either 5% BSA (phosphorylated proteins) or 5% non-fat dry milk (NFDM) in Tris buffered saline with 0.05% Tween 20 [TTBS; 150 mM NaCl, 3 mM KCl, 25 mM Tris, 0.05% Tween 20, dH<sub>2</sub>O, pH 7.5] for 1 h at RT with gentle shaking. The membranes were then immunoblotted with the specific primary antibody (p53 [Santa Cruz, sc-6243], MDM2 [Sigma-Aldrich, M4308], p-Ser-15-p53 [Cell Signalling Technology #9284], HDAC1 [Abcam, Ab19845], a-CBP (K1535)/p300 (K1499) [Cell Signalling Technology #4771S], 1:1 000 dilution; a-K382-p53 [Cell Signalling Technology #2525] and p-Ser-47-Sirt1 [Cell Signalling Technology #2314L], 1: 500 dilution) for 1 h at RT on a rotator and then overnight at 4°C. The membranes were washed five times with TTBS (10 min each, RT) and incubated with the respective horse-radish peroxidase (HRP)-conjugated secondary antibody [1:10 000 dilution in 5% BSA (goat anti-rabbit, sc-2004) and 1:10 000 dilution in 5% NFDM (goat anti-mouse, sc-2005)] for 2 h at RT with gentle shaking. Membranes were washed five times with TTBS (10 min each, RT). The Clarity™ Western ECL Substrate Kit (catalog no. #170-5060, Bio-Rad) was used for the visualization of protein bands and detected using the ChemiDoc™ XRS+ Molecular Imaging System (Bio-Rad). After detection, the membranes were quenched using hydrogen peroxide (5%, 30 min, 37°C), washed once with TTBS (10 min, RT), blocked in 5% BSA in TTBS (1 h, RT) and probed with the housekeeping protein, anti- $\beta$ -actin (catalog no. a3854, Sigma-Aldrich, 1:5 000 dilution in 5% BSA, 30 min, RT). Protein expression was analyzed using the Image Lab Software version 5.0 (Bio-Rad) and the results were quantified as relative band density (RBD). Protein expression was normalized against the housekeeping protein,  $\beta$ -actin. Fold-change was also determined relative to the control.

#### HOECHST 33342 ASSAY

The Hoechst 33342 assay was used to determine the effect of FA on apoptosis in HepG<sub>2</sub> cells. HepG<sub>2</sub> cells (500,000 cells/well) were seeded into a six-well plate and allowed to adhere overnight. Thereafter, the CCM was removed; cells were rinsed three times in 0.1M PBS and treated with FA for 24 h. Three technical replicates were prepared. Following treatment, the cells were rinsed three times in 0.1M PBS and fixed using 10% paraformaldehyde (500  $\mu$ l/well, 5 min, RT). Once fixed, the paraformaldehyde was removed and the cells were rinsed three times in 0.1M PBS. The Hoechst 33342 working solution (catalog no. B2261, Sigma-Aldrich; 5  $\mu$ g/ml) was added and the plate was incubated (15 min, 37°C). Thereafter, the cells were rinsed three times in 0.1M PBS and viewed using the Olympus IX51 inverted fluorescent microscope with 350 nm excitation and 450 nm emission filters. Three images per sample replicate were captured at 20 $\times$  magnification.

## STATISTICAL ANALYSES

The data were analyzed using GraphPad Prism version 5.0 (Graph-Pad Prism Software Inc., La Jolla). The D'Agostino and the Pearson normality tests were used to determine if the data followed a normal distribution. Since, the data was normally distributed, the unpaired *t*-test with Welch's Correction and the One Way Analysis of Variance (ANOVA) with the Bonferroni test (multiple comparisons) was used to analyze the data. All results were represented as the mean  $\pm$  standard deviation with a 95% confidence interval, unless otherwise stated. A value of  $P < 0.05$  was considered statistically significant.

## RESULTS

### FUSARIC ACID INDUCED DNA DAMAGE IN HepG<sub>2</sub> CELLS

We first aimed to determine if FA was genotoxic to HepG<sub>2</sub> cells. The comet assay was used to assess DNA damage in the FA treated and untreated HepG<sub>2</sub> cells (Fig. 1A). There was a significant increase (2.65-fold) in comet tail lengths in the FA treated HepG<sub>2</sub> cells compared to the control (Fig. 1B,  $89.98 \pm 10.36 \mu\text{m}$  vs. control:  $33.99 \pm 6.76 \mu\text{m}$ ,  $P < 0.0001$ ).

### FUSARIC ACID DECREASED THE PROTEIN EXPRESSION OF p53 AND INCREASED THE EXPRESSION OF MDM2 IN HepG<sub>2</sub> CELLS

DNA damage is the most common activator of p53. Due to the observed genotoxic effects of FA, we evaluated the protein expression of p53. Fusaric acid decreased the protein expression of p53 in HepG<sub>2</sub> cells (0.24-fold) compared to the control (Fig. 2A; control vs. FA:  $0.43 \pm 0.02$  RBD to  $0.33 \pm 0.03$  RBD,  $P = 0.0020$ ). The

expression of p53 was also decreased in SP 141 treated cells when compared to the control (control vs. SP 141:  $0.43 \pm 0.02$  RBD to  $0.31 \pm 0.01$  RBD,  $P = 0.0020$ ). The difference in p53 expression between the FA treated and SP 141 treated HepG<sub>2</sub> cells was not significant (FA vs. SP 141:  $0.33 \pm 0.03$  RBD to  $0.31 \pm 0.01$  RBD).

The E3 ubiquitin ligase, MDM2, plays a pivotal role in regulating p53 expression in the absence of cellular stress. It promotes p53 degradation through a ubiquitin-dependent pathway on nuclear and cytoplasmic 26S proteasomes. The protein expression of MDM2 was assessed to determine if the decrease in p53 expression was due to MDM2. The expression of MDM2 was significantly elevated (1.83-fold) in the FA treated HepG<sub>2</sub> cells compared to the control (Fig. 2B; control vs. FA:  $0.31 \pm 0.04$  RBD to  $0.56 \pm 0.01$  RBD,  $P < 0.0001$ ). The expression of MDM2 was significantly decreased in the SP 141 treated cells when compared to the control and FA treated HepG<sub>2</sub> cells (control vs. SP 141:  $0.31 \pm 0.04$  RBD to  $0.12 \pm 0.02$  RBD, FA vs. SP 141:  $0.56 \pm 0.01$  RBD to  $0.12 \pm 0.02$  RBD,  $P < 0.0001$ ).

### FUSARIC ACID INCREASED THE PHOSPHORYLATION AND ACETYLATION OF p53 ON THE Ser-15 AND K382 RESIDUE IN HepG<sub>2</sub> CELLS

The phosphorylation and acetylation of p53 on Ser-15 and K382, respectively are the most common post-translational modifications that occur during DNA damage. We determined if FA post-translationally modifies p53 via phosphorylation and acetylation in HepG<sub>2</sub> cells; and if the decrease in p53 expression observed had an effect on its phosphorylation and acetylation status. The protein expression of p-Ser-15-p53 and a-K382-p53 were divided by the protein expression of total p53 to determine the ratio of

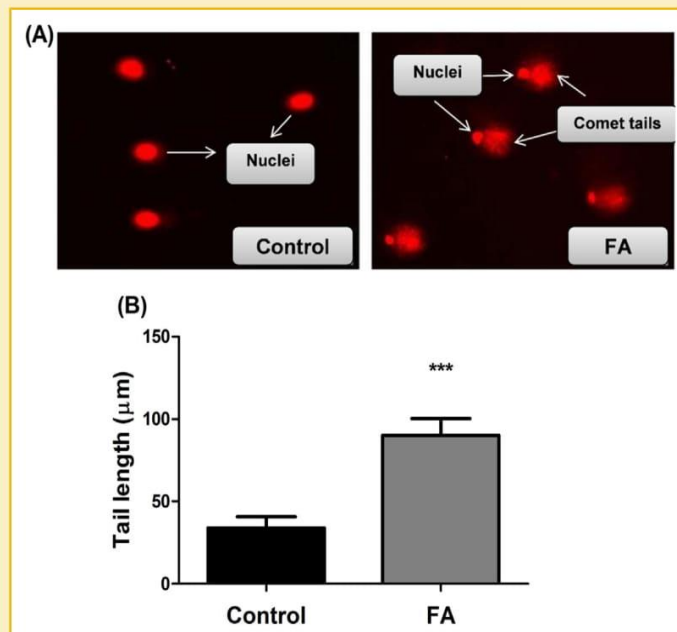


Fig. 1. Fusaric acid induced DNA damage in HepG<sub>2</sub> cells. Comet tails of the FA treated and control HepG<sub>2</sub> cells (20 $\times$  magnification) (A). Fusaric acid increased comet tail lengths in HepG<sub>2</sub> cells at 24 h (\*\* $P < 0.0001$ ) (B).

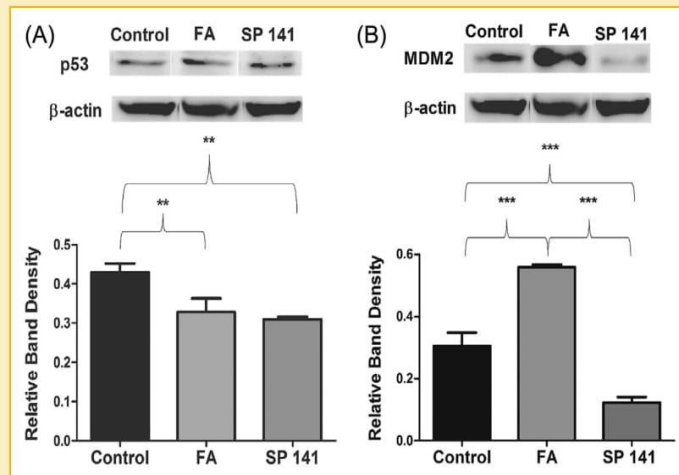


Fig. 2. Protein expression of p53 (A) and MDM2 (B) in FA and SP 141 treated HepG<sub>2</sub> cells. Fusaric acid significantly decreased the expression of p53 (A; \*\**P* < 0.005) and increased the expression of MDM2 (B; \*\*\**P* < 0.0001) in HepG<sub>2</sub> cells compared to the control.

phosphorylated and acetylated p53. Fusaric acid significantly increased the phosphorylation of p53 on the Ser-15 residue in HepG<sub>2</sub> cells (12.74-fold) compared to the control (Fig. 3A;  $1.38 \pm 0.25$  RBD vs. control:  $0.11 \pm 0.02$  RBD, *P* = 0.0126). Acetylated p53 on the K382 residue was significantly increased (2.24-fold) in the FA treatment compared to the control (Fig. 3B;  $0.61 \pm 0.07$  RBD vs. control:  $0.27 \pm 0.07$  RBD, *P* = 0.0096). These results indicate that FA not only alters the protein expression of p53, but also the phosphorylation and acetylation status of p53 in HepG<sub>2</sub> cells.

#### FUSARIC ACID DECREASED THE PROTEIN EXPRESSION OF THE HISTONE ACETYLTRANSFERASE, a-CBP (K1535)/P300 (K1499) AND ALTERED THE EXPRESSION OF THE HISTONE DEACETYLASES, HDAC1, AND p-Ser-47-Sirt1

The increase in a-K382-p53 expression led to the assessment of a-CBP (K1535)/p300 (K1499), HDAC1, and p-Ser-47-Sirt1. These

proteins both regulate the acetylation status of p53 on the K382 residue. Fusaric acid significantly decreased the expression of a-CBP (K1535)/p300 (K1499) (0.42-fold) in HepG<sub>2</sub> cells compared to the control ( $0.44 \pm 0.05$  RBD vs. control:  $0.76 \pm 0.03$  RBD, *P* = 0.0023; Fig. 4A).

The expression of HDAC1 was significantly decreased (0.16-fold) in the FA treated HepG<sub>2</sub> cells compared to the control ( $0.56 \pm 0.04$  RBD vs. control:  $0.66 \pm 0.04$  RBD, *P* = 0.0386; Fig. 4B). However, the protein expression of p-Ser-47-Sirt1 was higher (1.22-fold) in the FA treatment compared to the control ( $0.74 \pm 0.02$  RBD vs. control:  $0.61 \pm 0.03$  RBD, *P* = 0.0020; Fig. 4C).

#### FUSARIC ACID INHIBITS CELL PROLIFERATION AND INDUCES APOPTOSIS IN HepG<sub>2</sub> CELLS

The acetylation of p53 indicates an increase in p53 stability and activity. Since, p53 functions to regulate cell proliferation by further

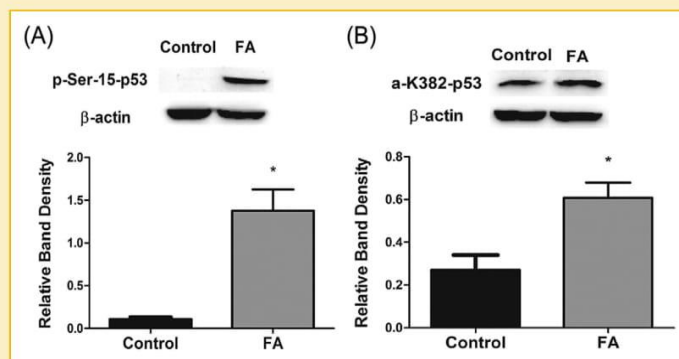


Fig. 3. Fusaric acid post-translationally modifies p53 in HepG<sub>2</sub> cells. The expression of p-Ser-15-p53 (A; \**P* < 0.05) and a-K382-p53 (B; \**P* < 0.05) was elevated in the FA treated cells compared to the control.

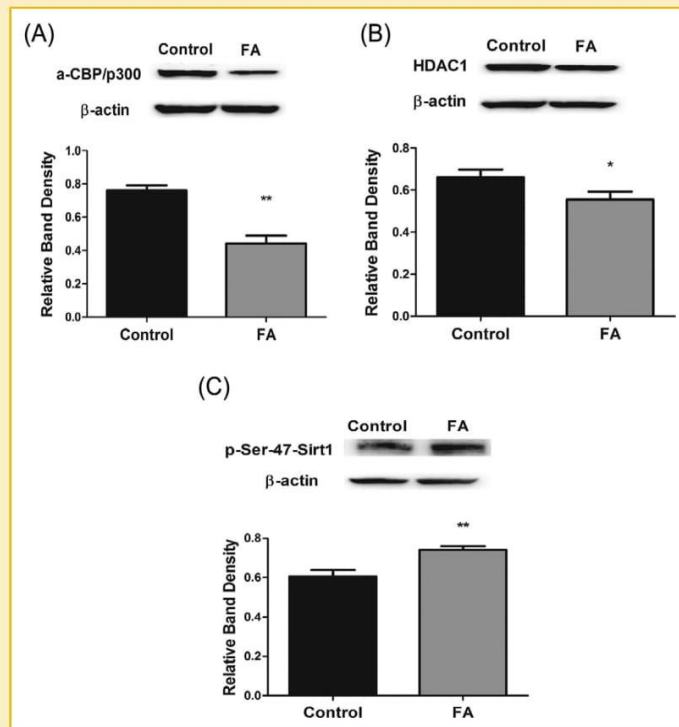


Fig. 4. The effect of FA on the protein expression of a-CBP (K1535)/p300 (K1499) (A), HDAC1 (B) and p-Ser-47-Sirt1 (C) in HepG<sub>2</sub> cells. Fusaric acid decreased the protein expression of a-CBP (K1535)/p300 (K1499) (A; \*\*  $P < 0.005$ ) and HDAC1 (B; \*  $P < 0.05$ ) and increased the expression of p-Ser-47-Sirt1 (C; \*\*  $P < 0.005$ ) in HepG<sub>2</sub> cells compared to the control.

regulating genes that control the cell cycle and apoptosis; the Hoechst 33342 assay was used to determine the effect of FA on cell proliferation and apoptosis in HepG<sub>2</sub> cells (Fig. 5). Hoechst analysis of HepG<sub>2</sub> cells displayed fewer cells with the presence of several apoptotic bodies in the FA treated cells (Fig. 5B) compared to the control (Fig. 5A). Therefore, FA inhibited cell proliferation and induced apoptosis in HepG<sub>2</sub> cells.

## DISCUSSION

Fusaric acid is a common mycotoxin that contaminates several food commodities [Bacon et al., 1996]. Fusaric acid exerts low to moderate toxicity in plants [D'Alton and Etherton, 1984; Pavlovkin et al., 2004; Diniz and Oliveira, 2009; Li et al., 2013] and animals [Hidaka et al., 1969; Dowd, 1988; Bacon et al., 1995; Smith et al., 1997; Voss et al., 1999; Fairchild et al., 2005]; however, the mechanism by which this mycotoxin exerts its toxicity is currently unclear. Several studies have shown FA to exert its toxicity by elevating oxidative stress [Sapko et al., 2011; Abdul et al., 2016; Devnarain et al., 2016] and causing DNA damage [Stack et al., 2004]; however, others show that FA is a potent chelator of divalent cations and thus may exert its toxicity by removing essential metal ions [Fernandez-Pol et al., 1993; Reddy et al., 1996; Stack et al., 2004; Devaraja et al., 2013; Yin et al., 2015]. We hypothesized that FA caused DNA damage and

post-translationally modified the tumor suppressor protein, p53 in the HepG<sub>2</sub> cell line; and that the activation of p53 may provide a possible mechanism of FA induced toxicity.

Due to its continuous replication, DNA is highly susceptible to damage by both endogenous and exogenous agents. Damage to cellular DNA disrupts normal functioning of the cell and can lead to death of the cell or malignant transformation [Salmon et al., 2004]. The longer comet tail lengths observed in the FA treated cells compared to the control (Fig. 1) indicate that FA induced significant DNA damage in HepG<sub>2</sub> cells. The increase in DNA damage may occur as a result of oxidative damage as it was previously shown that FA induces oxidative stress in HepG<sub>2</sub> cells [Abdul et al., 2016]. Oxidative stress refers to an increase in ROS and a decrease in antioxidants. Reactive oxygen species are highly reactive molecules that contain oxygen including superoxide radical ( $O_2^-$ ), hydroxyl radical ( $OH^-$ ) and hydrogen peroxide ( $H_2O_2$ ); that are capable of causing damage to cellular macromolecules [Salmon et al., 2004]. Reactive oxygen species damage cellular DNA by oxidising DNA bases, causing breaks in the DNA molecules (single- and double-strand breaks) and by forming highly toxic and mutagenic DNA lesions [Salmon et al., 2004].

p53 is a major stress response protein that is activated in response to DNA damage [Sakaguchi et al., 1998]. Extensive DNA damage increases the steady-state level and activity of p53 leading to cell cycle arrest, inhibition of cell proliferation and apoptosis. Fusaric

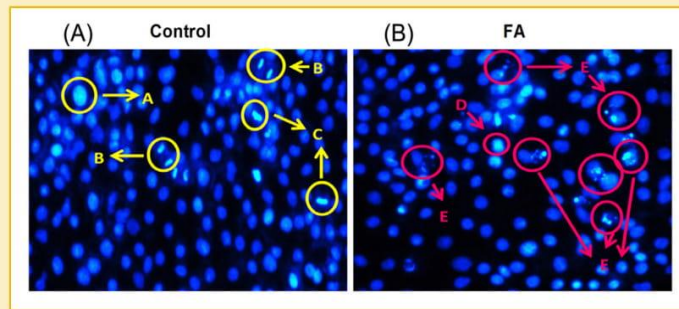


Fig. 5. Hoechst 33342 staining of the control (A) and FA treated (B) HepG<sub>2</sub> cells at 24 h (20× magnification) [A–prophase, B–anaphase, C–metaphase, D–hyper-condensed chromatin, and E–apoptotic bodies].

acid significantly decreased the protein expression of p53 in HepG<sub>2</sub> cells (Fig. 2A). p53 is a metalloprotein that requires a zinc ion to maintain structural stability. The zinc ion is tetrahedrally coordinated by a histidine (His179) and three cysteine side chains (Cys176, Cys238, and Cys242) [Bullock et al., 2000; Joerger and Fersht, 2007; Quinn and Thayer, 2015] and is essential for maintaining the wild-type conformation and stability of the p53 protein [Ostrakhovitch et al., 2006; Quinn and Thayer, 2015]. Chelation of the zinc ion by FA may cause changes in the stability of the coordination complex thereby, destabilizing the p53 protein resulting in local structural perturbations and loss of sequence-specific DNA binding [Ostrakhovitch et al., 2006; Quinn and Thayer, 2015].

The p53 protein is subjected to a variety of post-translational modifications that enhance its stability and activity as a transcription factor [Shieh et al., 1997; Sakaguchi et al., 1998; Tang et al., 2008]. During DNA damage, the kinases ATM, ATR, and DNA-PK are activated to phosphorylate p53 on Ser-15 [Shieh et al., 1997; Sakaguchi et al., 1998; Barlev et al., 2001]. The phosphorylation of p53 on Ser-15 is a major focal point in the activation of p53 as it enhances p53 stability by alleviating its inhibition by MDM2 [Shieh et al., 1997]. Fusaric acid significantly increased the expression of p-Ser-15-p53 in HepG<sub>2</sub> cells (Fig. 3A).

The phosphorylation of p53 on Ser-15 is known to prime p53 for acetylation by stimulating the association of p53 with histone acetyltransferases (HATs), such as CBP and p300 [Barlev et al., 2001; Tang et al., 2008; Loughery et al., 2014]. Fusaric acid significantly increased the expression of a-K382-p53 in HepG<sub>2</sub> cells (Fig. 3B) despite the significant decrease in the expression of a-CBP (K1535)/p300 (K1499) (Fig. 4A). The acetylation of CBP on K1535 and p300 on K1499 is known to enhance the HAT activity of CBP and p300 [Thompson et al., 2004]. These transcriptional co-activators function by directly binding to a variety of transcriptional regulators where they recruit additional CBP and p300 molecules to acetylate histone and non-histone proteins thereby, activating their transcriptional activity [Sakaguchi et al., 1998; Thompson et al., 2004; Tang et al., 2008; Loughery et al., 2014]. The structure of CBP/p300 plays a major role in its HAT function [Park et al., 2013]. CBP/p300 contain several well-conserved domains, three of which bind zinc and are required for maintaining a stable folded structure [Park et al., 2013]. The decrease in the expression of a-CBP/p300 observed in the FA

treatment may be attributed to the removal of the zinc ions from the CBP/p300 protein leading to structural destabilization. CBP/p300 are auto-acetylated in the presence of acetyl-CoA and a decrease in CBP/p300 will ultimately lead to a decrease in a-CBP (K1535)/p300 (K1499). The decrease in a-CBP (K1535)/p300 (K1499) did not affect the acetylation of p53 as the phosphorylation of p53 on Ser-15 enables a-CBP/p300 to bind to p53 with a high affinity leading to C-terminal acetylation and enhanced transcriptional activity of p53 [Lambert et al., 1998; Barlev et al., 2001; Tang et al., 2008; Loughery et al., 2014].

The acetylation of p53 promotes p53 mediated gene activation which ultimately determines cellular response to stress in the form of senescence, cell growth arrest, and apoptosis [Barlev et al., 2001]. Hoechst analysis of HepG<sub>2</sub> cells showed that FA inhibited cell growth and induced apoptosis, as shown by the absence of dividing cells and the presence of apoptotic bodies (Fig. 5). This is in accordance with the study by Abdul et al. (2016) in which FA induced apoptosis in HepG<sub>2</sub> cells by elevating the activity of the executioner caspases-3/7. Fusaric acid also effectively induced apoptosis in human promyelocytic leukaemia (HL-60) cells [Ogata et al., 2001] and oesophageal cancer (SNO) cells [Devnarain et al., 2016].

Histone deacetylation plays an important role in inhibiting p53-dependent transcriptional activity. The major deacetylases involved in regulating p53 are HDAC1 and Sirt1. HDAC1 is a zinc-dependent enzyme closely related to the yeast counterpart, *RPD3*. HDAC1 is found mainly in the nucleus and is known to deacetylate p53 on several lysine (K320, K373, and K382) residues [Luo et al., 2000]. Fusaric acid significantly decreased the protein expression of HDAC1 and increased the expression of p-Ser-47-Sirt1 in HepG<sub>2</sub> cells (Fig. 4B and C, respectively). Sirt1 is a class III NAD<sup>+</sup>-dependent deacetylase that is responsible for deacetylating p53 specifically on K382 [Solomon et al., 2006]. It catalyzes the deacetylation of acetyl-lysine residues in a unique reaction that utilises NAD<sup>+</sup> and generates nicotinamide and O-acetyl ADP-ribose [Solomon et al., 2006]. Nicotinamide is a non-competitive inhibitor of Sirt1 activity and the inhibition of Sirt1 activity has been reported to suppress cell growth as well as induce cell cycle arrest and apoptosis in vitro [Solomon et al., 2006]. The function of Sirt1 is regulated by phosphorylation. Several protein kinases have been shown to phosphorylate Sirt1; however, whether or not Sirt1 is activated by phosphorylation is

largely dependent on the protein kinase that phosphorylates it [Sasaki et al., 2008]. For example, the phosphorylation of Sirt1 on Ser-47 by JNK1 (c-Jun kinase) promotes its nuclear localization and enzymatic activity [Nasrin et al., 2009] whereas the phosphorylation of Sirt1 on Ser-47 by mTOR (mammalian target of rapamycin) was found to inhibit Sirt1 deacetylase activity [Back et al., 2011].

Sirt1 also contains a multi-functional domain known as the C-pocket that is capable of directly binding NAD<sup>+</sup> and is involved in mediating NAD<sup>+</sup> cleavage, base exchange activity and nicotinamide regulation [Avalos et al., 2005]. Pyridine derivatives are able to undergo exchange reactions with the nicotinamide moiety of NAD<sup>+</sup> thereby, forming NAD<sup>+</sup> analogues. Fusaric acid is a pyridine derivative and a nicotinic acid related compound that may bind to the C-pocket of Sirt1 and inhibit its activity by preventing NAD<sup>+</sup> from binding to the C-pocket and catalysing the deacetylation reaction. Fusaric acid may also mimic the structure of nicotinamide, bind to the C-pocket of Sirt1 and inhibit Sirt1 activity. Although FA increased the expression of p-Ser-47-Sirt1, it may not necessarily be active as an increase in the expression of a-K382-p53 was also observed.

MDM2 is the main regulator of p53. MDM2 binds to and ubiquitinates p53, targeting it for degradation by the 26S proteasome [Rodriguez et al., 2000]. This enables p53 to be maintained at low levels in the absence of cellular stress. However, excessive p53 activation can increase the expression of MDM2 in a negative feedback loop to decrease p53 expression and activation [Rodriguez et al., 2000]. Fusaric acid significantly increased the expression of MDM2 in HepG<sub>2</sub> cells when compared to the control and SP 141 treated cells (Fig. 2B). SP 141, a specific inhibitor of MDM2, is a cell permeable pyro [3,4-b] indole derivative that binds directly to the hydrophobic groove of MDM2 and acts by reducing MDM2 expression and promoting its ubiquitination and proteasomal degradation [Wang et al., 2014]. This process occurs regardless of the p53 status within the cell [Wang et al., 2014]. The acetylation of p53 on K382 indicates an increase in p53 stability and activity [Sakaguchi et al., 1998; Barlev et al., 2001]. Therefore, the increase in MDM2 expression may occur in response to the increase in a-K382-p53 (increase in p53 activity) observed in the FA treated HepG<sub>2</sub> cells. The decrease in p53 protein levels may not necessarily be attributed to the increase in MDM2 expression as the phosphorylation of p53 on Ser-15 prevents the interaction between p53 and MDM2 thereby, inhibiting its ubiquitination and degradation in the presence of DNA damage [Shieh et al., 1997]. Furthermore, in addition to phosphorylating p53, ATM, and DNA-PK also phosphorylate MDM2. DNA-PK mediated phosphorylation of MDM2 on Ser-17 prevents MDM2 from binding and ubiquitinating p53 [Mayo et al., 1997] whereas the phosphorylation of MDM2 on Ser-395 by ATM inhibits the export of p53 from the nucleus to the cytoplasm [Maya et al., 2001]. This prevents p53 degradation and may provide a possible explanation for how p53 trans-activates the MDM2 gene but is not initially inhibited by the resulting increase in MDM2 protein [Mayo et al., 1997; Maya et al., 2001].

This study provides a possible mechanism of FA induced toxicity in the human liver using the HepG<sub>2</sub> cell line. The results indicate that FA is genotoxic and post-translationally modified p53 leading to cell growth arrest and apoptosis of HepG<sub>2</sub> cells. Interestingly, the results

also indicate a control for p53 acetylation and highlight the importance of the regulation of p53 and MDM2 for cell development, proper protection from DNA damage, cell cycle control, and apoptosis. Furthermore, the results indicate that Ser-15 phosphorylation is required for the function of p53 and this may suggest a possible universal role in promoting p53-transcriptional activity.

## ACKNOWLEDGMENTS

The authors acknowledge the National Research Foundation (NRF) and the College of Health Sciences (University of Kwa-Zulu Natal) for funding this study.

## REFERENCES

- Abdul NS, Nagiah S, Chuturgoon AA. 2016. Fusaric acid induces mitochondrial stress in human hepatocellular carcinoma (HepG2) cells. *Toxicol* 119:336-344.
- Avalos JL, Bever KM, Wolberger C. 2005. Mechanism of sirtuin inhibition by nicotinamide: Altering the NAD<sup>+</sup> cosubstrate specificity of a Sir2 enzyme. *Mol Cell* 17:855-868.
- Back JH, Rezvani HR, Zhu Y, Guyonnet-Duperat V, Athar M, Ratner D, Kim AL. 2011. Cancer cell survival following DNA damage-mediated premature senescence is regulated by mammalian target of rapamycin (mTOR)-dependent inhibition of sirtuin 1. *J Biol Chem* 286:19100-19108.
- Bacon C, Porter J, Norred W, Leslie J. 1996. Production of fusaric acid by *Fusarium* species. *Appl Environ Microbiol* 62:4039-4043.
- Bacon CW, Porter JK, Norred WP. 1995. Toxic interaction of fumonisin B1 and fusaric acid measured by injection into fertile chicken egg. *Mycopathologia* 129:29-35.
- Barlev NA, Liu L, Chehab NH, Mansfield K, Harris KG, Halazonetis TD, Berger SL. 2001. Acetylation of p53 activates transcription through recruitment of coactivators/histone acetyltransferases. *Mol Cell* 8:1243-1254.
- Bullock AN, Henckel J, Fersht AR. 2000. Quantitative analysis of residual folding and DNA binding in mutant p53 core domain: Definition of mutant states for rescue in cancer therapy. *Oncogene* 19:1245.
- D'alton A, Etherton B. 1984. Effects of fusaric acid on tomato root hair membrane potentials and ATP levels. *Plant Physiol* 74:39-42.
- Devaraja S, Girish KS, Santhosh MS, Hemshekhar M, Nayaka SC, Kemparaju K. 2013. Fusaric acid, a mycotoxin, and its influence on blood coagulation and platelet function. *Blood Coagul Fibrinolysis* 24:419-423.
- Devnarain N, Tiloke C, Nagiah S, Chuturgoon AA. 2016. Fusaric acid induces oxidative stress and apoptosis in human cancerous oesophageal SNO cells. *Toxicol* 126:4-11.
- Dimiz S, Oliveira R. 2009. Effects of fusaric acid on *Zea mays* L. seedlings. *Phyton (Buenos Aires)* 78:155-160.
- Dowd PF. 1988. Toxicological and biochemical interactions of the fungal metabolites fusaric acid and kojic acid with xenobiotics in *Heliothis zea* (F.) and *Spodoptera frugiperda* (JE Smith). *Pestic Biochem Physiol* 32:123-134.
- Fairchild A, Grimes J, Porter J, Croom W, Jr, Daniel L, Hagler W, Jr. 2005. Effects of diacetoxyscirpenol and fusaric acid on poult: Individual and combined effects of dietary diacetoxyscirpenol and fusaric acid on turkey poult performance. *Int J Poul Sci* 4:350-355.
- Fernandez-Pol JA, Klos DJ, Hamilton PD. 1993. Cytotoxic activity of fusaric acid on human adenocarcinoma cells in tissue culture. *Anticancer Res* 13:57-64.
- Hidaka H, Nagatsu T, Takeya K, Takeuchi T, Suda H, Kojiri K, Matsuzaki M, Umezawa H. 1969. Fusaric acid, a hypotensive agent produced by fungi. *J Antibiot* 22:228-230.

- Joerger A, Fersht A. 2007. Structure-function-rescue: The diverse nature of common p53 cancer mutants. *Oncogene* 26:2226–2242.
- Lambert PF, Kashanchi F, Radonovich MF, Shiekhattar R, Brady JN. 1998. Phosphorylation of p53 serine 15 increases interaction with CBP. *J Biol Chem* 273:33048–33053.
- Li C, Zuo C, Deng G, Kuang R, Yang Q, Hu C, Sheng O, Zhang S, Ma L, Wei Y. 2013. Contamination of bananas with beauvericin and fusaric acid produced by *Fusarium oxysporum* f. sp. *cubense*. *PLoS ONE* 8:1–11.
- Loughery J, Cox M, Smith LM, Meek DW. 2014. Critical role for p53-serine 15 phosphorylation in stimulating transactivation at p53-responsive promoters. *Nucl Acids Res* 42:7666–7680.
- Luo J, SU F, Chen D, Shiloh A, GU W. 2000. Deacetylation of p53 modulates its effect on cell growth and apoptosis. *Nature* 408:377–381.
- Maya R, Balass M, Kim S-T, Shkedy D, Leal J-FM, Shifman O, Moas M, Buschmann T, Ronai ZE, Shiloh Y. 2001. ATM-dependent phosphorylation of Mdm2 on serine 395: Role in p53 activation by DNA damage. *Genes Dev* 15:1067–1077.
- Mayo LD, Turchi JJ, Berberich SJ. 1997. Mdm-2 phosphorylation by DNA-dependent protein kinase prevents interaction with p53. *Cancer Res* 57:5013–5016.
- Nasrin N, Kaushik VK, Fortier E, Wall D, Pearson KJ, DE Cabo R, Bordone L. 2009. JNK1 phosphorylates SIRT1 and promotes its enzymatic activity. *PLoS ONE* 4:1–9.
- Ogata S, Inoue K, Iwata K, Okumura K, Taguchi H. 2001. Apoptosis induced by picolinic acid-related compounds in HL-60 cells. *Biosci Biotechnol Biochem* 65:2337–2339.
- Ogunbo S, Broomhead J, Ledoux D, Bermudez A, Rottinghaus G. 2007. The individual and combined effects of fusaric acid and T-2 toxin in broilers and turkeys. *Int J Poult Sci* 6:484–488.
- Ostrakhovitch EA, Olsson P-E, Jiang S, Cherian MG. 2006. Interaction of metallothionein with tumor suppressor p53 protein. *FEBS Lett* 580:1235–1238.
- Park S, Martinez-Yamout MA, Dyson HJ, Wright PE. 2013. The CH2 domain of CBP/p300 is a novel zinc finger. *FEBS Lett* 587:2506–2511.
- Pavlovkin J, Mistrik I, Prokop M. 2004. Some aspects of the phytotoxic action of fusaric acid on primary *Ricinus* roots. *Plant Soil Env* 50:397–401.
- Prives C, Hall PA. 1999. The p53 pathway. *J Pathol* 187:112–126.
- Quinn T, Thayer K. 2015. Structural point mutations of p53 protein and their effects on the zinc coordination complex. *FASEB J* 29:–712.23.
- Reddy RV, Larson CA, Brimer GE, Frappier BL, Reddy CS. 1996. Developmental toxic effects of fusaric acid in CD1 mice. *Bull Environ Contam Toxicol* 57:354–360.
- Rodriguez MS, Desterro JM, Lain S, Lane DP, Hay RT. 2000. Multiple C-terminal lysine residues target p53 for ubiquitin-proteasome-mediated degradation. *Mol Cell Biol* 20:8458–8467.
- Sakaguchi K, Herrera JE, Saito SI, Miki T, Bustin M, Vassilev A, Anderson CW, Appella E. 1998. DNA damage activates p53 through a phosphorylation-acetylation cascade. *Genes Dev* 12:2831–2841.
- Salmon TB, Evert BA, Song B, Doetsch PW. 2004. Biological consequences of oxidative stress-induced DNA damage in *Saccharomyces cerevisiae*. *Nucl Acids Res* 32:3712–3723.
- Sapko O, Utarbaeva AS, Makulbek S. 2011. Effect of fusaric acid on prooxidant and antioxidant properties of the potato cell suspension culture. *Russ J Plant Physiol* 58:828–835.
- Sasaki T, Maier B, Koclega KD, Chruszcz M, Gluba W, Stukenberg PT, Minor W, Scrable H. 2008. Phosphorylation regulates SIRT1 function. *PLoS ONE* 3:1–13.
- Shieh S-Y, Ikeda M, Taya Y, Prives C. 1997. DNA damage-induced phosphorylation of p53 alleviates inhibition by MDM2. *Cell* 91:325–334.
- Singh VK, Upadhyay RS. 2014. Fusaric acid induced cell death and changes in oxidative metabolism of *Solanum lycopersicum* L. *Bot Stud* 55:1.
- Smith TK, Mcmillan EG, Castillo JB. 1997. Effect of feeding blends of *Fusarium* mycotoxin-contaminated grains containing deoxynivalenol and fusaric acid on growth and feed consumption of immature swine. *J Anim Sci* 75:2184–2191.
- Solomon JM, Pasupuleti R, Xu L, Mcdonagh T, Curtis R, Distefano PS, Huber LJ. 2006. Inhibition of SIRT1 catalytic activity increases p53 acetylation but does not alter cell survival following DNA damage. *Mol Cell Biol* 26:28–38.
- Stack BC, Hansen JP, Ruda JM, Jaglowski J, Shvidler J, Hollenbeak CS. 2004. Fusaric acid: A novel agent and mechanism to treat HNSCC. *Otolaryngol Head Neck Surg* 131:54–60.
- Tang Y, Zhao W, Chen Y, Zhao Y, Gu W. 2008. Acetylation is indispensable for p53 activation. *Cell* 133:612–626.
- Terasawa F, Kameyama M. 1971. The clinical trial of a new hypotensive agent, "fusaric acid (5-butylpicolinic acid)": The preliminary report. *Jpn Circ J* 35:339–357.
- Thompson PR, Wang D, Wang L, Fulco M, Pediconi N, Zhang D, An W, Ge Q, Roeder RG, Wong J. 2004. Regulation of the p300 HAT domain via a novel activation loop. *Nat Struct Mol Biol* 11:308–315.
- Voss K, Porter J, Bacon C, Meredith F, Norred W. 1999. Fusaric acid and modification of the subchronic toxicity to rats of fumonisins in *F. moniliforme* culture material. *Food Chem Toxicol* 37:853–861.
- Wang W, Qin J-J, Voruganti S, Srivenugopal KS, Nag S, Patil S, Sharma H, Wang M-H, Wang H, Buolamwini JK. 2014. The pyrido [b] indole MDM2 inhibitor SP-141 exerts potent therapeutic effects in breast cancer models. *Nat Commun* 5:1–12.
- Wu H-S, Bao W, Liu D-Y, Ling N, Ying R-R, Raza W, Shen Q-R. 2008. Effect of fusaric acid on biomass and photosynthesis of watermelon seedlings leaves. *Caryologia* 61:258–268.
- Ye J, Montero M, Stack BC, Jr. 2013. Effects of fusaric acid treatment on HEP2 and docetaxel-resistant HEP2 laryngeal squamous cell carcinoma. *Chemotherapy* 59:121–128.
- Yi J, Luo J. 2010. SIRT1 and p53, effect on cancer, senescence and beyond. *Biochim Biophys Acta* 1804:1684–1689.
- Yin ES, Rakhmankulova M, Kucera K, De Sena Filho JG, Portero CE, Narvaez-Trujillo A, Holley SA, Strobel SA. 2015. Fusaric acid induces a notochord malformation in zebrafish via copper chelation. *Biomaterials* 28:783–789.

## SUPPORTING INFORMATION

Additional supporting information may be found in the online version of this article at the publisher's web-site.

## ADDENDUM B

### Ethical Approval Letter – *In Vitro* Study



29 May 2019

Ms T Ghazi (211504090)  
School of Laboratory Medicine and Medical Sciences  
College of Health Sciences  
[terishaghazi@gmail.com](mailto:terishaghazi@gmail.com)

Dear Ms Ghazi

Protocol: An investigation into the epigenetic effects of fusaric acid in human liver (HepG2) cells  
Degree: PhD  
BREC Ref No: BE316/19

#### EXPEDITED APPLICATION: APPROVAL LETTER

A sub-committee of the Biomedical Research Ethics Committee has considered and noted your application received 05 April 2019.

Please ensure that site permissions are obtained and forwarded to BREC for approval before commencing research at a site.

This approval is valid for one year from 29 May 2019. To ensure uninterrupted approval of this study beyond the approval expiry date, an application for recertification must be submitted to BREC on the appropriate BREC form 2-3 months before the expiry date.

Any amendments to this study, unless urgently required to ensure safety of participants, must be approved by BREC prior to implementation.

Your acceptance of this approval denotes your compliance with South African National Research Ethics Guidelines (2015), South African National Good Clinical Practice Guidelines (2006) (if applicable) and with UKZN BREC ethics requirements as contained in the UKZN BREC Terms of Reference and Standard Operating Procedures, all available at <http://research.ukzn.ac.za/Research-Ethics/Biomedical-Research-Ethics.aspx>.

BREC is registered with the South African National Health Research Ethics Council (REC-290408-009). BREC has US Office for Human Research Protections (OHRP) Federal-wide Assurance (FWA 678).

The sub-committee's decision will be noted by a full Committee at its next meeting taking place on 11 June 2019.

Yours sincerely

Prof V Rambiritch  
Chair: Biomedical Research Ethics Committee

cc: Postgrad admin: [dudhrajhp@ukzn.ac.za](mailto:dudhrajhp@ukzn.ac.za) Supervisor: [CHUTUR@ukzn.ac.za](mailto:CHUTUR@ukzn.ac.za) [Nagiah.savania@gmail.com](mailto:Nagiah.savania@gmail.com)

Biomedical Research Ethics Committee  
Professor V Rambiritch (Chair)

Westville Campus, Govan Mbeki Building  
Postal Address: Private Bag X54001, Durban 4000

Telephone: +27 (0) 31 260 2486 Facsimile: +27 (0) 31 260 4609 Email: [brec@ukzn.ac.za](mailto:brec@ukzn.ac.za)

Website: <http://research.ukzn.ac.za/Research-Ethics/Biomedical-Research-Ethics.aspx>



Founding Campuses: Edgewood Howard College Medical School Pietermaritzburg Westville

## ADDENDUM C

### Ethical Approval Letter – *In Vivo* Study



18 September 2018

Professor Anil Chuturgoon (34866)  
School of Laboratory Medicine & Medical Sciences  
Howard College Campus

Dear Professor Chuturgoon,

**Protocol reference number: AREC/079/016**

**Project title:** The molecular and epigenetic effects of selected mycotoxins on C57B/6 black mice

**Full Approval – Renewal Application**

With regards to your renewal application received on 24 August 2018. The documents submitted have been accepted by the Animal Research Ethics Committee and **FULL APPROVAL** for the protocol has been granted.

**Please note: Any Veterinary and Para-Veterinary procedures must be conducted by a SAVC registered VET or SAVC authorized person.**

**Any alteration/s to the approved research protocol, i.e Title of Project, Location of the Study, Research Approach and Methods must be reviewed and approved through the amendment/modification prior to its implementation. In case you have further queries, please quote the above reference number.**

Please note: Research data should be securely stored in the discipline/department for a period of 5 years.

**The ethical clearance certificate is only valid for a period of one year from the date of issue. Renewal for the study must be applied for before 18 September 2019.**

Attached to the Approval letter is a template of the Progress Report that is required at the end of the study, or when applying for Renewal (whichever comes first). An Adverse Event Reporting form has also been attached in the event of any unanticipated event involving the animals' health / wellbeing.

I take this opportunity of wishing you everything of the best with your study.

Yours faithfully

.....  
Professor S Islam, PhD  
Chair: Animal Research Ethics Committee

/ms

Cc Acting Academic Leader Research: Dr Brenda de Gama  
Cc Registrar: Mr Simon Mokoena  
Cc NSPCA: Ms Anita Engelbrecht  
Cc BRU – Dr Linda Bester

---

Animal Research Ethics Committee (AREC)  
Ms Mariette Snyman (Administrator)  
Westville Campus, Govan Mbeki Building

Postal Address: Private Bag X54001, Durban 4000

Telephone: +27 (0) 31 260 8350 Facsimile: +27 (0) 31 260 4609 Email: [animaethics@ukzn.ac.za](mailto:animaethics@ukzn.ac.za)  
Website: <http://research.ukzn.ac.za/Research-Ethics/Animal-Ethics.aspx>



100 YEARS OF ACADEMIC EXCELLENCE

Founding Campuses: ■ Edgewood ■ Howard College ■ Medical School ■ Pietermaritzburg ■ Westville

## ADDENDUM D

### Quantification of DNA Methylation

The Methylated DNA Quantification Kit (ab117128) is a colorimetric assay used to measure 5-methylcytosine on DNA. It is a highly sensitive assay, detecting as little as 0.2ng of methylated DNA, and is based on the principle of an ELISA. First, DNA together with a series of 5-methylcytosine standards (0, 1, 2, 5, and 10 ng/ $\mu$ l) are bound to strip wells that are specifically treated to have a high affinity for DNA; and 5-methylcytosine is detected using capture and detection antibodies that result in a color change from yellow to blue. The optical density (OD) is measured spectrophotometrically at a wavelength of 450 nm. The ODs of the 5-methylcytosine standards are used to construct a standard curve from which the percentage 5-methylcytosine in each sample is determined (Figure A1). The amount of methylated DNA is proportional to the OD intensity measured.

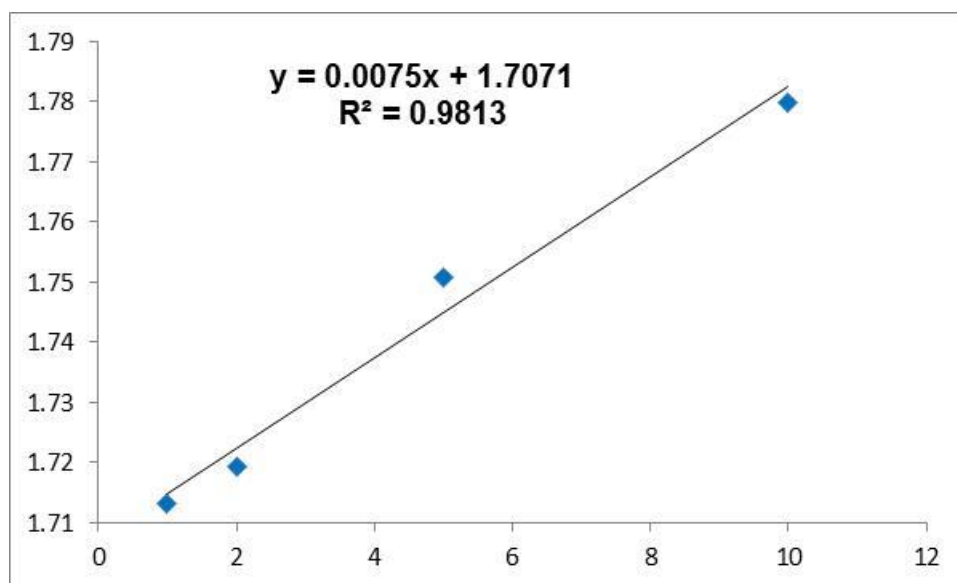


**Figure A1** Standard curve used to determine 5-methylcytosine in DNA

## ADDENDUM E

### Quantification of M6A RNA Methylation

The m6A RNA methylation quantification kit (ab185912) is a highly sensitive, detects as little as 10 pg of m6A, colorimetric assay that utilizes the principle of antigen-antibody binding to measure m6A levels in total RNA. First, total RNA together with various m6A standards (0, 0.01, 0.02, 0.05, and 0.1 ng/ $\mu$ l) are bound to strip wells using a high affinity RNA binding solution. Thereafter, m6A is detected using a specific m6A capture and detection antibody. The detected signal is enhanced and the OD is measured at a wavelength of 450 nm using a microplate spectrophotometer. The ODs of the standards are used to construct a standard curve from which the percentage m6A in each sample is determined (Figure A2). The amount of m6A is proportional to the intensity of the OD measured.

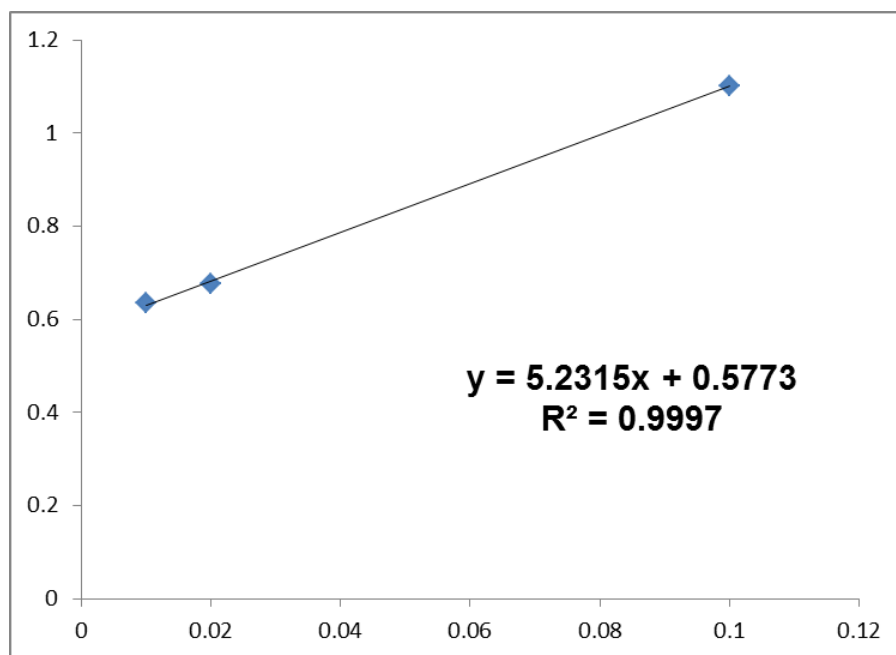


**Figure A2** Standard curve used to determine m6A levels in total RNA

### Fusaric Acid Increases Total M6A Levels in HepG2 Cells

We determined the effect of FA on total m6A levels in HepG2 cells. Briefly, total RNA was isolated from control and FA-treated HepG2 cells, as previously described (Ghazi et al., 2019). The RNA was then quantified using the Nanodrop2000 spectrophotometer, standardized to 500 ng/ $\mu$ l, and m6A levels were measured using the colorimetric m6A RNA methylation quantification kit (ab185912), as per manufacturer's instructions. FA significantly increased the percentage of m6A in HepG2 cells in a dose-dependent manner compared to the control ( $p = 0.0005$ ; Figure A3).

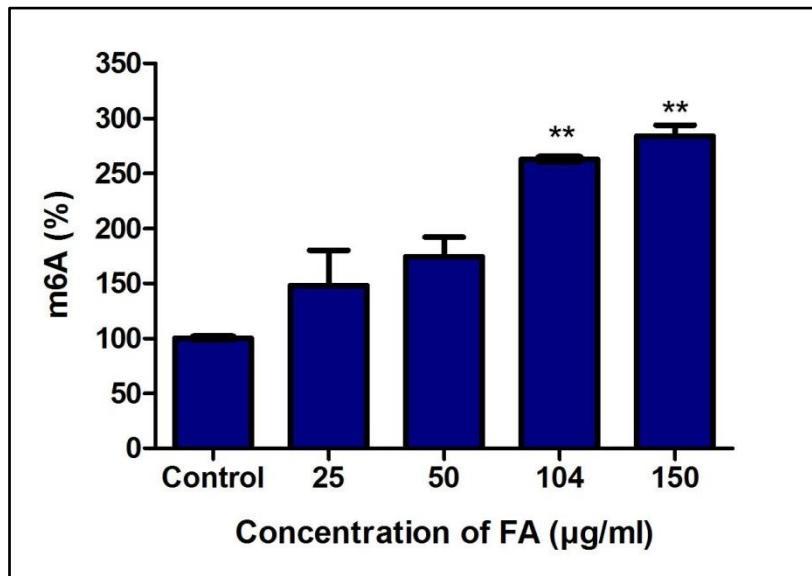


**Figure A3** The effect of FA on total m6A levels in HepG2 cells. FA increased the percentage m6A RNA methylation in HepG2 cells. Results are represented as the mean  $\pm$  SD ( $n = 3$ ). Statistical significance was determined using the one-way ANOVA with the Bonferroni multiple comparisons test (\*\* $p < 0.005$ ).